TESIS DE LA UNIVERSIDAD DE ZARAGOZA
2025
28

Ruth Mafalda Soler Agesta

Impact of mitochondrial function in the response of cancer cells to PT-112

Director/es
Anel Bernal, Luis Alberto
Moreno Loshuertos, Raquel

ISSN 2254-7606

Prensas de la Universidad
Universidad Zaragoza

Universidad de Zaragoza
Servicio de Publicaciones

ISSN 2254-7606

Universidad Zaragoza
1542

Tesis Doctoral

IMPACT OF MITOCHONDRIAL FUNCTION IN THE RESPONSE OF CANCER CELLS TO PT-112

Autor

Ruth Mafalda Soler Agesta

Director/es

Anel Bernal, Luis Alberto
Moreno Loshuertos, Raquel

UNIVERSIDAD DE ZARAGOZA
Escuela de Doctorado

Programa de Doctorado en Bioquímica y Biología Molecular

2024

Universidad Zaragoza

FACULTY OF SCIENCE

DEPARTMENT OF BIOCHEMISTRY, MOLECULAR AND CELL BIOLOGY

Doctoral Thesis

IMPACT OF MITOCHONDRIAL FUNCTION IN THE RESPONSE OF CANCER CELLS TO PT-112

Ruth Mafalda Soler Agesta

June 2024

Dr. LUIS ALBERTO ANEL BERNAL, Catedrático en Bioquímica y Biología Molecular y Dr. RAQUEL MORENO LOSHUERTOS, Profesor contratado doctor en Bioquímica y Biología Molecular, ambos miembros del Departamento de Bioquímica y Biología Molecular y Celular de la Universidad de Zaragoza.

Certifican:

Que la tesis titulada "IMPACT OF MITOCHONDRIAL FUNCTION IN THE RESPONSE OF CANCER CELLS TO PT-112" ha sido realizada por Ruth Mafalda Soler Agesta en el Departamento de Bioquímica y Biología Molecular y Celular de la Facultad de Ciencias de la Universidad de Zaragoza, bajo nuestra dirección y reúne, a nuestro juicio, las condiciones requeridas para que su autor pueda optar al grado de Doctor en Bioquímica, Biología Molecular y Celular por la Universidad de Zaragoza.

Zaragoza, junio 2024

Fdo. Luis Alberto Anel Bernal

Fdo. Raquel Moreno Loshuertos

Esta tesis doctoral ha sido realizada gracias a la ayuda financiera recibida por la Asociación Española Contra el Cáncer (AECC) asociada al proyecto PRDAR21487SOLE y con el apoyo de Promontory Therapeutics Inc.

ACKNOWLEDGEMENTS

"Science is always a collective adventure"

-Guido Kroemer-

Todo empezó con, “ni de coña hago una tesis doctoral”, ¿pero te acuerdas del dicho? Nunca digas nunca. Pues aquí estamos casi 5 años de mi vida con esta tesis, unas cuantas canas más y probablemente más celulitis por las interminables horas que he pasado sobre una silla escribiendo. Por no decir, las noches sin dormir, los dolores de espalda y los ataques de corazón cada vez que pasaba algo o con los experimentos, o con la redacción de esta tesis. Para los que ya habéis escrito una y estéis leyendo estas líneas ya sabréis lo que todo esto supone. Es casi como una aventura que no le ves el final, pero que deseas que llegue a su fin tan pronto como sea. Bueno pues nada, aquí estoy en Nueva York, una ciudad en la que nunca me hubiera imaginado acabar cuando empecé en el mundo de la ciencia. Y es en estos momentos tan intensos y especiales, que un domingo a las seis de la tarde me he puesto a escribir esta parrafada desde el laboratorio (parece que las horas extras no remuneradas en la ciencia es algo universal, pasa aquí y en la China). Es con esta tranquilidad intermitente por el ruido de las ambulancias aquí en el pleno corazón de Manhattan que me entra una nostalgia tremenda al pensar en todas aquellas personas que han pasado por mi vida durante estos intensos pero alucinantes 5 años. Yo solo espero no dejarme a nadie, y si fuera el caso me disculpo de antemano por mi capacidad recurrente de olvidarme de las cosas. Algún día me darán un premio por eso o una mañana moriré achicharrada por olvidarme la cafetera hirviendo en los fogones de mi piso de Nueva York, que son por cierto de la época de María Antonieta. Antes de empezar a enumerar a la gente, quisiera dejar claro que el orden que voy a utilizar no refleja lo más o menos importante que ha sido esa persona para mí durante este viaje ya que todos y cada uno de vosotros me habéis aportado y enseñado cosas distintas, pero cada una con un valor incalculable.

En primer lugar, quisiera agradecer a mis directores de tesis al Dr. Alberto Anel y a la Dra. Raquel Moreno por su apoyo incondicional en todo lo que me he propuesto des de que trabajo con ellos. Mi suerte es infinita por haberos encontrado. He aprendido tanto con vosotros que podría escribir otra tesis. Gracias por todo, siempre seréis un referente para mí.

También agradecer a María Barreiro, la mujer del Dr. Alberto Anel, la “mami”, y es que ella también lo sabe, que es como si fuera mi segunda madre. Gracias por cuidarme como si fuera de los tuyos, y sobre todo por hacerme reír tanto. Oye, enserio, algún día me mataras de la risa. ¡Que afortunada soy en tenerte en mi vida también!

Ahora toca a la familia. Creo que van a ser unas líneas duras porque desde que empecé esta tesis muchos nos han abandonado.

En primer lugar, quiero agradecer a mi querida madre María Ángeles Agesta por haberme dado la vida. Gracias por tu apoyo incondicional, tu amor infinito hacia mí. Gracias por TODO. Yo no podría haber hecho esto si no fuera por ti. Te quiero mama.

En segundo lugar, agradecer a mi padre Ramon Soler, tú también has sido imprescindible para que esto pase. Gracias por esforzarte en intentar hacer las cosas lo mejor que pudiste. Aunque no nos veamos mucho, pienso en ti muy a menudo. Hoy soy la mujer que soy gracias a ti.

También quisiera mencionar a mi familia más cercana, mis difuntos abuelos Ascensión Gracia y Alfredo Agesta. Os fuisteis cuando yo estaba muy lejos. Aunque no nos hayamos podido despedir siento que estáis aquí, conmigo, dándome todo vuestro apoyo. Siempre seréis un referente de fortaleza para mí. Nunca os olvidare.

A mi Yaya Pepa Fabregat, la matriarca, t'estimo molt.

Mencionar también a mis tías Mari Paz Agesta (mi madrina) y en especial a Àngels Soler por haber cuidado de la familia cuando yo he estado terminando esta tesis en otro país. Sois ejemplo de valentía y fortaleza. Gracias a las dos.

Bueno, ahora toca hablar de alguien muy especial, Mario Andrés Lituma, al que quiero agradecerle infinitamente todo el apoyo que me ha dado durante la redacción de esta tesis. Especialmente por los cafés mañaneros y por esas cenas tan buenas que me preparas después de un largo día de trabajo. Gracias por ser el mejor. Te quiero mucho.

En la misma línea, quisiera también agradecer a la familia Córdova (la tía Rosy, el tío Fernando, Gigi, Pacho, Erika y al Choco) por esas comidas de fin de semana tan deliciosas acompañadas de alegría, risas y cariño incondicional. Aunque no lo creáis, habéis sido un apoyo enorme cuando el *burnout* de la tesis empezaba a hacer mella. Gracias por tratarme como uno de los vuestros. Os quiero.

Y por fin llego a las raíces, donde todo esto empezó. Mi grupo de investigación Apoptosis, Inmunidad y Cáncer de la Universidad de Zaragoza, en el que yo casi aprendí a usar una pipeta. Ya han pasado 7 años desde aquel octubre de 2017 en el que entre como estudiante de Máster. Durante todo este tiempo han pasado muchas personas por el laboratorio. Aquí hay algunos nombres que me gustaría resaltar:

Dra. Raquel Ibáñez, Dra. Patricia Guerrero y Dra. Martha Minjarez que des el principio de mi tesis hemos "vivido" juntas en el laboratorio. Compartiendo momentos inolvidables y chismes para escribir

telenovelas. Ahora que ya sois las tres doctoras y yo ya estoy en camino, solo puedo decir que ¡el tiempo vuela!

Al Dr. Joaquín Marco por haber sido mi principal guía al inicio de esta aventura. Gracias por enseñarme casi todo lo que sabias sobre ciencia. ¡Fuiste un compañero de laboratorio genial!

A mis estudiantes de grado Mario Belio, Fernando De la Figuera que también me han enseñado cosas que ni siquiera yo sabía de mí misma. Los dos habéis despertado en mi la pasión por enseñar. Estoy muy orgullosa de veros evolucionar tanto personalmente como profesionalmente. Y bueno, a mi Cristina Ripollès que no sé muy bien si meterte con mis estudiantes o con la sección de grupo de apoyo psicológico. Que te voy a decir que no sepas pequeña. Te admiro como persona y como científica. ¡ERES MUY GRANDE! A Andrea Redrado, gracias por esas charlas tan bonitas e inspiradoras. Me he dado cuenta de que eres una bellísima persona.

Al Dr. Manuel Beltrán, mi Manueeeeee. Aquel chico tímido de mi grupo de investigación que ahora casi vive conmigo en otro país. Vaya aventura en la que nos hemos metido, pero estoy feliz que hayas sido tú, ¡siempre supe que eras un crack!

A los demás compañeros de laboratorio: Evelyn Galanos, mi cubana que recién llego de la otra punta del mundo. Te deseo el más bonito de los futuros. ¡Lo más duro ya está hecho, ahora solo toca subir y subir! A Laura Cambronero, el alma inquieta del laboratorio. Confía un poco más en ti misma, yo sé que eres capaz de mucho ¡Se te quiere y se te echa de menos! A la Dra. Chantal Reina, una mujer muy especial. Te agradezco la generosidad que tú y tu familia siempre habéis mostrado hacia mí durante todo este tiempo. Ya sabes que tienes una casa en Nueva York, ven a visitarme cuando quieras. A Pilar Corral, que a pesar de llegar al laboratorio cuando yo ya estaba casi en los finales de mi tesis, he podido compartir momentos muy agradables contigo. Te mando mucha fuerza para lo que te queda por recorrer. También quería mencionar a la Dra. Andrea Benedí, la Dra. Nelia Jiménez, la Dra. Isabel Marzo, el Dr. Javier Naval, la Dra. Eva Latorre, la Dra. Pilar Mozas, la Dra. Ana Gallego y el Dr. David Giraldos. El Dr. Javier Amezcua, aunque fuiste del *team* mitocondrias, siempre te he considerado como uno de los nuestros.

En fin, gracias a cada uno de vosotros por entregarme vuestra amistad, regalar sabiduría y compartir momentos inolvidables en nuestro pequeño laboratorio. Siempre os recodare con cariño.

A nuestros técnicos Manoli, Ester, Fina y a nuestra más preciada secretaria Marta Fajes, ¡qué haríamos sin vosotras!

A los de mitocondrias, el Dr. Patricio Fernández, la Dra. Ester López, la Dra. Nuria Garrido y la Dra. Pilar Bayona. Gracias por ayudar a resolver mis dudas científicas sobre mitocondrias y sobre la ciencia en general.

A las chicas del servicio de microscopia electrónica de la Facultad de Medicina, Concepción Junqueras, Rosa Bueno y María José Marín. Gracias por enseñarme tanto y apoyarme con mis investigaciones. Sois unas grandes mujeres y profesionales.

To my Promontory co-workers, Matthew Price, Dr. Tyler Ames, Dr. Cristina Yim, Robert Fallon, Marie Congenie and Dr. Jose Jimeno. Thank you for all your support and for offering the opportunity to move to New York City. You definitely have changed my scientific career for the best.

Thanks to Dr. Lorenzo Galluzzi, that I truly admire and respect. You are source of inspiration and an example to me, thank you for allowing me to be part of your lab. Also, to Dr. Aitzibier Buqué, and all the former and current members of Galluzzi Lab that composed or compose this amazing crew of crazy scientists. Dr. Claudia Galassi, Ai Sato, Dr. Norma Bloy, Cristina Ibiarren, Nina Boeck, Dr. Peter Holiček, Dr. Takahiro Yamazaki. To the students Giovanni Manara, Millie Nathanson and Flavie Naulin. With a special mention to Dr. Emma Guilbaud who has been my closest mentor in a lot of aspects and my *camarade* of scientific discussions. It is always nice to found people as passionate for science as you are. You have a brilliant scientific career ahead. Merci, et que le pouvoir de la mitochondrie t'accompagne!

Ginevra Campia, la mia piccola Gini. I do not have enough words to explain how important your support was, especially at the beginning of my adventure in New York city. You have been like my little sis, my confident and the one that made me laugh in my darkest moments. I will always remember you!

And also, other members of the Radiation Oncology department at Weill Cornell Medicine: Dr. Maud Charpentier and my Argentinian girls Dr. Mara De Martino and Dr. Cecilia Lira. You are amazing woman and scientists. Thank you for your support and kindness. Also, I would like to thank Jeffrey Kraynak, always ready to help!

To my next-door neighbors of the 32-02 34th Ave Joe Feldman and Emily Owens and Alicia What can I say? You are live savers! I am happy I have encountered you during this adventure.

Also, to acknowledge Marcus Rutter. This last year would not have been possible without your support. Thank you for helping me during my move to NYC. ¡Gracias por todo!

A David Clemente, la persona que me ha visto evolucionar a lo largo de estos 7 años. Parece mentira todo lo que ha sucedido desde que me mude a ese piso de calle Tarragona y trabajaba en las cocinas de aquel restaurante *Morroputa*. Qué tiempos aquellos y todo lo que he podido aprender... ¡Gracias Dav!

Así mismo, agradecer a otros colaboradores como José Enríquez, Raquel Martínez y Raquel Justo del Centro Carlos III en Madrid. ¡Me abristeis las puertas de vuestra casa y me tratasteis estupendamente!

Finalmente, agradecer a la Asociación Española Contra el Cáncer por apoyar financieramente este trabajo. Gracias a todo el equipo de la sede de Zaragoza, en especial al Patxi López y Juan Antonio Pérez. Gracias de corazón. Sin esta ayuda esto no podría haber salido adelante. Habéis hecho realidad mi sueño de ser Doctora.

Pues para que veáis el apoyo de cuánta gente se ha necesitado para que esto suceda. Y es que como dijo Guido Kroemer una vez: *"Science is always a collective adventure"*.

A mi mayor Tesoro,

Mi madre

ABSTRACT/RESUMEN

“Believe there are no limits but the sky”

-Miguel de Cervantes-

RESUMEN

PT-112 es una nueva molécula de uso quimioterapéutico que presenta una estructura de platino conjugada con un pirofosfato, la cual se ha demostrado que tiene baja afinidad de unión al ADN comparado con otros análogos de platino. En la actualidad, PT-112 se encuentra en desarrollo clínico de fase 2 y se ha demostrado su actividad en pacientes diagnosticados con tumores sólidos que se encuentran en enfermedad avanzada, incluyendo el cáncer de próstata metastásico resistente a la castración. Estudios previos apuntan a que PT-112 inhibe la biogénesis ribosómica e induce muerte celular inmunogénica, la cual culmina en una respuesta inmune antitumoral. La capacidad de PT-112 de estimular el sistema inmunitario fue en parte descubierta por experimentos realizados con ratones inmunocompetentes que demostraron que la vacuna preparada a partir de un extracto de células previamente expuestas a PT-112 permite generar protección inmunológica frente al desarrollo de tumores inoculados con células del mismo tipo. En ese mismo estudio también se reportó que PT-112 es capaz de establecer sinergia con los inhibidores de puntos de control inmunológicos anti-PD-1 o anti-PD-L1, lo que permite controlar el crecimiento de tumores inoculados en huéspedes inmunológicamente competentes. De acuerdo con dichos antecedentes, el objetivo la presente investigación es ampliar el estudio del mecanismo de acción de PT-112 así como tratar de elucidar los mecanismos que subyacen a la muerte inmunogénica inducida por este compuesto.

En este trabajo se ha podido demostrar que PT-112 sensibiliza preferentemente a las células de cáncer que presentan disfunciones mitocondriales y que, además, presenta selectividad tanto citostática como citotóxica por células humanas de cáncer próstata, sin afectar significativamente a la línea sana de próstata RWPE-1, a las concentraciones ensayadas. Así mismo, se ha demostrado que, en la mayor parte de las células tumorales ensayadas, PT-112 induce muerte celular a través de la vía apoptótica mitocondrial mediada por la oligomerización de BAK1 y BAX y la activación de caspasa-3. Además, la muerte celular inducida por PT-112 está asociada con fenómenos de estrés mitocondrial como la producción de especies reactivas de oxígeno, cambios en el potencial de membrana mitocondrial, alteración en la capacidad respiratoria, reorganización del sistema de supercomplejos respiratorios asociados al complejo III, así como cambios en la morfología del organelo.

En este trabajo se ha validado también la capacidad de PT-112 de inducir muerte celular inmunogénica en modelos celulares no ensayados anteriormente. Concretamente, se ha podido demostrar

que PT-112 induce un aumento en la liberación de ATP, en la exposición de calreticulina, en la secreción de HMGB1 y de IFN tipo I, esta última precedida por un aumento en el ADN de doble hebra citosólico. Además, se ha demostrado que la acumulación de este ADN en el citosol es parcialmente dependiente de las proteínas pro-apoptóticas BAK1 y BAX. Finalmente, se ha demostrado que PT-112 podría tener la capacidad de modular la actividad de las células presentadoras de antígeno de acuerdo con el aumento en la expresión del MHC de clase I en la superficie de las células cancerosas observado. En conjunto, los datos obtenidos en este trabajo proporcionan información adicional sobre el estrés mitocondrial y las vías relacionadas con muerte celular inmunogénica en respuesta al PT-112, las cuales podrían tener futuras aplicaciones clínicas.

ABSTRACT

PT-112 is a novel pyrophosphate-platinum conjugate with low DNA-binding affinity compared to other platinum analogs. PT-112 is currently under phase 2 clinical development and its activity in advanced pretreated solid tumors, including in metastatic castration-resistant prostate cancer (mCRPC), has been demonstrated. In previous studies, PT-112 has been shown to cause ribosomal biogenesis inhibition followed by immunogenic cell death (ICD), culminating in anticancer immunity. In line with this, immunocompetent mice vaccinated with cancer cells previously exposed *in vitro* to PT-112, efficiently protected it from challenge with living cancer cells of the same type. Additionally, it has been observed that PT-112 synergizes with PD-1 or PD-L1 blockade controlling mouse tumors that were developed in immunologically competent hosts. Thus, according with what has been previously observed, the aim of this research is to extent the study of PT-112's mechanism of action and to elucidate the underlying mechanisms of PT-112-induced ICD.

During this work it has been demonstrated that PT-112 further sensitizes cancer cells with mitochondrial dysfunctions and exhibits cancer cell selectivity by inhibiting cell growth and leading to cell death of prostate cancer cells without affecting non-tumorigenic epithelial prostate cell line RWPE-1 at the concentrations tested. PT-112 also triggers BAK1 and BAX oligomerization-mediated mitochondrial apoptosis, and caspase-3 activation, that is preceded by several events indicating mitochondria stress including mitochondrial ROS generation, compromised organelle membrane integrity, altered respiration capacity, reorganization of the complex-III containing respiratory supercomplexes as well as morphological changes in the organelle. Furthermore, it has been validated PT-112's ability to induce ICD in other cancer cell models never tested before. PT-112's capacity to induce ICD was demonstrated by an increase in ATP release, calreticulin exposure, HMGB1 and type I IFN secretion, preceded by an increase of the cytosolic dsDNA molecules which accumulation was demonstrated to be partially dependent on the pro-apoptotic proteins BAK1 and BAX. Moreover, it has been demonstrated that PT-112 display the capacity to modulate the activity of the professional antigenic presenting cells (DCs) by increasing the expression of MHC class I molecules on the surface of cancer cells. Altogether, the data obtained in this work provide additional insight into mitochondrial stress and ICD-relevant pathways in response to PT-112 which could have future relevant clinical applications.

ABBREVIATIONS

A	**ABB,** annexin binding buffer
	ACD, accidental dell death
	AIF, apoptosis-inducing factor
	ALP, alcaline phosphatase
	ANXA, annexin
	Apaf 1, apoptotic protease activating factor 1
	APCs, antigen presentation cells
	Apo2L/TRAIL, TNF-related apoptosis-Inducing ligand
	AR, androgenic receptor
	AR, androgenic receptor
	ATP, adenosine triphosphate
B	**BCA,** bicinchoninic acid assay
	BCL2, B-cell leukemia/lymphoma 2 gene
	BH, bcl-2 homology
C	**CAR**, chimeric antigen receptor
	CASP, caspase
	cFLIP, cellular FLICE Inhibitory Protein
	CoQ, coenzyme Q
	CRPC, castration-resistant prostate cancer
	CALR, calreticulin
	CTCs, circulating tumor cells
	CTL, cytotoxic lymphocytes
	CXCL10, C-X-C motif chemokine ligand 10
	CXCR3, CXC-chemokine receptor 3
D	**DAMPs**, danger associated molecular patterns
	DAMPs, danger-associated molecular patterns
	DAPI, 4′,6-diamidino-2-phenylindole
	dATP, deoxyadenosine triphosphate
	DCA, dichloroacetate
	DcR, decoy receptor
	DCs, dendritic cells
	DD, death domain
	DED, death effector domain
	DISC, death-inducing signaling complex
	DMSO, dimethyl sulfoxide
	DR, death receptor

dsDNA, double-stranded DNA
DTCs, disseminated tumor cells

E

ELISA, enzyme-linked immunosorbent assay
EMT, epithelial-mesenchymal transition
ER, endoplasmic reticulum
ETC, electron transport chain

F

FADD, Fas-associated death domain
FBS, fetal bovine serum
FDA, food, and drugs administration
FPR, formyl peptide receptor
FPPS, farnesyl pyrophosphate synthase

G

GLOBOCAN, global cancer observatory
GSDM D, gasdermin D
GSDM, gasdermin
GZMB, granzyme

H

HLA-I, human leukocyte antigen I
HMGB1, non-histone chromatin-binding protein high-mobility group box 1
HR, hormone receptor

I

IAPs, inhibitor of apoptotic proteins
ICD, immunogenic cell death
IDH, isocitrate dehydrogenase
IFN, interferon
IFNAR1; interferon α/β-receptor subunit 1
Ig, immunoglobulin
IL, interleukin
IM, inner membrane
IRF, interferon regulatory factor
IRF9, interferon regulatory factor 9
ISGF3, interferon-stimulated gene factor 3
ISGs, interferon-stimulated genes

J

JAK1, janus kinase 1

L

LC3, microtubule-associated protein 1A/1B-light chain
LRP1, LDL receptor related protein 1

M

MCL1, myeloid cell leukemia 1
mCRPC, metastatic castration-resistant prostate cancer
MET, mesenchymal-epithelial transition
mETC, mitochondrial electron transport chain
MHC-I, major histocompatibility complex-I

MICs, metastasis-initiating cells
MOA, mechanism of action
MOMP, mitochondrial outer membrane permeabilization
MPT, mitochondrial permeability transition
mtDNA, mitochondrial DNA
mtROS, mitochondrial reactive oxygen species
MTT, dimetil-tiazolil-difeniltetrazolium bromide

N

NF-KB, nuclear factor- KB
NK, natural killer
NLPR3, NLR family pyrin domain-containing 3
NLR, nucleotide-binding domain and leucine-rich repeat-containing

O

OM, outer membrane
OXPHOS, oxidative phosphorylation

P2RX7, purinergic receptor P2X7

P2RY2, purinergic receptor P2Y2

PARP1, polyadenine diphosphate ribose polymerase
PBS, Phosphate Buffered Saline
PGE_2, prostaglandin E_2
PI, propidium iodide

PINK1, PTEN-induced kinase 1
PRRs, pattern recognition receptors
PS, phosphatidylserine
PSA, prostatic specific antigen
PSMA, prostate specific membrane-antigen
PTEN, phosphatase tensin homolog
PVDF, polyvinylidene difluoride

R

RCD, regulated cell death
RIPK3, necroptotic kinase receptor-interacting serine-threonine kinase 3
RNS, reactive nitrogen species
ROS, reactive oxygen species
RT, radiation therapy

S

SDS, sodium dodecyl sulphate
SMAC/DIABLO, second mitochondrial activator of caspases/ direct IAP-binding protein with low pI
SNP, single nucleotide polymorphism

SOD, superoxide dismutase
STING, stimulator of interferon genes

STING1, stimulator of interferon genes 1

T

TCA, tricarboxylic acid

TEMED, N, N, N, N'-tetrametiletilendiamine

TLRs, toll-like receptors

TME, mesenchymal-epithelial transition

TME, tumor microenvironment

TNF, tumor necrosis factor

TNFR1, tumor necrosis factor receptor 1

TNF-α, Tumor Necrosis Factor- α

TYK2, tyrosine kinase 2

V **VEGF,** vascular endothelial growth factor

W **WHO**, World Health Organization

X **XIAP,** X-linked inhibitor of apoptotic protein

Z **Z-VAD-fmk,** benciloxicarbonil-Val-Ala-DL-Asp-fluorometilceton

γδ T cells, gamma delta T cells

$\Delta\psi_m$, mitocondrial membrane potential

7-AAD, 7-aminoactinomycin D

Table of Contents

1. Introduction 1

1.1 Cancer: general concepts, incidence, and mortality 1

1.1.1 Tumoral transformation- early stages of tumor development 2

1.1.2 Metastasis 3

1.1.2.1 Factors priming metastasis 4

1.2 Hallmarks of cancer 5

1.3 Cell death 7

1.3.1 Regulated cell death 7

1.3.1.1 Apoptosis 8

1.3.1.1.1 Intrinsic or mitochondrial apoptotic pathway 10

1.3.1.1.2 Extrinsic apoptotic pathway 12

1.3.1.1.2 BCL2 family of pro- and anti-apoptotic proteins 14

1.3.1.2 Necroptosis 17

1.3.1.3 Pyroptosis 19

1.3.1.4 Others forms of regulated cell death 20

1.3.1.5 Accidental cell death (ACD) 20

1.4 Immune system 21

1.4.1 Basic concepts 21

1.4.1.1 Innate immune system 22

1.4.1.2 Adaptive immune system 23

1.4.2 The immune system in cancer 23

1.4.2.1 Immunosurveillance 23

1.4.2.2 Cancer immunoediting 24

1.4.3 Cancer immunotherapy 25

1.5 Immunogenic cell death 26

1.5.1 Definition and its implication in cancer 26

1.5.2 Calreticulin 28

1.5.3 Extracellular ATP 30

1.5.4 HMGB1 release 30

1.5.5 Annexin A1 32

1.5.6 Type I IFN signaling 32

1.5.7 Implication of autophagy in cancer and ICD 36

1.5.8 Immunogenic cell death inducers 38
1.6 Cancer metabolism 38
1.6.1 Alterations in glucose metabolism -The Warburg effect 38
1.7 Mitochondria and cancer 43
1.7.1 Characteristics and functions of mitochondria 43
1.7.2 Mitochondrial dynamics 44
1.7.3 The mitochondrial electron transport chain (mETC) and the oxidative phosphorylation system (OXPHOS) 46
1.7.3.1 Composition, organization, and dynamics of the mECT 46
1.7.4 Role of mitochondrial in cancer 48
1.7.4.1 Implications of mitochondrial DNA mutations 49
1.8 Mitochondrial role in ICD 51
1.8.1 Cytosolic dsDNA sensor: the CGAS/STING1 pathway 53
1.8.2 Specific autophagy: mitophagy 55
1.9 The L929/L929dt mouse model 57
1.9.1 *In vitro* and *in vivo* characterization of a new L929-derived cell line 57
1.9.2 Transmitochondrial cybrid generation between L929 and L929dt cells 58
1.10 Prostate cancer 60
1.10.1 Basic concepts of the disease 60
1.10.2 Molecular basis of prostate cancer 62
1.10.3 Castration-resistant prostate cancer (CRPC) and metastatic castration-resistant prostate cancer (mCRPC) 63
1.10.3.1 Current therapies 64
1.10.4 Prostate cancer metabolism 65
1.10.5 mtDNA mutations in prostate cancer 68
1.11 Breast cancer 68
1.11.1 Breast cancer classification 69
1.11.2 Molecular bases of breast cancer 70
1.11.3 Current therapies 71
1.12 Platinum-based chemotherapy 72
1.12.1 Origin and use for cancer therapy 72
1.12.2 New generation of platinum agents 73
1.12.3 Mechanism of action (MOA) of platinum drugs 73
1.12.4 PT-112, a next generation platinum agent 76

2. Background and objectives 80
3. Experimental procedures 83
3.1 Cell culture 83
3.2 CRISPR/Cas9 genetic edition 83
3.3 Cell viability assays 84
3.4 Cytotoxicity assays and cell death quantification 84
3.5 Clonogenic assays 85
3.6 ROS production, mitochondrial membrane potential and mitochondrial mass measurement by flow cytometry 85
3.7 Apoptosis and necroptosis inhibition assays 85
3.8 Analysis of CASP3 activation 85
3.9 Autophagosome formation measurement 86
3.10 MHC-I and CALR surface expression 86
3.11 Protein extraction and immunoblot analysis 86
3.12 Coenzyme Q quantification 87
3.13 Cell morphology assessments 88
3.14 OXPHOS performance and metabolism measurements 88
3.15 Mitochondria purification (for Blue Native analysis) 89
3.16 Blue Native electrophoresis and immunoblot analysis 89
3.17 Enzymatic activity analysis of respiratory complexes 90
3.18 Transmission electron microscopy 90
3.19 DAMP emission 91
3.20 Immunofluorescence microscopy 91
3.21 Statistical analysis and data processing 91
4.CHAPTER I: Mitochondrial effects on the murine model 93
5.CHAPTER II: Mitochondrial effects on human prostate cancer cells 108
6.CHAPTER III: Mitochondrial implications on ICD 157
7.General discussion 175
8.1 Conclusions 182
8.2 Conclusiones 183
9.Bibliography 184

INTRODUCTION

“Knowledge is power”

-Sir Francis Bacon-

1. Introduction

1.1 Cancer: general concepts, incidence, and mortality

Cancer is a large group of diseases that are characterized by the uncontrolled division and growth of cells from a specific tissue, leading eventually to the invasion of adjoining parts of the body, spreading to other organs and colonizing other tissues (NIH, 2021).

Although to date we still not have the *so-called* cure for cancer and the prevalence appears to be high in numbers (19.3 million new cases reported in 2021) (Sung et al., 2021), during the last decades of clinical trials and basic research, researchers have managed to develop new therapeutical strategies that were able to increase the quality of life and the overall survival of cancer patients (NIH, 2024b). Indeed, discoveries such the ones made by M.D. Bert Vogelstein and his team in the 90's were of special relevance in the history of cancer research. Professor Vogelstein was the pioneer in discovering the causes of the tumoral transformation, providing an accurate description of its origin and the principles governing its pathogenesis (Vogelstein & Kinzler, 1993).

The term *cancer* was first described near the year 1600 B.C. in the antique Egypt. Later, Hippocrates (460-370 B.C.) considered the "Father of Medicine" was the first one to use the term *karkinoma* to refer to it. However, it was not until the emergence of the Roman empire that this term was latinized and transformed to the word *cancer,* as we currently know it (NIH, 2024c).

According to the most recent statistics provided by the World Health Organization (WHO) (WHO, 2024), cancer is the second leading cause of death globally, with an estimated average of 9.9 million of deaths per year. Going deeper into the statistics, the Global Cancer Observatory (GLOBACAN) (Sung et al., 2021) points to breast cancer as the cancer type with highest rate worldwide (see figure 1). Moreover, lung, prostate, colorectal, stomach and liver cancer are the most common types of cancer in men while breast, colorectal, lung, cervical and thyroid cancer are the most common among women. Regarding the mortality rates, the data that we currently hold indicate that lung cancer is the one that causes more deaths per year in both sexes, followed by breast cancer which is also the deadliest type of cancer in women (for more information see section 1.11).

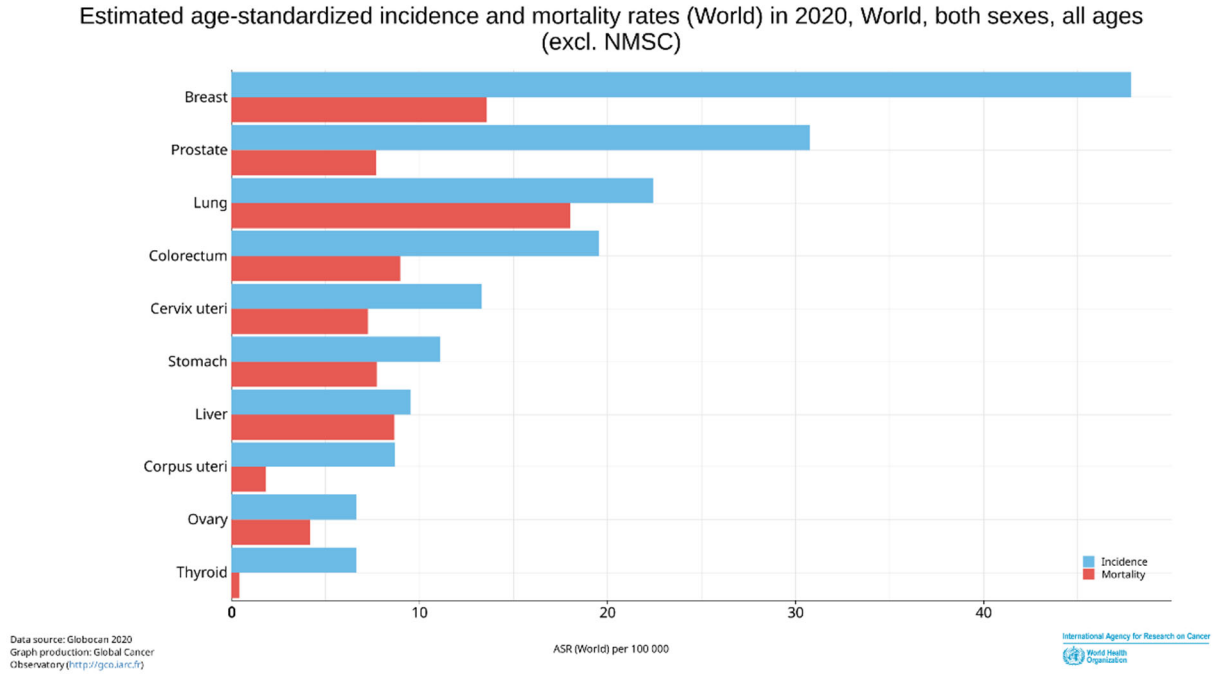

Figure 1. Graph bar provided by the International Agency for Research of Cancer, representing the estimate age-standardized worldwide incidence and mortality rates in 2020 for both sexes and all ages. Blue bars represents the incidence and red bars the mortality (Observatory, 2024).

1.1.1 Tumoral transformation- early stages of tumor development

Tumoral transformation can have multiple causes and be aggravated by external factors such as tobacco and alcohol consumption, unhealthy diet, exposure to ionizing sources, physical inactivity, infections, among others. All of these factors are well known for favoring the apparition of DNA mutations, compromising the genome stability of normal cells (Sung et al., 2021). The accumulation of several mutations can eventually lead to the cells to multiply, disorganize and transform into a malignant version that over the time will contribute to a tumor mass formation (Vogelstein & Kinzler, 1993). In essence, cancer debuts with the transformation of a normal cell into a tumor cell with the ability to escape apoptosis signaling (see section 1.3.1.1). If the immune system does not respond against this primary tumor, it will have the opportunity to keep growing and dividing without regulation. It is important to note that the process by which the immune system controls the emergence of tumors is referred as **cancer immunosurveillance** (Zitvogel et al., 2006), and it will be discussed later in section 1.4.2.1.

In general, most tumor cells acquire resistance to death mechanisms that the immune system uses to maintain the cellular homeostasis. Indeed, the main mechanism that regulates the apoptotic signaling is mainly caused by genetic abnormalities that encode the P53 protein (Junttila & Evan, 2009). However, this

explanation seems to be very simplistic, since a large number of factors that are directly related to the oncogenesis process have been described over the recent years (D. Hanahan & Robert A. Weinberg, 2011). These factors are known as **hallmarks of cancer**, and they will be also introduced in section 1.2 of this work.

1.1.2 Metastasis

Metastasis is the ultimate and most lethal manifestation of cancer which is characterized by the growth of cells in organs distant from the one where it initially originated. In fact, the vast majority of cancer patients die as a consequence of their metastatic disease and not because of their primary tumors (Gerstberger et al., 2023). During this process, the future metastatic cancer cells progressively acquire the capacity to invade the mucosa and reach the lymph nodes and blood vessels that can act as a *hallway* for cancer cells (in this stage also known as a **circulating tumor cells** (CTCs)) and allows them to freely travel through the body and attain other tissues. However, this process is not abrupt but gradual, and it can take from days to months or even years. In consequence, cancer cells need to develop different strategies in order to survive in transit, to adapt to the environmental changes, as well as to evade the immune system antitumor activity (Quail & Joyce, 2013).

The studies dedicated to understanding this complex succession of events, referred as **metastatic cascade** (Lambert et al., 2017; Massagué & Ganesh, 2021), have made it possible to differentiate three different phases of this process that can overlap in time: **dissemination**, **dormancy**, and **colonization** (Gerstberger et al., 2023) (see **figure 2**).

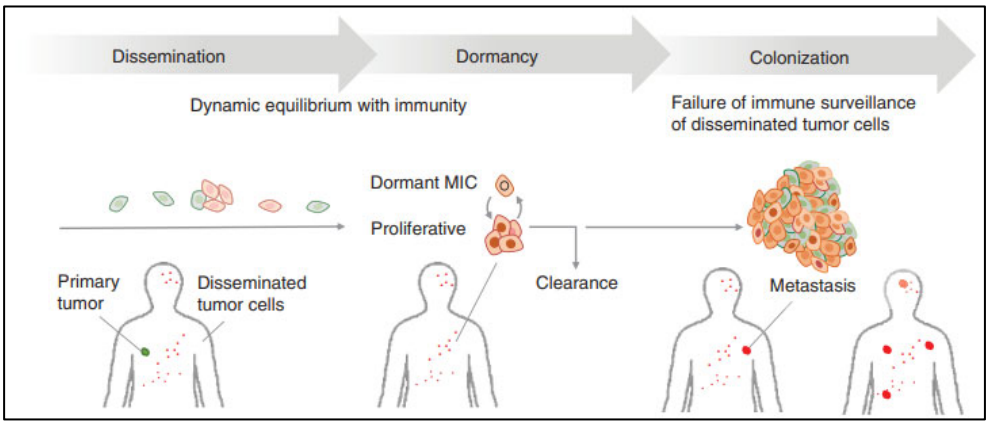

Figure 2. Schematic representation of different stages of the metastatic process. Modified from (Massagué & Ganesh, 2021).

The ignition point begins when cells from a primary tumor acquire the ability to undergo migration. This step is often stimulated by a multiplicity of factors that are associated, but not only, with the **tumor microenvironment** (TME).

In brief, the early form of metastatic cells is known as **metastasis-initiating cells** (MICs) and are originated from the primary tumor. In this stage, cells acquire the ability to penetrate the blood vessels (**intravasation**) and freely circulate through the bloodstream. During this step those cells adopt the name of **circulating tumor cells** (CTCs). This process is known as **epithelial-mesenchymal transition** (EMT). During this event, most of the CTCs will not be able to survive to the physical, redox, and immune stressors and thus, they are cleared from the bloodstream system. However, a small but significant part of the CTCs will be able to adapt in the absence of a niche-specific-growth factors, abandon the blood vessels (**extravasation**) and migrate into organ parenchyma. This reverse step is known as **mesenchymal-epithelial transition** (MET).

Afterwards, **disseminated tumor cells** (DTCs) would encounter the necessity to adapt to the new environment and some remain in a dormancy stage (now known as **dormant MIC**). However, at some stage of the process, these cells can exit the dormancy and start actively dividing and ultimately forming a clinical detectable metastasis (see **figure 3**) (Gerstberger et al., 2023).

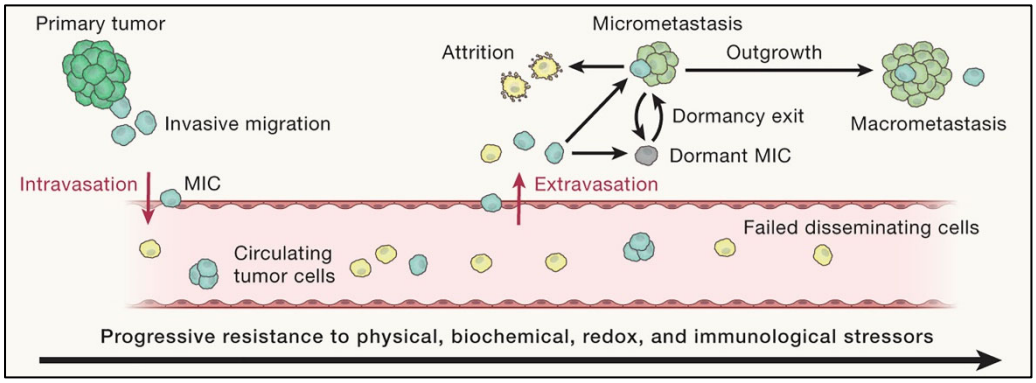

Figure 3. Stages of metastasis - the metastatic cascade. Modified from (Gerstberger et al., 2023).

1.1.2.1 Factors priming metastasis

As previously mentioned, the emergence of metastasis is a complex and intricate process that requires several numbers of traits for it to occur. Most of these features are the result of genetic mutations that the tumor cells have acquired in the primary site (Samuel F. Bakhoum et al., 2018). Accordingly, most

of the cells originated in the primary lesion are exposed to a major evolutionary bottleneck and are unable to survive. Indeed, only a few portions of cells that develop metastatic-specific traits will be positively selected and able to endure. Generally, the main factors that have been identified priming metastasis are: **epigenetic factors** (e.g., aging, and circadian rhythm disruptions (Kaur et al., 2019; Masri & Sassone-Corsi, 2018)), **adhesive signals from the extracellular matrix components** (e.g., collagen, fibrin (Kai et al., 2019)) **extracellular mechanical pressures** (e.g., tension and compression (Follain et al., 2018)), **cell-cell interactions**, **soluble signals** (e.g., growth factors and cytokines (Coffelt et al., 2015)) and the **intratumoral microbiota** (Helmink et al., 2019) (Fares et al., 2020).

1.2 Hallmarks of cancer

Several characteristics have been identified as common markers of tumor cells (Hanahan, 2022; D. Hanahan & Robert A. Weinberg, 2011). Those considered of major relevance are described thereafter:

- **Dysregulation in cell growth**: Cancer cells are able to produce their own growth factors that stimulate their own cell surface receptors by an autocrine-dependent secretion. This characteristic let tumor cells the ability to autonomously control their growing rate even in absence of external stimulation. Also, but not only, cancer cells can increase the number of receptors anchored on their membrane, resulting in an intensification of the signaling pathway activation. Moreover, cancer cells are also able to internally activate intracellular pathways in absence of its ligand stimulator.

- **Apoptosis evasion**: The evasion of the apoptotic stimuli it is a very well-known characteristic of cancer cells (Evan & Littlewood, 1998). In fact, tumor cells are able to develop apoptosis resistance by hijacking the mechanisms that regulate this process. Some of those strategies implies overexpressing anti-apoptotic proteins such as BCLXL, BCL2 or MCL1, or blocking the expression of proteins that prime apoptosis such as BAX, BIM or PUMA, between others, cancer cells can also *short circuit* the signaling pathways that are regulated by death ligands such as Fas and TRAIL (Fulda, 2009). All the details related to the regulation of this pathway are explained in section 1.3.1.1.2.1.

- **Unlimited replicative potential**: Different to normal cells, tumor cells have no limits for division. This is due, in part, to the reacquisition of the **telomerase**, the enzyme that protects chromosomes from the reduction of their telomeres during the replicative process and thus preventing tumor cells from entering into a senescence stage (Blasco, 2005).

- **Prolonged angiogenesis**: Like any organ, tumors need oxygen and nutrient supply from the bloodstream system. Tumor cells are able to locally stimulate the formation of new blood vessels by releasing pro-angiogenic growth factors (e.g., VEGF or TSP-1) in the tumor microenvironment. This increases tumor irrigation necessary for sustaining cell growth and division (Ferrara & Kerbel, 2005).

- **Inactivation of tumor suppressor genes**: Frequently, tumor cells can acquire specific mutations in tumor suppressor genes that are in charge of controlling cell cycle and apoptosis. Consequently, any type of mutation affecting their transcription and functionality would eventually promote tumor development. Accordingly, the most notorious tumor suppressor gene is *p53* which is also referred as "the guardian of the genome" (Donehower et al., 1992; Finlay et al., 1989; Nigro et al., 1989).

- **Gain of activity of proto-oncogenes**: Proto-oncogenes are genes that under normal conditions encode for proteins that are responsible of cell growth regulation. However, the acquisition of critical mutations in those genes can promote the transcription of pathological version of those proteins, causing cell growth dysregulation. The aberrant version of those genes are known as **oncogenes** (Thomas et al., 2007).

- **Remodeling of energy metabolism**: Neoplastic transformation is often associated with rewriting cancer cell metabolic pathways. This process permits cancer cells to control and adapt the nutrient supply according with their energy demands. For instance, remodeling of glucose metabolism, also known as a **Warburg effect**, is one of the most well-known metabolic changes found in cancer cells (Vander Heiden et al., 2009; Otto Warburg, 1956) that will be fully detailed in section 1.6.1.

- **Evasion of the immune response**: Among all the strategies put in place by cancer cells to evade the immune response, the most relevant is the expression of immunomodulatory molecules (immune checkpoints) used by the immune system to control antitumor responses. For example, PD-L1 and PD-L2 cell surface expression on tumor cells inactivates immune cell effectors by PD1 ligation and thus, protects cancer cells from their attack (Sharma & Allison, 2015). On the other hand, cells can also slip past of the immune system by decreasing the expression of antigen presentation cell surface molecules such as HLA-I (MHC-I in mice) (Garrido et al., 2010), necessary for the antigen recognition and correct activation of $CD8^+$ cytotoxic T lymphocytes (see section 1.4).

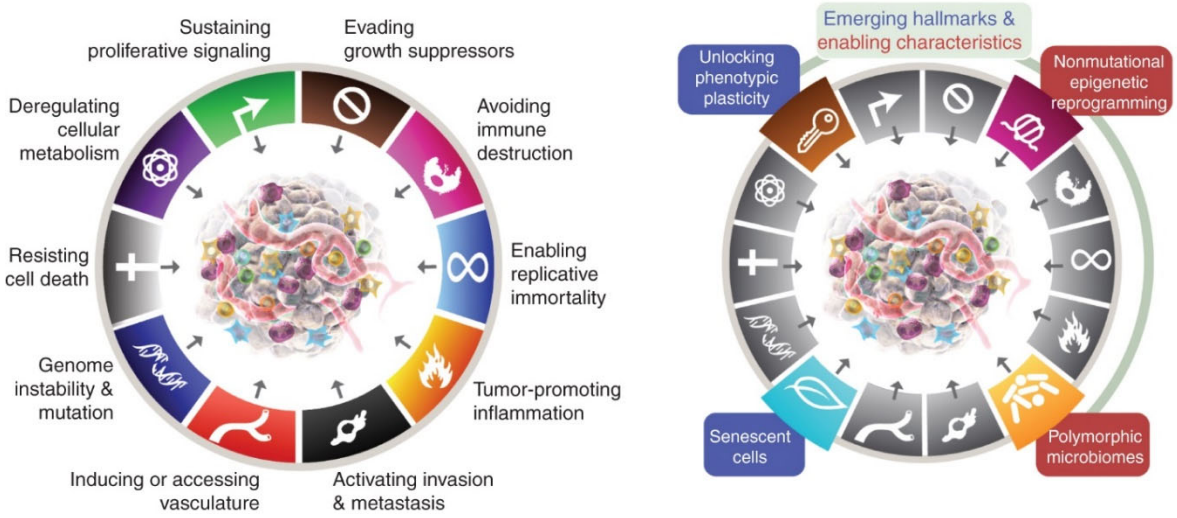

Figure 5. Hallmarks of cancer (Hanahan, 2022).

1.3 Cell death

1.3.1 Regulated cell death

Regulated cell death (RCD) is the form of cell death activated when cells are under stressful conditions and it is controlled by a genetic machinery that results from one or more signal transduction modules, meaning that it can be regulated by genetic or pharmacological ways (L. Galluzzi et al., 2018)

When cells are stressed, they attempt to survive by activating cellular mechanisms that facilitates their adaption to the environmental changes. A few examples of these mechanisms are the DNA damage response pathway or the activation of the autophagy machinery (see section 1.5.7). However, if the cells

cannot cope with that stress, they are provided with genetic mechanisms that can be activated and will determine their fate (Newton et al., 2024). In some cases, cells can also enter in a stage of **senescence** (i.e., cellular stage of irreversible loss of proliferative potential associated with specific morphological and biochemical features). The other alternative will be the activation of one of the regulated cell death types. For instance, **apoptosis**, **necroptosis**, **pyroptosis**, **anoikis** and **ferroptosis** are some of the cell death types included in the last update in the classification of RCD (Lorenzo Galluzzi Ilio Vitale, et al., 2018), and certain of them will be explained in the following paragraphs of this section.

Contrary, in cases when cell death is not preceded by and attempt of stress adaptation that it is classified as **accidental dell death** (ACD) that will be briefly described in section 1.3.1.5.

1.3.1.1 Apoptosis

Apoptosis is a form of RCD characteristic of the eukaryotic organisms participating in the regulation of development, growth, and homeostasis. The main function of apoptosis in adults is the elimination of excessively damaged and potentially harmful cells (e.g., cancer cells or cells infected with pathogens) (Vitale et al., 2023). However, this process also participates during embryonic and post-embryonic development contributing to morphogenesis (e.g., finger separation) (Ke et al., 2018; Newton et al., 2024). Apoptosis is also involved in key events to preserve the health of the individual. For instance, it participates in the negative selection of autoreactive immune cell lines during hematopoiesis as well as the maintenance of the effector function of **cytotoxic lymphocytes** (CTLs) and **natural killer** (NK) **cells** (van Parijs et al., 1998). Therefore, alterations in the apoptotic pathway are associated to pathologies such as neurological, cardiovascular, renal, or hepatic disorders, autoimmune diseases as well as hematological malignancies, and solid cancers (Vitale et al., 2023). In most cases of cancer, the apoptotic pathway is either altered or the tumor cell have developed mechanisms to evade the apoptotic stimuli. For example, the overexpression of anti-apoptotic proteins (e.g., BCL2, BCLXL or MCL1) or the loss of the expression of genes encoding pro-apoptotic proteins (e.g., BIM) are the more common alterations of the apoptotic pathway found in cancer cells (Bedoui et al., 2020; Singh et al., 2019).

Apoptosis can be activated through two different pathways: the **extrinsic pathway** (see section 1.3.1.1.2) which is triggered from an external cell signal, and the **intrinsic** one (see section 1.3.1.1.1), that can be triggered from both an internal and external cell stimulus.

Both apoptotic pathways are regulated by caspases, proteins of the protease family that are specifically cleaved after an aspartic acid amino acid residue. Caspases are classified based on the level where they display its activity within the **apoptotic cascade**. For instance, caspase 8 (CASP8) or CASP10 are considered the initiator caspases since they are located upstream of the cascade while CASP3 and CASP7 are assigned as effector caspases due to the fact that they activity is exhibited downstream in the pathway (see **figure 7**).

For the caspase to reach its functional/active form, the non-active form named **procaspase** must be cleaved between specific domains leading to the formation of a heterotetrametric structure (Nicholson, 1999). Caspase activity is regulated by the IAP proteins such as XIAP - that binds to the executioner caspases promoting their degradation - or cFLIP which blocks the activation of initiator CASP8 (Bagnoli et al., 2010).

Apoptosis starts with the condensation of the cytosol and the compaction of the chromatin (pyknosis), forming visible aggregates at the vicinity of the cell membrane. Subsequently, endonucleases digest the DNA into fragments of approximately 180 base pairs long. Simultaneously, the dilation of the endoplasmic reticulum along with a membrane blebbing takes place (see **figure 6**). Finally, the cell is segregated into fragments called **apoptotic bodies** that exposes “eat me” signals in the outer membrane such as **phosphatidylserine** (PS) that will be recognized by macrophages which will end up phagocyting the apoptotic cell. The phagocytosis of the dying cells (also known as **efferocytosis**) also prevents the release of cellular DAMPs but the release of immunosuppressors that maintains an immunosilent environment (Chen et al., 2001; Gao et al., 1998; Sisirak et al., 2016). The outcome of this process is a “clean” and “silent” cell death that typically does not initiate an inflammatory process (Elmore, 2007).

Even so, the attribution of apoptosis as a poorly immunogenic event has been a matter of debate. Indeed, for many years apoptosis has been attribute as an event with low capacity to stimulate the immune system. However, several works have shown that apoptosis can also engage immune responses (Blachère et al., 2005; Guermonprez et al., 2002).

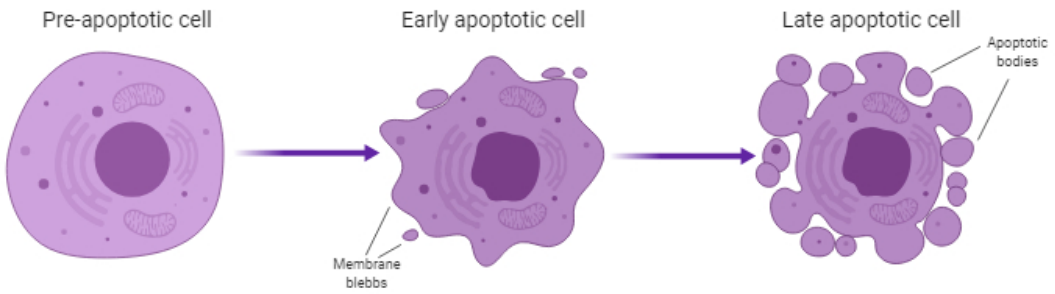

Figure 6. Progression of the cell morphology during apoptosis. Image created with BioRender®.

1.3.1.1.1 Intrinsic or mitochondrial apoptotic pathway

The intrinsic pathway of apoptosis is the most conserved pathway in evolutionary terms, also known as the mitochondrial apoptotic pathway since the main spot of regulation is the mitochondria. It is an autonomous cell death, specific to the cell, and activated in response to certain internal or external stimuli such as absence of growing factors, ionizing radiation, oxidative stress, DNA damage, microtubular alterations, among others (Vitale et al., 2023).

For this modality to be triggered, it is needed the activation of the pro-apoptotic proteins of the BCL2 family (BAX, BAK and BOK) with capacity to dimerize and create a pore in the outer mitochondrial membrane (MOMP), causing the release of the apoptogenic factor cytochrome c and SMAC (second mitochondrial activator of caspases, also known as DIABLO) into the cytosol. This event is known to be accompanied by the dismantling of the **mitochondrial electron transport chain** (mETC) and drop of the mitochondrial membrane potential (ΔΨm). Afterwards, the cytochrome c in the cytosol interacts with Apaf 1 together with dATP forming the **apoptosome** that recruits and activates CASP9 (Li et al., 1997). Simultaneously, the release of SMAC in the cytosol induces the degradation of members of the IAP family (caspase inhibitors), which preserves functional activated caspases. This cascade of events culminates with the activation of CASP3 by the activity of the CASP9, and the death of the cell (see **figure 7**).

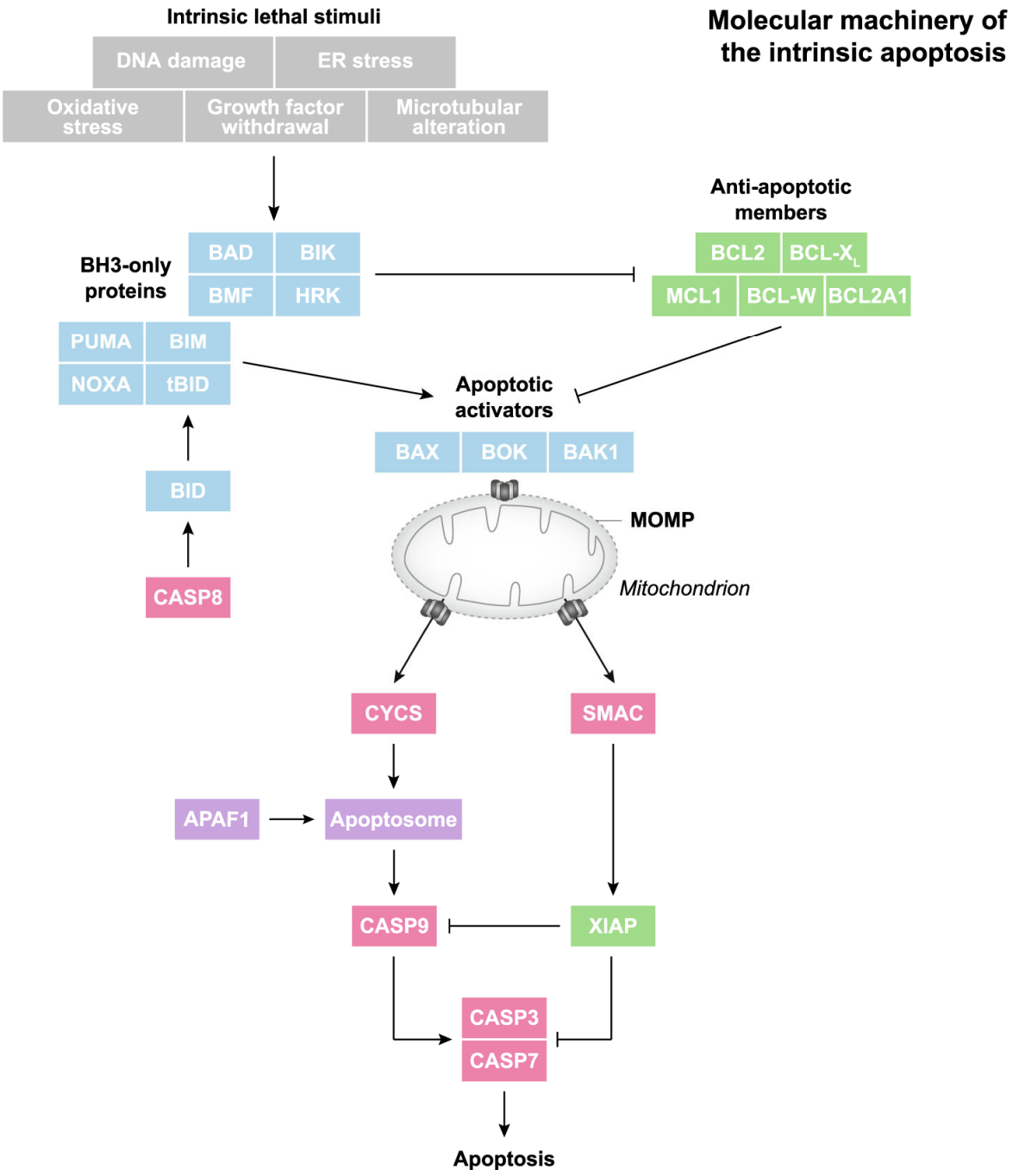

Figure 7. Molecular regulation of the intrinsic apoptotic pathway. Schematic representation of the most relevant proteins involved in the apoptotic cascade and their interactions (Vitale et al., 2023).

1.3.1.1.2 Extrinsic apoptotic pathway

1.3.1.1.2.1 Mediated by death receptors

Different to the mitochondrial pathway, the extrinsic pathway is exclusively triggered by an external stimulus, and it is manly activated by the binding of the death ligands FasL, Apo2L/TRAIL and TNF, to their corresponding transmembrane receptors Fas, DR4/DR5 and TNF-R1, respectively. The death ligand receptors are constituted of an intracellular death domain (DD) that interacts with the DD domain of the adapter protein FADD. Subsequently of its stimulation, the death effector domains (DED) of the FADD protein binds to the DED domains of the pro-caspases 8 and 10. The homotypic interaction between these proteins forms a complex known as DISC that allows the activation of the caspases (Nagata, 1997). Later, the activation of the pro-caspase 8 promotes the cleavage and activation of the CASP3 and CASP7, culminating the process with the death of the cell (see **figure 8**).

Death ligands can be expressed on the cell surface of activated T cells, or they can be stored in the cytoplasm, mainly associated with intraluminal vesicles of multivesicular bodies upon an additional activation. These intraluminal vesicles are secreted in the form of exosomes (Martínez-Lorenzo et al., 1999; Monleón et al., 2001).

1.3.1.1.2.2 Mediated by cytotoxic granules

Apoptosis can also be induced by molecules specifically secreted by the immune system. Indeed, in the cytoplasm of activated CTL and NK cells are stored granules containing cytotoxic proteins such as perforin, granzymes and granulysin with the capacity to activate the apoptotic signal when they are secreted and establish contact with the membrane of the target cell. This process is referred as **granular exocytosis,** and it is exclusive of the immune cells (Keefe et al., 2005; Pardo et al., 2009; Peters et al., 1991).

For this event to happen in CTLs, it is necessary the interaction between the T-cell receptor (TCR) of the $CD8^+$ T cells and the peptide -MHC I complex exposed on the external membrane of the target cell. Simultaneously, the interaction between the LFA-1 integrin from the T-cell with the ICAM-1 integrin of the target cell must occur for a successful activation (Grakoui et al., 1999; Makgoba et al., 1988; Monks et al., 1998; Weiss & Littman, 1994). All these signals promote the reorganization of the cytoskeleton inside of the T lymphocyte that facilitates the fusion of the cytotoxic granules with the plasma membrane and the subsequent release of the granule contact into the immunological synapse (Stinchcombe et al., 2011).

Cell death induced by cytotoxic granules is mediated by the perforin-facilitated entry of granzymes in the cytosol of the target cell (Martínez-Lostao et al., 2015). **Granzyme B** (GZMB) is a serin-protease, active at neutral pH with cleavage specificity at Asp residues, similar to caspases. Early *in vitro* experiments initially demonstrated that GZMB was able to directly cleave and activate CASP3 (Darmon et al., 1995). Experiments performed with whole CTL either using granzyme or caspase inhibitors (Anel et al., 1997) or using CTL from granzyme and/or perforin knockout mice (Pardo et al., 2008; Pardo et al., 2004) demonstrated that perforin/GZMB system was able to induce apoptotic cell death through caspase activation, either directly or through the mitochondrial apoptotic pathway. Regarding granzyme A (GZMA), although it was initially thought to induce caspase-independent (Fan et al., 2003; Pardo et al., 2004), it was later demonstrated that its cytolytic potential was much lower than that of GZMB, especially in the case of the human proteases, and that it was rather implicated in the promotion of inflammation (Metkar et al., 2008). In those studies it was also demonstrated that an additional caspase- and mitochondria-independent non-apoptotic cell death pathway was activated by cytotoxic granules (Pardo et al., 2004). Later on, it was demonstrated that GZMB is able to cleave **gasdermin E** (GSDME), a protein that when cleaved is able to induce membrane pores leading to **pyroptosis** (see section 1.3.1.1.3)(Zhang et al., 2020). Thus, **granzyme A** (GZMA) is also able to induce **gasdermin B** (GSDMB) cleavage and pyroptosis, explaining its less-efficient and caspase-independent cell death ability (Zhou et al., 2020).

1.3.1.1.2.3 Connection between the intrinsic and the extrinsic pathway

Although in this work both extrinsic and intrinsic pathways have been introduced as if they were two unrelated pathways, there exists a connecting point between them through the activation of the BH3-only protein BID that promotes **MOMP** formation (see **figure 8**). In fact, the activation of the initiator CASP8 and 10 from the extrinsic results in the proteolytic cleavage of BID, generating the truncated active form of the protein tBID (Scaffidi et al., 1998). The dependence on the mitochondrial apoptotic pathway when activated the extrinsic apoptotic pathway allow for the classification of cells as **type II**, if they are dependent, or **type I**, if they are independent (Scaffidi et al., 1998).

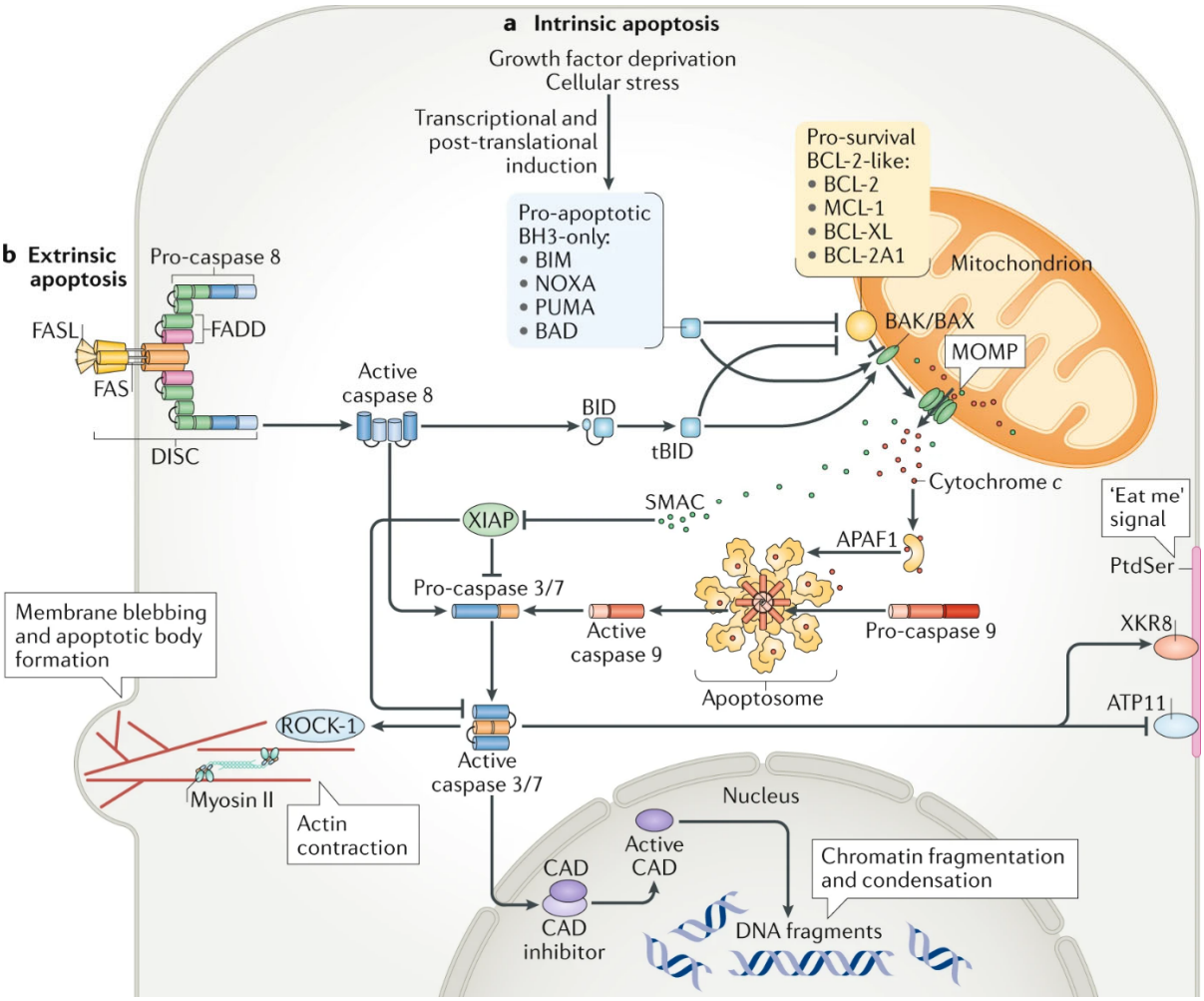

Figure 8. Connection between the extrinsic and the intrinsic apoptotic pathway (Bedoui et al., 2020).

1.3.1.1.2 BCL2 family of pro- and anti-apoptotic proteins

As already mentioned, the apoptotic machinery is controlled by proteins of the BCL2 family which are grouped in three subfamilies according to their homology between their four protein domains BH1, BH2, BH3 and BH4:

-Anti-apoptotic proteins (BCL2, BCLXL, BCLW, MCL1, BFL1): They interact with the pro-apoptotic proteins and inhibits their activity. They controls the release of apoptogenic proteins from mitochondria (Wei et al., 2001).

-Multidomain pro-apoptotic proteins (BAX and BAK1): Activated by an apoptotic stimulus, BAX (located in the cytosol) and BAK (associated with the mitochondrial membrane) are able to oligomerize and built pore channels in the mitochondrial membrane (referred as a MOMP), resulting in the release of cytochrome c

into the cytoplasm. Accordingly, BAK and BAX proteins act as a gatekeeper for the cytochrome c release process (Wei et al., 2001).

-**BH3-only pro-apoptotic proteins (BID, BAD, BIK, BLK, BIML, PUMA, NOXA, among others)**. They can exert their function in two ways: (1) by its association with anti-apoptotic proteins and inhibiting their function (specifically BIM and PUMA) or (2) by directly associating with the multidomain pro-apoptotic proteins BAX and BAK (Gonzalo et al., 2023; Kim et al., 2006).

As previously mentioned in this work, it is very common to found abnormalities in the apoptotic pathway of tumor cells. Thus, targeting BCL2 family proteins seems to be a rational for cancer treatment (Diepstraten et al., 2022; Kaloni et al., 2023). Over the past years several antiapoptotic inhibitors have been developed with the expectation of attaining human clinical trials. However, most of them some are still only in preclinical development and till the date the only that have received the approval by the Food and Drugs Administration (**FDA**) is the BCL2 mimetic **venetoclax** as it has been observed to be effective in certain types of cancer. A summary table of some of those therapies is included thereafter:

Table 1. Current state of development of BH-3 mimetics drugs (adapted from (Diepstraten et al., 2022)).

Target	Compound	Owner/inventor	Status
BCL2, BCLXL and BCLW	ABT-737	AbbVie and Idun	Preclinical
	ABT-263 (also known as navitoclax)	AbbVie	Phase I/II
BCL2	ABT-199 (also known as venetoclax)	AbbVie, Genentech and WEHI	Approved
	S55746	Servier and Novartis	Phase I
	APG-2575 (also known as lisaftoclax)	University of Michigan and Ascentage	Phase I
BCLXL	WEHI-539	WEHI and Genentech	Preclinical
	A-1331852	AbbVie, WEHI and Genentech	Preclinical
MCL1	S63845	Vernalis and Servier	Preclinical

	S64315	Vernalis, Servier and Novartis	Phase I
	AMG-176	Amgen	Phase I (on hold)
	AZD5991	AstraZeneca	Phase I/II
	VU661013	Vanderbilt University	Preclinical

The main reason of why cancer cells display heterogenous responses to a different to BH-3 mimetics is because of their "addiction" to the apoptotic proteins of the BCL2 family (Certo et al., 2006). Actually, over the last decade, Dr. Letai's research group have been dedicated to understanding this concept. Emerging from their investigations, Dr. Letai and co-workers develop a functional approach that can be used to accurately predict cellular responses after a cell perturbation based on the use of a panel of BH-3 domain peptides (Del Gaizo Moore & Letai, 2013). This technique is known as a **BH-3 profiling** and it can be exploited to predict clinical cancer responses to BH-3 mimetics such as venetoclax (Chonghaile et al., 2011).

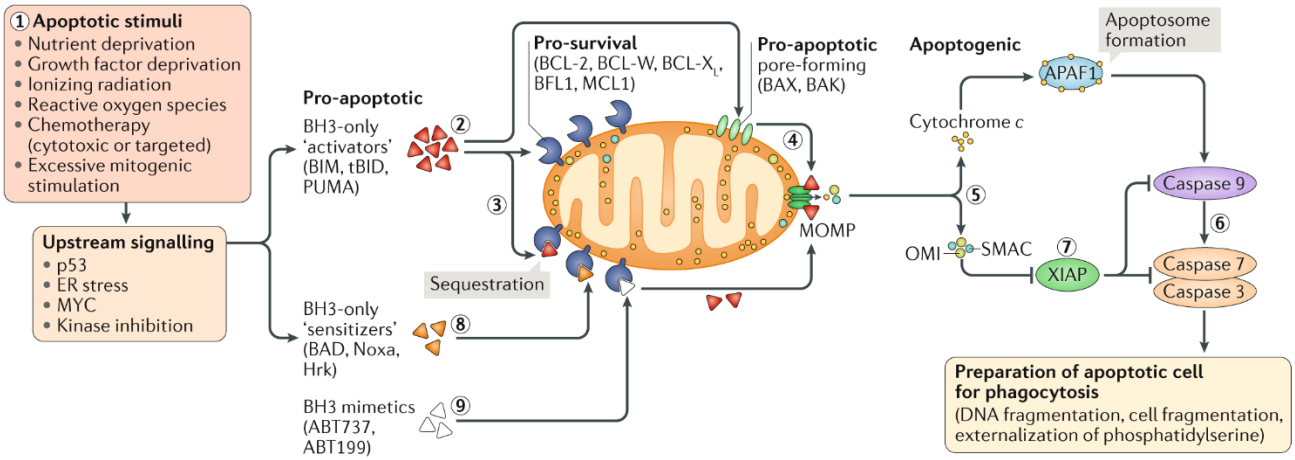

Figure 9. The mitochondrial apoptotic pathway and therapeutical strategies targeting pro and anti-apoptotic proteins (Singh et al., 2019).

1.3.1.2 Necroptosis

Necroptosis is a regulated form of necrosis that is characterized by the rupture of the cell membrane and the release of the cellular components to the extracellular media with capacity to activate the immune system. This type of cell death is thought to play a role in killing cells infected with pathogens and/or cells that have been damaged by degenerative disorders (Newton & Manning, 2016).

Necroptosis can be triggered by several immune signaling pathways through the activation of transmembrane receptors such as TLRs, death receptors or RIG-I-like receptors. The stimulation of these transmembrane proteins promotes the phosphorylation of the necroptotic kinase **receptor-interacting serine-threonine kinase 3** (RIPK3) (or **RIPK1** if the stimulation is done through death receptors) that ultimately activates by phosphorylation the pseudokinase **mixed lineage kinase domain like** (MLKL) (Sun et al., 2012), promoting the migration of this protein to the plasma membrane in where it will disrupt cell osmolarity and membrane potential (Bedoui et al., 2020). These events will culminate on cell lysis and death. Although the molecular cascade of this pathway is well documented, the precise mechanism by which MLKL can compromise the membrane integrity remains unclear.

Interestingly, despite apoptosis and necroptosis are two separate pathways, they are deeply interconnected (Vercammen, Brouckaert, et al., 1998). Indeed, necroptosis is negatively regulated by CASP8 which is also known to act as initiator of the apoptotic pathway mediated by death ligands (e.g., **tumor necrosis factor**, TNF) (see section 1.3.1.1.2.1) (Bedoui et al., 2020). Thus, in conditions in which the active form of CASP8 is present, necroptosis is blocked by preventing RIPK1 phosphorylation (Oberst et al., 2011). This blockage is mediated by cFLIP that directly controls the activity of CASP8 (Bagnoli et al., 2010; BOATRIGHT et al., 2004). In this scenario, the stimulation of the death receptors will terminate on apoptosis activation. Contrary, when CASP8 is absent, inhibited or its activity is compromised by the apoptosis inhibitors cIAP1 and cIAP2 (Deveraux et al., 1997; Roy et al., 1997), cell death induction through death receptors will activate necroptosis (Vercammen, Beyaert, et al., 1998).

As a relevant fact, CASP8-dependent cell death regulatory mechanisms were for the first time described in *in vitro* conditions in the murine fibrosarcoma cell line L929 in which it was demonstrated that blocking caspases increased their sensitivity to necrosis mediated by TNF (Vercammen, Beyaert, et al., 1998). Later on, Vanlangenakker and colleagues also demonstrated that stimulation of the **tumor necrosis**

factor receptor 1 (TNFR1) by TNF along with *Casp8* knockdown genes promotes necroptotic cell death, corroborating Vercammen previous findings (Vanlangenakker et al., 2011) (see figure 11). It is important to note that the L929 cell line model will be detailed in section 1.9 of this introduction, and it is especially relevant for this work.

Moreover, it has been reported that CASP8 not only promotes cell death by activating the extrinsic apoptotic pathway but also displays a pro-survival activity by blocking necroptosis in specific conditions as in embryogenesis (Newton et al., 2019). Accordingly, genetic ablation of CASP8 results in embryonic lethality which also supports the pro-survival activity of the CASP8 (Varfolomeev et al., 1998).

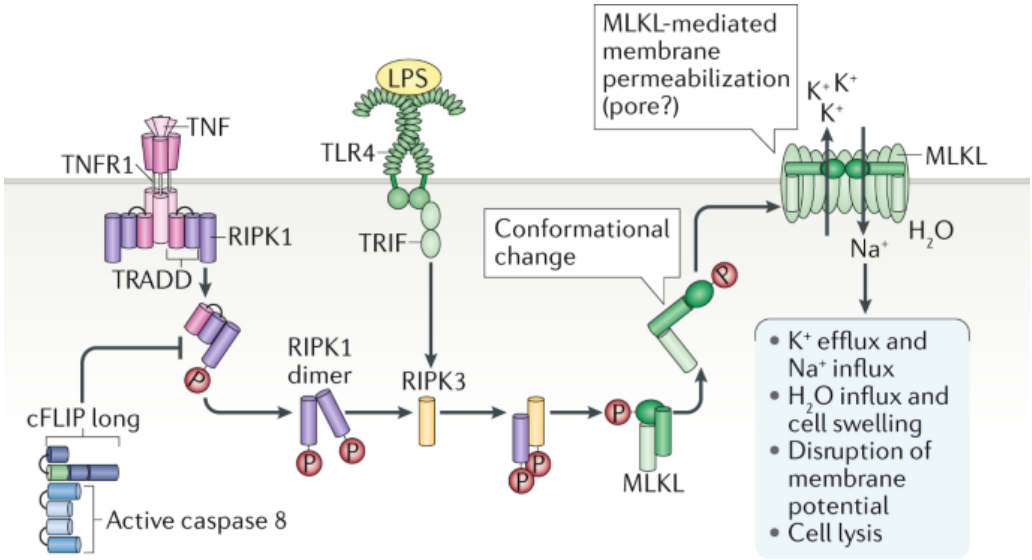

Figure 10. Molecular mechanisms of necroptosis (Bedoui et al., 2020).

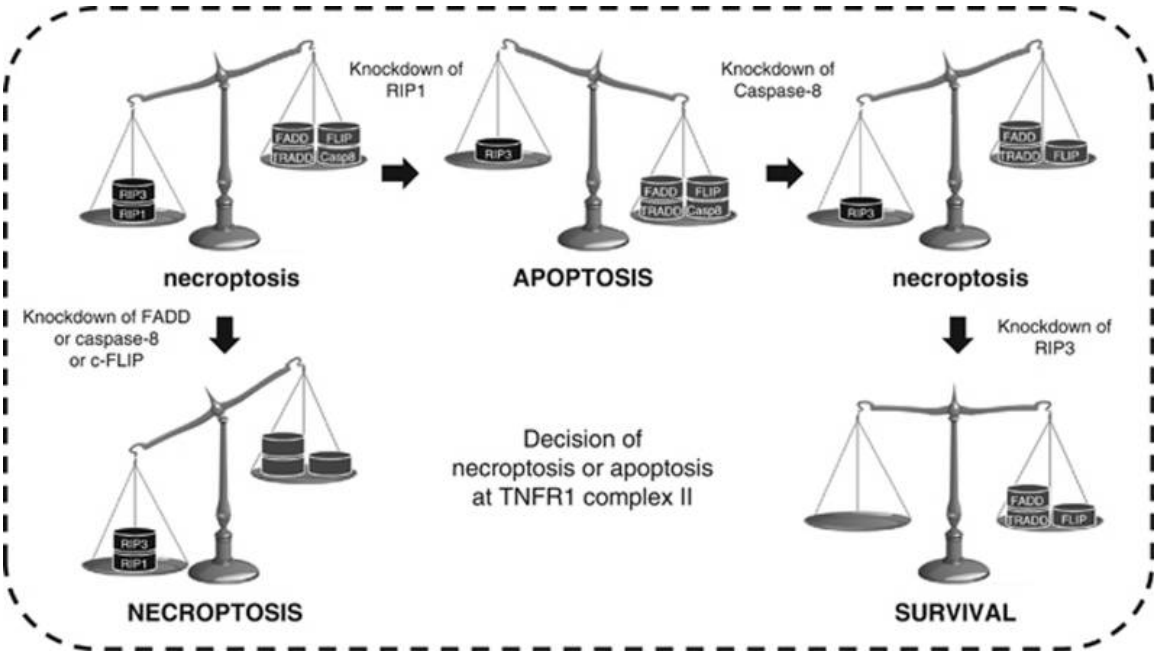

Figure 11. Necroptosis and apoptosis regulation proposed workflow (Vanlangenakker et al., 2011).

1.3.1.3 Pyroptosis

Pyroptosis is a type of regulated cell death that was first described in macrophages infected with *Salmonella typhimurium* (Hersh et al., 1999). This event is typically stimulated by bacterial or viral infection through a CASP1-dependent cellular mechanism as it was observed in both *in vitro* and *in vivo* conditions (Hersh et al., 1999; Monack et al., 2000). However, it has also been demonstrated that changes in ion fluxes (K^+ efflux, Ca^{2+} signaling, Na^+ efflux and chloride efflux) are critical events that can trigger pyroptosis through inflammasome activation (Green et al., 2018; Muñoz-Planillo et al., 2013; Murakami et al., 2012). All those cells' disturbances can stimulate the **nucleotide-binding domain and leucine-rich repeat-containing** (NLR) family receptors such as **NLR family pyrin domain-containing 3** (NLPR3) that in association with pro-caspase 1 and the adaptor protein **ACS** form the **inflammasome**, a large cytosolic multiprotein complex that activates CASP1. The release of CASP1 promotes the proteolytic conversion of pro-IL-1β and pro-IL-18 into their active forms, and the oligomerization of **GSDMD** that create pores of approximately 2 nm in the cell membrane facilitating the release of **IL-1β** and **IL-18** before the execution of cell death (Brough & Rothwell, 2007; Yang et al., 2019). As a consequence, the morphology of the cell undergoing pyroptosis is characterized by cytoplasmic swelling and the lysis of the plasma membrane due to osmotic changes which

are precisely caused by the formation of pores in the membrane by GSDMD (Fink & Cookson, 2006). As described previously in the granule-induced cell death mechanism in section 1.3.1.1.2.2, pyroptosis can be also activated by direct cleavage of GSDM by granzymes or caspases (Zhou et al., 2020).

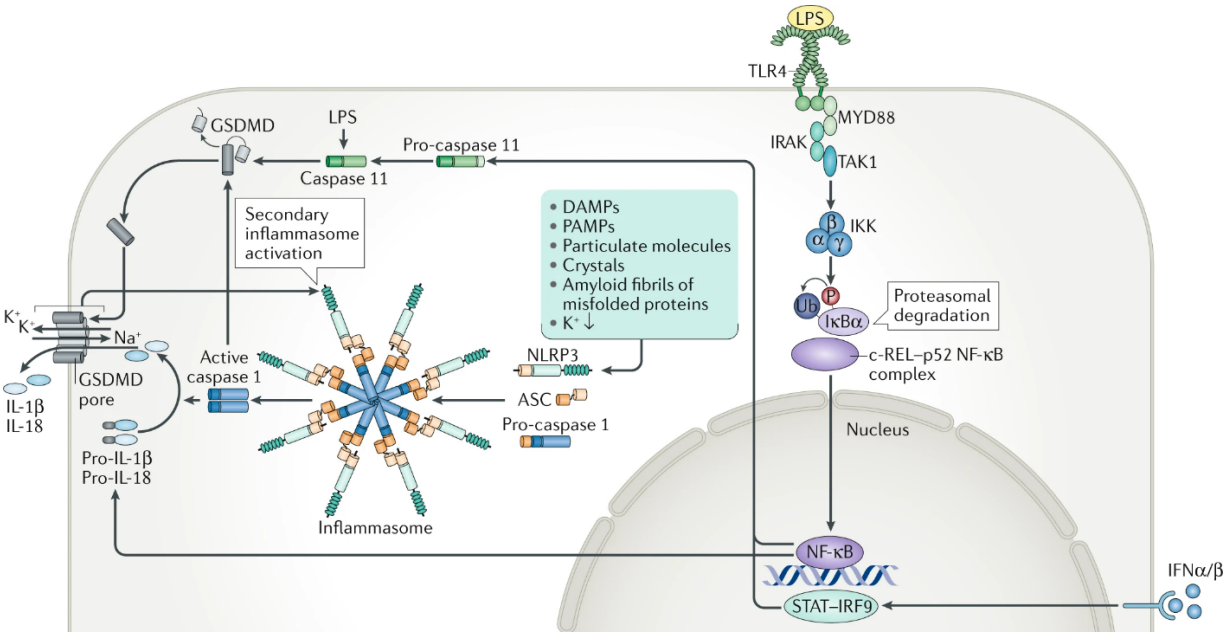

Figure 12. Inflammasome activation and pyroptosis pathway (Bedoui et al., 2020).

1.3.1.4 Others forms of regulated cell death

Since the discovery of apoptosis as a type of RCD in the early 1970s (Kerr et al., 1972), the list of other types of RCD has not stopped growing. Nowadays, there is around 20 modalities/types of RCD that have been identified. Necrosis, anoikis, autophagy-dependent cell death, autosis, efferocytosis, entotic cell death, ferroptosis, lysosome-dependent cell death, mitochondrial permeability transition (MPT)-driven necrosis, mitotic cell death, NETotic cell death, parthanatos and pyroptosis are some of them include in this list (L. Galluzzi et al., 2018).

1.3.1.5 Accidental cell death (ACD)

Accidental dell death is another modality of cell death that it is characterized by not being preceded by and attempt of the cell to adapt to the stress. The official definition is an instantaneous and uncontrollable form of cell death that is associated with the rupture of the plasma membrane and triggered by and extreme physical, chemical, or mechanical cause. Consequently, this phenomenon is naturally irreversible (L. Galluzzi et al., 2018).

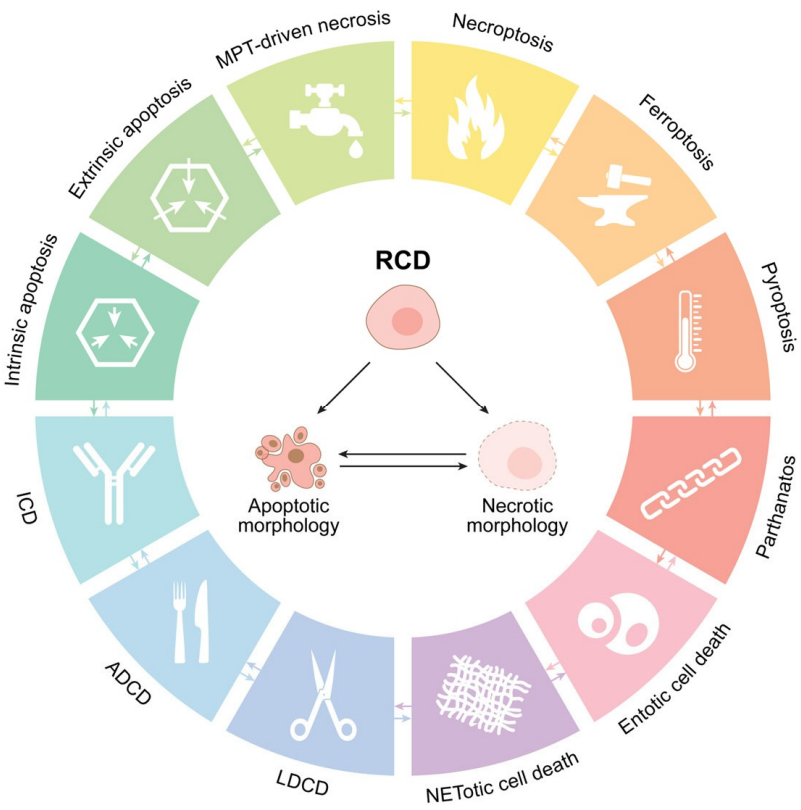

Figure 13. Schematic representation of the cell death types identified in the last recommendations of the Nomenclature Committee on Cell Death in 2018 (L. Galluzzi et al., 2018).

1.4 Immune system

1.4.1 Basic concepts

Our bodies are constantly exposed to external agents from our environment such as pathogenic organisms, chemical substances and physical conditions that threat our health. These external factors might be able to penetrate in our bodies through the mucosae or trespass the skin, leading to the development of diseases.

The immune system is an interactive network formed by lymphoid organs, cells, chemical substances, and humoral factors. Its essential function is to host defense against foreign agents, and thus, to protect us from the development of pathologies that could ultimately cause our death. Therefore, the inactivity and/or defect in the immune system action often result in severe and recurrent infections, and more significant for this work, the apparition of tumors (Parkin & Cohen, 2001).

Immunity can be divided into two parts determined by the speed and the specificity of the reaction: the **innate** and the **adaptative** immune system. However, it is important to note that this classification is a simplistic approach to compartmentalize different events that are in fact, deeply interconnected. Both modalities will be detailed thereafter.

1.4.1.1 Innate immune system

Innate immunity is the first line of defense of the organism that is activated during primary infection and is the responsible for maintaining homeostasis and preventing microbe invasion. It is a quick and unspecific response against pathogens or external agents which is involved in the activation of the adaptive immunity.

The components of the innate immune system include external physical barriers such as skin and mucosa, humoral mechanisms including antibodies, cytokines, antimicrobial peptides and cellular types such as granulocytes, monocytes, macrophages, dendritic and NK cells (see **figure 14**) (Riera Romo et al., 2016). Additionally, the innate immune system plays a role in cancer development and elimination. All these concepts are discussed in sections 1.4.2.1 and 1.4.2.2.

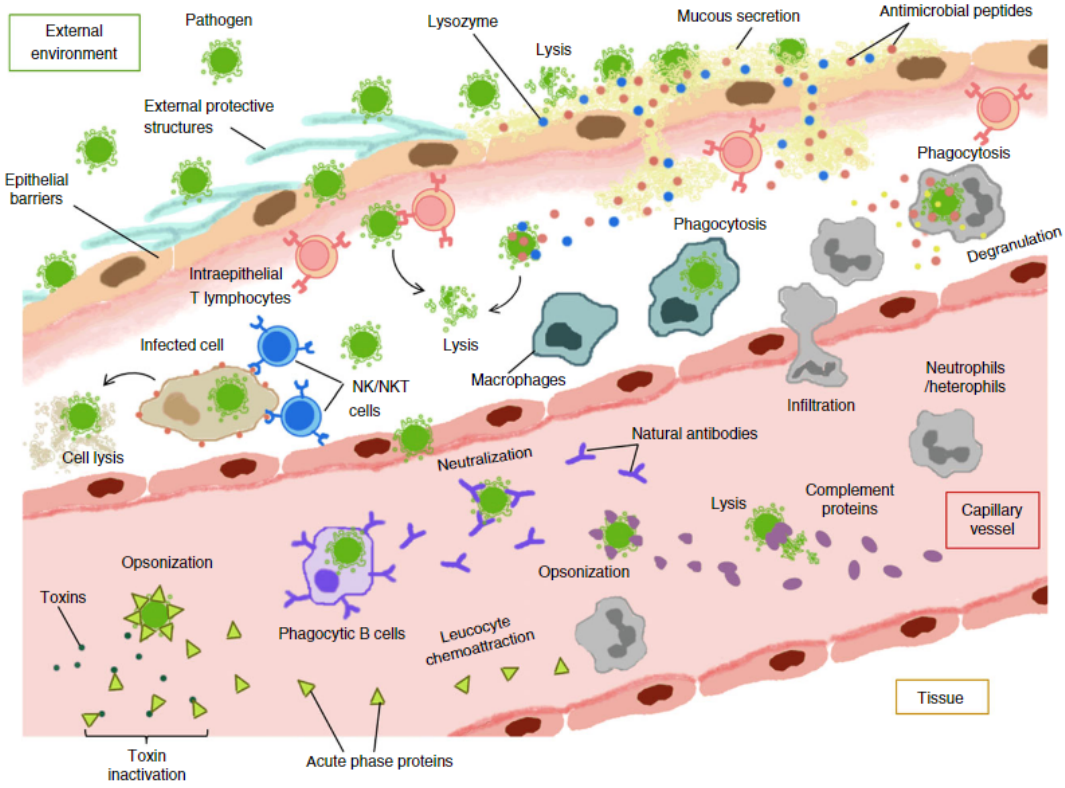

Figure 14. Overview of the innate immune response (Riera Romo et al., 2016).

1.4.1.2 Adaptive immune system

Differently from the innate, the adaptive immune system is characterized by its antigenic specificity which is given by the **interaction antigen-receptor**. Indeed, the immune cells of the adaptive system are equipped with receptors that after its activation -triggered by the interaction with the foreign antigen- are able to attack and kill the infectious agent.

Despite this is a slower response as it often takes several days to set up, it is characterized by being considerably stronger than the innate and with the additional advantage to create **immunological memory**. Thus, in case of a second exposure to the same pathogen, the immune system is capable to recognize the infection and respond more rapidly and efficiently.

The principal components of the adaptive immune system are two specialized cell types, **T cells** and **B cells**, each one playing a specific role depending on the nature of the infection. For the activation of this type of immunity it is necessary a phenomenon known as **clonal expansion** which is characterized by the rapid division and increase in number of cells after their activation through its specific antigen receptor. It is important to note that this event is essential for an efficient antitumoral and antibacterial immune response (Medzhitov & Janeway, 2000).

1.4.2 The immune system in cancer

1.4.2.1 Immunosurveillance

In 1909, the Nobel Prize in Medicine Paul Ehrlich, anticipated the concept of the immune system opposing tumor development and suggested that the antibody-based therapies could be “the magic bullet” against cancer.

Later in 1950, Burnet and Thomas introduced the early concept of **cancer immunosurveillance** (Burnet, 1967, 1971; Thomas, 1982). According to them, the immune system is the responsible of controlling the development of cancer and eliminating tumors in immunocompetent individuals. However, their theory was highly debated by the scientific community until the beginning of the 21st century (van den Broek et al., 1996) (Shankaran et al., 2001), especially after the studies published by Osias Stutman between 1974 and 1980 in nude mice using 3-methylcholanthrene (Stutman, 1974) that contradicted the immunosurveillance hypothesis.

Certainly, until the beginning of this century, cancer has been always associated with the concept of a cell-intrinsic disease with genetic or epigenetic components. However, the role of the tumor

microenvironment it is nowadays considered as a key actor controlling tumor growth. The process by which the immune system represses cancer development is referred as **immunosurveillance**, and it is the basic principle of modern cancer therapy (Finn, 2018). Accordingly, it has been more than 6 decades since Prehn and Main discovered that immunocompetent mice are able to generate specific immunological memory against carcinogen-induced self-tumors (Prehn & Main, 1957). Years later, Klein and colleagues reproduced the same experiment and demonstrated that mice that could have developed an immune response after tumor removal remained immune and would reject the challenge after being inoculated with the same previous tumor (Klein et al., 1960). However, the discovery of mutant mouse without thymus lacking T cells (known as a *nude*) (Flanagan, 1966; Pantelouris, 1968) add a new level of complexity to this idea, especially after the notorious experiments performed by Stutman and colleagues that *a priori* disproved the initial hypothesis. Interestingly, at the same time that the Stutman studies contradicted the immunosurveillance hypothesis, NK cells were discovered (Herberman et al., 1975) and the same Stutman group demonstrated that they were present and active in nude mice (Stutman et al., 1980).

It would take at least 20 years to understand the connection of the innate and the adaptive immune response that would definitely explain the anti-tumor immune response.

In 2022, Robert Schreiber and co-workers proposed an improved version of the cancer immunosurveillance hypothesis that was referred as the **cancer immunoediting theory** (Dunn et al., 2002) and will be discussed in next section.

1.4.2.2 Cancer immunoediting

Years of research has been needed to demonstrate that the immune system plays a double role in the development of cancer: not only it has the possibility of controlling and eliminating cancer cells, but it would also be responsible for sculpting the tumor phenotype. That is, the immune system would also promote the selection of variant clones with reduced immunogenicity, providing developing tumors with mechanisms to escape immunological detection and elimination. This clonal selection is known as the **cancer immunoediting** process (Schreiber et al., 2011). Altogether, cancer immunoediting encompasses three stages:

1. **Elimination**: The immune system recognizes clones of transformed cells and eliminate them before the apparition of clinical signs of the disease. This step is usually mediated by the recognition of effector molecules and the action of pro-inflammatory cytokines from the immune system, especially IFN-γ.

2. **Equilibrium or editing**: During this stage the immune system positively "selects" the clones that survive from the attack of the immune system due to their low immunogenicity. This process can be extended for years.
3. **Escape**: In this step, selected cells proliferate without control causing a clinically observable disease (Schreiber et al., 2011).

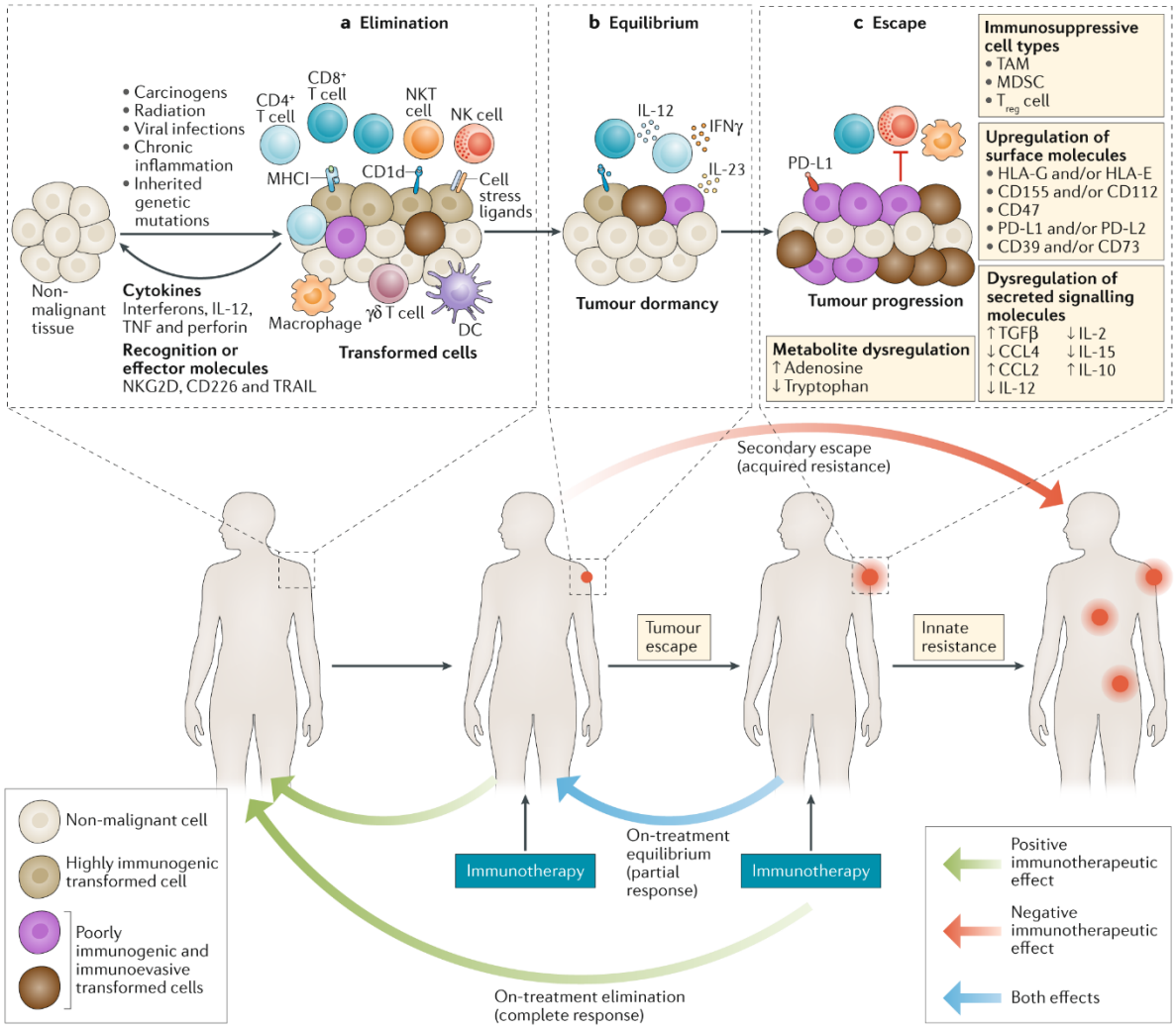

Figure 15. Stages of the cancer immunoediting process (O'Donnell et al., 2019).

1.4.3 Cancer immunotherapy

Basic work developed over the years by the research groups of Dr. Jim Allison and Dr. Tasuku Honjo on the function of the immune checkpoints CTLA4 and PD-1, initially discovered at the end of the 80's (Brunet et al., 1987; Ishida et al., 1992), led to successful clinical assays using blocking antibodies against them in 2010 and 2012 (Hodi et al., 2010; Topalian et al., 2012). These two researchers received the Nobel

Prize in 2018 for those works and since then, immunotherapy has gained ground in the field of cancer research (Sharma & Allison, 2015). Consequently, over the past 15 years, members of the scientific community started to focus on the development of cancer treatments based on the stimulation of the immune system, leading to the emergence of a new era for cancer therapy (Korman et al., 2006). Certainly, immunotherapy is nowadays considered a desirable treatment alternative as it is known to display lower toxicities -compared to traditional chemotherapeutic regimens- and show greater antitumor selectivity. Nevertheless, only a portion of the patients can beneficiate from this treatment. Thus, major efforts are needed to develop new strategies with the aim to increase the number of cancer patients eligible for this type of treatment. This idea is directly related with the concept of immunogenic cell death that is discussed in the next section 1.5 of this work.

CAR T cells-based therapies, immunogenic cell death inducers, immune checkpoint inhibitors, oncolytic viruses, prophylactic vaccines, tumor-targeting monoclonal antibodies, antibody-drug conjugates or immunotoxins are some of the US Food and Drug Administration-approved immunotherapies that are currently in the clinic (Kroemer et al., 2024; Sanz et al., 2021).

For instance, the goal of tumor antigen vaccines is to activate the patient's immune system against specific tumor cell antigens (Lin et al., 2022). Adoptive cell therapy is based on the same concept but the immune cells from the patient are isolated by apheresis, activated *in vitro* against antigens from their own tumor and reinfused into the patient. Some of the examples are CAR-T, TCR-T, CAR-NK, CAR-macrophages, dendritic cells (DCs) cells and TILs cell therapy (Dougé et al., 2024; Liu et al., 2023).

Other therapies, such as the already commented checkpoint inhibitors, are based on the use of monoclonal antibodies that binds to CTLA-4 or PD-1 molecules exposed on the surface of activated CTLs. These antibodies are currently used for the treatment of a wide variety of cancers and have provided encouraging results. The anti-CTLA-4 antibody **ipilimumab**, the anti-PD-1 antibodies **nivolumab** or **pembrolizumab**, and the anti-PD-L1 antibodies **atezolizumab** or **durvalumab** are some of these successful treatments (Wei et al., 2018).

1.5 Immunogenic cell death

1.5.1 Definition and its implication in cancer

As discussed in the previous section, a substantial fraction of cancer patients will be classified as not responders for immunotherapy. This is mainly due to the low immunogenicity of their tumors.

Accordingly, tumors can be classified as *cold* or *hot* depending on the type and the quantity of immune cells present within the tumoral mass. This concept was introduced as soon as 2005 by the group of Dr. Jérôme Galon (Pagès et al., 2005) which demonstrated upon genetic analysis of colorectal tumor biopsies that these immune infiltrations following a TH_1 signature has better prognosis than tumors without immune infiltration. Accordingly, this strategy seeks to develop immunological tools to use as (1) a prognostic of tumor progression and (2) a predictor for immunotherapy responses. Gallon and colleagues referred to this concept as **immunoscore** (Galon & Lanzi, 2020) and it has demonstrated its validity in recent clinical assays (Locke et al., 2024).

As per definition, *hot* tumors are characterized by a noticeable immune infiltration in the tumor-limiting area and consequently they tend to respond better to the immunotherapy. Contrary, *cold* tumors are characterized by a low immune cell infiltration and thus considered as poorly immunogenic. Predictably, those patients show poor responses when they are treated with immunotherapy.

For all of these reasons, it is necessary to develop new therapeutical strategies that can transform *cold* tumors into *hot* tumors, enabling patients to obtain benefits from this therapy (Sharma & Allison, 2015). One of the most likely approaches is to employ chemotherapeutic drugs that by its specific mechanism of action can kill cancer cells in a way that they can become recognizable for the immune system. This concept is known as immunogenic cell death (**ICD**) and seeks to increase the immune infiltration on the tumor site, rendering the immunotherapy effective in those patients.

The concept of ICD was introduced for the first time by the research group of Guido Kroemer in 2005 with the aim to differentiate cases of regulated cell death that drive antigen-specific immune responses and generates immunological memory from cases of RCD that only are able to engage the innate immune system (Casares et al., 2005). Nowadays, this term is used to define the mode of action of anti-cancer agents such as chemotherapy and radiation therapy (RT) with capacity to engage tumor-targeting immune responses (L. Galluzzi et al., 2020).

By definition, immunogenic cell death is a type of cell death with the capacity to activate the immune response against dead-cell antigens (Green et al., 2009). Therefore, this process involves the change of the cell surface as well as promotes the release of soluble mediators that operate as a signal on the receptors expressed by dendritic cells, and subsequently contribute to the antigenic presentation to T cells (Green et al., 2009). Indeed, many works have demonstrated that some types of cell death, but not all, can elicit signals that stimulates the immune system (also known as **immunogenic**). Some of the

examples are **calreticulin** (CALR) exposure and on the cell surface as well as **ATP** release, the non-histone chromatin-binding protein high-mobility group box 1 (**HMGB1**) and **type I IFN** extracellular secretion (Fucikova et al., 2020). All of them will be detailed in the following sections of this chapter. Contrary, it has been demonstrated that cell signs such as **phosphatidylserine** (PS) exposure, **prostaglandin E_2** (PGE_2) release or caspase activation display immunosuppressive potential that accompany immunologically silent cell death events (Fadok et al., 1998; Kalinski, 2012; Lauber et al., 2003).

The perception of cell death as immunogenic depends on several factors that rely on the cytotoxic stimulus, the dying cell, and the host (L. Galluzzi et al., 2020). For this event to take place it is necessary in first instance that the cell dies in a context of failing in adaptation to stress. In addition, it is required that dying cells express antigens that are not involved in peripheral tolerance but able to emit ICD-associated DAMPs (Holicek et al., 2024).

Certainly, the concept of immunogenic cell death is proved to be relevant for the cancer treatment. Accordingly, clinical evidence showed that situations in where immunogenic cell death is compromised (e.g., poorly immunogenic regiments) are often associated with bad outcomes and therapeutic failures in cancer patients. Contrary, a clinical context favoring immunogenic cell death seem to correlate with successful long-term clinical responses. Thus, these observations point to ICD as a highly desirable event in the clinical context that is changing the paradigm of cancer therapy.

1.5.2 Calreticulin

Calreticulin (CALR) is a chaperone protein localized in the lumen of the endoplasmic reticulum (ER) which plays a role in preserving calcium homeostasis (Johnson et al., 2001) in nascent protein folding in the ER (e.g., MHC class I molecule (Del Cid et al., 2010; Fucikova et al., 2021; Howe et al., 2009)). However, in cases of cellular stress, CALR can be exported and anchored to the outer plasma membrane, known as **ecto-calreticulin** (ecto-CALR). Ecto-CALR in turn displays a potent "eat me" signal for innate immune cells, especially for the antigen presentation cells (**APCs**). Moreover, CALR exposure not only facilitates the phagocytosis of the cells by the APCs and the activation of innate immunity (Guilbaud et al., 2023; Sen Santara et al., 2023) (see **figure 16**), but also contributes to the activation of the adaptive immune response (Chen et al., 2017) generating immunological memory which is a crucial event for tumor immunosurveillance (see section 1.4.2.1).

CALR membrane exposure linked with ICD is regulated by the phosphorylation of **eIF2α** which is involved int the ER stress response via the **protein kinase R (PKR)-like endoplasmic reticulum kinase** (PERK),

a sensor of accumulation of misfolded proteins located in the ER membrane (Bezu et al., 2018; Costa-Mattioli & Walter, 2020; Hetz & Papa, 2018).

Accordingly, several works point to CALR levels as a predictive value for cancer prognosis. However, it is still not clear if this correlation is direct or indirect. Indeed, low CALR levels in cancer cells have been associated with hyperproliferative phenotypes and poor clinical outcomes (Alur et al., 2009). Contrary, high levels of CALR expression have been linked to improved disease control in several malignancies (Fucikova et al., 2016; Hsu et al., 2005; Peng et al., 2010; Schardt et al., 2009). Other works demonstrated that high levels of ecto-CALR, at least in multiple myeloma malignant blasts, are associated with a failed immune response bad prognosis (Serrano Del Valle et al., 2022). Even if this correlation is still under research, data seems to point to CALR to influence disease progression and response to therapy (Fucikova et al., 2021).

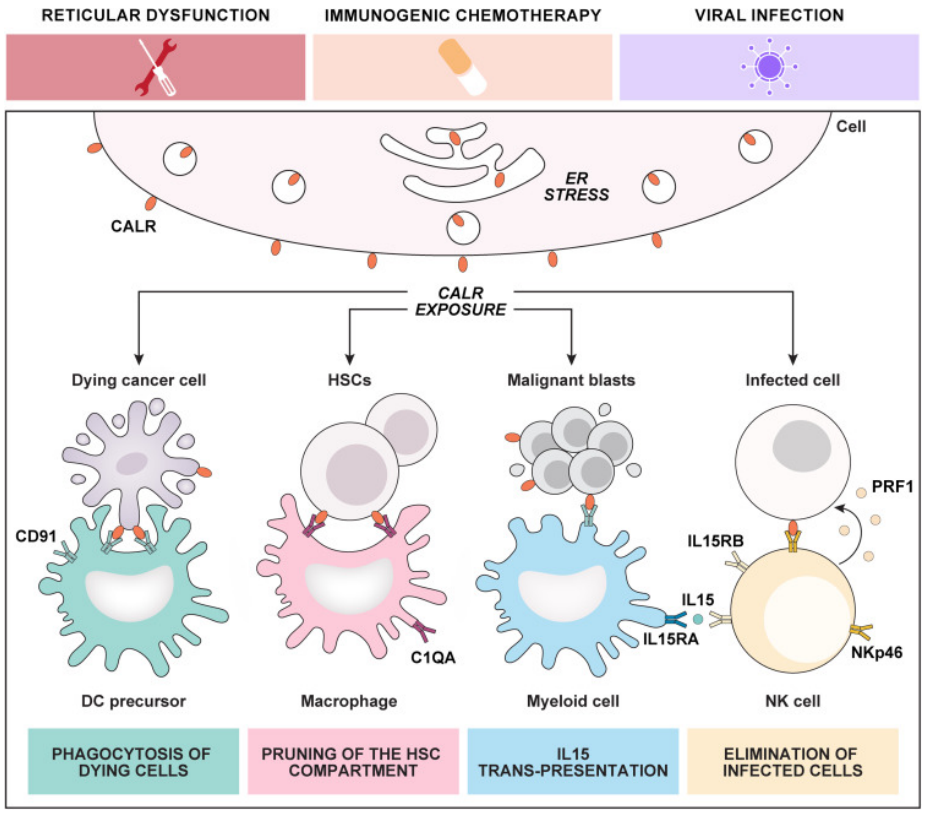

Figure 16. Effects of calreticulin exposure in innate immune response (Guilbaud et al., 2023).

CALR exposure can be directly monitored by different techniques. For instance, cytofluorometric assay that use an specific anti-CALR antibody together with vital dyes such as 4′,6-diamidino-2-phenylindole (DAPI), propidium iodide (PI) or 7-aminoactinomycin D (7-AAD), used to exclude dead cells with permeabilized plasma membrane from the analysis and avoid false-positive results, it is one of the most

usual and simple way to quantify it (Fucikova et al., 2020). Still, other techniques such as immunochemistry are routinely used to evaluate paraffin-embedded samples (Fucikova et al., 2016).

1.5.3 Extracellular ATP

Another marker of immunogenic cell death is ATP release that is mediated through pannexin channels reported to take place in an autophagic-dependent manner (Martins et al., 2012; Martins et al., 2014b; Wang et al., 2013). The secretion of ATP displays a robust signal for dendritic cells precursors and macrophages since it binds to purinergic receptors **P2Y2** (P2RY2) and **P2X7** (P2RX7) which facilitates the recruitment of myeloid cells to the same location as the ICD is occurring (Elliott et al., 2009; Kaur & Dora, 2023). Additionally, the presence of ATP in the extracellular space induces the activation of the CASP1-dependent NLRP3 inflammasome that stimulates the secretion of IL-1β and IL-18 by dendritic cells. All these events culminate with the activation of **T CD8$^+$** and **gamma delta T cells** (γδ T cells) boosting the adaptative antitumor-immune response (Ghiringhelli et al., 2009; Mariathasan et al., 2006). Consistent with this, it has been demonstrated that the immunogenicity of cell death can be blocked in cases where the purinergic pathway cannot be activated, suggesting the importance of the adenosine signaling in the context of anticancer therapies (Galluzzi, Buqué, et al., 2017). Thus, falling ATP accumulation in the tumor microenvironment, either by the action of the ATP-degrading enzyme ENTPD1 or a loss-of-function of the purinergic receptors (P2RX7 or P2RY2) in the myeloid compartment are some of the markers that has been associated with immunosuppressive outcomes (Ghiringhelli et al., 2009; Nagate et al., 2021; Stagg et al., 2012; Vijayan et al., 2017).

ICD-associated ATP secretion can be monitored *in vitro* by its quantification in cell supernatants using commercial luminescent-based kits. This assay is based on the quantification of light emission during the oxidation reaction of luciferin after adding the enzyme luciferase. Extracellular ATP levels can also be evaluated by quantifying the residual pool of intracellular ATP in cell lysates (Fucikova et al., 2020).

1.5.4 HMGB1 release

High mobility group box 1 (HMGB1) is a highly evolutionary conserved nuclear protein from the **high mobility group** (HMG) family protein, widely expressed in mammalian cells and tissues with multiple functions according to its subcellular location (Chen et al., 2022; Goodwin & Johns, 1973). In normal physiological conditions, HMGB1 is in the nucleus, associated to DNA molecules where it acts as a chaperone and helps to maintain the structure and function of chromosomes. However, in specific stress conditions this protein can shuttle to the cytoplasm and be passively released outside the cells in where it

acquires the function as a **damage-associated molecular pattern** (DAMPs) molecule, acting as a mediator of inflammation, immunity, and metabolic responses (Scaffidi et al., 2002; Tsung et al., 2005). Once liberated to the extracellular space, HMGB1 can bind to several membrane receptors of the immune cells such as TLR4 which is the primary receptor need for macrophage simulation and cytokine release (Jong Sung Park et al., 2006; Yanai et al., 2011; Yang et al., 2010) .

Due to the fact that HMGB1 lacks a leader sequence in its protein structure, its release to the extracellular space is not associated with the conventional endoplasmic reticulum-Golgi secretory pathway. Thus, two models of secretion have been identified for this protein that can be grouped in **active** and **passive** release, depending on the event that is taking place during its liberation (Chen et al., 2022).

Within the active secretory modality, two major subcategories can be differentiate: (1) HMGB1 can freely be released into the cytoplasm, a process that seems to be associated with the activation of a cell by a stimulus (Youn & Shin, 2006) or (2) enclosed in intracellular vesicles, preceded by its fusion with the cell membrane (Gardella et al., 2002).

Oxidative stress (ROS and RNS production), disruption of calcium ion levels, tumor necrosis factor (TNF) release as well as the activation of the classical inflammatory pathways NF-κB or NOTCH, MAPK, and STAT signaling cascades, are some of the events that have been identified to regulate HMGB1 secretion (Chen et al., 2022). Moreover, it is has been reported that HMGB1 can be found associated to the tumor protein **TP53**, forming a protein complex in processes responding to DNA repair and to the regulation of the apoptotic/autophagic flux balance which is known to be relevant in the cancer setting (Livesey et al., 2012).

In line with the above, it has also been observed that the release of HMGB1 into the extracellular space can be also linked to cell death processes such as apoptosis, necroptosis, pyroptosis, necrosis, ferroptosis, NETosis, and lysosome-mediated and autophagy-dependent cell death (Morinaga et al., 2010; Murakami et al., 2014). However, this type of secretion is not caused by the death process itself, but it is a consequence of the events that are directly associated with it. This secretory modality it is categorized as **passive,** and it is known to be regulated by molecules such as PARP1, RIPK3, cathepsin, DNase, caspases, ATG and alkaliptosis (Chen et al., 2022).

Due to the fact that HMGB1 is known to contribute to inflammatory processes -as it has been reported to be secreted by monocytes and macrophages (Bonaldi et al., 2003; Wang et al., 1999)- and to mediate immune responses (Yanai et al., 2009), it is considered nowadays a marker of **immunogenic cell death** that can be easily monitored *in vitro* (Fucikova et al., 2020). Nonetheless, it is important to note that

since extracellular HMGB1 is also associated in cell death processes, its analysis cannot be interpreted as a reliable sign of ICD and thus, it has to be complemented with the analysis of other ICD-markers (Fucikova et al., 2020).

1.5.5 Annexin A1

Annexin A1 (ANXA1) appertains to the multigene family of Ca^{2+}-regulated proteins with affinity for acidic phospholipids in a calcium-dependent manner (Gerke et al., 2005). Its pro-inflammatory activity is mediated through its interaction with the **formyl peptide receptor 2** (FPR2) when it is secreted or surface-exposed (Perretti & D'Acquisto, 2009). FPR1 is expressed by myeloid cells, especially by intratumoral dendritic cells, supporting the importance of this molecule in anti-tumor immunity (Cucolo & Minn, 2015; Del Prete et al., 2023; Le Naour et al., 2021; E. Vacchelli et al., 2015).

In line with this, it has been reported that malignant cells lacking ANXA1 expression present limited sensitivity to anthracycline-based chemotherapy *in vivo* (Erika Vacchelli et al., 2015). Moreover, in the same work, Vacchelli and colleagues reported that loss-of-function variants exhibiting **single nucleotide polymorphisms** (SNPs) of its receptor FRP1 in samples of breast cancer patients were associated with compromised clinical responses to cisplatin and anthracycline-based therapy. Altogether, these data points to the relevance of both ANXA1 and FRP1 in the antitumor immune response and supports the idea that polymorphisms in FRP1 could be used as a predictive biomarker for chemotherapy response and disease aggressiveness (Erika Vacchelli et al., 2015).

In the past, the detection of extracellular ANXA1 was performed by semiquantitative Western blot analysis. However, it is rather monitored by using a commercial ELISA assay with increased sensitivity and specificity (Baracco et al., 2019).

1.5.6 Type I IFN signaling

Type I IFN belongs to a proinflammatory cytokine family that was initially discovered as a fundamental component of the mammalian first-line defense system against pathogenic viruses (Hardy et al., 2004). Type I IFN was first identified in chicks as a soluble factor secreted the chorioallantoic membrane after exposure to influenza virus A (Isaacs & Lindenmann, 1957; Isaacs et al., 1957).

Its secretion can be initiated in innate immune cells by the interaction of a variety of pathogen-derived molecules (also known as MAMPs) with **pattern recognition receptors** (PRRs) such as plasma membrane-associated **toll-like receptors** (TLRs) -also able to recognize HMGB1 (see section 1.5.4) (J. S. Park

et al., 2006), double-stranded DNA (dsDNA) CpG containing motifs (Hemmi et al., 2000), dsDNA sensor cyclic GMP-AMP synthase (CGAS) (Sun et al., 2013)(see section 1.8.1), among others.

In line with this, in all nucleated cells provided of functional IFN type I (**IFNAR1** and **IFNAR2**), type I IFN ligand can bind to them and activate an intracellular cascade that involves in first place the activation of the Janus kinase 1 (**JAK1**) and/or the tyrosine kinase 2 (**TYK2**). Subsequently, the formation of the supramolecular complex composed by STAT1, STAT2 and interferon regulatory factor 9 (IRF9) is induced which ultimately stimulates the transcription of the **interferon-stimulated genes** (ISGs). There are several factors involved in the inhibition of viral replication as well as for immunostimulatory molecules and chemotactic factors such as C-X-C motif chemokine ligand 10 (**CXCL10**) (see **figure 17**) (de Weerd et al., 2013; Holicek et al., 2024; Schoggins, 2019). Additionally, it has been described that type I IFN exert immunomodulatory effects (Parker et al., 2016) such as an increase in MHC class I expression on the surface of cancer cells, increasing tumor immunogenicity (Greiner et al., 1984). Indeed, type IFN is necessary for a correct T-cell-cross priming with dendritic cells (Fuertes et al., 2011) and it is also an efficient activation of NK cells (Mizutani et al., 2012). In addition, it is required for the generation of $CD8^+$ memory T cells (Lu et al., 2019; Marrack et al., 1999; Mescher et al., 2006), for the differentiation of $CD4^+$ T cells to the T_H1 phenotype and lymphocytes B into antibody-secretion plasma cells (Jego et al., 2003). Accordingly, a great variety of preclinical data show that defects in the IFN type I pathway as well as in PRR signaling can favor oncogenesis and tumor progression in addition to restrain responses to therapy (Holicek et al., 2024).

Type I IFN associated with ICD events can be monitored *in vitro* by different laboratory techniques. One of them consists in analyzing the intracellular expression of *Ifnb1* mRNA transcripts by RT-PCR. However, this technique has its drawbacks as an increase in transcripts is not necessarily associated with its translation and secretion. Thus, type I IFN in cell supernatants analyzed by ELISA-based techniques appears to be more reliable with superior sensitivity (Fucikova et al., 2020).

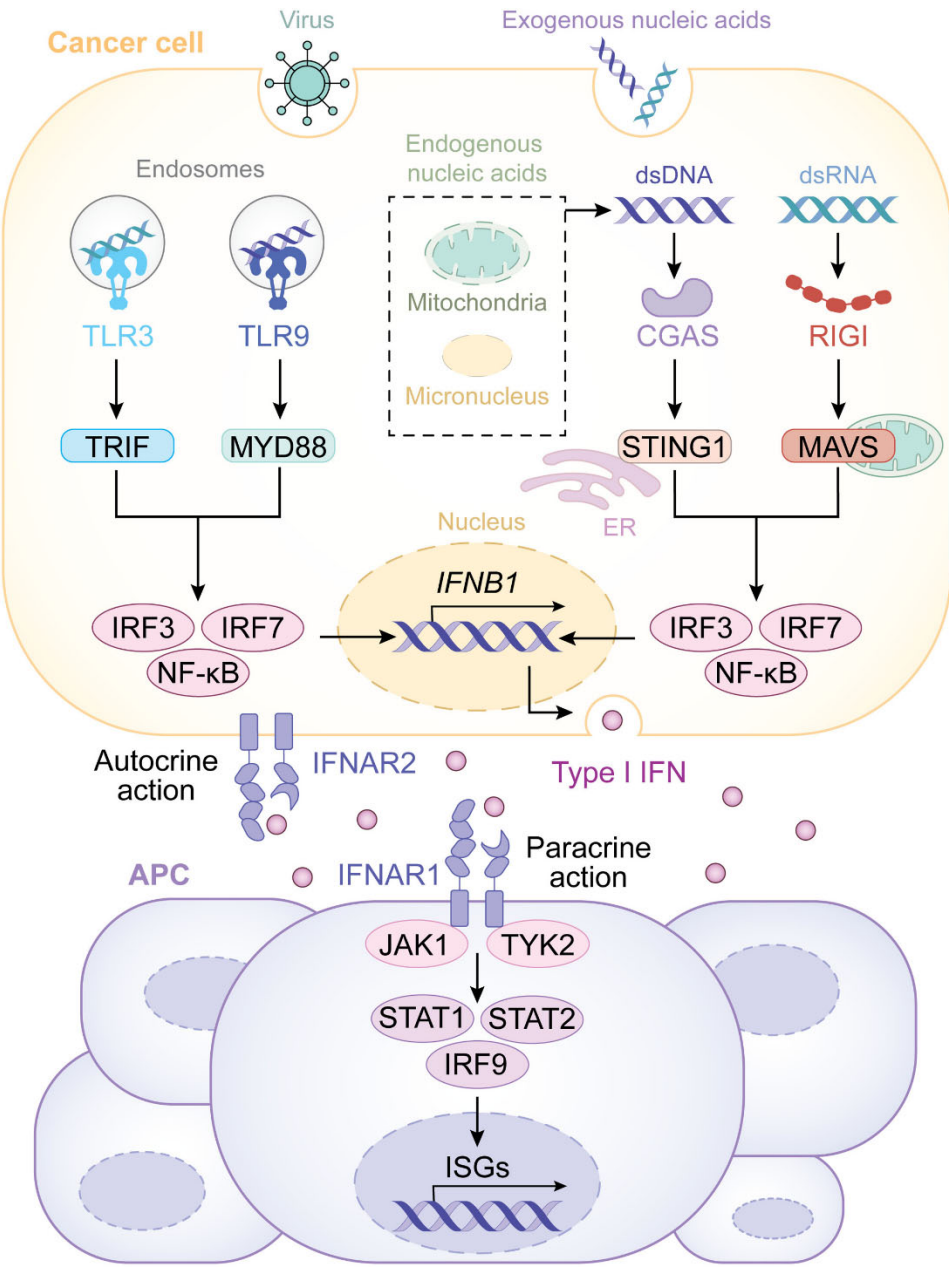

Figure 17. Type I IFN signaling (Holicek et al., 2024).

A summary of the molecular mechanisms leading to ICD is schematically depicted thereafter:

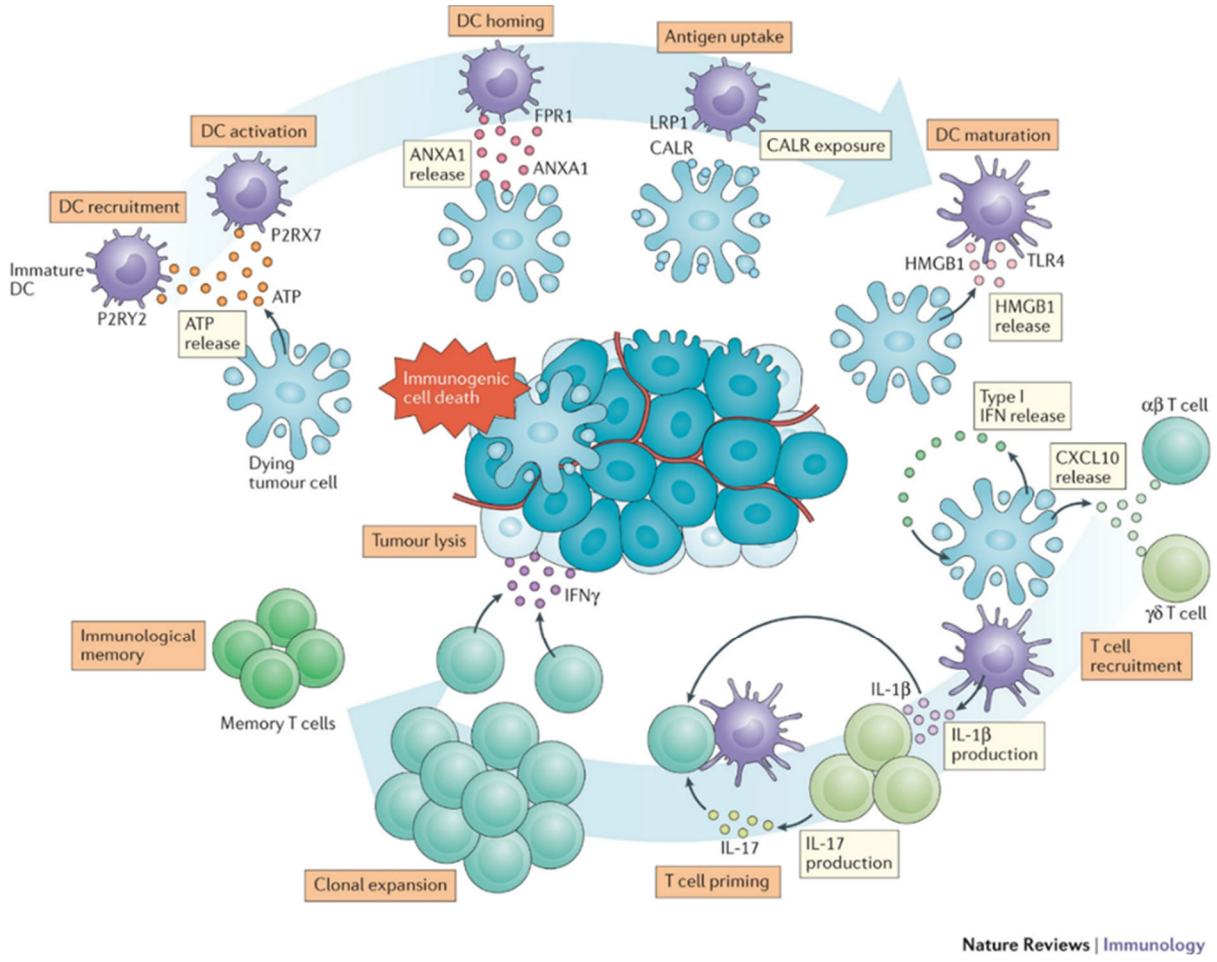

Figure 18. Effects of ICD in immune cells activation and antigenic presentation (Galluzzi, Buqué, et al., 2017). In response to immunogenic cell death inducers, cancer cells are able to emit a plethora of signals engaging antitumor immune responses. For instance, dying cells can expose calreticulin (CALR) on the surface of their membranes as well as secrete ATP, type I IFN, annexin 1 and HMGB1. Those molecules bind on the surface receptors of immune cells promoting the maturation of dendritic cells (DC) that will acquire the capacity to activate the adaptive immune response mediate by the antigenic presentation. All these events eventually prime immunological memory and control tumor growth by eradicating chemotherapy resistant cells via IFN gamma secretion mechanism.

1.5.7 Implication of autophagy in cancer and ICD

Autophagy is a highly conserved cellular lysosome-mediated degradation pathway exclusive of the eukaryotic organisms which is controlled by autophagy-related (ATG) family proteins (Levine & Kroemer, 2019). The main role of this process is to clear cells from their "molecular trash" (e.g., damaged organelles, protein aggregates, nucleic acids, lipids) in order to maintain cell homeostasis and promote differentiation, development, and survival (Galluzzi, Baehrecke, et al., 2017).

Different types of autophagy have been described depending on the mechanism that mediates the delivery of cargo to lysosomes for degradation. The three different types of autophagy are: (1) **macroautophagy**, (2) **microautophagy** and (3) **chaperone-mediated autophagy**, the latest only occurs in mammalian cells and it is regulated by an entire different set of proteins without involving membrane dynamics (Kaushik & Cuervo, 2018; Klionsky et al., 2021). Both macroautophagy and microautophagy can be classified as **selective** and **non-selective.** It refers as non-selective autophagy when the process occurs randomly with the indiscriminate engulfment of the cytosolic components in response to nutrient starvation. Contrary, selective autophagy degrades specific targets such as damaged organelles and bacteria (Vargas et al., 2023).

Selective autophagic process involves two major steps: in first place, the dysfunctional organelles or other molecules are typically tagged by ubiquitylation by the action of **E3 ubiquitin ligases** and selectively enclosed in a double-membrane system known as **autophagosome.** Secondly, the autophagosomes fuse with the **lysosomes** which are organelles containing hydrolases. The fusion of these two membranous systems originated the **autophagolysosome** in where the hydrolases digest the molecular content.

The initiation of this process is mediated by the **ULK complex** containing the **kinase UNC-51-like kinase 1** (ULK1) **and 2** (ULK2), **FIP200**, **ATG13**, **ATG101** together with **ATG9** promotes the autophagosome formation. This complex is controlled by cellular signaling pathways involved in nutrient and energy sensing such as **mechanistic target of rapamycin complex 1** (mTORC1) and it is facilitated by cargo adaptors such as **p62**, **NDP52**, **TAX1BP1** and **OPTN**.

Downstream of the ULK molecular complex, the **class III phosphatidylinositol 3-kinase complex I** (PI3KC3-C1) formed by **beclin-1**, **VPS34**, **VSP15 ATG14 and NRBF2** are associated with the ULK1 complex that catalyzes the production of **phosphatidylinositol-3-phosphate** (PI3P) which is the main effector for the elongation of the autophagosome membrane. Subsequently, PI3P recruits **ATG16L1-ATG5-ATG12**, **ATG3**

and ATG7 that act as a facilitators for lipid conjugation of autophagy-related genes 8 (ATG8) family members, including microtubule-associated protein 1A/1B-light chain 3 (MAP1LC3), also referred as LC3 that is lipidated into a LC3-II form by its association to phosphatidylethanolamine. Finally, the autophagosome fusions with the lysosome by the action of PLEKHM1, EPG5 and RAB7 as well as two SNARE complexes containing STX17–SNAP29–VAMP7/8 and YKT6–SNAP29–STX7 proteins (Yamamoto et al., 2023).

Accordingly, many works associate general autophagy as a mechanism used by cancer cells to cope with difference sources of stress, contributing to apoptosis evasion and therapy resistance (Jarauta et al., 2016; White et al., 2021). Indeed, several studies points to autophagy as an advantage for cancer development and growth (Levy et al., 2017). However, there is also scientific evidence suggesting that autophagy could act as a repressor for cancer cells (Bhutia et al., 2013; Eskelinen, 2011). Therefore, manipulating autophagy (either inducing it or repressing it) is nowadays considered as a strategy for cancer treatment, especially in combination with other anticancer therapies (Ramakrishnan et al., 2012; Sui et al., 2013).

It has been shown that autophagy is essential for the immunogenic release of ATP from dying cells (Michaud et al., 2011) which act as a recruiter of immune cells into the tumor bed when is actively secreted. For instance, Martins and colleagues demonstrated that knocking down the autophagic-related genes (ATG3, ATG5, ATG7 and BECN1) abolished the secretion of ATP during death of several mice cell lines (Martins et al., 2012). Additionally, a work published by Yamazaki and colleagues demonstrate that autophagy blocks CGAS/STING1 induced- type I IFN secretion a process initiated by cytosolic mitochondrial DNA in response to radiotherapy (Takahiro Yamazaki et al., 2020). In line with this, it has also been documented that the autophagic protein ATG9a and STING (which is activated by CGAS, see section 1.8.1) co-localized in vesicles and can limit the production of type I IFN production mediated by dsDNA in mouse embryonic fibroblasts (Saitoh et al., 2009). In addition, many works investigating bacterial and viral infection have reported that the activation of STING1 by CGAS in this context initiates several types of autophagy (Collins et al., 2015; Rasmussen et al., 2011; Yamashiro et al., 2020). Thus, all this scientific evidence points to STING1 not only as a component of the autophagic machinery but also as a modulator of immunogenic cell death through the activation of type I IFN secretion. Other works showed that autophagy activation is necessary for a successful anti-cancer immune response in the context of chemotherapy (Follo et al., 2019; Michaud et al., 2011). However, the role of autophagy in cancer development and immunogenic cell death remains controversial and still unclear.

1.5.8 Immunogenic cell death inducers

Immunostimulatory drugs also known as a "**ICD inducers**" are routinely used in the clinic for the treatment of a wide range of cancer types (Lorenzo Galluzzi et al., 2020). Paradoxically, before the immunotherapy era initiated in 2010, traditional chemotherapeutic drugs received the FDA-approval according to their specific effects on cancer cells and skipping the fact that they could also act on anti-tumor immunity (Zitvogel et al., 2008). Indeed, experimental data point that chemotherapeutic agents (Solari et al., 2020) as well as radiotherapy (Dewan et al., 2009; Golden et al., 2012) can also have a positive effect on the antitumor action of the immune system. Some of the examples are cyclophosphamide (Schiavoni et al., 2000), anthracyclines (Casares et al., 2005; Orsini et al., 1977), taxanes (Senovilla et al., 2012) or some platinum-based compounds (see section 1.12) (O. Kepp & G. Kroemer, 2020; Tesniere et al., 2010a).

The immunostimulatory capacity of these compounds is explained by the fact that they are able to induce ICD, a rationale to combine them with immunotherapy regimes. Nevertheless, further investigations are needed to demonstrate their clinical potential when combined with immunotherapy.

1.6 Cancer metabolism

Unicellular organisms such as bacteria are constantly exposed to an evolutionary pressure to reproduce as quick as possible when nutrients are available. Consequently, when the nutrients are scarce there is a need to control and adapt their metabolism according with the nutrient supply and to extract the maximum energy from those resources. Accordingly, different regulatory mechanisms have been developed to control metabolic pathways in proliferating versus non-proliferating cells. Thus, it is also expected that cancer cells have adopted similar strategies in order to meet their high energy demands even in the most austere nutrient conditions (Vander Heiden et al., 2009).

1.6.1 Alterations in glucose metabolism -The Warburg effect

The role of metabolism as a hallmark of cancer (Hanahan, 2022; D. Hanahan & Robert A. Weinberg, 2011) was postulated for the first time by Otto Warburg in the 20's (Warburg, 1924). According to Warburg´s theory, cancer cells undergo a process of metabolic reprogramming – initially deemed a sequela of primary damaged mitochondria (see also section 1.7.4.1) - which increases the levels of glucose consumption and induces the redirection of the pyruvate obtained from the glycolysis to lactate fueling the

lactic fermentation process pathway, also referred as **aerobic glycolysis** (O. Warburg, 1956) (see **figure 19**). It is currently accepted by most of the scientific community that this feature represents an advantage for cancer cells to grow faster (Ralph J. DeBerardinis & Navdeep S. Chandel, 2020; Liberti & Locasale, 2016; Lunt & Vander Heiden, 2011; Vander Heiden et al., 2009; Peter Vaupel & Gabriele Multhoff, 2021) and to escape from the immune system's antitumoral activity (Catalán et al., 2015; Huber et al., 2017; Xia et al., 2021).

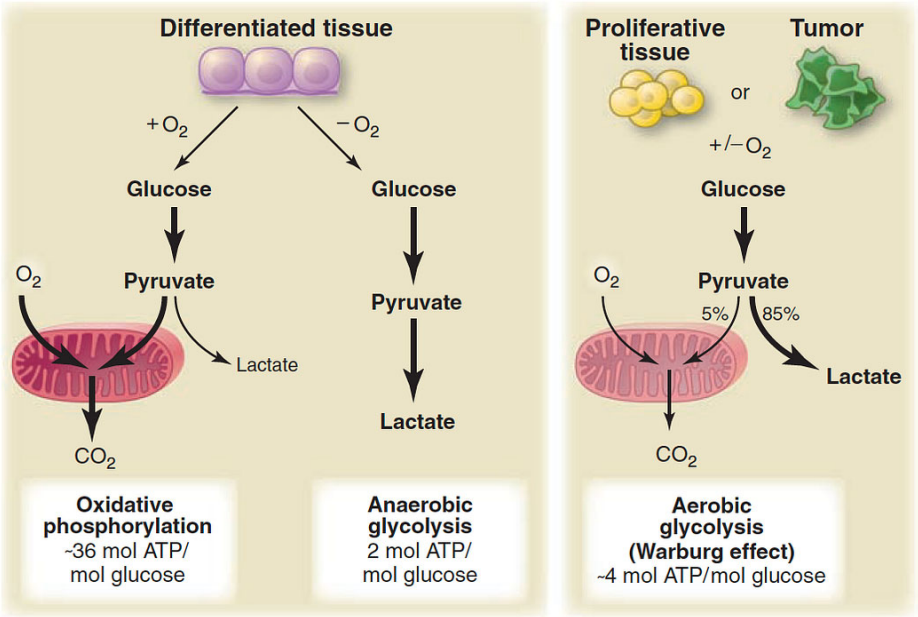

Figure 19. The Warburg effect (Vander Heiden et al., 2009).

But what drives cancer cells to perform aerobic glycolysis and why is this feature associated with proliferation? Proliferating cells require large amounts of ATP to meet their increased needs for biomass synthesis. According to the efficiency in terms of ATP production, aerobic glycolysis is much less efficient compared to oxidative phosphorylation (see section 1.7.3.1), producing 4 mol of ATP per 1 mol of glucose versus 38 ATP molecules per 1 mol of glucose, respectively (see **figure 19**) (Vander Heiden et al., 2009). One possible explanation of why this metabolic rewriting implies an advantage for cancer cells is that increasing glucose consumption provides important biosynthetic precursors that fuel anabolic reactions such as lipid, nucleosides, or protein synthesis pathways. However, this explanation appears to be incomplete as most of the glucose consumed by cancer cells is secreted as lactate, and the major precursor

of biomass derives from amino acids rather than glucose (Hosios et al., 2016). Thus, some theories propose that aerobic glycolysis also facilitates the production of electron carriers such as NADPH that are required as a cofactor for redox reactions. Moreover, other models cognate the idea that this metabolic phenotype would result from an adaptation of molecular crowding (Vazquez & Oltvai, 2011) or even caused by mitochondria saturation due to the excessive glucose consumption (Wang & Patti, 2023). That said, Warburg postulated that malignant cells largely depend on glucose for bioenergetic metabolism as a consequence of mitochondrial dysfunction (O. Warburg, 1956) a possibility that has now been invalidated (P. Vaupel & G. Multhoff, 2021; Vyas et al., 2016; Zong et al., 2016). Indeed, accrued glucose uptake by malignant cells appears to mainly fuel anabolic (rather catabolic) metabolism in support of lipid and nucleotide biosynthesis (which are crucial for accelerated proliferation), mitochondrial ATP remaining the major source of energy (R. J. DeBerardinis & N. S. Chandel, 2020; Locasale et al., 2011; Lunt & Vander Heiden, 2011; Vander Heiden et al., 2009). Moreover, mitochondrial metabolism at large – including catabolic and anabolic components thereof – is fundamental for all steps of oncogenesis, including malignant transformation, tumor progression and response to treatment (Hanahan, 2022; D. Hanahan & R. A. Weinberg, 2011; Porporato et al., 2018).

Certainly, cell metabolic reprogramming towards aerobic glycolysis favors **lactate** secretion leading to an acidification of the **tumor microenvironment** (TME). This creates an immunosuppressive niche that impairs immune cell infiltration and function and favors tumor growth (Apostolova & Pearce, 2022).

Through the last years, the study of glucose metabolism in the context of cancer has led to the emergence of different therapeutical approaches. For instance, drugs targeted towards glucose transporters and glycolytic enzymes (e.g., GLUT1, HK-2) are currently undergoing clinical trials (Sainero-Alcolado et al., 2022; Tilekar et al., 2020). Interestingly, **metformin** which is the most widely used drug for the clinical management of type II diabetes, has been associated with lower cancer cases in these patients (Allende-Vega et al., 2022; Pollak, 2012). Other drugs such **dichloroacetate** (DCA) which targets the **pyruvate dehydrogenase kinase 1** (PDK1) displays antitumor effects *in vitro* and target specifically cells with mitochondrial DNA mutations (de Mey et al., 2020; Dunbar et al., 2014; Marco-Brualla et al., 2019; Tataranni & Piccoli, 2019).

Undoubtedly, pharmacological blockade of glucose uptake by cancer cells or shutting off the biosynthesis of metabolic intermediates is a rationale that would directly affect tumoral growth (X. S. Chen et al., 2016; Ghanavat et al., 2021; Yu et al., 2016).

Apart from the strategies based on the inhibition of aerobic glycolysis, therapeutical approaches directed against other metabolic pathways such as glutamine, nucleotide metabolism, and de novo fatty acid synthesis (Luengo et al., 2017; Stine et al., 2022) are currently being studied (see **figure 20** and **table 2**).

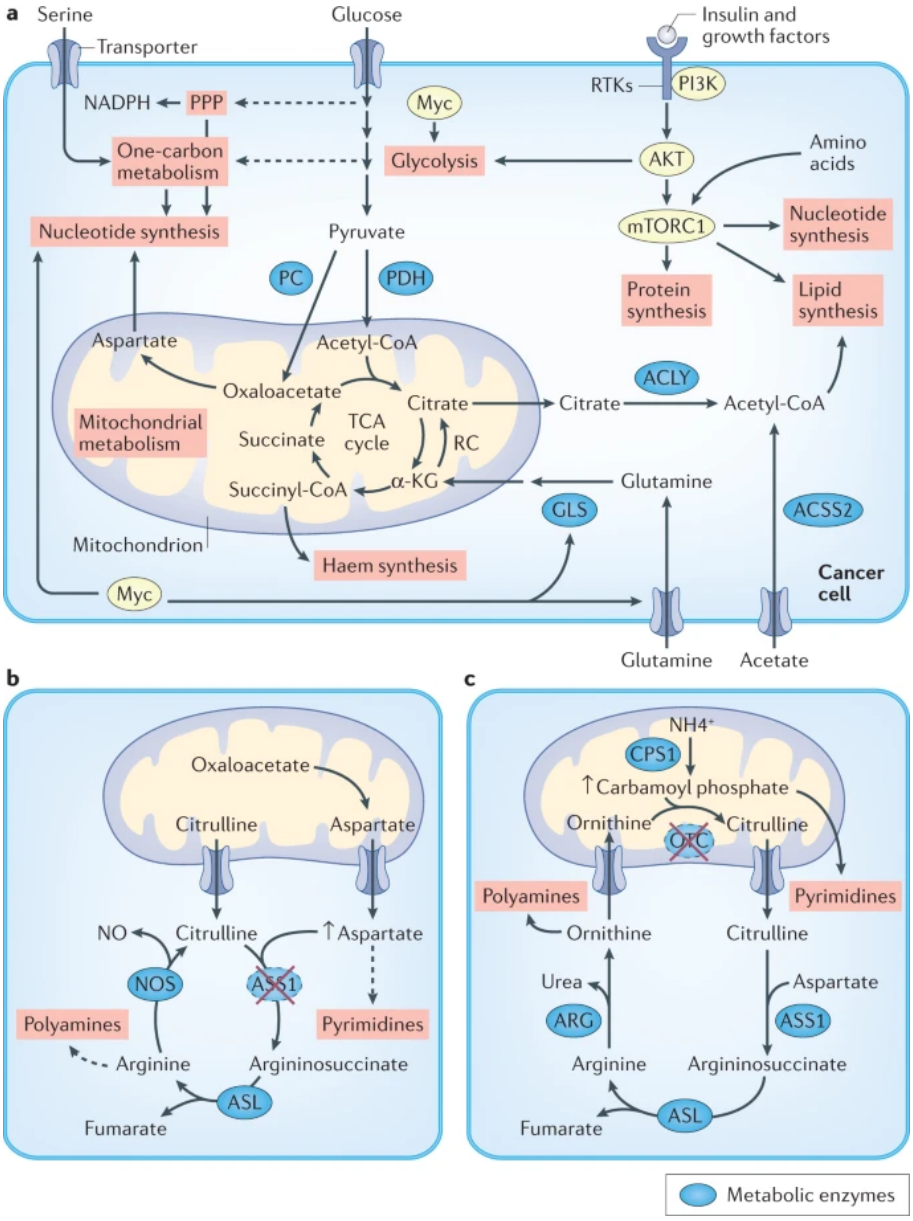

Figure 20. Metabolic and molecular pathways supporting tumor biomass synthesis in cancer cells. α-KG, α-ketoglutarate; ARG, arginase; PC, pyruvate carboxylase; PPP, pentose phosphate pathway (Martínez-Reyes & Chandel, 2021).

Table 2. Drugs targeting cell metabolism.

Agent	Target	Function	Indications
Pemetrexed	TYMS, DHFR	dUMP to dTMP conversion; folate to THF conversion	NSCLC
5-Fluorouracil	TYMS	dUMP to dTMP conversion	CRC, gastric and breast cancer
Hydroxyurea	RNR	Ribonucleotide to deoxyribonucleotide conversion	CML, HNSCC
Gemcitabine	DNA incorporation	Nucleotide analogues	Pancreatic, ovarian and breast cancer; NSCLC
Fludarabine	DNA incorporation	Nucleotide analogues	CLL
6-Mercaptopurine	PPAT	Purine synthesis	ALL
Methotrexate	DHFR	Folate to THF conversion	Breast, HNSCC, lung, non-Hodgkin lymphomas
Enasidenib	Mutant IDH2	2-Hydroxyglutarate synthesis	AML
Ivosidenib	Mutant IDH1	2-Hydroxyglutarate synthesis	AML
Metformin	Complex I	Oxidative metabolism	Type 2 diabetes mellitus
Leflunomide	DHODH	Pyrimidine metabolism	Rheumatoid arthritis
Bempedoic acid	ACLY	Lipid synthesis	Heterozygous familial hypercholesterolemia, established atherosclerotic cardiovascular disease
Hydroxychlorquine	Autophagy	Removal of damaged cellular components	Rheumatoid arthritis
Sulfasalazine	SLC7A11/xCT	Cystine/glutamate exchange	Ulcerative colitis
CPI-613	Mitochondria	Oxidative metabolism	Pancreatic cancer, AML, solid tumors, lymphoma
IM156	Mitochondria	Complex I	Solid tumors, lymphoma
IACS-010759	Mitochondria	Complex I	AML, advanced solid tumors
CB-839	Glutaminase	Glutamine to glutamate conversion	Leukemia, CRC, breast cancer, RCC
IPN60090	Glutaminase	Glutamine to glutamate conversion	Advanced solid tumors
DRP-104	Glutamine-utilizing enzymes	Glutamine-dependent enzymes	NSCLC, NHSCC, advanced solid tumors

AZD-3965	MCT1	Lactate symporter	Advanced cancers
TVB-2640	FASN	Fatty acid synthesis	NSCLC, CRC, breast cancer, astrocytoma
AG-270	MAT2A	Production of S-adenosylmethionine	Advanced solid tumors or lymphoma
SM-88	Tyrosine metabolism	Oxidative stress	Sarcoma, prostate, breast and pancreatic cancer
Indoximod	IDO1	Kynurenine synthesis	Melanoma, breast and pancreatic cancer

ACLY, ATP-citrate synthase; ALL, acute lymphatic leukemia; AML, acute myeloid leukemia; CLL, chronic lymphocytic leukemia; CML, chronic myeloid leukemia; CRC, colorectal cancer; DHFR, dihydrofolate reductase; DHODH, dihydroorotate dehydrogenase; FASN, fatty acid synthase; HNSCC, head and neck squamous cell carcinoma; IDH, isocitrate dehydrogenase; IDO1, indoleamine 2,3-dioxygenase 1; MAT2, S-adenosylmethionine synthase isoform type 2; MCT1, monocarboxylate transporter 1; NSCLC, non-small-cell lung cancer; PPAT, phosphoribosyl pyrophosphate amidotransferase; RCC, renal cell carcinoma; RNR, ribonucleotide reductase; THF, tetrahydrofolate; TYMS, thymidylate synthase. Modified from (Stine et al., 2022).

1.7 Mitochondria and cancer

1.7.1 Characteristics and functions of mitochondria

Mitochondrion is an intracellular organelle present in almost all eukaryotic organisms, also known as the *powerhouse* of the cell, due to the fact it is the hub of ATP synthesis. Apart from energy production, mitochondria participate in other cellular key functions such as biomass synthesis, control of Ca^{2+} homeostasis, autophagy, apoptosis regulation (Desagher & Martinou, 2000), and even immunogenic cell death (Riley et al., 2018)(see section 1.8).

This organelle is composed by a double membrane (the **inner** (IM) and the **outer membrane** (OM)) that delimitates two compartments with differential functions: the **matrix** and the **intermembrane space** (IMS). Through this membranous system, mitochondria form a dynamic and interconnected network with the rest of the cell compartments (Xia et al., 2019). Typically, the inner membrane -which is in contact with the matrix- is shaped by numerous bag-like invaginations, referred as a **mitochondria cristae,** in which the molecular machinery in charge of ATP production -known as **electron transport chain** (ETC)- is anchored (see section 1.7.3.1) (Kühlbrandt, 2015).

It was in the 1960s, when Lynn Margulis hypothesize that mitochondria come from prokaryotic organisms incompletely endocytosed by an elderly anaerobic eukaryotic cell (Sagan, 1967). This symbiotic alliance provided an advantage to the host cell as it developed the capacity to produce energy in aerobic conditions (Lane & Martin, 2010; Pittis & Gabaldón, 2016). Nowadays, this concept is accepted as the **endosymbiotic theory**, and it would eventually explain how the multicellular organisms have emerged and why current mitochondria display unique features that evoke regular bacteria.

Certainly, mitochondria are the only organelles in animal cells that contain their own genetic material (known as **mitochondrial DNA** (mtDNA)) which is located within the mitochondrial matrix compartment. Contrary to nuclear DNA, mtDNA is a super-coiled double-stranded closed circular genome formed by 37 genes: **2 ribosomal RNAs** (12s and 16s rRNAs, similar to bacteria), **22 transfer RNAs** (tRNAs) and **13 genes** that encodes for 13 protein subunits of the respiratory complexes composing the ETC (see **figure 23**) (Anderson et al., 1981; Andrews et al., 1999; Montoya et al., 2006). The mtDNA is characterized by a series of unique features when is compared with the nuclear DNA. First, the mtDNA is inherited exclusively from the maternal lineage and second, it is found in multiple copies (polyploidy) in the same cell.

More than 1,500 proteins composing mammalian mitochondria have been identified, indicating that this organelle strongly depends on the nuclear genes to maintain its basic functions (Schmidt et al., 2010). Thus, it is assumed that during years of evolution, the mtDNA genes that were originally from the alpha-protobacterium began to migrate to the nucleus and were incorporated into the nuclear genome resulting in the mtDNA as currently known (Adams & Palmer, 2003). This process is known as **numtogenesis** and it seems to be an ongoing process in some pathologies such as cancer (Ju et al., 2015; Srinivasainagendra et al., 2017).

1.7.2 Mitochondrial dynamics

Mitochondria are highly plastic organelles implicated in a plethora of cell functions. For instance, mitochondria intervene in fundamental process that are involved in cardiac function (Bonora et al., 2019). From metabolic functions to immunostimulatory effects (Weinberg et al., 2015), mitochondria dynamics are indispensable to preserve the correct functioning of the cell. Certainly, mitochondria undergo a continuous process of fission, fusion, transportation, and elimination (known as **mitophagy**, see section 1.8.2) that controls their morphology, quantity, disposition, and function (R. Quintana-Cabrera & L. Scorrano, 2023). Thus, dysregulation of mitochondrial dynamics and function is often associated with

pathologies such as cardiac disease and ischemia (Ding et al., 2017; Ong et al., 2010) or even cancer (Giampazolias & Tait, 2016).

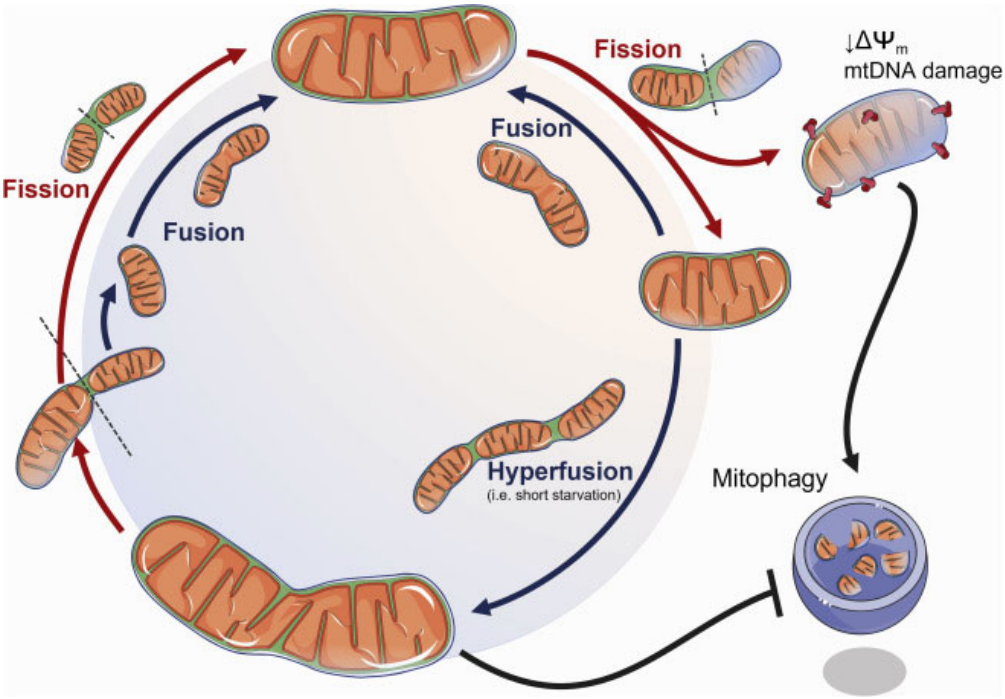

Figure 21. Mitochondrial fusion, fission and elimination cycle (Rubén Quintana-Cabrera & Luca Scorrano, 2023).

Mitochondria can undergo fission, typically in cases where mtDNA is damaged or mitochondria are depolarized ($\Delta\Psi_m$) (Kleele et al., 2021). During this process, the damaged components are pushed towards the part that will be segregated and subsequently eliminated by mitophagy (see **figure 21**).

However, this process is reversible as a daughter mitochondria resulting from the fission can fuse with other new mitochondria to generate a recomposed larger organelle fusion. Once the insult is resolved, hyperfused mitochondria enters in a new cycle of fission and fusion in order to preserve the mitochondrial network of the cell (Rubén Quintana-Cabrera & Luca Scorrano, 2023).

1.7.3 The mitochondrial electron transport chain (mETC) and the oxidative phosphorylation system (OXPHOS)

1.7.3.1 Composition, organization, and dynamics of the mECT

The majority of the cellular ATP pool is generated by the electron transport chain which is a supramolecular complex composed by respiratory complexes, electron carriers and the H^+-ATP synthase (Enríquez, 2016). The elements of the **oxidative phosphorylation system** (OXPHOS) couple the oxidation of the **nicotinamide adenine nucleotide** (NADH) and **flavine adenine dinucleotide** ($FADH_2$) to the pumping of protons across the inner membrane, generating a proton electrochemical gradient that is used by the **complex V** or **ATP synthase** to produce ATP from ADP (Acín-Pérez et al., 2008). Within the OXPHOS system, 5 respiratory complexes that are directly anchored in the IM can be distinguished:

- **Complex I (CI)**, also known as **NADH/ubiquinone oxidoreductase**, its function consists in accepting the electrons from the NADH and transfer them to the ubiquinone (also known as coenzyme -Q (CoQ)) to be reduced into $CoQH_2$. During this step, 4 H^+ per molecule of NADH are pumped into the intermembrane space.
- **Complex II (CII)**, also known as **succinate dehydrogenase**, accept the electrons from the $FADH_2$ obtained from the enzymatic conversion of succinate into fumarate during tricarboxylic acid (TCA) cycle. These electrons are subsequently transferred to the CoQ, promoting its reduction into $CoQH_2$. In this step, no protons are pumped.
- **Complex III (CIII)**, also known as **ubiquinol-cytochrome c reductase**, assists the electron transfer from $CoQH_2$ to the cytochrome c. During this oxidation-reduction reaction, 4 H^+ are pumped into the intermembrane space for each pair of electrons transferred.
- **Complex IV (CIV)**, also known as **cytochrome c oxidase**, is the final acceptor of the electrons proceeding from the CIII and that are transferred to O_2 in this step. During this process it is produced H_2O and 2 H^+ per NADH molecule are pumped to the intermembrane space.
- **Complex V (CV)**, also known as **ATP synthase**, is in charge of catalyzing the conversion of ADP into ATP to the mitochondrial matrix by the incorporation of a phosphate group. This reaction is sustained by the energy generated from the electrochemical proton gradient originated during the electron transport from CI to CIV. For the ATP synthesis, the protons from the intermembrane space are transferred back to the matrix through the pore formed by the F_o region of the ATP

synthase. The energy obtained during this step is used by the region F_1 of the CV to catalyze the formation of ATP by a rotary movement of this protein complex (see **figure 22**).

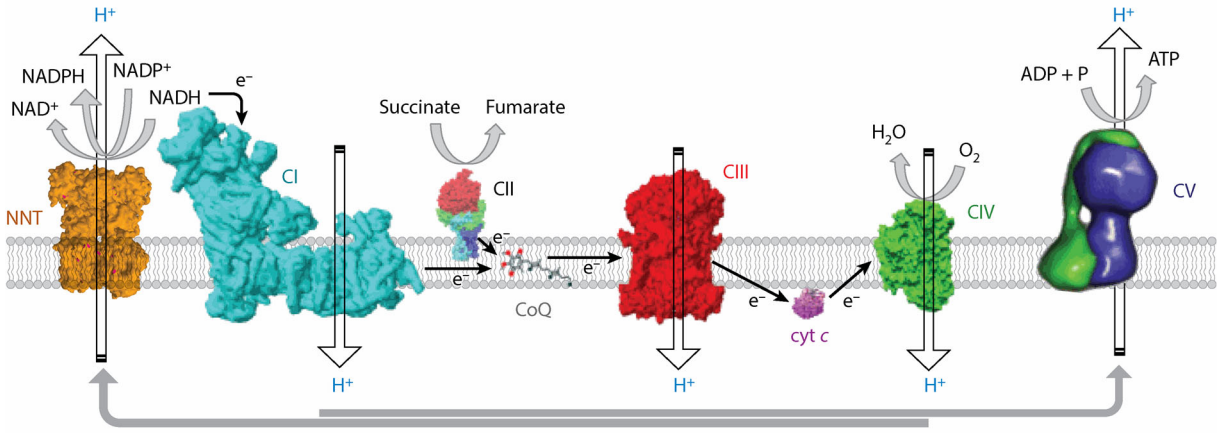

Figure 22. The electron transport chain. The electrons flow from the complex I to complex IV and the protons (H^+) are pumped from the intermembrane space into the mitochondrial matrix. At the end of the ETC, the protons from the matrix return to the intermembrane space through the complex V facilitating the production of ATP. Adapted from (Enríquez, 2016).

According to the plasticity model, respiratory complexes can be freely anchored in the mitochondrial membrane or establish associations between them forming a supramolecular protein complex referred a **supercomplexes** (when associated more than one) and **respirasomes** (the totality of the supercomplexes associations) (Acín-Pérez et al., 2008; Enríquez, 2016; Lobo-Jarne & Ugalde, 2018) (see **figure 24**). The type and the association level between all the complexes can vary from one cell type to another as it is known to be modulated by the cell energy demands, the type of tissue, nutrient resources availability or even by the dysfunction of the respiratory complexes (Lapuente-Brun et al., 2013; Marco-Brualla et al., 2019).

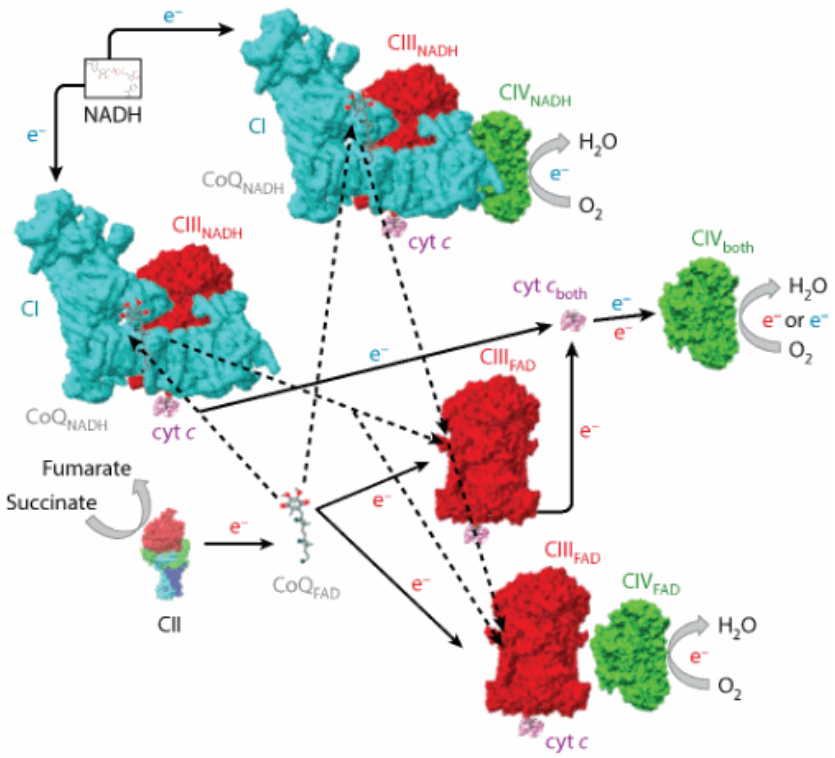

Figure 23. The plasticity model of the organization of the ETC. Modified from (Enríquez, 2016).

1.7.4 Role of mitochondrial in cancer

By virtue of all of its functions, mitochondria are essential organelles in life as they are the main intracellular components that controls cell homeostasis and survival. In consequence, dysfunctionality of mitochondria has been related to carcinogenesis (Galluzzi et al., 2010). Over the last years, numerous studies concerning mitochondrial implication in cancer have been carried out (Ahn & Metallo, 2015; Ghosh et al., 2020; Giampazolias & Tait, 2016; Grasso et al., 2020; Marco-Brualla et al., 2019; Porporato et al., 2018), and a plethora of processes that are directly interconnected with mitochondria have been identified as potentials hallmarks of cancer (Hanahan, 2022; D. Hanahan & Robert A. Weinberg, 2011). For example, cancer cell evasion from cell death is a process that ultimately implicates mitochondria (Carneiro & El-Deiry, 2020; Igney & Krammer, 2002). Indeed, the partial loss of P53 activity contributes to the resistance to the mitochondrial apoptotic pathway induced by DNA-damage (Muller & Vousden, 2013). Up-regulation of the anti-apoptotic proteins (e.g., BCLXL, BCL2, MCL1) or failure in MOMP formation are also known to contribute to apoptotic-cell death evasion and therapy resistance (see section 1.3.1.1.2).

1.7.4.1 Implications of mitochondrial DNA mutations

Mitochondria is in charge of cellular energetics which are de-regulated in cancer cells in order to sustain their increased nutrient demands. The metabolic adjustments observed can be a direct consequence of mutations in metabolic enzymes that could act as oncogenic drivers. For instance, recurrent mutations in isocitrate dehydrogenase (IDH), the enzyme that catalyzes the oxidation of isocitrate to α-ketoglutarate in mitochondria have been identified in cases of glioblastoma, sarcoma and myeloid leukemia (Chen et al., 2013; Lu et al., 2013; Rohle et al., 2013). Moreover, mutations in mtDNA or in mitochondrial genes localized in the nucleus can affect both mitochondrial function and mitochondrial-associated metabolic pathways. For instance, several mutations in CII components have been reported in neuroendocrine tumors (Gimm et al., 2000; Niemann & Müller, 2000). Indeed, malfunction of the electron transport chain is known to cause ROS production which represents a source of DNA-damage (Kowaltowski & Vercesi, 1999). For a summary of mtDNA mutations associated with different types of cancer see **figure 24**.

There is a large list of mitochondrial effects on cancer cells that have been documented and yet there is a lot more to explore. For obvious reasons, this work will focus only on a minimal part of this subject.

According to what has been discussed in previous sections, mitochondria are the only extra-nuclear cell compartment that contains its own DNA. Despite being surrounded by a double membrane, its genetic material is located within the mitochondrial matrix exposed to numerous mutagenic agents such as ROS that are produced as a result of the electron transport chain's activity (Ishikawa et al., 2008; Raimondi et al., 2020; Yakes & Van Houten, 1997; Yang et al., 2016). As previously mentioned, mtDNA is also found in many copies per cell. Thus, the combination of these factors predisposes to the acquisition of *de novo* mtDNA mutations that could affect the correct functioning of the organelle and it would contribute to the development of pathologies (Chinnery et al., 2000; Kopinski et al., 2021).

mtDNA mutations can either affect all the DNA molecules or only a portion of them. The presence of two or more variants of mtDNA copies is referred as **heteroplasmy** while a cell harboring identical copies of their mitochondrial genome is referred as **homoplasmy**. The level of the heteroplasmy can vary between cells within the same tissue or organ, and between members of the same family (He et al., 2010; Stewart & Chinnery, 2015). However, the degree of heteroplasmy and the threshold level of mtDNA mutations that a cell must exceed to exhibit clinical pathologies is still not well defined (Kopinski et al., 2021). It is believed

that mutation heteroplasmy under clinical thresholds equal to 60 or less are not relevant for the immediate manifestation of the disease (Kim et al., 2022).

Consistently, a wide range of mtDNA mutations has been reported in many cancer types (Brandon et al., 2006; Chinnery et al., 2002; J. F. Hopkins et al., 2017; Lu et al., 2009; Petros et al., 2005; Reznik et al., 2016; Yuan et al., 2023). Indeed, tumoral cells deprived of mtDNA – known as **rho 0** (ρ^0) cells – exhibit a reduced proliferation rate as well as delayed tumor formation (Cavalli et al., 1997; Morais et al., 1994; A. S. Tan et al., 2015), a fact that sustains the influence of mtDNA in cancer development (Cruz-Bermúdez et al., 2015). Indeed, mtDNA mutations could affect the ETC activity that would impair their respiratory capacity and their ability to generate ATP. As Otto Warburg postulated more than a century ago, mtDNA mutations could drive cancer cells to rewrite its metabolism to adapt and survive. These metabolic changes could also affect to other cellular pathways that are directly associated with tumorigenesis (Martínez-Reyes & Chandel, 2021). One of the examples is the hypoxia inducer factor 1 alfa (HIF-1α) that has been demonstrated to be active in cells undergoing the Warburg effect (Bao et al., 2021) which is also known to be associated with cancer and metastasis (Birner et al., 2000; Bos et al., 2003; Schindl et al., 2002; Semenza, 2003).

Despite all the scientific evidence that exists around this topic, mtDNA mutations could partially but not totally explain the metabolic rewriting observed in cancer cells which is nowadays considered as one of the hallmarks of cancer (D. Hanahan & Robert A. Weinberg, 2011). The degree of impact that mtDNA mutations could have in this scenario remains unclear. Hence, further studies are needed to comprehend these pathways as well as to characterize tumor-associated mitochondrial phenotypes.

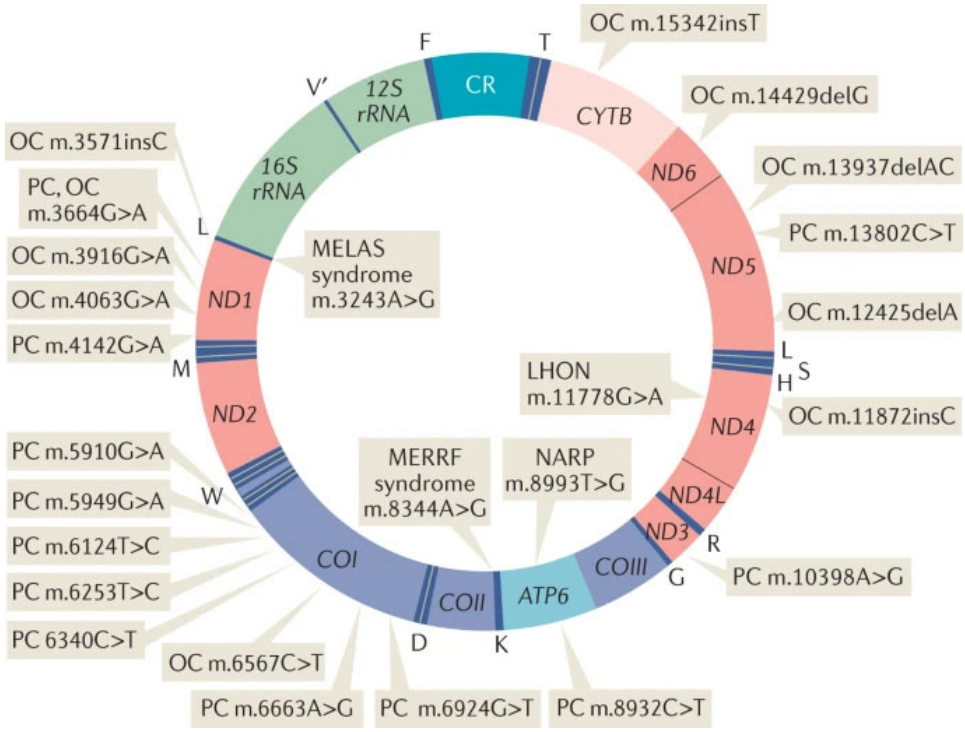

Figure 24. Human mtDNA map and different variants identified as potential pathogenic (Kopinski et al., 2021). PC, prostate cancer; OC, oncocytoma; CR, control region; MELAS, mitochondrial encephalomyopathy and stroke-like episodes syndrome; LHON, Leber hereditary optic neuropathy; MERRF, myoclonic epilepsy and ragged red fiber; NARP, neurogenic muscle weakness retinitis pigmentosa.

1.8 Mitochondrial role in ICD

In connection with what has been discussed in the previous sections of this work, it has been demonstrated that mitochondria is a source of danger signals with capacity to regulate the activation of inflammation (Jin et al., 2017). The exceptional similarities between mitochondria and bacteria (see section 1.7.1 for more information) leads to the engagement of pathogenic-like immune responses in situations when mitochondrial internal components are released into the cytosol (see **figure 25**). mtDNA, **mitochondrial antiviral signaling protein** (MAVS), mtROS production, cardiolipin, N-formyl peptides (NFPs), ATP and succinate (Rodríguez-Nuevo & Zorzano, 2019) are some of the key triggers for the activation of inflammatory pathways, and that are usually linked to cell death processes (Vringer & Tait, 2023).

For instance, the hypermethylated CpG rich motifs of mtDNA can stimulate the endosomal Toll-like receptor 9 (TLR9) and activate the innate immune response (Latz et al., 2004). Another example of mitochondrial DAMP that is shared with bacteria is the phospholipid cardiolipin. This molecule located within the mitochondrial matrix can activate mitophagy when is externalized in the OMM (Chu et al., 2013) promoting the activation of the NLRP3 inflammasome (see section 1.3.1.3). Moreover, the discovery of the CGAS/STING1 signaling pathway as a sensor of cytosolic dsDNA and its connection with type I IFN-mediated immune responses confirm the immunostimulatory capacity of this organelle (Kwon & Bakhoum, 2020).

The release of signals that activate pro-inflammatory pathways occur during MOMP which is also the converging point for the activation of the mitochondrial apoptotic cell death pathway (see section 1.3.1.1.1). This observation indicates that the activation of the apoptotic pathway triggers, at least partially, inflammation. However, caspases, which are the main executioners of this molecular signaling have been identified as inhibitors of pro-inflammatory pathways after MOMP formation (Ning et al., 2019; Rodriguez-Ruiz et al., 2019; A. Rongvaux et al., 2014; White et al., 2014). This fact supports the idea that apoptosis is an immunosilent event when caspases are activated. Consequently, caspases appear to be the key determinants in the inflammatory output accompanying the cell death process. Thus, blocking caspases could be presented as a strategy to boost anti-tumor immune responses induced by radiotherapy and/or chemotherapy (Giampazolias et al., 2017; Rodriguez-Ruiz et al., 2019). In fact, this manipulation would induce a rather necroptotic cell death process, especially if elicited by death receptors (see section 1.3.1.1.2.1).

Nonetheless, the pan-caspase inhibitor Emricasan known to accumulate in the liver, is now in clinical trials for the management of **non-alcoholic fatty liver disease** (NASH) and liver transplants showing limited beneficial effects (Frenette et al., 2019; Harrison et al., 2020).

Despite all previously mentioned, the molecular process by which mtDNA is released into the cytosol and promotes inflammation is a matter of debate. On one hand, scientific evidence points that the canonical mtDNA release to the cytosol is mediated via the MOMP pore formed by BAX and BAK oligomerization (Cosentino et al., 2022; McArthur et al., 2018; Riley et al., 2018). However, there are also scientific evidence suggesting that the formation of the **mitochondrial permeability transition pore** (mPTP) would be sufficient for the release of the mtDNA to the cytosol despite its much-reduced size (Nakahira et al., 2011). Even though we understand the fundamentals of this pathway, the discovery of new alternative regulation mechanisms adds more complexity to this question (Riley & Tait, 2020).

In any case, it is beyond the doubt that mitochondrial-driven inflammation can enhance immunogenic cell death and it may be therapeutically exploited to improve cancer treatment (Vringer & Tait, 2023).

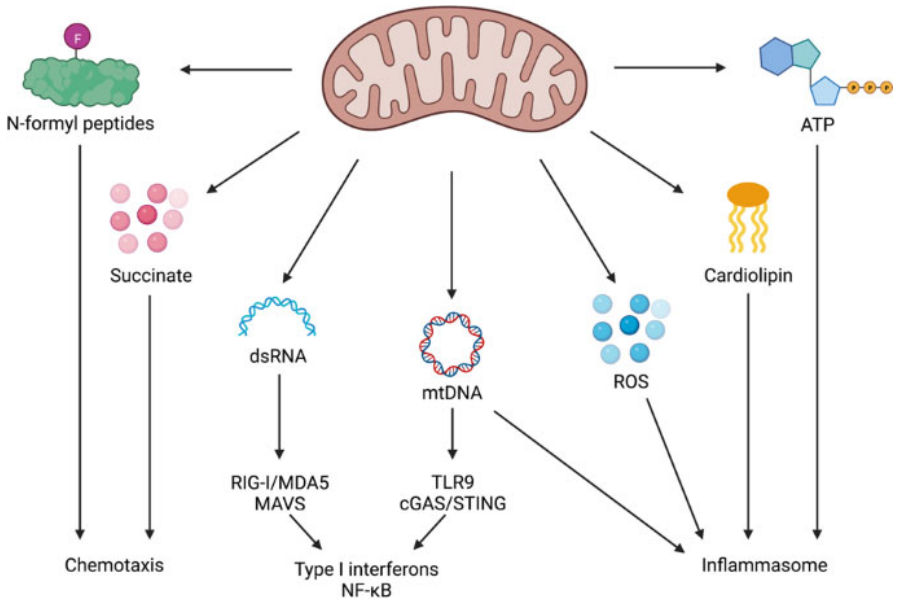

Figure 25. Mitochondria-derived DAMPs and the possible outcomes (Vringer & Tait, 2023).

1.8.1 Cytosolic dsDNA sensor: the CGAS/STING1 pathway

The **CGAS/STING1** pathway is an evolutionary preserved molecular mechanism that mediates immune responses against pathogenic infections (Ishikawa & Barber, 2008; Jenson & Chen, 2020; West et al., 2015). CGAS is a DNA sensor that recognizes extracellular double strand DNA (dsDNA) -from viral, bacterial or plasmid origin- as well as cytoplasmic free self-dsDNA from nuclear and/or mitochondrial origin. The acquisition of DNA breakages in precancerous cells during tumorigenesis, exposure to classical mitochondrial -targeting chemotherapy or micronucleus formation are some of the main causes of DNA fragmentation and release to the cytosol. In this scenario, CGAS recognizes free DNA fragments and catabolizes the CGAMP production by employing ATP and GTP as a substrate for the reaction. Subsequently, CGAMP binds and activate the **stimulator of interferon genes** (STING1) which is associated to the endoplasmic reticulum (ER) membrane. At this level, STING1 mediates the activation by the NF-κB pathway and/or the phosphorylation of IRF3, both transcription factors with the capacity to migrate to the nucleus and stimulate the transcription of type I IFN and other proinflammatory cytokines, such as TNF-α and IL-6

(see **figure 26**) (Kim et al., 2023; Sun et al., 2013). Among others, type I IFN plays an important role in antitumor responses as it mediates the connection between the innate immune response (Stetson & Medzhitov, 2006) and T-cell immunity (Ishikawa & Barber, 2008). Due to the fact that this pathway is involved in the activation of the innate immune system (Woo et al., 2014), its dysregulation has been linked with a broad range of human pathologies including cancer (Samson & Ablasser, 2022).

However, it seems that the CGAS/STING1 pathway could have a dual role in tumor development. From one point of view, it could display a pro-tumor role by inducing chronic inflammation (S. F. Bakhoum et al., 2018; Q. Chen et al., 2016). For instance, it has been reported that chronical stimulation of the CGAS/STING1 pathway by some carcinogenics such as DMBA may innduce inflamation-driven tumorigenesis (Ahn et al., 2014). In this particular case, targeting CGAS/STING1 signaling seems to be an attractive therapeutic option for cancer (Conlon et al., 2013; Tang et al., 2016), including its use as adjuvant in combination with chemotherapy or radiotherapy (Khoo & Chen, 2018). From other perspective, there are some works that supports that the activation of the CGAS/STING1 patway supresses cancer development by inducing cellular senenscense and by promoting immuno-surveillance (Glück et al., 2017; Yang et al., 2017). Moreover, it has been reported that functional cGAS/STING1-type I IFN pathway is requiered to obtain sucessful radiation-mediated antitumor responses (Deng et al., 2014).

According with the mentioned before, the combination of CGAS/STING1 activators with immunotherapy (e.g., immunocheckpoint blockade) could result into an improval of the anticancer treatments efficacy (Wang et al., 2017).

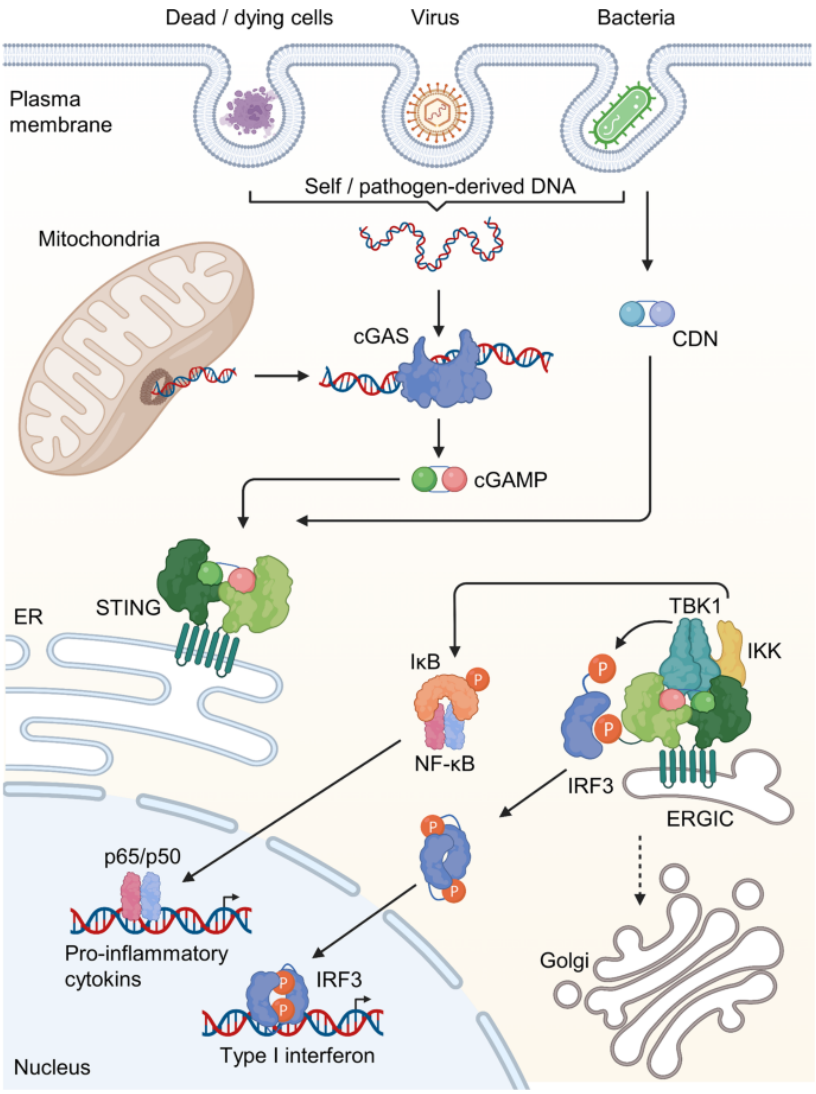

Figure 26. Overview of the CGAS/STING1 signaling pathway (Kim et al., 2023).

1.8.2 Specific autophagy: mitophagy

Mitophagy is a specific form of autophagy that selectively removes dysfunctional, damaged, or superfluous mitochondria to preserve cell homeostasis (Palikaras et al., 2018). Mitophagy works in coordination with mitochondrial dynamics and biogenesis (see section 1.7.2) controlling the quality and the quantity of these organelles within the cell.

The canonical pathway of mitophagy is mainly controlled by **phosphatase and tensin homologue (PTEN)-induced putative kinase 1 (PINK1) - Parking** pathway. In healthy physiological conditions, PINK1, is rapidly cleaved and degraded in a proteasome-dependent manner. Contrary, in conditions of

depolarization of the IMM, PINK1 is not degraded and stabilized on the OMM (Gan et al., 2022). Subsequently, PINK1 recruit Parking that ubiquitinates several mitochondrial components of the OMM for organelle degradation. The ubiquitinated proteins recruits general autophagy adapters such as **p62** and **optineurin**. Then, the tagged mitochondria interacts with **LC3**-positive autophagosomes that eliminate the damaged organelles (Palikaras et al., 2018).

Considering mitophagy as a system of mitochondrial fitness surveillance, impaired mitophagy causes the accumulation of dysfunctional mitochondria which has been associated with the development of several neurodegenerative disease such as Parkinson, Alzheimer or Huntington disease (Chen et al., 2018; Fang et al., 2019; Hwang et al., 2015) as well as with cancer development (Chang et al., 2017).

In the cancer setting, mitophagy appears to play a dual role, depending on the type and status of the cell. On one hand, in early stages of tumor development, mitophagy maintains cell homeostasis by removing dysfunctional ROS-producing mitochondria that could potentially promote tumorigenesis (Raimondi et al., 2020). However, once the tumors are already progressing, mitophagy can represent a cytoprotective mechanism for cancer cells against radiotherapy/chemotherapy-induced mitochondrial damage or apoptosis (Yan et al., 2017).

Moreover, mitochondria is known to be involved in inflammatory processes that are linked to the activation of the immune system. As previously described, damaged mitochondrial can release its own mtDNA into the cytosol and activate the CGAS/STING1 pathway, promoting the production and release of type I IFN (see **figure 26**). Thus, it seems logical to hypothesize that, activated mitophagy would also contribute to tumor-immune evasion by reducing the ability of the "ICD inducers" to boost antitumor immune responses (see section 1.5.8). Indeed, over the last few years, several works that supports this hypothesis have been published (Glytsou et al., 2023; Li et al., 2019; Limagne et al., 2022; Liu et al., 2020; Villa et al., 2017; Yao et al., 2019; Zhao et al., 2022).

In addition, Yamazaki and colleagues demonstrates that autophagy (but not specific mitophagy) represses the **abscopal effect** observed in the context of radiotherapy by limiting the CGAS/STING1-type I IFN-dependent signaling (Takahiro Yamazaki et al., 2020). In the same line, Glytsou and co-workers showed that mitophagy promotes resistance to BH3 mimetics in acute myeloid leukemia (Glytsou et al., 2023). Moreover, a recent work in the context of inflammation and aging demonstrated that mitophagy is involved in the clearance of cytosolic mtDNA from old-damaged mitochondria. This directly impairs the activation

of CGAS/STING1 pathway restricting type I IFN production and inhibiting chronic inflammation (Jiménez-Loygorri et al., 2024).

Hence, blocking mitophagy seems a rationale for the improvement of anti-cancer therapies, especially in combination with immunotherapy, although a lot of work is still needed to deeply characterize this mechanism.

1.9The L929/L929dt mouse model

1.9.1 *In vitro* and *in vivo* characterization of a new L929-derived cell line

L929 was one of the first cell lines to be established in continuous culture. It is an immortalized fibroblast mouse cell line growing in adherent monolayer derived from the L strain of a normal subcutaneous areolar and adipose tissue from a 100-day-old male C3H/An mouse. After the 95th subculture passage, in March 1948, the clone 929 was isolated by the capillary technique for single cell isolation (Gavilondo et al., 1982; Rodríguez et al., 1984; Sanford et al., 1956).

In a previous work carried out by our research group, we have generated a L929-subline by collecting spontaneous detached cells that were present floating in the culture dish which were referred as L929dt (dt coming from English "detached"). Interestingly, after several passages, these cells kept growing in suspension and never re-acquired the adherent phenotype (Catalán et al., 2015).

Later, the characterization study revealed that L929dt cells displayed some of the typical characteristics of tumor cells that are in an advanced metastatic stage of the disease. The findings related to this new L929-derived cell line are listed below (Marco-Brualla et al., 2019):

1. Accelerated growth and division: L929dt grow faster compared to L929 when maintained in fermentative medium (high-glucose), with almost 2-fold increase in the duplication time when cultured in galactose restricted media.
2. Metabolic changes: Seahorse analysis revealed that L929dt cells are higher glucose consumers than L929 cells together with an increased in lactate production and a drastic reduction in their oxygen consumption rate. These features suggest that these cells underwent a Warburg-like metabolic remodeling displaying an elevated acidification rate typically observed in cells with a fermentative phenotype (see section 1.6.1).

3. **Acquisition of two mtDNA mutations in the *ND2* subunit of the respiratory complex I**: Two variations in the C4859T and C4206T mtDNA sequences caused the replacement of a histidine to a tyrosine at position 316, and a replacement of a methionine for a threonine at position 98, respectively.
4. **Changes in the activity and dynamics of the components of the ETC**: A reduction in the formation of supercomplexes containing complex I (I + III and I + III + IV) was observed as well as a partial reduction of the individual complex I expression. Moreover, complex I activity (individually or in association with CIII) was demonstrated to be substantially reduced in L929dt cells compared to the parental L929. Contrary, CII and CII + CIII activity was detected to be increased, revealing the existence of a compensatory mechanism in response to CI malfunction. Those defects in the ETC were also confirmed by testing L929dt sensitivity to the PDK1 inhibitor DCA which resulted especially toxic against L929dt cells.
5. **Increased general and mtROS production levels as well increased activity of antioxidant enzymes**: Superoxide levels appeared to be higher in L929dt cells, probably as a result of the defects in the ETC already mentioned. In addition, the activity of the ROS detoxification enzymes **catalase** and **superoxide dismutase** (SOD) were greatly enhanced L929dt cells. This feature has been associated with an adaptation of metastatic cells to oxidative stress due to cell detachment (Piskounova et al., 2015).
6. **Lower antigenicity**: L929dt cells showed a reduction in their antigenic presentation capacity due to a drastic reduction of MHC-I exposure on their membrane surface.
7. **Higher tumorigenicity *in vivo***: According to *in vivo* experiments, L929dt cells are able to form bigger tumors at higher rate than L929 cells and to generate higher number of metastasis.

1.9.2 Transmitochondrial cybrid generation between L929 and L929dt cells

After the identification of specific mtDNA mutations harboring by L929dt cells, our research group sought to understand if the genetic changes acquired during the generation of these cells were the responsible of their increased tumorigenic and aggressive phenotype both *in vitro* and *in vivo*. For this purpose, Marco-Brualla and our team generated transmitochondrial cybrids between L929 and L929dt cell lines consisting in two step-process: (1) the previous elimination of the mitochondria from the recipient cell line and (2) the subsequent repopulation with mitochondria from a different cell type (Bacman et al., 2020; King & Attardi, 1989; Liao et al., 2020; Marco-Brualla et al., 2019) (see **figure 27**). The result of this

procedure allowed us to obtain two transmitochondrial cybrids that were named as $L929^{dt}$ and dt^{L929}. The $L929^{dt}$ cybrid harbors the nuclear background of the parental L929 cells but the mutated mitochondria of the L929dt cells. Contrary, dt^{L929} cybrid contains the nuclear background of the L929dt cells but the **wild type** (WT) mitochondria from the L929 cells.

Remarkably, the mitochondrial exchange between cells caused in the repopulated mitochondrial recipient cell lines the acquisition of the same phenotype than their respective mitochondrial donor: parental L929 cells with L929dt mitochondria lost matrix attachment and MHC-I expression. Conversely, L929dt cells with the L929 mitochondrial background re-acquired the adherence to the culture dish and MHC-I expression. In addition, cybrid cells showed the same pattern of sensitivity to DCA-induced cell death and *in vivo* tumorigenic properties than mitochondrial donor cells. This model will be used in this work performed on this Doctoral Thesis.

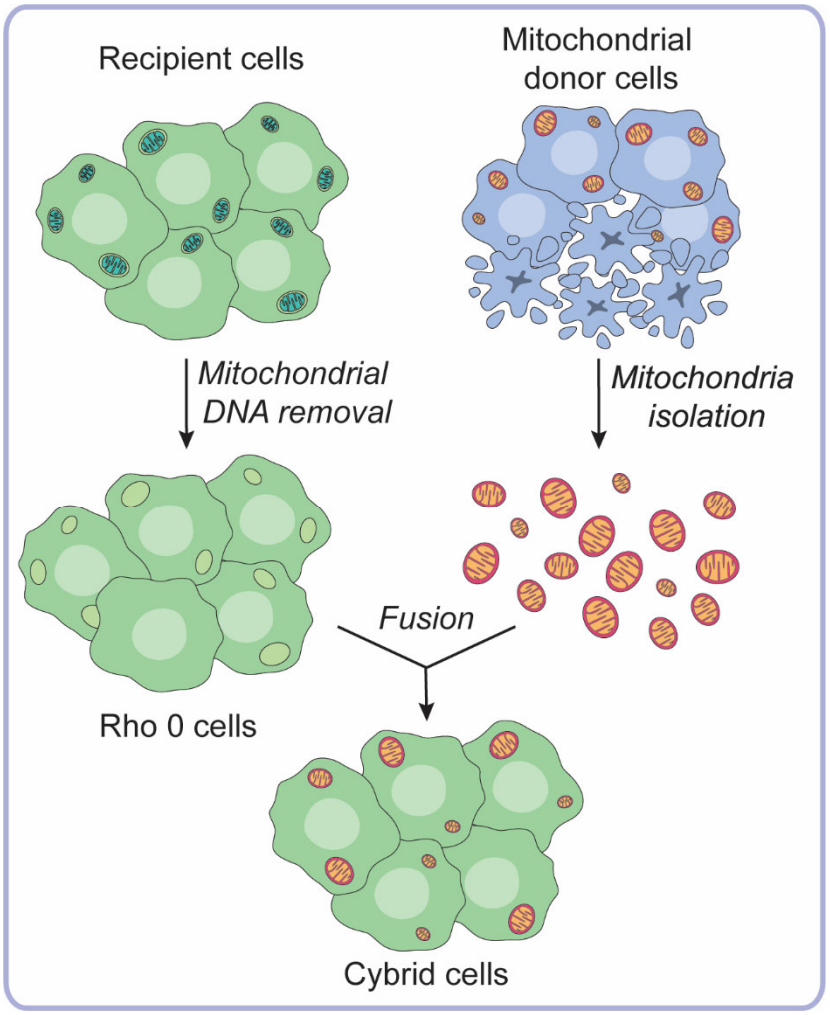

Figure 27. Schematic representation of the transmitochondrial cybrid generation process (Soler-Agesta, 2024).

1.10 Prostate cancer

1.10.1 Basic concepts of the disease

The prostate is a small and rubbery gland of the male reproductive system located below the bladder in between the penis and the rectum. Its principal function is the production of the seminal fluid that forces the semen through the urethra during ejaculation (NIH, 2024a).

According to the World Health Organization, prostate cancer is the leading cancer diagnosed among men and the second most common overall with 288,300 expected cases (WHO, 2024).

Most of the prostate cancer types are **adenocarcinomas** derived from the prostate gland cells. However, there are other forms of prostate cancer such as **small cell carcinoma** (regular or neuroendocrine), **large cell carcinoma**, **transitional cell carcinoma** and **sarcoma,** but they are very rare (American Cancer Society, 2024). Typically, prostate cancer is relatively a slow-growing type of cancer and its main sustain are the androgens hormones, mainly testosterone (Prostate Cancer Foundation, 2024). Its diagnosis is based on complementary techniques such as digital rectal examination that seeks for lumps or hard areas, the analysis of the levels of the **prostatic specific antigen** (PSA) in serum, biopsies from the prostate gland as well as magnetic resonance imaging (MRI) and computed tomography (CT) scan.

The stage of the disease is classified according to the **Gleason Grade** given by the pathologist after the examination of the biopsy. Grades 1-5 rate the primary and secondary most common pattern of cells within the biopsy. Usually, malignant tissues scores 6 or more in the Gleason scale. A score of 7 means that it is an intermediate risk of cancer, and higher scores from 8-10 means there is a high risk that the cancer keeps growing and generate metastasis (Swanson et al., 2021).

In most cases, prostate cancer does not cause any symptoms, specially at early stages. However, if the cancer has already spread to other parts of the body (also known as a **metastatic prostate cancer**, see next section 1.10.3) the patients can experience continuous back or bone pain with risk of fracture, tiredness, and loss of weight.

Nowadays, there are different types of treatment options available for localized, no metastatic prostate cancer cases. The three most common treatments are the following (Cancer Research UK, 2024b):

1. **Radiotherapy**:

   - ✓ **External beam radiotherapy for prostate cancer**. It consists in using high energy waves similar x-rays to irradiate the patient from the outside of the body. This treatment option is frequently combined with hormone therapy.

   - ✓ **Brachytherapy for prostate cancer** is a type of internal radiotherapy performed inside of the prostate. Also known as **permanent seed brachytherapy,** the radiation might stay inside of the organ, and it is gradually released over the months. In this modality it also exists the **high dose rate brachytherapy** (or **temporary brachytherapy**) which consists in the irradiation of the internal part of the prostate but for a short time period of about 15 to 40 minutes.

2. **Hormone therapy**: Due to the fact that prostate cancer cells depend on testosterone to grow, hormone therapy seeks to block the action of this hormone in order to control cancer cell growing. There are three types of hormonotherapy that are currently used in the clinic**:** (1) **Luteinizing hormone-releasing hormone agonists** (LHRH agonists or LH blockers) such as leuprolerin, goselerin acetate, triptorelin, that regulates the **luteinizing hormone** (LH). (2) **Gonadotrophin-releasing hormone antagonists** (GnRH blocker) that blocks the pituitary gland from producing the follicle-stimulating hormone (FSH). Both LH and FSH are in charge of controlling the amount of testosterone produced by the testicles. (3) **Anti androgens** that block the testosterone receptor of prostate cells. Some of the examples are enzatulamide or cyproterone acetate.

3. **Surgery**. **Radical prostatectomy** is the type of surgery that consists in removing the entire prostate gland and the surrounding lymph nodes to reduce the testosterone levels in the body.

   In advanced stages of the disease, when the patient does not respond to the androgen deprivation therapy, and the cancer has metastasized, is referred as **metastatic castration-resistant prostate cancer** (mCRPC) stage that it is detailed in the following section 1.10.3.

Usually, the disease evolution and the treatment effectiveness is controlled by monitoring the levels of PSA in blood. Nonetheless, PSA level does not seem to be a reliable marker because (1) fails to

discern between an indolent and aggressive prostate cancer and (2) PSA is also found in normal prostate cells. Thus, in recent years, **prostate specific membrane-antigen** (PSMA) has gain interest in the oncology field (Ahmadi et al., 2023). PMSA is type II transmembrane glycoprotein only expressed in prostate cells that has been considered as more reliable biomarker for **theragnosis**, a treatment strategy that combines both diagnosis and therapy by employing radioligands. For instance, **lutetium-177 (177Lu)-PSMA-617** is a radioligand that delivers beta-particle radiation to PSMA-expressing cells that is currently in clinical trials for the detection and treatment of mCRPC (see **figure 28**) (Almuradova et al., 2024; Sartor et al., 2021).

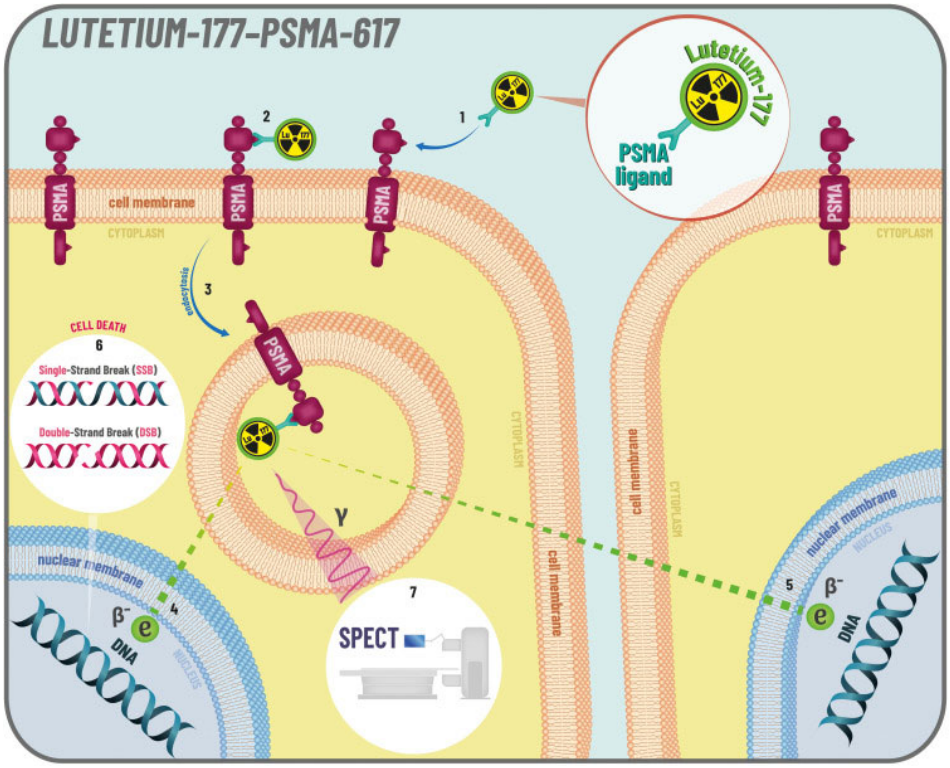

Figure 28. Mechanism of action of lutetium-117-PSMA-617, a radioligand used for diagnosis and treatment (Ferretti et al., 2023).

1.10.2 Molecular basis of prostate cancer

Prostate cancer is known to be an heterogenous disease with many molecular alterations and chromosomal aberrations reported. Chromosome mutations in the **ETS-related gene** (ERG) oncogene which is involved in hematopoiesis, angiogenesis, and bone development are frequent in prostate cancer.

Indeed, ETS is overexpressed in 50% of prostate cancer cases and often presents 5' aberrant gene fusions (Hermans et al., 2006; Soller et al., 2006; Tomlins et al., 2005).

Defects in the genes coding for the **androgenic receptor** (AR) are other common chromosomal abnormalities found in prostate cancer. The AR is essential as it controls the normal physiological function of the prostate gland. This intracellular receptor is highly sensitive to dihydrotestosterone (DHT) that upon binding to the AR induces the release of heat-shock proteins and receptor dimerization and phosphorylation. Subsequently, the AR receptor is translocated to the nucleus where it acts as a transcriptional activator of several genes (M. H. E. Tan et al., 2015). The AR-V7 or AR3 **splicing variations** are the most frequent AR variations encountered in prostate cancer (Guo et al., 2009). Indeed, most of the cases of castration resistance (i.e., the tumor keeps growing even if the gonads are not producing androgens) are related to genetic alterations that lead to the production of AR lacking ligand-binding domain and maintains the receptor constitutively active (Attard et al., 2016).

Somatic mutations in **phosphatase and tensin homolog** (PTEN) tumor suppressor gene has also been identified as recurrent feature of the disease. PTEN converts the phosphatidylinositol 3,4,5 triphosphate (PIP_3) into phosphatidylinositol 4,5-biphosphate (PIP_2) which blocks the activation of the PI3K/AKT/mTOR molecular cascade. Thus, certain mutations in PTEN or the loss-of-function of this phosphatase results in the activation of the PI3K/AKT pathway that is involved in controlling cell metabolism, growth, proliferation and apoptosis (Engelman et al., 2006). Activation of PI3K signaling correlates with resistance to castration and poor outcomes (McMenamin et al., 1999). In addition, AR activity is directly interconnected with this pathway (Carver et al., 2011; Tortorella et al., 2023). Moreover, pathogenic variants of ***BRCA 2*** gene – involved in the DNA damage response pathway – has been associated with higher prostate cancer risk (Agalliu et al., 2009; Gallagher et al., 2010). Additional inheritance and other genetic factors such as RAS, RAF, c-MYC and P53 are also known to have a significant function in prostate cancer (Gandhi et al., 2018).

1.10.3 Castration-resistant prostate cancer (CRPC) and metastatic castration-resistant prostate cancer (mCRPC)

As discussed in the previous section, deprivation hormone therapy is one of the main strategies to control the early stages of prostate cancer. Unfortunately, the general trend for these patients is the development of a castration-resistant disease which is in most of the cases inevitable, complex to manage

and with high lethality rate (Devasia et al., 2023). In addition, the acquisition of resistance to hormone deprivation therapy is normally associated with metastasis.

The most common metastasis sites are the inguinal lymph nodes (causing the swelling of the legs, known as lymphoedema), liver, lungs (causing respiratory problems) and bones (spine, pelvis ribs and skull). When the tumor spreads to the spine can cause the compression of the spinal cord which is considered a life-threating condition (Cancer Research UK, 2024a; Loblaw et al., 2005).

1.10.3.1 Current therapies

Nowadays, the indication regimes to treat **CRPC** and **mCRPC** patients are very diverse. The most common are **chemotherapy** such as docetaxel and cabazitaxel that acts inhibiting microtubular polymerization, and **platinum-based therapy** such as cisplatin and carboplatin that form adducts with the DNA and blocks cell replication (see section 1.12). Radiotherapy with radium-223 or ^{177}Lu-PSMA-617 are less frequent as they still under investigation. Targeted therapies such as PARP or PI3K/Akt/ mTOR inhibitors have also shown benefits in patients with terminal disease (Schaeffer et al., 2022).

For patients with bone metastases, it is indicated the use of bone maintenance therapy such as a **zoledronic acid** or **RANK ligand inhibitors** that bocks the reabsorption of the bone by osteoclasts and prevents from bone fractures and skeletal-related events (Saad et al., 2004).

Despite we are in the era of cancer immunotherapy, prostate cancer is still one of the tumor types with lower responses. Actually, clinical trials using the anti-PD-1 **nivolumab** in mCRPC did not show significant response rates (Topalian et al., 2012), neither with **pembrolizumab** (Philippou et al., 2020). Other phase II and phase III clinical trials of the immune check-point inhibitor anti-CTLA-4 **ipilimumab** after receiving chemotherapy or in combination with radiotherapy, showed no objective and no long-term safety signals in a cohort including mCRPC patients (Fizazi et al., 2020). Hence, the limited activity of the single-agent check-point inhibitors in advanced disease suggest the need of combinatorial regimes to expand the benefits of immunotherapy in this type of cancer.

Sipuleucel-T based on autologous dendritic cells vaccine or other tumor-associated based vaccines as well as adoptive cell therapy are showing encouraging results but still in preliminary stages of development (Sridaran et al., 2023).

1.10.4 Prostate cancer metabolism

Prostate secretory epithelial cells have a specialized function as they are in charge of secreting the seminal liquid which is remarkably rich in **citric acid** (around 12-fold higher than blood plasma levels). The physiological role of citrate produced by the prostatic glands is to acidify the vagina introitus and to favor the spermatozoid motility and fecundation ability (Verze et al., 2016). Accordingly, normal prostate cells transforms glucose into acetyl-CoA that fuels the **tricarboxylic acid** (TCA) **cycle** in where the citrate is produced. In other cellular types, citrate would be oxidized to produce metabolic intermediates but in this case accumulated is and secreted into the prostatic lumen (Barron & Huggins, 1946). The impaired oxidation of citrate is mainly due by the inhibition of **mitochondrial aconitase** (m-aconitase) which is the enzyme responsible to catalyze the isomerization of citrate to isocitrate within the TCA cycle. The activity of the enzyme aconitase is controlled by **zinc** levels that results to be extremely high in this tissue compared to normal blood plasma levels (around 200-fold increase). Thus, zinc accumulation in mitochondria blocks the activity of the aconitase that truncates the TCA cycle and leads to the accumulation of citrate (see **figure 29**) (Costello & Franklin, 1981; Costello et al., 1997). As a result, normal prostate cells are highly reliant on glycolysis and less dependent on OXPHOS metabolism.

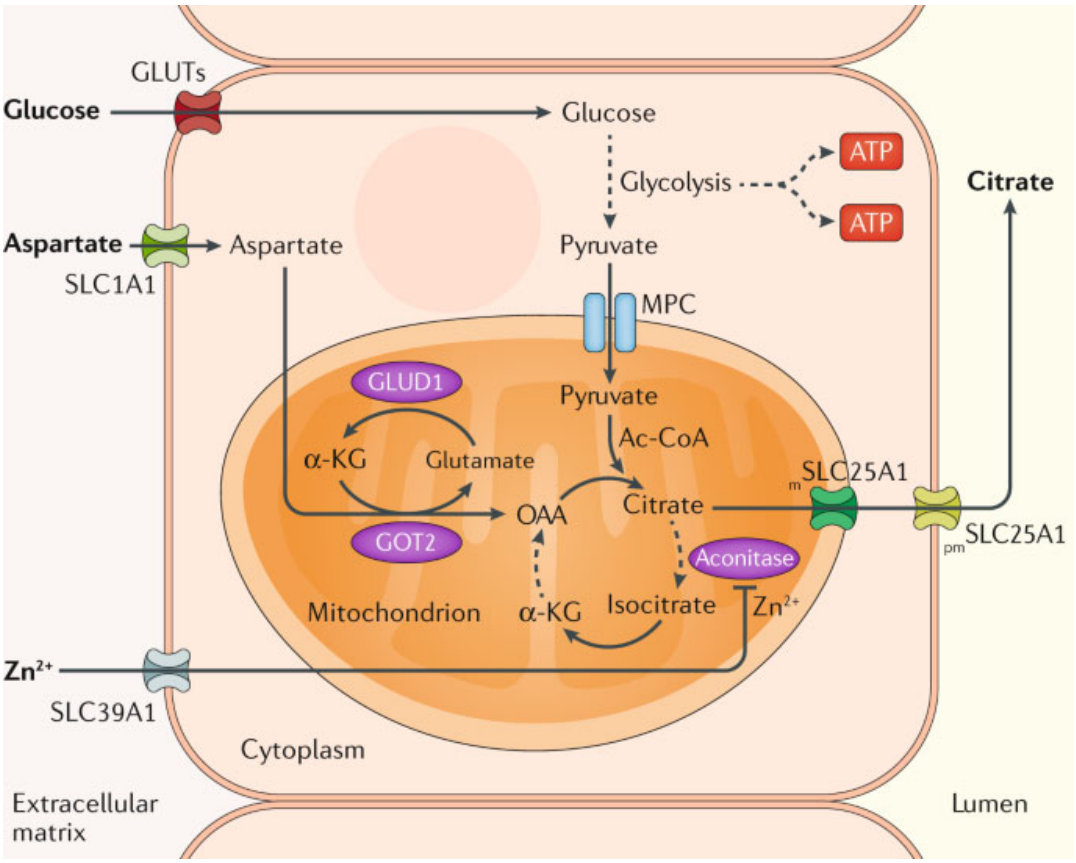

Figure 29. Metabolism of a normal epithelial prostate cell (Bader & McGuire, 2020).

Contrary, prostate cancer cells use citrate as a source of energy instead of being secreted. Indeed, as a substrate of the TCA cycle, citrate can be an attractive source of energy for neoplastic cells with high energy demands. In this regard, Franklin and Costello postulated "the bioenergetic theory of prostate cancer" and demonstrated that prostate cancer cells develop the ability to oxidize citrate in order to complete the TCA cycle and fueled OXPHOS machinery to produce ATP (see **figure 30**). Accordingly, prostate cancer cells display reduced levels of citrate and zinc (Liu et al., 1997) that allows the reactivation of the activity of the m-aconitase. This feature seems to be characteristic of the early stages of prostate cancer development (Costello & Franklin, 1994) and it is accompanied by an increase of lipid metabolism (Scaglia et al., 2021; Watt et al., 2019).

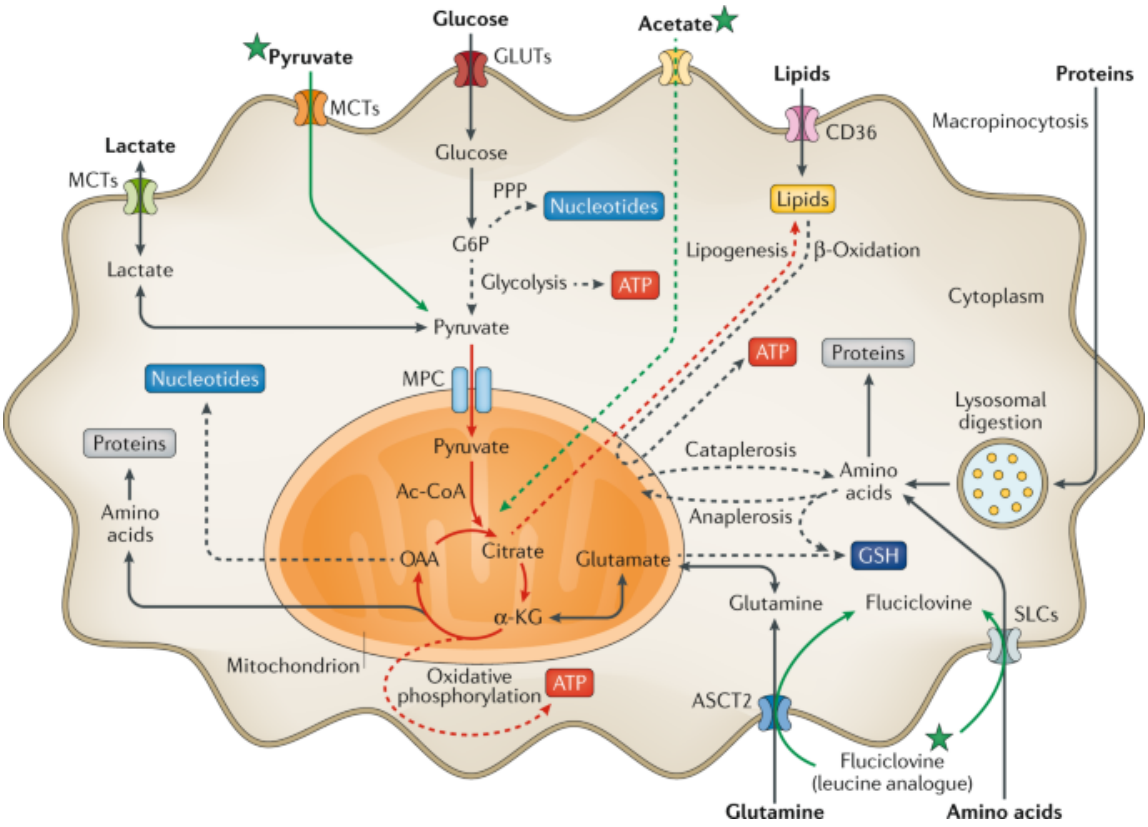

Figure 30. Metabolism of a prostatic adenocarcinoma (Bader & McGuire, 2020).

Costello and Franklin also demonstrated that the accumulation of zinc (Costello & Franklin, 1998) as well as the regulation of the aconitase gene expression (Costello et al., 2000) is controlled by prolactin and testosterone levels. Moreover, most of the molecular machinery that characterizes the unique metabolism of prostate cells seems also to be controlled by AR signaling (Costello & Franklin, 1991; Massie et al., 2011). Hence, the metabolic shift encountered in prostate cancer is most likely linked to the AR status - as it has been observed to favor lipogenesis (Swinnen et al., 1996) and oxidative phosphorylation – as well as to the loss of zinc transporters during tumorigenesis (Desouki et al., 2007).

Certainly, clinical imaging studies employing radiolabeled glucose 18F-fluorodeoxygluocose use for the detection of tumors by positron emission tomography (PET) scan consistently fail to detect prostate cancer tumors, supporting the idea that primary prostate tumors do not rely in glycolysis (Liu et al., 2001).

Despite the discovery of the metabolic bases that governate prostate cancer, the complexity of tumor metabolism together with the genetic and epigenetic components makes prostate cancer an incurable disease.

1.10.5 mtDNA mutations in prostate cancer

As previously described in this work, mtDNA mutations are the most common genetic events found in cancer cells (Kim et al., 2022). One of the earliest records of describing mtDNA mutations in tumors came from Polyak and coworkers in 1998 who reported the presence of small number of homoplasmic mutations in colorectal cancer cells (Polyak et al., 1998). However, its contribution in cancer still needs some clarity as not all the tumors harbor mtDNA mutations.

As an exception, pathogenic mutations in mtDNA have been described as a major contributor in prostate cancer development (Julia F. Hopkins et al., 2017; Petros et al., 2005). Certainly, large deletions, non-synonymous, autosomal, and somatic mutations have been reported in mtDNA from patients with malignant prostate (Jerónimo et al., 2001; Jessie et al., 2001; Lindberg et al., 2013). Furthermore, mutations in mtDNA have been associated with high PSA levels and higher Gleason Scores (see section 1.10.1) (Chen et al., 2002; Gómez-Zaera et al., 2006; Kloss-Brandstätter et al., 2010).

That being the case, how mtDNA mutations can suppose an advantage for cancer cells if they directly affect the central hub of ATP production and impairs the cell redox balance? At the present time this question still has not a final answer. According to the prostate cancer cases reported, mtDNA mutations not only contribute to the disease but they are involved in metastasis (Arnold et al., 2009; Ishikawa et al., 2008). One of the probable explanations is the elevated ROS production - possible as a subproduct of a malfunction of the ECT- that has been linked to a high grade of invasiveness and more aggressive phenotypes (Ishikawa et al., 2008; Kumar et al., 2008; Marco-Brualla et al., 2019). Yet, this observation appears to be just the *tip of the iceberg.*

1.11 Breast cancer

Breast cancer is a heterogenous disease that is characterized by a numerous molecular and cell pathways dysregulations with a wide range clinical outcomes.

In 2024, more than 2.0 million people will be diagnosed with cancer in the United States and around 600,000 cancer deaths are expected. Among all of them, an estimated of 310,720 women and 2,790 men will be diagnosed with breast cancer which makes it the most common cancer diagnosis with almost 42,780 estimated deaths in both sexes (Siegel et al., 2024).

Breast is a secretory organ manly composed by glandular tissue (also known as **mammary gland**), fat, and connective tissue which is surrounded by an abundant lymph node network. Due to the fact that this organ belongs to the reproductive system, its development and functional is mainly regulated by hormones, especially for the mammary gland (Petersen et al., 1987). Consequently, the most common and widely accepted classification of breast cancer is founded on immunohistochemical features which are based according on the expression of the hormone **receptors estrogen** (ER), **progesterone** (PR) and **human epidermal growth factor** (HER2) (Orrantia-Borunda et al., 2022).

1.11.1 Breast cancer classification

As mentioned above, breast cancer can be classified according to the presence of the hormone receptors (HR) progesterone, estrogen, and human epidermal growth factor in tumor biopsies, meaning if they are able to respond to hormone therapy deprivation. As an abbreviation, patients presenting at least one of the receptors are referred as HR positive (HR^+). Contrary, patients that do not express any hormonal receptor are referred as HR negative (HR^-) and they result to have lower rate responses to endocrine treatments. The different breast cancer subtypes according to this classification are listed hereafter (Inic et al., 2014):

- **HER2-negative breast cancer** (HER2-):
  - ✓ **Luminal A subtype:** Luminal A breast cancer tumors are characterized by the presence of both PR and ER but the absence of HER2. This subtype it is known for its slow growing rate (low expression of the **proliferation marker Ki-67**), and this is the one with the best prognosis which shows high response rates to hormone therapy (e.g., tamoxifen and aromatase inhibitors (see section 1.11.3).

  - ✓ **Luminal B subtype:** It represents 10-20 % of luminal tumors. Compared to luminal A subtype, luminal B tumors are positive for ER, negative for HER2 but it can be also negative for PR. These are of high grade with worst prognosis as it usually presents an elevated Ki-67 (Inic et al., 2014). Most of the cases they benefit from hormone therapy regimes combined with chemotherapy.

- **HER2-positive breast cancer** (HER2+): It represents 10-15% of breast cancer, and it is characterized by an elevated expression of the hormone receptor HER2. The HER2-positive type is known to be more aggressive and fast-growing than HER2-negative type, especially

it is known for having worst prognosis. Within this group, it can be distinguished **luminal HER2-positive**, also positive for ER and PR, and **HER2-enriched** which is characterized to be negative for ER and PR. Both subtypes required from HER2-specific targeted therapies such as trastuzumab (see section 1.11.3). For this type of disease, bones are the most typical dissemination sites.

- **Triple negative breast cancer** (TNBC): This tumor type is ER, PR and HER2 negative and it is constituted around 20% of all breast cancers. It is characterized by its aggressiveness, high proliferation rate, early relapses and it is often present in advances stages of the disease. From a genetic point of view, it often presents alterations in DNA repair genes and high genomic instability. Within this group, two categories can be distinguished from a histological point of view: **basal** and **non-basal TNBC**.

With an increased on the understanding of the molecular bases of breast cancer over the past years, the traditional classification detailed above may also benefit from other molecular markers such as specific miRNAs levels, and mutations in *p53*, *BRCA1* and *2* genes).

1.11.2 Molecular bases of breast cancer

The exact etiology of breast cancer is still unknown. However, there are some determinants of risk that are mainly associated with genetic heritance. The most common inherited genes identified that predisposes to develop breast cancer are ***BRCA1*** (Miki et al., 1994), ***BRCA2*** (Wooster et al., 1995), ***TP53*** **(Shahbandi et al., 2020).** However, a small portion of the cases shown allele variants and single nucleotide polymorphisms (SNPs) in the **fibroblast growth receptor** (FGFR2) (Hunter et al., 2007), **thymocyte selection-associated high mobility group box 9** (TNRC9), **mitogen-activated kinase 1** (MAP3K1), **lymphocyte-specific protein** (LSP1), **CASP8** (Cox et al., 2007) and **TGFB1**.

HER2 overexpression is one of the most common markers that correlates with breast tumoral transformation (Seshadri et al., 1989) which is also used as a criteria to classify breast cancer subtypes (see section 1.11.1) Indeed, *HER2/neu* oncogene, is a member of family of genes that encodes for HER2 transmembrane receptor which has been found to be amplified from 2 to 20 times-fold in breast cancer cases and it has been shown to be a reliable predictor of both overall survival and relapse time. Accordingly, the implication of the HER2 receptor become relevant in the clinic when it was demonstrated that HER2-positive breast cancers have a worse prognosis than the HER2-negative cancer types (Slamon et al., 1987).

In the same line, mutations in PI3K/AKT/mTOR pathway have been reported in breast cancer and to be associated with tumoral transformation and drug resistance (Araki & Miyoshi, 2018; Guerrero-Zotano et al., 2016). Certainly, this pathway plays a central role in controlling proliferation, survival and metabolism, among others (Engelman et al., 2006). Related to this, mutations, or loss of function in *PTEN* seems to occur in over 70% of breast cancer cases ("Comprehensive molecular portraits of human breast tumours," 2012) which is also directly associated with the regulation of the PI3K pathway, a feature that is shared with other tumor types (see section 1.10.2).

1.11.3 Current therapies

Due to the heterogeneity of the disease, there are several therapeutic strategies for the management of breast cancer. Here under it is listed the most used in the clinic:

1. **Hormonal therapy:** They are designed to target tumors that responds to hormone deprivation.
   - ✓ **Hormone receptor blockers**: They act by directly binding to the HR and competing with estrogen. The most notorious are **tamoxifen** (Jordan, 2003) and **trastuzumab** (Modi et al., 2022).
   - ✓ **Selective estrogen receptor degraders (SERDs)**: They act similar to the hormone receptor blockers, but they additionally promote HR degradation. They are often used in tamoxifen-acquired resistance cases. One of the examples is **fulvestrant.**
   - ✓ **Aromatase inhibitors**: They inhibit the aromatase enzyme which controls the estrogen levels. Some of the examples are **anastrozole**, **letrozole** and **exemestane**.
2. **Agonists of the luteinizing hormone-releasing hormone** (see section 1.10.1)
3. **Chemotherapy:**
   - ✓ **CDK 4/6 inhibitors**: Blocks the activity of cyclin D -in charge of regulating the cell cycle - which is reported to be highly expressed in ER^+ breast cancer (Gillett et al., 1994; Kenny et al., 1999). Palbociclib is one of the CDK 4/6 inhibitors that is currently being used in the clinic (Morrison et al., 2024).
   - ✓ **PI3K and mTOR inhibitors**: Acts blocking the activity of PI3K or mTOR which are involved in the PI3K/AKT/mTOR signaling pathway. **Everolimus** (François-Martin et al., 2023) and **apelisib** (André et al., 2019) are two examples of mTOR and PI3K inhibitors, respectively.
4. **Radiation:** Uses high-energy X rays and it can be total or partial, depending on the extent of the breast area irradiated. This is usually performed following surgery (Polgár et al., 2022).

5. **Surgery:** This can be breast-conserving surgery which preserves the surrounding tissue and only the part of the breast containing cancer is removed, or mastectomy which consist in the removal of the entire breast. The choose of the type of surgery is usually dictated by the tumor size (Gradishar et al., 2021).

1.12 Platinum-based chemotherapy

1.12.1 Origin and use for cancer therapy

Around 1950, the concept of cancer chemotherapy was born as a result of an extension research with mustard gas that started during the First World War. Apart to be use for extermination purposes in Jewish camps, mustard gas was found to have anti-cancer properties. During that decade, oncologists begun to acquire interest in analog compounds that they would have demonstrated to block cell replication by acting as alkylating DNA agents.

Many years before, in 1844, the chemist Michele Peyrone was the first to report the synthesis of **diamminedichloroplatinum (II)** (also referred to **cisplatin**) (Kauffman et al., 2010) but it was until 1965, when Dr. Barnett Rosenberg discovered by accident its anti-proliferative properties in a model of *Escherichia coli* (Rosenberg et al., 1965). Similar to mustard gas, scientist demonstrated that cisplatin acts as an alkylating agent analog preventing cell division. As a result, in 1978, cisplatin was the first platinum compound approved by the FDA to be used in the clinic as an anticancer agent (Rottenberg et al., 2021). Almost 45 years later, in 2019, platinum-based drugs were approved in the USA for the treatment of metastatic prostate cancer, ovarian and bladder cancer (FDA, 2024).

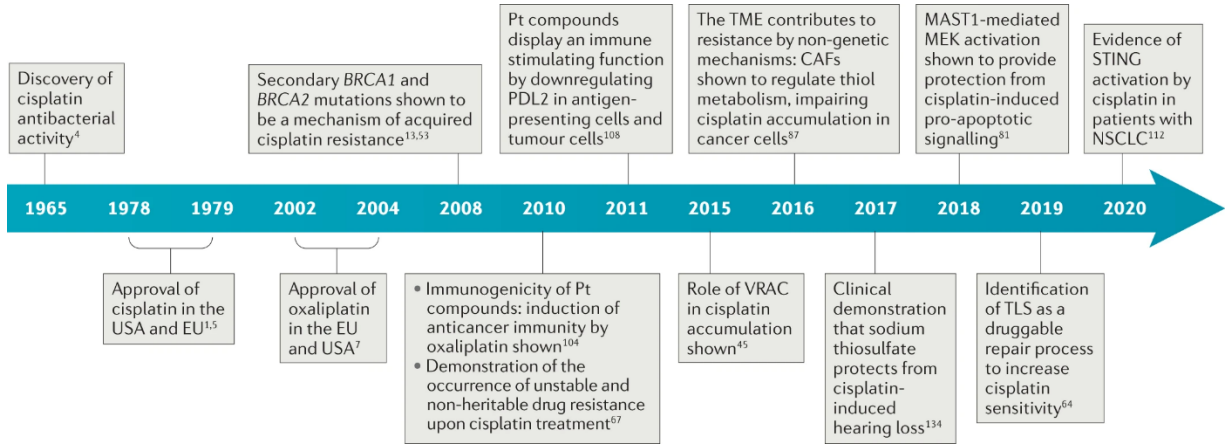

Figure 31. Timeline of the milestones in platinum-based chemotherapeutics in both research and clinics (Rottenberg et al., 2021).

1.12.2 New generation of platinum agents

Despite the discovery of cisplatin revolutionizing cancer treatment, numerous cases of patients suffering from acquired resistances started to be documented. As consequence, thousands of platinum analogs have been synthesized as an attempt to overcome this problem (Kelland et al., 1999), but only few of them received the FDA clinical approval. One of the examples is **carboplatin** that was the second platinum analog to be approved for its use in the clinic. After, in 2002, **oxaliplatin** was introduced first in Europe and later in the USA, as third-generation platinum compound able to overcome the resistances observed with cisplatin and carboplatin (Perego & Robert, 2016).

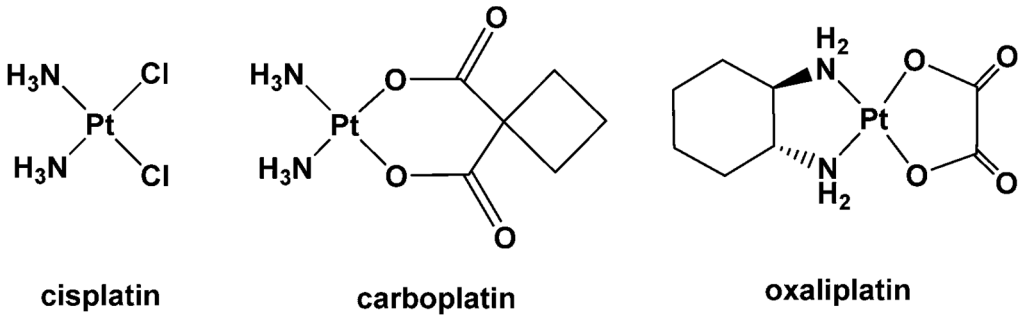

Figure 32. Chemical structure of the three FDA-approved chemotherapeutic platinum-based agents for cancer treatment (Apps et al., 2015).

1.12.3 Mechanism of action (MOA) of platinum drugs

DNA is the primary target identified of platinum-based agents forming monoadducts and crosslinks with the DNA molecule (Jamieson & Lippard, 1999). More precisely, the platinum atoms form covalent bonds to the N^7 position of the guanine (G) in the double helix (Au-Yeung et al., 2006) (see **figure 33**), having a direct impact on DNA functions, inhibiting replication, causing cell-cycle arrest, and cell death. Accordingly, following the formation of DNA adducts, they can be recognized by HMG box family proteins (see section 1.5.4) that activates TP53 (Jayaraman et al., 1998) triggering several cell responses and inducing apoptosis.

The lack of cell specificity of this compounds implies that they can interact with all the DNA molecules without discriminate if they are normal or cancer cells. In consequence, this type of drugs are known to provoke nephrotoxicity and neurotoxicity. Even if some of them can be easily managed, neurotoxicity can imply severe side-effects such as peripheral neuropathy that are linked to life-threatening clinical complications. Compared to cisplatin, carboplatin shows to be better tolerated but with the same cross-resistance than cisplatin (Martelli et al., 2006). Interestingly, oxaliplatin seems to be effective in cisplatin-resistant cells (Tashiro et al., 1989) and display different associated-toxicities even if both *a priori* have the same primary target. This is probably due to the diaminocyclohexane (DACH) carrier ligand variation (see **figure 32**) that can to form platinum-DNA adducts with major capacity to block DNA replication which result as an advantage to overcome the mismatch repair DNA system (Perego & Robert, 2016) but also by influence its accumulation capacity (Martelli et al., 2006).

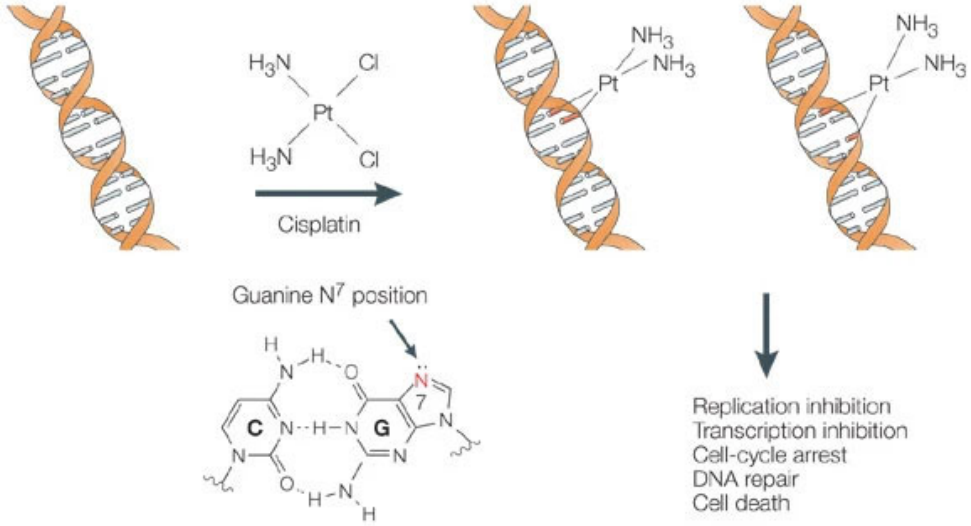

Figure 33. Molecular interactions between gDNA and cisplatin. Modified from (Au-Yeung et al., 2006).

In line with this, some of the resistance observed have been attributed to drug inactivation by glutathione, metallothionein or sulfur-containing molecules, changes in the drug incorporation efflux as well as an increase in the activity of DNA damage response pathways (Lord & Ashworth, 2012).

The mechanisms by which cisplatin and other platinum compounds are incorporate inside of the cell are not yet fully understood. Some works indicate that they can enter by a mechanism of passive diffusion through the plasmatic membrane. However, more recent studies carried out in yeast and mice suggests that cisplatin is incorporated via copper transporters as a decreased expression of these transporters has been linked to cell resistance (Holzer et al., 2004; Ishida et al., 2002; Komatsu et al., 2000).

In addition, it is known that both cisplatin and carboplatin but not oxaliplatin can be internalized trough the volume-regulated anion channel (VRAC) (Hall et al., 2008).

After several years of deep exploration of the MOA of oxaliplatin, in 2017, Hemann's and Lippard's research group demonstrated that oxaliplatin induces cell death by ribosomal stress rather than by a DNA damage response (Bruno et al., 2017). This alternative MOA would explain the differences in clinical applications and side effects reported when compared with both cisplatin and carboplatin. Indeed, it has been documented that oxaliplatin establishes less crosslinks per base than cisplatin and its interaction with DNA would be minimum leading to the inhibition of ribosomal RNA (rRNA) synthesis which would cause the ribosomal stress and induce apoptosis (Bruno et al., 2017).

Probably linked to its MOA, oxaliplatin but not cisplatin has also been reported to induce ICD. Certainly, Dr. Guido Kroemer's research group was the first to propose that certain chemotherapeutic drugs can activate adaptive immune responses as they have the ability to induce ICD (Casares et al., 2005). Concretely, they demonstrated that oxaliplatin and cisplatin are equally able to induce HMGB1 release (see section 1.5.4) but only oxaliplatin is able to induce pre-apoptotic exposure of CALR (see section 1.5.2) in colon cancer cell lines followed by a successful induction of anticancer immune response *in vivo* (Tesniere et al., 2010b).

In line with the previously mentioned, it has been reported that platinum-based agents can also interact with mtDNA causing mtDNA dysfunction (Cullen et al., 2007; Yang et al., 2006). Indeed, several works indicates that mitochondria play a role in developed resistance to cisplatin as observed in cisplatin-resistant cells to exhibit elevated mitochondrial membrane potential (Andrews & Albright, 1992; Isonishi et al., 2001). Other works have demonstrated that cisplatin treated cells increases their mitochondrial mass and the mtROS production in response to the treatment (Kleih et al., 2019) supporting the mitochondrial effect of cisplatin and its link with its capacity to induce cell death. Certainly, many investigations points to mitochondria as one of the organelles targeted by platinum-based agents as it has been demonstrates that cells lacking mtDNA (known as **rho 0 cells**) are less susceptible to toxicity from cisplatin (Park et al., 2004; Yang et al., 2006). Thus, it is very probable that some of the immunostimulatory capacities that have been attributed to those compounds (Chang et al., 2023) could also be directly linked by mitochondrial damaged (see section 1.7.4.1).

1.12.4 PT-112, a next generation platinum agent

PT-112 (also known as **imifoplatin**) is the first conjugated platinum-pyrophosphate molecule (see **figure 34**) under the license of **Promontory Therapeutics Inc.** since 2010 (Promontory Therapeutics, 2024) and currently in clinical development for solid tumors including phase II in mCRPC (Bryce et al., 2023), phase I in no small cell lung cancer (NSCLC) (Imbimbo et al., 2022) and phase II in thymic epithelial tumors (NIH, 2024d) (see **figure 36**).

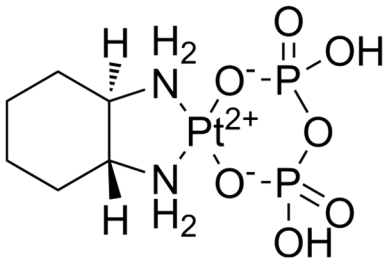

Figure 34. Chemical structure of PT-112 (MedChemExpress, 2024).

From a chemical point of view, PT-112 appertains to the family of **phosphaplatins** compounds which are characterized by containing a **diaminocyclohexane** core structure similar to oxaliplatin, but with the replacement of the oxalate group by a **pyrophosphate ligand**. Interestingly, these type of molecules have been shown to exhibit higher efficacy and reduced toxicities compared to the traditional platinum agents (Bose et al., 2008). Certainly, PT-112 was rationally designed to circumvent the toxicity and the cell mechanisms associated to chemotherapy resistance (Ames et al., 2017). In fact, early *in vitro* and *in vivo* studies in 2012, demonstrated that PT-112 can induced inhibition of growth and death of ovarian A2780 cancer cell line cross resistant to cisplatin and carboplatin (Moghaddas et al., 2012).

Despite containing a platinum atom within its chemical structure, Corte-Rodríguez and colleagues confirmed that, as the rest of phosphaplatins, PT-112 shows a reduced capacity to stablish adducts with DNA when compared to traditional platinum agents such as cisplatin and oxaliplatin (Corte-Rodríguez et al., 2015) which could also explain why PT-112 appears to be effective in cells with acquired resistance to other platinum compounds (Moghaddas et al., 2012).

In line with its chemical properties, it has been reported that PT-112 displays a tendency to accumulate in the bone (also know as **osteotropism**) (see **figure 35**) (Ames et al., 2017), meaning that PT-112's biodistribution profile could be effective in cancers that originate in or metastasize to the bone such as multiple myeloma, breast, or prostate cancer. This particular feature may be explained at least in part by PT-112's organic pyrophosphate moiety, chemically similar to a bisphosphonate which is used for the clinical management of skeletal complications and/or bone metastases (Russell et al., 2008).

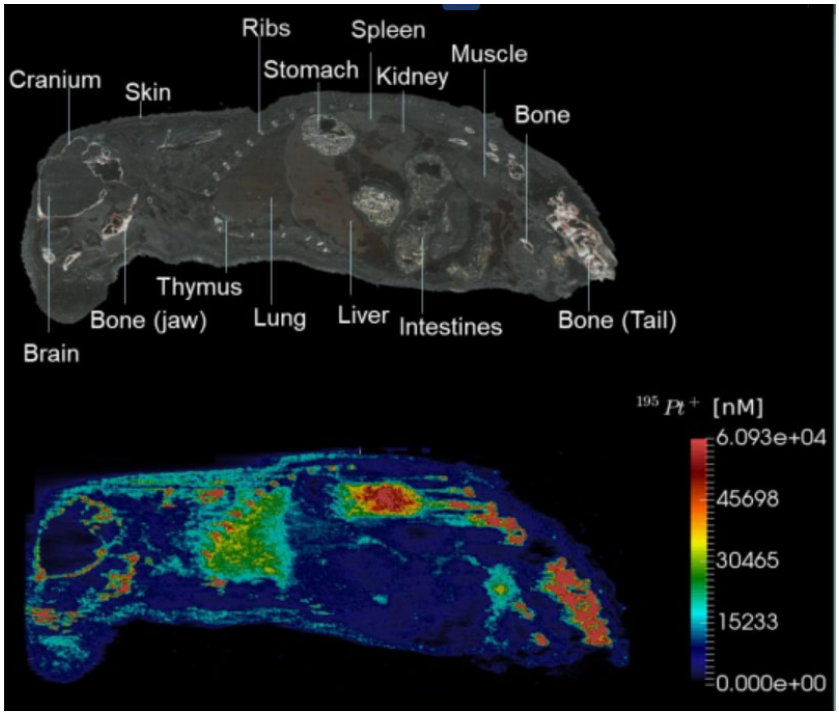

*Figure 35. Platinum distribution in Vk*MYC mice with established multiple myeloma treated with 90 mg/kg of PT-112 for 24 h via tail vein injection. PT-112 reaches several tissues such as liver, lung, and the highest concentrations in mineralized bone. Colorimetric scale indicate platinum accumulation in nanomoles (Ames et al., 2017).*

Since Promontory Therapeutics launched its first-in-human phase I clinical trial in solid tumors in 2014 (ClinicalTrials.gov ID: NCT02266745), PT-112 have demonstrated to be **safe**, **active** and **well-tolerated**, especially in in **late-stage heavily pretreated patients** with a median of 4 prior treatment lines (Karp et al., 2018; Karp et al., 2022). In this study they reported prolonged responses against thymoma and lung cancer as well as an improvement of serum and radiographic markers in prostate cancer.

Furthermore, PT-112 has been atributed to induce immunogenic cell death as it has been demonstrated (1) by the release of DAMPs such as calreticulin, ATP and HMGB1 *in vitro* (2) by succesuful vaccination assays and abscopal reponses *in vivo* (T. Yamazaki, A. Buqué, et al., 2020). Morover, clinical trials in combination with PD-L1 inhibitor avelumab in mCRPR showed bone pain improvement and a reduction in volumen tumor, PSA and alcaline phosphatase (ALP) in almonst all patients enrolled (Alan Haruo Bryce et al., 2021; Bryce et al., 2020). In consequence, on September 13, 2022, Promontory Therapeutics obtained, and extension of the patent entitled "Phosphaplatin Compounds as Immuno-Modulatory Agents and Therapeutic Uses Thereof" (U.S. Patent No. 11,439,619 B2).

Figure 36. On-going clinical trials with PT-112 in monotherapy or in combination with immunotherapy. Besides of indicated, PT-112 is in Phase I trial pending to approval for the American Society of Hematology (ASH) in multiple myeloma.

According to the most recent findings from Yim and colleagues, PT-112-treated human cells shown evidence of nucleolar stress and ribosome biogenesis inhibition *in vitro* (Christina Y. Yim et al., 2023). This was demonstrated by the analysis of nascent RNA sequencing in human cancer cells form non-small cell lung, prostate, and renal carcinoma after short incubation times with this compound. During these experiments they documented that PT-112 induces the relocation of NPM1 from nucleoli to nucleoplasm,

which is typically a hallmark of nucleolar stress, as well as a substantial suppression genes associated with ribosomes a feature that is also associated with ribosome inhibition.

BACKGROUND AND OBJECTIVES

"Where there is a will, there is a way"

-George Herbert-

2. Background and objectives

Despite immunotherapy has revolutionized cancer treatment (Sharma & Allison, 2015), major efforts are still needed to make it accessible to the patients that are not responding to this therapy. Seeking to solve this problem, scientists worldwide are searching new single or combinatorial therapies that could kill cancer cells in a way that they become recognizable by the immune system. The main goal of this strategy is to increase the immune infiltration on the tumor site, making immunotherapy effective in patients who still do not obtain any clinical benefit. This strategy arises from of immunogenic cell death (ICD) concept (Green et al., 2009) that was introduced for the first time by Dr. Guido Kroemer's research group in 2005, demonstrating that anthracycline-base therapies are able to boost antitumor-immune responses (Casares et al., 2005). Many works published later also demonstrated that radiotherapy and several traditional chemotherapies such as oxaliplatin, can activate the anti-tumor immune response through its capacity to induce ICD (L. Galluzzi et al., 2020). As a result of the investigations dedicated to ascertaining the molecular mechanisms that regulates this phenomenon, a direct connection between mitochondria and ICD has been established over the past decade (A. Rongvaux et al., 2014; White et al., 2014). According to this, other works have demonstrated that this organelle is also implicated in pathways controlling inflammation and anti-tumor immune responses such as type I IFN secretion or antigen presentation by MHC-I (Charni et al., 2010; Mangalhara et al., 2023; Marchi et al., 2023).

The new anti-tumor drug PT-112 appears to be one of those emergent treatment candidates with a promising antitumor-activity profile and immunomodulatory capacity (T. Yamazaki, A. Buqué, et al., 2020). PT-112 is the first conjugated platinum-pyrophosphate molecule currently in clinical development for solid tumor treatment. This drug operates with mechanisms that differ from conventional DNA-damaging chemotherapies: it has been demonstrated to have low affinity for DNA compared to traditional platinum agents such as cisplatin or oxaliplatin (Corte-Rodríguez et al., 2015), and to overcome acquired *in vitro* resistance to other platinum compounds (Moghaddas et al., 2012). This observation could most likely be explained because of its chemical structure. As in the case of oxaliplatin, PT-112 has been demonstrated to induce ribosomal stress (Christina Y. Yim et al., 2023). Indeed, PT-112 and oxaliplatin shares very similar chemical structures if the pyrophosphate moiety present in PT-112 chemical structure is not considered. However, oxaliplatin still have minimal but significant affinity for DNA while PT-112 does not seem to have at all (Corte-Rodríguez et al., 2015). This feature could explain why PT-112 can overcome cases of platinum-acquired resistances (Moghaddas et al., 2012) and show encouraging results in heavily pretreated patients

that previously underwent treatment with platinum-based agents (Karp et al., 2022). Despite all the scientific evidence obtained until date, the mechanism of action of PT-112 in not yet fully understood. Thus, the specific objectives that has been established for the **first chapter** of this Doctoral Thesis are:

1. Generate transmitochondrial cybrids as a model to investigate the possible role of mitochondria in PT-112's mechanism of action.
2. Investigate if PT-112 exhibits selectivity *in vitro* for cells with defective mitochondria in the L929dt cell model harboring mtDNA mutations.
3. Evaluate PT-112's mitochondrial effects in the L929dt cell model.
4. Evaluate the ability of PT-112 to induce ICD in cells showing sensitivity to PT-112-induced cell death.

In line with the results obtained in clinical trials, PT-112 has shown to procure prolonged responses in thymoma and lung cancer as well as a clinical improvement in prostate cancer patients (Karp et al., 2018; Karp et al., 2022). In cases of mCRPC in which the standard of care therapies are exhausted and novel treatment options are urgently needed, PT-112 seem to be a promising therapy. Indeed, among all the clinical trials currently ongoing with PT-112, mCRPC is the one that is at more advance stage. Supporting this idea, it has been found that PT-112 has affnity for the bone matrix (Ames et al., 2017), meaning that its bone distribution could be an advantage to treat cancers that originate in or metastasize to the bone, as it is the case of prostate cancer. Thus, due to the relevance of prostate cancer for the clinical development of this drug, the objectives of the **second chapter** of this Doctoral Thesis are:

1. Investigate *in vitro* the profile of sensitivity of PT-112 in a panel of human prostate cancer cell lines.
2. Evaluate PT-112's mitochondrial effects in human prostate cancer cell lines.
3. Analyze the ability of PT-112 to induce ICD in human prostate cell lines.

Moreover, previous work from Yamazaki et al. in 2020 has demonstrated in mouse mammary adenocarcinoma TS/A cell lines that PT-112 elicits *in vitro* danger signals that are linked to ICD and promote *in vivo* protection in vaccination models. Accordingly, *in vitro* treated TS/A cells with PT-112 efficiently protected immunocompetent, tumor naïve-mice when they were challenged with living cancer cells of the same type (T. Yamazaki, A. Buqué, et al., 2020). In concordance with this, positive data obtained from phase I clinical trials in combination with the immune checkpoint blocker avelumab (Alan Haruo Bryce et al., 2021) supports PT-112's modulatory and immunostimulatory capacity. Because of the link between mitochondria and ICD already mentioned, preliminary data have evidenced that PT-112 promotes mitochondrial

dysfunction as demonstrated by an increase in mtROS generation and hyperpolarization, all together coupled with cytosolic mtDNA accumulation (Yamazaki et al., 2022). Accordingly, BH-3 family proteins are known to regulate the mitochondrial apoptotic process as well as to modulate cytosolic mtDNA accumulation which generally leads to type I IFN secretion (Cosentino et al., 2022; McArthur et al., 2018; Riley et al., 2018). Thus, the objectives of the **third chapter** of this Doctoral Thesis are:

1. Investigate the PT-112's cytostatic and cytotoxic effects in parental TS/A cells and in genetically modified BCL2/BCLXL KO and BAK1/BAX KO cells.
2. Investigate the *in vitro* mitochondrial effects of PT-112 in parental TS/A cells and in genetically modified BCL2/BCLXL KO and BAK1/BAX KO cells.
3. Investigate the capacity of PT-112 to induce ICD in parental TS/A cells and in genetically modified BCL2/BCLXL KO and BAK1/BAX KO cells.
4. Identify the link between mitochondrial effects and PT-112's immunostimulatory capacity.

EXPERIMENTAL PROCEDURES

"Practice makes perfect"

-Bruce Lee-

3. Experimental procedures

3.1 Cell culture

Cells were maintained according to ATCC recommendations. Mouse fibroblast cell lines L929 and L929-derived, "detached" cells (L929dt) were routinely cultured in high glucose DMEM medium with GlutaMAX (Life Technologies) supplemented with 10 % of fetal bovine serum (FBS; Sigma), penicillin (1000 U/mL) and streptomycin (10 mg/mL) (PanBiotech). The cybrid cell lines $L929^{dt}$ and dt^{L929} were cultured with the identical medium as parental cells. For L929-ρ^0 cells, complete DMEM medium was also supplemented with pyruvate (110 µg/mL) and uridine (50 µg/mL).

Human prostate cell lines PC-3, DU-145, and VCap were cultured in high glucose DMEM medium with GlutaMAX (Life Technologies). LNCap and 22Rv1 were cultured in RPMI 1640 medium (Life Technologies). LNCap-C4 and LNCap-C4-2 were cultured in a mixture of DMEM: F12 (4:1) supplemented with biotin (4.9 ng/mL), adenine (251.8 ng/mL), insulin (0.1 ng/mL), and transferrin (88.6 ng/mL). RWPE-1 (immortalized, non-tumorigenic human prostate cell line) was cultured in Keratinocyte-SFM supplemented with EGF human recombinant (5 ng/mL) and bovine pituitary extract (50 µg/mL) (Gibco). All cell culture media used for prostate cancer cell lines were supplemented with 10 % FBS, penicillin (1000 U/mL) and streptomycin (10 mg/mL) (PanBiotech). PC3, LNCap, VCap, and RWPE-1 cell lines were kindly provided by Dr. M. Jesús Vicent from CIPF, Valencia, while DU-145, LNCap C4, LNCap C4-2 and 22Rv1 cell lines were a kind gift of Dr. Santiago Ramón y Cajal from Hospital Vall d'Hebron (Barcelona).

TS/A cells (SCC177) were obtained from Millipore Sigma and maintained in culture as per manufacturer's recommendations. Wild-type (WT) TS/A and TS/A-derived clones were routinely cultured in DMEM containing 1 mM sodium pyruvate, 1mM HEPES buffer, 4.5 g/L glucose (Corning®) and supplemented with 10 % FBS (GeminiBio), 100 µg/mL streptomycin sulfate, 100 U/mL penicillin sodium and 290 µg/mL L-glutamine (Gibco™). All the cells were maintained at 37°C and 5 % CO_2 using standard procedures.

3.2 CRISPR/Cas9 genetic edition

TS/A cells were transfected with a control commercial CRISPR-cas9 plasmid (CRISPR06-1EA, Sigma) or customized CRISPR-cas9 plasmids based on CRISPR06-1EA targeting *Bak1*, *Bax*, *Bcl2*, *Bcl2l1* (Sigma), harnessing the TransIT-CRISPR manufacturer protocol. After transfection, individual GFP-expressing cells

were sorted into 96-well plates using a FACS Symphony S6 Sorter (BD Biosciences) for cell expansion. Immunoblotting validation was performed according to conventional procedures (T. Yamazaki, A. Kirchmair, et al., 2020) with primary antibodies specific for BAK1 (#12105, Cell Signaling Technology, 1:500), BAX (#2772, Cell Signaling Technology, 1:1,000), BCL2 (#3498, Cell Signaling Technology, 1:500), BCL-X_L (#2764, Cell Signaling Technology, 1:500) and ACTB1 (#3700, Cell Signaling Technology, 1:2,000) as a loading control. After washing and incubation with horseradish peroxidase-conjugated anti-rabbit (#NA934, GE Healthcare Life Sciences, 1:5,000) or anti-mouse secondary antibodies (#NA931, GE Healthcare Life Sciences, 1:5,000), the SuperSignal West Femto Maximum Sensitivity Substrate (#34094, Thermo Fisher) was employed to visualize protein expression on an Azure 600 Imaging System operated by Azure capture v.1.9.0.0406 (Azure Biosystems).

3.3 Cell viability assays

Relative cell growth was measured using a modified Mossman method (Mosmann, 1983) for microplates. Briefly, 2 x 10^4 cells were seeded per well in a 96-well flat-bottom plate and incubated with increasing concentrations of PT-112 or cisplatin (2, 6 and 10 µM) for 24–72 h at 37 °C. Then, 10 µL of a 5 mg/mL 3-(4,5-Dimethylthiazol-2-yl)-2,5-Diphenyltetrazolium Bromide (MTT) solution was added to each well and incubated for 3 h. During the incubation time, viable cells reduced the MTT solution to insoluble purple formazan crystals, which were subsequently solubilized with a mixture off isopropanol and 0.05 M HCl, and the absorbance was measured in a microplate reader (Dynatec). The MTT method in mitochondria-defective cell lines has been used in other studies, as MTT reduction is performed not only by mitochondrial enzymes but also by other cellular oxidoreductases (Loveland et al., 1992). Control cell lines were included in each growth experiment.

3.4 Cytotoxicity assays and cell death quantification

Cytotoxicity induced by PT-112 was measured as follows: 2 x 10^5 cells were seeded in a 96-well plate and incubated with increasing concentrations of PT-112 (2, 6, and 10 µM) or cisplatin (10 µM) for 24-72 h at 37°C. Cell death in untreated and treated samples was analyzed by flow cytometry using a FACSCalibur flow cytometer (BD Biosciences) after simultaneous incubation with annexin-V-FITC and 7-Aminoactinomycin D (7-AAD;BD Biosciences) in annexin binding buffer (ABB; 140 mM NaCl, 2.5 mM $CaCl_2$, 10mM HEPES/NaOH, pH 7.4) for 10 minutes (min). For WT and derived TS/A cells, dead cells number was evaluated by flow cytometry using the Attune NxT flow cytometer (Thermo Fisher Scientific) upon staining with 0.5 µg/mL 4',6-diamidino-2-phenylindole (DAPI; Sigma).

3.5 Clonogenic assays

Seven days after treatment initiation colonies were fixed with 70% ethanol and stained with 0.1% crystal violet (Electron Microscopy Sciences), according to conventional procedures (Serrano-Mendioroz et al., 2023). Colonies were manually counted with the eCountTM Colony counter (Heathrow Scientific).

3.6 ROS production, mitochondrial membrane potential and mitochondrial mass measurement by flow cytometry

Total and mitochondrial ROS (mtROS) production, mitochondrial membrane potential and mitochondrial mass were measured using a FACScalibur flow cytometer (BD Biosciences). For mitochondrial membrane potential and total ROS production, pretreated cells with PT-112 were incubated with 20 nM DiOC6 (Molecular Probes) and 2 µM DHE (Molecular Probes) for 30 min at 37 °C, respectively. For mitochondria-specific superoxide production analysis, pretreated cells were incubated with 5 µM MitoSOX™ (ThermoFisher) for 30 min at 37 °C. To analyze alterations in mitochondrial membrane potential in DU-145 and LNCap-C4 cells, simultaneously incubated with 20 nM TMRE (Molecular Probes) and annexin-V-DYE-634 (Sigma) for 30 min at 37°C.

For TS/A cell lines, mitochondrial membrane potential and mitochondrial mass were analyzed by flow cytometry using the Attune NxT flow cytometer (Thermo Fisher Scientific) upon staining with 100 nM MitoTracker™ Deep Red FM (Invitrogen™), 150 nM MitoTracker™ green FM (Invitrogen™), and 0.5 µg/mL DAPI (Sigma-Aldrich) which was used as a vital dye. All dyes were incubated for 30 min at 37 °C.

3.7 Apoptosis and necroptosis inhibition assays

2 x 10^4 cells were seeded in a 96-well plate and incubated with 50 µM of pan-caspase inhibitor Z-VAD-fmk (MedChem Express) and/or 30 µM RIPK-1 inhibitor necrostatin-1 (MedChem Express) for 1 h. Next, cells were treated with 10 µM of PT-112 and incubated for 48 h at 37 °C. Both inhibitors were refreshed in their corresponding well after 24 h. Finally, cell death was assessed using flow cytometry using a FACSCalibur flow cytometer (BD Biosciences) after incubation with annexin-V-FITC and 7-AAD in ABB for 10 min.

3.8 Analysis of CASP3 activation

CASP3 activation was measured using a FITC-labelled antibody against cleaved CASP3 (BD Pharmingen™). Cells pretreated with 10 µM of PT-112 were fixed with 4 % paraformaldehyde (PFA) solution for 15 min at 4 °C. Then, cells were washed with PBS buffer, permeabilized using a 0.1 % saponin dilution

supplemented with 5 % FBS and incubated for 15 min at room temperature (RT). After washing them, samples were incubated with the antibody anti CASP3 for 30 min at RT and analyzed by flow cytometry using a FACSCalibur flow cytometer (BD Biosciences).

3.9 Autophagosome formation measurement

The autophagosome formation after treatment with PT-112 was evaluated using a Cyto-ID® probe (Enzo Life Sciences). Cells pretreated with 10 µM of PT-112 were incubated with 1 µL of Cyto-ID® dye reagent for 30 min at 37 °C. Subsequently, cells were washed with PBS buffer and analyzed by flow cytometry. For autophagy-positive controls, cells were treated with 1 µM of rapamycin at least 12 h before the analysis.

3.10 MHC-I and CALR surface expression

CALR surface expression upon incubation with PT-112 (24–72 h) in L929dt cell model was analyzed by flow cytometry. Cells treated with PT-112 were incubated with primary rabbit anti-calreticulin antibody (Abcam, #AB2907 1:700 in PBS) at 4 °C for 1 h. Then, cells were washed with PBS and incubated simultaneously with secondary goat anti-rabbit IgG antibody conjugated with Alexa Fluor488® (#A11034, Invitrogen) and 7-AAD. To rule out non-specific interactions, untreated cells were incubated only with secondary antibody. 7-AAD-positive cells were excluded from the analysis.

MHC-I and CALR surface expression in TS/A cell lines were evaluated as follows: pretreated cells were washed with PBS and stained with Zombie Aqua™ Fixable Viability Kit (BioLegend) for 15 min. Subsequently, cells were washed and incubated with the Calreticulin (D3E6) XP® rabbit monoclonal antibody PE Conjugate (#19780S, Cell Signaling, 0.5 µL/sample) and PE anti-mouse H-2 Antibody anti-H-2 - M1/42 (#125505, BioLegend, 1 µL/sample) in 0.5 % BSA in PBS (FACS buffer) for 25 min at 4°C in the dark. Then, cells were washed and fixed with eBioscience™ Intracellular Fixation & Permeabilization Buffer Set (Invitrogen) for 30 min at 4°C in the dark, incubated with the permeabilization buffer eBioscience™ Intracellular Fixation & Permeabilization Buffer Set (Invitrogen) for 5 min, washed and resuspended in FACS buffer for analysis by flow cytometry (Attune NxT flow cytometer, Thermo Fisher Scientific). Zombie Aqua™ positive cells (*i.e.*, dead cells) were excluded from the analysis.

3.11 Protein extraction and immunoblot analysis

A total of 5×10^6 cells were lysed with 100 µL of 1× lysis buffer (1 % Triton-X-100; 150 mM NaCl; 50 mM Tris/HCl pH 7,6; 10 % v/v glycerol; 1 mM EDTA; 1 mM sodium orthovanadate; 10 mM sodium

pyrophosphate; 10 µg/mL leupeptin; 10 mM sodium fluoride; 1 mM methyl phenyl sulfide, Sigma) for 30 min on ice. The mixture was ultra-centrifugated at 13,500 xg for 20 min at 4 °C. The protein concentration in the supernatant was analyzed using the BCA assay (Thermo Fisher) and was mixed with 3× lysis buffer (SDS 3 % v/v; 150 mM Tris/HCl; 0.3 mM sodium molybdate; 30 % v/v glycerol; 30 mM sodium pyrophosphate; 30 mM sodium fluoride; 0.06 % p/v bromophenol blue; 30 % v/v 2-mercaptoethanol, all purchased from Sigma). Protein separation was performed using SDS-PAGE (6 % or 12 % polyacrylamide gel), and proteins were transferred to nitrocellulose membranes using a semi-dry electro-transfer (GE Healthcare). Membranes were blocked with TBS-T buffer (10 mM Tris/HCl, pH 8.0; 120 mM NaCl; 0.1 % Tween-20, 0.1 g/L thimerosal, Sigma) containing 5 % skimmed milk. Protein detection was performed by western blot using specific antibodies against p62 (#SC-28359, Santa Cruz), LC3BI/II (#L7543, Sigma) and HIF-1α (#NB100–479, Novus) that were incubated overnight at 4 °C in agitation. Anti-rabbit or anti-mouse secondary antibodies labeled with peroxidase (#A9044, Sigma) were incubated for 1 h at RT. Blots were analyzed with Pierce ECL Western Blotting Substrate (Thermo Scientific) using an Amersham Imager 680 (GE Healthcare Life Sciences). Protein expression was quantified by densitometry using ImageJ software. β-actin or tubulin levels were used as a reference to normalize data (#3700, Cell Signaling).

3.12 Coenzyme Q quantification

Mitochondria were isolated from cultured cell lines as previously described (Schägger & Pfeiffer, 2000) with small modifications (Acín-Pérez et al., 2008). The mitochondrial pellet was immediately frozen in liquid nitrogen under anaerobic conditions. Then, lipids extraction and CoQ determination were performed as described previously (Brea-Calvo et al., 2006). Briefly, mitochondrial samples (0.6 mg of mitochondrial protein for each measurement) were lysed with 1 % SDS and vortexed for 1 min. Then, a mixture of ethanol:2-propanol (95:5) was added and the samples vortexed again for 1 min. To recover CoQ, 5 mL of hexane was added, and the samples were centrifuged at 1000 ×g for 5 min at 4 °C. The upper phases from two extractions were recovered and dried using a rotary evaporator. Lipid extracts were suspended in 1 mL ethanol, dried in a speed-vac and stored at −20 °C. Samples were resuspended in a suitable volume of ethanol prior to HPLC injection. Lipid components were separated with an Alliance HPLC system (Waters) equipped with a 2707 autosampler and 2996 photodiode array detector, with HSST3 column (4.6 × 150 mm, 3.5 µm, Waters), preceded by a pre-column (4.6 × 20 mm, 3.5 µm, Waters), with a flow rate of 1 mL/min and a mobile phase containing 40:60 methanol/2-propanol. Commercial CoQ10 (Sigma) was used as an internal standard to detect the CoQ10 peak in the samples.

3.13 Cell morphology assessments

Cells were treated with or without 10 µM of PT-112 for 72 h. Images were taken using an inverted microscope (Nikon Eclipse TE300). For cell morphology assessments using transmission electron microscopy (TEM), refer to *Transmission Electron Microscopy (TEM)*.

Confocal fluorescence microscopy was used to visualize mitochondrial membrane polarization. 2 x 10^4 cells (LNCap and DU-145) per well were plated in an optical plastic bottom 384-well plate (Aurora Microplates) and, after overnight attachment, treated with control buffer or 25 µM PT-112 for 72 h. Cells were then stained live with Hoechst 33342 (#62249, ThermoFisher, 1:5,000) and either TMRE (#T669, ThermoFisher, 1:1,000) or JC-1 (#T3168, ThermoFisher, 1:1,000) for 30 min. Next, cells were imaged on a Yokogawa CV8000 high-throughput spinning disk confocal using a 20x/1.0 water objective capturing a 10 µm z-stack in 9 fields of view per condition. Images were then projected at maximum intensity for quantification. Image analysis was performed using the CellPathfinder software (Yokogawa). Briefly, nuclei were identified using the Hoechst channel, followed by a dilation step to include the mitochondrial signal ("virtual cell") from where intensity-based measurements were extracted. The experiment was repeated three independent times with four technical replicates per biological replicate.

3.14 OXPHOS performance and metabolism measurements

Oxygen consumption rate (OCR) measurements of 3 x 10^4LNCap-C4 cells treated with or without 10 µM PT-112 for 24 h were performed using the Seahorse XF Cell Mito Stress Test Kit and the XF96 Extracellular Flux Analyzer (Seahorse Biosciences). Cells were incubated in Seahorse media (1 mM pyruvate, 2 mM glutamine, 1 M glucose at pH 7.4) for 30 min at 37°C without CO_2. According to the manufacturer's instructions, OCR was measured in basal conditions and after sequential addition of oligomycin (CV inhibitor), FCCP (respiration and ATP synthesis uncoupler), and rotenone + antimycin A (AA + Rot, CI and CIII inhibitors, respectively). Final drug concentrations were 1 µM. OCR data were normalized to the number of viable cells as determined by the CyQuant Cell Proliferation Assay (Thermo Fisher).

Energy maps were constructed using the XF96 Extracellular Flux Analyzer (Seahorse Biosciences) following the manufacturer's instructions. The energetic phenotype of LNCap-C4 cells was determined based on measurements of OCR and extracellular acidification rate (ECAR) indicative of OXPHOS and glycolysis, respectively, in untreated, control cells and following 10 µM PT-112 treatment for 24 h.

3.15 Mitochondria purification (for Blue Native analysis)

Mitochondria were purified as previously described (Acín-Pérez et al., 2008; Schägger & Pfeiffer, 2000) with small modifications (Acín-Pérez et al., 2008). Briefly, 2×10^7 cells were centrifuged, washed twice with cool PBS, and frozen at -80°C for, at least, 1 h. Pellets were resuspended in a volume of hypotonic buffer (10 mM MOPS, 83 mM saccharose, pH 7.2) equal to 7× the cell pellet volume and incubated on ice for 2 min. Samples were then homogenized with 8 to 10 strokes using a Potter-Dounce homogenizer with a Teflon piston (Deltalab). After adding an equal volume of a hypertonic buffer (30 mM MOPS, 250 mM saccharose, pH 7.2), the samples were centrifuged at 1000 xg for 5 min at 4°C, and only the supernatants were centrifuged again at 11,000 xg for 2 min at 4°C. Finally, mitochondria-containing pellets were washed with media A (10 mM Tris, 1 mM EDTA, 0.32 M saccharose, pH 7) and resuspended in a buffer containing 50 mM NaCl, 50 mM imidazole, 2 mM aminocaproic acid and 1 mM EDTA at pH 7.0, to obtain a final concentration of 10 mg/mL of the mitochondrial extract. Then, 4 mg of 10 % digitonin (50 mM NaCl, 50 mM imidazole, 5 mM aminocaproic acid, 4 mM phenylmethylsulfonyl fluoride) per mg of mitochondrial extract was added. Finally, loading buffer (5 % Coomassie Blue G in 0.75 M aminocaproic acid) was added to the samples in a proportion 1 to 3 of the final volume.

3.16 Blue Native electrophoresis and immunoblot analysis

Separation of respiratory complex (CI, CII, CIII, CIV and CV) and supercomplexes (SCs) proteins in mitochondrial extracts was performed using blue native electrophoresis in a gel gradient according to the published methodology (Wittig et al., 2007). Briefly, samples were loaded in NativePAGE™ 3-12% Bis-Tris Gel (Invitrogen) and run at 80 V for the first 30 min, then at 160-180 V limiting the current to 12 mA/gel until the dye reaches the bottom of gel (around 125-165 min. in total). For protein separation of protein extracts, SDS-PAGE (6 % and 12 % polyacrylamide gel) was used.

Proteins were transferred to PVDF membranes using semi-dry electrotransfer (GE Healthcare). Membranes were blocked with TBS-T buffer (10mM Tris/HCl, pH 8; 0.12 M NaCl; 0.1 % Tween-20, 0.1 g/L thimerosal; Sigma) containing 5 % skimmed milk. Protein detection was performed by immunoblot using specific antibodies (Invitrogen) against the individual complexes of the mitochondrial electron transport chain: CI (anti-NDUFA9; #459100), CII (anti-SDHA; #459200), CIII (anti-Uqcrc1; #459140), CIV (anti-COI; #459600), and CV (anti-α-F1-ATPase; #459240). Primary antibodies were incubated overnight at 4°C in agitation. Afterwards, anti-mouse (#A9044, Sigma) or anti-rabbit (#A9169, Sigma) secondary antibodies conjugated with peroxidase were incubated for 1 h at RT. Blots were analyzed with Pierce ELC Western

Blotting Substrate (Thermo Scientific) using Amersham Imager 680 (GE Healthcare Life Sciences). Protein expression was quantified by densitometry using ImageJ software.

3.17 Enzymatic activity analysis of respiratory complexes

Purified mitochondria from unfrizzed fresh pelleted cells treated with or without 10 µM PT-112 for 24 h were used to assess enzymatic activity of respiratory complexes via spectrophotometric quantification as previously described (Birch-Machin & Turnbull, 2001). For this specific assay, mitochondrial pellets were resuspended in MAITE buffer (25 mM saccharose, 75 mM sorbitol, 100 mM KCl, 0.05 mM EDTA-Na, 1 mM MgCl2, 10 mM Tris-HCl pH 7.4 and 10 mM of K_3PO_4, pH 7.4) or B media (250 mM saccharose, 2 mM HEPES, 0.1 mM EGTA). Briefly, activity of individual complexes and supercomplexes was measured using a spectrophotometer (Fisher Scientific) based on the following: CI (NADH-dehydrogenase) activity via oxidation of NADH at 340 nm, CII (succinate dehydrogenase) activity via reduction of 2,6'dichlorophenolindophenol at 600 nm, CIV (cytochrome c oxidase) activity via oxidation of cytochrome c at 550 nm, CI+III (NADH cytochrome c oxido-reductase) via reduction of cytochrome c at 550 nm when NADH is added, and CII+III (succinate cytochrome c oxido-reductase) activity via reduction of cytochrome c at 550 nm when succinate is added.

3.18 Transmission electron microscopy

Samples for TEM were prepared as follows: 5×10^4 DU-145 cells were seeded overnight in an 8-well Nunc™ Lab-Tek® Chamber Slide™ (Thermo, Rockford). Cells were treated with 10 µM PT-112 for 1, 6, 24 and 48 h, and after incubation, the medium was removed. Cells were carefully washed 3× for 2 min with 0.1 M PBS at RT and a solution containing 2.5 % glutaraldehyde in 0.1 M phosphate buffer (PB; Na_2HPO_4 + NaH_2PO_4 4:1, pH 7.4) was added. The chamber slide was then incubated at 37 °C for 5 min. The glutaraldehyde solution was refreshed, and the chamber slide was again incubated for additional 2 h at 4 °C. It was subsequently washed 4× (5 min each) with 0.1 M PB before adding a solution of 0.05% NaN_3 in 0.1 M PB and storing the chamber slide at 4 °C. For the fixation process, samples were washed 5× (5 min each) with PBS and incubated with 2 % OsO_4 in PB for 1 h. Next, 3 washes (5 min each) with cold distilled water were performed and samples were dehydrated with increasing concentrations of ethanol (30 %, 50 % and 70 %) before staining with 2 % uranyl acetate in 70 % ethanol for 2 h 30 min. Samples were dehydrated a second time with increasing concentrations of ethanol (70 %, 96 %, 100 %), gradually included in resin, transferred to a 100 % epoxy resin, and incubated overnight. The next day, 3 changes of epoxy resin were performed (30 min each), and samples were embedded in the molds with epoxy resin and dried

in the oven for 48-72 h at 70°C. Finally, ultrafine 50 nm cuts were performed and stained with Reynol's solution. Images were taken using a transmission electron microscope (JEOL 1010) at 80 kV.

3.19 DAMP emission

HMGB1, type I IFN and ATP release were quantified with the HMGB1 express ELISA Kit (Tecan), the IFN-β ELISA kit, High Sensitivity (PBL Assay Science) and the Enliten ATP Assay (Promega), respectively, as per manufacturer's recommendations. Sample absorbance at 450 nm or light emission were measured on a FlexStation 3 Multi-Mode Microplate Reader operated by SoftMaxPro v.5.4.6 (Molecular Devices LLC). Absolute quantification was calculated based on standard curves with $R^2 \geq 0.99$.

3.20 Immunofluorescence microscopy

For cytosolic dsDNA analysis, between 5 x 10^3 to 10 x 10^3 cells growing on glass coverslips were fixed with 4 % paraformaldehyde (#sc-281692, Santa Cruz Biotechnology), plasma membrane was permeabilized with 0.1 % Tween20 and 0.01 % Triton X-100 in PBS followed by incubation with specific dsDNA primary antibody (#ab27156, Abcam, 1:1,000). Cells were next washed with PBS-Tween and incubated with Goat Anti-Mouse IgG H&L (Alexa Fluor® 488) preadsorbed (#ab150117, Abcam). Finally, samples were washed and mounted on slides with Hoechst 33342-containing ProLong Glass Antifade Mountant (Thermo Fisher Scientific).

Images were acquired with an EVOS FL Imaging System operated by embedded software v.1.4 (Rev 26059) (Thermo Fisher Scientific). Quantitative dsDNA analyses were performed on ≥10 randomly selected images per condition. Briefly, blue (nuclear) and green (dsDNA) levels were normalized with a LUT file optimized for each sample set on Photoshop v.25.7.0 (Adobe), followed by the identification of nuclear and cytoplasmic regions of interest, which were quantified for the presence and relative localization of dsDNA spots above a predefined threshold size (to account for background noise) with Cell Profiler v.4.2.1 (Broad Institute). All steps were performed with commands that are publicly available at https://cellprofiler.org/ (Sato et al., 2022{Sato, 2021 #786)}.

3.21 Statistical analysis and data processing

Prism v. 10 (GraphPad) and Excel 2021 (Microsoft) were used for data processing, plotting and statistical analysis. Illustrator 2020 (Adobe) was used for figure preparation. Otherwise noted, for statistical analysis, significance was evaluated using Student's t-test for simple comparisons and two-way ANOVA uncorrected Fisher's LSD were applied in comparisons involving two or more groups. For samples not following a Gaussian distribution, statistical significance was assessed by Wilcoxon test. Data obtained by

flow cytometry were analyzed using FlowJo v. 10.9.0 (Tree star Inc.). Unless otherwise noted, all experiments were performed at least in two independent replicates.

4.CHAPTER I: Mitochondrial effects on the murine model

jove

Transmitochondrial Cybrid Generation Using Cancer Cell Lines

Ruth Soler-Agesta[1], **Joaquín Marco-Brualla**[1], **Patricio Fernández-Silva**[1,2], **Pilar Mozas**[1,3], **Alberto Anel**[1], **Raquel Moreno Loshuertos**[1,2]

[1] Department of Biochemistry, University of Zaragoza [2] Institute for Biocomputation and Physics of Complex Systems, University of Zaragoza [3] Sequencing and Functional Genomics Unit, University of Zaragoza-IACS

Corresponding Author

Raquel Moreno Loshuertos
raquelml@unizar.es

Citation

Soler-Agesta, R., Marco-Brualla, J., Fernández-Silva, P., Mozas, P., Anel, A., Moreno Loshuertos, R. Transmitochondrial Cybrid Generation Using Cancer Cell Lines. *J. Vis. Exp.* (193), e65186, doi:10.3791/65186 (2023).

Date Published

March 17, 2023

DOI

10.3791/65186

URL

jove.com/video/65186

Abstract

In recent years, the number of studies dedicated to ascertaining the connection between mitochondria and cancer has significantly risen. However, more efforts are still needed to fully understand the link involving alterations in mitochondria and tumorigenesis, as well as to identify tumor-associated mitochondrial phenotypes. For instance, to evaluate the contribution of mitochondria in tumorigenesis and metastasis processes, it is essential to understand the influence of mitochondria from tumor cells in different nuclear environments. For this purpose, one possible approach consists of transferring mitochondria into a different nuclear background to obtain the so-called cybrid cells. In the traditional cybridization techniques, a cell line lacking mtDNA (ρ^0, nuclear donor cell) is repopulated with mitochondria derived from either enucleated cells or platelets. However, the enucleation process requires good cell adhesion to the culture plate, a feature that is partially or completely lost in many cases in invasive cells. In addition, another difficulty found in the traditional methods is achieving complete removal of the endogenous mtDNA from the mitochondrial-recipient cell line to obtain pure nuclear and mitochondrial DNA backgrounds, avoiding the presence of two different mtDNA species in the generated cybrid. In this work, we present a mitochondrial exchange protocol applied to suspension-growing cancer cells based on the repopulation of rhodamine 6G-pretreated cells with isolated mitochondria. This methodology allows us to overcome the limitations of the traditional approaches, and thus can be used as a tool to expand the comprehension of the mitochondrial role in cancer progression and metastasis.

Introduction

Reprogramming energy metabolism is a hallmark of cancer[1] that was observed for the first time by Otto Warburg in the 1930s[2]. Under aerobic conditions, normal cells convert glucose into pyruvate, that then generates acetyl-

coA, fuelling the mitochondrial machinery and promoting cellular respiration. Nevertheless, Warburg demonstrated that, even under normoxic conditions, most cancer cells convert pyruvate obtained from the glycolysis process into lactate, shifting their way to obtain energy. This metabolic adjustment is known as the "Warburg effect" and enables some cancer cells to supply their energetic demands for rapid growth and division, despite generating ATP less efficiently than the aerobic process[3,4,5]. In recent decades, numerous works have supported the implication of metabolism reprogramming in cancer progression. Hence, tumor energetics is considered an interesting target against cancer[1]. As a central hub in energetic metabolism and in the supply of essential precursors, mitochondria play a key role in these cell adaptations that, to date, we only partially understand.

In line with the above, mitochondrial DNA (mtDNA) mutations have been proposed as one of the possible causes of this metabolic reprogramming, which could lead to an impaired electron transport chain (ETC) performance[6] and would explain why some cancer cells enhance their glycolytic metabolism to survive. Indeed, it has been reported that mtDNA accumulates mutations within cancer cells, being present in at least 50% of tumors[7]. For example, a recent study carried out by Yuan et al. reported the presence of hypermutated and truncated mtDNA molecules in kidney, colorectal, and thyroid cancers[8]. Moreover, many works have demonstrated that certain mtDNA mutations are associated with a more aggressive tumor phenotype and with an increase in the metastatic potential of cancer cells[9,10,11,12,13,14,15,16].

Despite the apparent relevance of the mitochondrial genome in cancer progression, the study of these mutations and their contribution to the disease have been challenging due to limitations in the experimental models and technologies currently available[17]. Thus, new techniques to understand the real impact of mitochondria DNA in cancer disease development and progression are needed. In this work, we introduce a protocol for transmitochondrial cybrid generation from suspension-growing cancer cells, based on the repopulation of rhodamine 6G-pretreated cells with isolated mitochondria, that overcomes the main challenges of traditional cybridization methods[18,19]. This methodology allows the use of any nuclei donor regardless of the availability of their corresponding ρ^0 cell line and the transfer of mitochondria from cells that, following the traditional techniques, would be difficult to enucleate (i.e., non-adherent cell lines).

Protocol

NOTE: All culture media and buffer compositions are specified in **Table 1**. Prior to cybrid generation, both mitochondrial and nuclear DNA profiles from the donor and recipient cells must be typed to confirm the presence of genetic differences in both genomes between cell lines. In this study, a commercially available L929 cell line and its derived cell line, L929dt, which was spontaneously generated in our laboratory (see[13] for more information) were used. These cell lines present two differences in the sequence of their *mt-Nd2* gene which can be used to confirm the purity of mtDNA once the cybridization process has been finished[13]. In this case, the purity of the nuclear background was confirmed by antibiotic sensitivity, since, contrary to L929dt cells, L929 were resistant to geneticin.

1. Mitochondrial depletion by rhodamine 6G treatment (recipient cells)

NOTE: The first step for successful cybrid generation is to completely and irreversibly abolish mitochondrial functions in the recipient cells. For this purpose, it is necessary to previously determine, for each cell line, the appropriate concentration and treatment duration with rhodamine 6G. This adequate concentration should be just below drug-induced cell death (the highest that does not kill the cells during the treatment). Perform the following once the optimal conditions are defined.

1. Seed 10^6 cells in a 6-well plate using complete culture medium (see **Table 1** for details) and treat them daily with the optimal concentration of rhodamine 6G for 3-10 days, depending on the cell line. Traditional concentrations range from 2 to 5 µg/mL for 3-10 days[20,21]. In this study, for L929-derived cells, 2.5 µg/mL rhodamine 6G for 7 days was the selected treatment[13,22].
2. To keep the cells alive, supplement the cell culture medium with 50 µg/mL of uridine and 100 µg/mL of pyruvate and renew it every 24 h.
3. After treatment and prior to fusion, change the medium of rhodamine 6G-treated cells to complete cell culture medium without rhodamine 6G, and leave them in this medium for 3-4 h in an incubator at 37 °C with 5% CO_2.
   NOTE: The rhodamine 6G toxic effect is irreversible, and cells with non-functional mitochondria should not recover[20]. Thus, after treatment, cells that do not receive functional mitochondria should die even in uridine-supplemented culture medium. Therefore, no nuclear selection should be necessary. However, a control fusion of rhodamine 6G-treated cells without mitochondria is recommended.

2. Expansion and mitochondrial isolation (donor cells)

1. Expand the mitochondria donor cells during the time lapse of rhodamine 6G treatment to obtain around 25 x 10^6 cells.
2. On day 7, harvest exponentially growing cells in a 50 mL tube and collect them by centrifugation at 520 x *g* for 5 min at room temperature (RT). Wash the cells 3x with cold phosphate-buffered saline (PBS) and sediment them by centrifugation at 520 x *g* for 5 min at RT. From now on, perform all the steps of mitochondrial extraction at 4 °C, using cold reagents and keeping the tubes with cells or mitochondria on ice.
3. After the third centrifugation, discard the supernatant by aspiration using a glass pipette coupled to a vacuum pump and resuspend the packed cells in a volume of hypotonic buffer equal to 7x the cell pellet volume. Then, transfer the cell suspension into a homogenizer tube and let the cells swell by incubating them on ice for 2 min.
4. Break the cell membranes by performing 8 to 10 strokes in the homogenizer coupled to a motor-driven pestle rotating at 600 rpm.
   NOTE: The step of cell membrane disruption can vary between cell types; thus, it has to be optimized for each cell type.
5. Add the same volume of hypertonic buffer to the cell suspension (7x the cell pellet volume) to generate an isotonic environment.
6. Transfer the homogenate into a 15 mL tube and centrifuge it in a fixed rotor at 1,000 x *g* for 5 min at 4 °C.

Then, collect only 3/4 of the supernatant leaving a large margin from the pellet, to avoid contamination with nuclei or intact cells, and transfer it to another tube. Repeat the same process twice. Note that the supernatant must be kept and the pellet discarded.

7. Save the mitochondrial fraction (supernatant). Transfer it into 1.5 mL tubes and centrifuge at maximum speed (18,000 x *g*) for 2 min at 4 °C.

8. Discard the supernatant and wash the mitochondria-enriched pellet with buffer A, combining the content of the two tubes into one and centrifuging at the same conditions as described in step 2.7. Repeat the same process until all the material is in only one tube.

9. Make an additional wash with 300 µL of buffer A and quantify the mitochondrial protein concentration using the Bradford assay[23]. For each cybridization assay, the optimal amount of mitochondria for the transfer procedure has to be determined (in our case, a concentration between 10-40 µg of mitochondrial protein per 10^6 cells).

10. Simultaneously, prepare the rhodamine 6G-pretreated cells for the fusion by collecting them in a 15 mL tube and centrifuging at 520 x *g* for 5 min at RT. Note that the pellet acquires a neon pink color due to rhodamine 6G treatment.

11. To ensure that both mitochondrial function abolishment in receptor cells as well as organelle purification from donors have been properly performed, seed a small number of rhodamine 6G-treated cells and isolated mitochondria using the complete culture medium in a 6-well plate and culture them for a month to check that no surviving cells remain in any of the wells (**Figure 2**).

12. In parallel, evaluate the absence of nuclei contaminants in the mitochondrial fraction by immunodetection of nuclear proteins (i.e., lamin beta, histone H3, etc.) or by quantitative polymerase chain reaction (qPCR) amplification of a nuclear gene (i.e., SDH, 18S rRNA, etc.).

    NOTE: To avoid contaminations, it is recommended to perform all the steps in aseptic conditions working under a laminar flow hood.

3. Fusion and cybrid generation

1. To proceed with the fusion, carefully add 10^6 of the rhodamine 6G-treated cells to the isolated mitochondria pellet (10-40 µg of mitochondrial protein) and centrifuge at 520 x *g* for 5 min to allow the cells to mix with the mitochondria.

2. Add 100 µL of polyethylene glycol (PEG, 50%) and gently resuspend the pellet for 30 s. Then, allow to rest untouched for another 30 s.

3. Finally, transfer the mix into a 6-well plate with fresh complete cell culture medium and place in the incubator at 37 °C with 5% CO_2. After a few days (usually 1 week), transmitochondrial cybrids should start growing (**Figure 2**), giving rise to clones that can be individually selected or mixed in a pool prior to their analysis.

4. Verification of both mitochondrial and nuclear background

NOTE: Once the new cell line has been established and cells begin to grow exponentially, the purity of their mitochondrial and nuclear DNAs must be verified. Thus, the original cell lines should harbor different mutations or polymorphisms within their genomes to make them recognizable.

1. Total DNA isolation
    1. Isolate the genomic DNA of all cell lines used for cybrid generation by employing a commercial genomic DNA extraction kit (see **Table of Materials**) or by performing a standard protocol using phenol-chloroform-isoamyl alcohol extraction and alcohol precipitation[24].
2. mtDNA evaluation (**Figure 3**)

    NOTE: Several techniques, such as sequencing, restriction fragment length polymorphism (RFLP) analysis, or allele-specific qPCR, can be performed to analyze the purity of mtDNA. To confirm the presence of mtDNA sequence variations by RFLP, follow the next protocol steps.
    1. Amplify an mtDNA fragment containing the nucleotide change by PCR.
        1. Here, L929dt cells present an mtDNA mutation at position 4206, within an *mt-Nd2* gene (m.4206C>T) that is absent in L929 cells. To confirm the presence of this substitution in the transmitochondrial cybrids, amplify a 397 bp fragment by PCR using a standard protocol and the following primers: 1) 5'-AAGCTATCGGG CCCATACCCCG-3' (positions 3862-3884) and 2) 5'-TAATCAGAAGTGGAATGGGGCG -3' (positions 4236-4258).
    2. Analyze the presence of the desired nucleotide substitution by RFLP, using a specific endonuclease that recognizes the sequence change and generates a different cut pattern for both cell lines.

        NOTE: When the L929dt mtDNA variant is present (4206T), the amplicon obtained in step 4.2.1 contains two restriction sites for SspI (see **Table of Materials**) that produces three DNA fragments of 306 bp, 52 bp, and 39 bp. The restriction site that generates the 52 and 39 bands is disrupted when the wild-type (WT) version C4206 is present, and a new band of 91 bp appears. Therefore, an internal control for full digestion for SspI is included in the analysis. The digestion reaction is performed at 37 °C, following the manufacturer's instructions.
    3. Separate the restriction fragments by electrophoresis and compare the band pattern.
        1. Once the digestion is performed, analyze the obtained restriction fragments by electrophoresis in 10% polyacrylamide-Tris-borate-EDTA (TBE) gels (see **Table 1** for 1x TBE composition). Run the electrophoresis at 80 V for 1 h at RT. Visualize the DNA fragments after gel staining in a solution of ethidium bromide in 1x TBE for 15 min at RT (see **Table 1** for gel staining solution composition).
3. Nuclear DNA genotyping

    NOTE: Nuclear DNA genotyping must be performed using the previous DNA extraction sample employed for RFLP analysis.
    1. Amplify 16 loci (D21S11, CSF1PO, vWA, D8S1179, TH01, D18S51, D5S818, D16S539, D3S1358, D2S1338, TPOX, FGA, D7S820, D13S317, D19S433, and AMEL) by using a pool of commercial-specific oligonucleotides (see **Table of Materials**).
    2. Perform electrophoresis by using a genetic analyzer in order to separate the fragments previously obtained.

NOTE: Once amplified, the different loci are analyzed by electrophoresis using a capilar system (see **Table of Materials**). The fragments are separated in a 50 cm long capilar filled with a commercial polymer. Cathode and anode buffers are also commercially available, as shown in the **Table of Materials**. Electrophoresis is performed at 19.5 kV for 20 min at 60 °C.

3. Use bioinformatical tools to determine the alleles corresponding to each amplified locus (see **Table of Materials**).

4. Compare the data obtained in step 4.3.3 with the nuclear DNA profile database (**Table 1**), to check if the nuclear DNA profile matches with the mitochondria receptor cell line profile (**Figure 4**).

Representative Results

After following the above-presented protocol, a homoplasmic cybrid cell line with a conserved nuclear background but with a new mitochondria genotype should be obtained, as represented in the schematics in **Figure 1** and **Figure 2**. The purity of the mitochondrial and nuclear DNA present in the cybrids can be confirmed by RFLP, as shown in **Figure 3**, and by nuclear DNA genotyping analysis, as shown in **Figure 4**.

If the mitochondrial transfer was done successfully, the results obtained with the RFLP analysis for the cybrid cell line must show different digestion band patterns compared to the recipient cell line and identical to the mitochondria donor cell line. For this purpose, the restriction enzyme must be chosen carefully, making sure that the band patterns obtained from the digestion are different in both cell lines. One example is given in **Figure 3**, in which the restriction fragments obtained after SspI digestion in WT mitochondria and mutant mitochondria (MUT) are shown. In the case of the new transmitochondrial cell lines, restriction fragments were identical to those obtained in their respective mitochondrial donors and different to those generated with the nuclei donor cell amplicons. Thus, this assay confirms that the mitochondrial exchange was performed as expected. Of note, a sample from recipient cells that was not subjected to the digestion procedure was included in this analysis as a negative control.

Regarding DNA nuclear genotyping, a typical profile obtained from the analysis of 16 nuclear loci for one of the cell lines used in this protocol is shown in **Figure 4**. Similar to RFLP, by comparing the peaks obtained for each locus, the results obtained from the mitochondria receptor cell line (nuclear donor) should match with the generated cybrid.

It is important to note that the results obtained may vary according to different factors. As we indicate in the protocol, not all cell lines are susceptible to the same amount of rhodamine 6G for removing the totality of functional mitochondria.

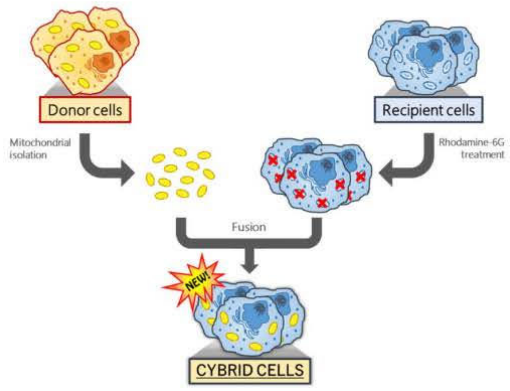

Figure 1: Schematical representation of cybrid generation, summarizing steps 1 to 3 of the protocol. Please click here to view a larger version of this figure.

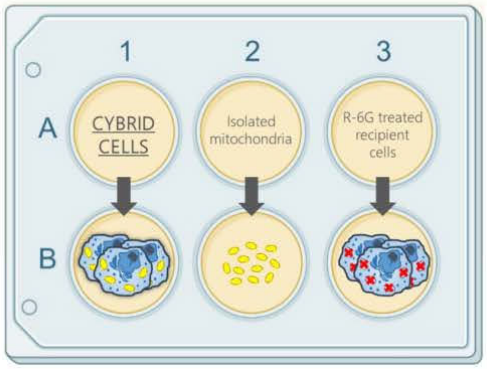

Figure 2: Schematical representation showing the design of the cell culture plate after the cybridization protocol. A new cybrid cell line and controls (isolated mitochondria and rhodamine 6G-treated recipient cells) are seeded separately in a 6-well plate. After a few days of culture, cybrid cells begin to grow, whereas no surviving cells remain in the control wells. Please click here to view a larger version of this figure.

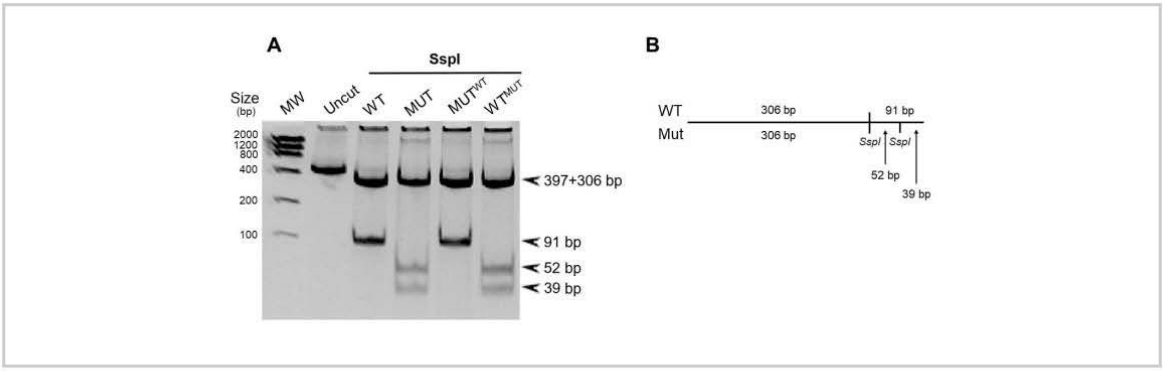

Figure 3: Molecular characterization of cybrids. (**A**) RFLP analysis of the m.4206C>T mutation in mitochondrial donor cell lines (WT and MUT, lanes 3 and 4, respectively) and their respective transmitochondrial cell lines (MUT^{WT} → lane 5, and WT^{MUT} → lane 6). MW: molecular weight marker (lane 1); uncut: non-digested PCR product (lane 2). (**B**) SspI restriction maps of the PCR product for WT and MUT mitochondria. Please click here to view a larger version of this figure.

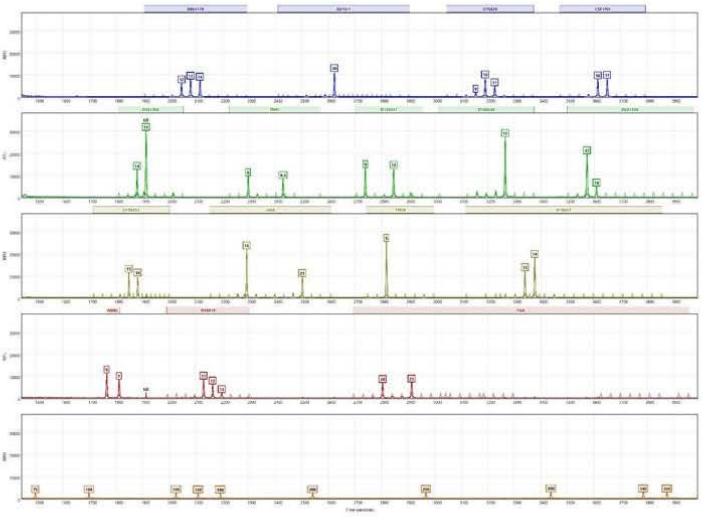

Figure 4: Representative results of nuclear DNA background analysis. Example of the nuclear DNA fingerprint obtained after PCR amplification of 16 loci and separation by capilar electrophoresis. The figure shows the characteristic peak pattern for each amplified loci of a cell line. This pattern must be different for the two cell lines used in the cybridization protocol to confirm nuclear DNA purity. Please click here to view a larger version of this figure.

Medium	Composition
Complete culture medium	DMEM high glucose with L-Gln and pyruvate + FBS (10%) + Penicillin-Streptomycin (1x)
Hypotonic buffer	10 mM MOPS, 83 mM sucrose, pH 7.2
Hypertonic buffer	30 mM MOPS, 250 mM sucrose, pH 7.2
Buffer A	10 mM Tris, 1 mM EDTA, 0.32 M sucrose, pH 7.4
TBE (1x)	50 mM Tris, 50 mM Boric acid; 1 mM EDTA
Gel staining solution	0.75 µg/mL Ethidium bromide in 1x TBE

Table 1: Buffers and media composition.

Discussion

Since Otto Warburg reported that cancer cells shift their metabolism and potentiate "aerobic glycolysis"[3,4] while reducing mitochondrial respiration, the interest in the role of mitochondria in cancer transformation and progression has grown exponentially. In recent years, mutations in the mtDNA and mitochondrial dysfunction have been postulated as hallmarks of many cancer types[25]. To date, numerous studies have analyzed the mtDNA variation of specific tumours[6,26,27,28,29,30,31,32], and the total burden of acquired mtDNA mutations has been considered a biomarker of tumorigenicity[30] in cancers such as prostate cancer[33]. In line with this, whereas mtDNA mutations are considered tumor initiators in some cases, such as in breast[34,35] or pancreatic[36] cancers, gynecological malignancies[37,38], lung adenocarcinoma metastases[15,39], or acute myeloid leukemia[40,41], they seem to be less relevant in glioblastomas[42].

Although many cancers harbor severe mtDNA mutations that are not found in healthy tissues[43] and could contribute to cancer initiation[30], others present polymorphic mtDNA variants that are common in various human populations. These variants promote milder changes that can be important for cancer cell adaptation once the transformation process has been initiated[30]. In any case, mtDNA mutations and mitochondrial metabolism alterations are involved in tumor progression, modifying different aspects of cell homeostasis such as reactive oxygen species production or redox status[44,45,46]. However, the mechanisms by which mtDNA mutations and variants can favor tumorigenesis are not completely understood yet. Besides, mtDNA mutations in cancer cells may coexist with alterations in nuclear genes[8,33], making it hard to determine which is the driver mutation. In other cases, the bioenergetic requirements of tumor cells are achieved by modulating the mtDNA copy number[47]. On the other hand, in some cases, mtDNA mutations could make tumor cells more susceptible to specific anti-tumor drugs[48].

To fully understand the role of mtDNA mutations in the pathophysiology of cancer, it is necessary to develop methodologies in which mutated mitochondria can be analyzed in a controlled nuclear environment. This can help avoid compensating effects of nuclear genes that could trigger cellular adaptation. For this purpose, transmitochondrial cybrids represent an appropriate model. Traditional methods of cybridization involve a mtDNA depleted cell line (ρ^0 cells) that act as a nuclei donor (and, therefore, mitochondria receptor) and a donor of mitochondria, usually an enucleated cell line or platelets[19], carrying the mtDNA variants or mutations of interest. The first challenge to be solved when trying to generate cybrids is the availability of ρ^0 cells harboring the nuclear background of choice. The obtention of these cells involves long-term treatment with ethidium bromide, a chemical compound that inhibits mtDNA replication. However, it can also induce the generation of mutations within the nuclear genome that could mask the effects of the mitochondrial alterations to be studied. Therefore, in this work, we propose the elimination of whole mitochondria in nuclei donor cell lines by treatment with rhodamine 6G, a drug that irreversibly damages mitochondria and would kill the cells unless fresh mitochondria are introduced in their cytoplasm[21,22,49].

Another challenge in traditional cybrid generation methods is related to the enucleation process of the mitochondrial donor cells. For this purpose, adherent cells are centrifuged in the presence of cytochalasin B, which allows the isolation of enucleated cytoplasts[18] by promoting the disorganization

of the cytoskeleton. If cells grow in suspension (such as hematological lines) or have lost cell-cell and cell-extracellular matrix adhesion (which may happen to those with a higher metastatic potential[50,51,52]), this enucleation protocol would be compromised, since cytoplasts would detach from the plate during the centrifugation to remove the nuclei, largely reducing their pool for the subsequent fusion procedure. To circumvent both challenges, we propose here a protocol in which isolated mitochondria are fused with rhodamine 6G pretreated cells in the presence of PEG, that has proven to be time-saving and efficient[21,22,49].

Once the transmitochondrial cell lines are generated, it is crucial to assess the purity of both mitochondrial and nuclear genomes. Therefore, it is critical to select donor cell lines with sequence differences within their mitochondrial DNA and with distinguishable characteristics, such as antibiotic resistance or differential microsatellites. As described above, some cancers have been reported to modulate their mtDNA copy number[47], evidencing the importance of analyzing the mtDNA load in both original and transmitochondrial cell lines and studying their OXPHOS performance under similar conditions.

The main pitfalls hidden in this procedure are linked to the process of mitochondria elimination with rhodamine 6G. Each cybridization experiment should be preceded by assays to establish the optimal conditions of drug concentration and treatment time for the selected nucleus donor cell line. If the rhodamine 6G concentration or the exposition time is not sufficient, the new cell line will have the contribution of two different mtDNAs, which will add more complexity to the phenotypic analysis. Moreover, if the time or dose exceeds the optimal ones, the cells will not survive even after mitochondria repopulation. Finally, it is essential to be careful during the mitochondria isolation process in order to avoid contamination with unbroken cells, which could alter the phenotypic characterization.

Despite the technical difficulties, the generation of transmitochondrial cybrids is a potent tool to unravel the mitochondrial contribution to cancer and metastasis processes and generate cell models where potential anticancer treatments using mitochondria as a therapeutical target can be tested.

Disclosures

The authors declare no conflicts of interest.

Acknowledgments

This research was funded by grant number PID2019-105128RB-I00 to RSA, JMB, and AA, and PGC2018-095795-B-I00 to PFS and RML, both funded by MCIN/AEI/10.13039/501100011033 and grant numbers B31_20R (RSA, JMA, and AA) and E35_17R (PFS and RML) and funded by Gobierno de Aragón. The work of RSA was supported by a grant from the Asociación Española Contra el Cáncer (AECC) PRDAR21487SOLE. The authors would like to acknowledge the use of Servicio General de Apoyo a la Investigación-SAI, Universidad de Zaragoza.

References

1. Hanahan, D. Hallmarks of cancer: new dimensions. *Cancer Discovery*. **12** (1), 31-46 (2022).
2. Wind, F., Warburg, O. H. *The Metabolism of Tumors: Investigation from the Kaiser Wilhelm Institute for Biology*. Berlin-Dahlem. Constable. (1930).
3. Warburg, O. On respiratory impairment in cancer cells. *Science*. **124** (3215), 269-270 (1956).

4. Warburg, O. On the origin of cancer cells. *Science*. **123** (3191), 309-314 (1956).
5. Weinhouse, S. On respiratory impairment in cancer cells. *Science*. **124** (3215), 267-269 (1956).
6. Brandon, M., Baldi, P., Wallace, D. C. Mitochondrial mutations in cancer. *Oncogene*. **25** (34), 4647-4662 (2006).
7. Ju, Y. S. et al. Origins and functional consequences of somatic mitochondrial DNA mutations in human cancer. *eLife*. **3**, e02935 (2014).
8. Yuan, Y. et al. Comprehensive molecular characterization of mitochondrial genomes in human cancers. *Nature Genetics*. **52** (3), 342-352 (2020).
9. Arnold, R. S. et al. Bone metastasis in prostate cancer: Recurring mitochondrial DNA mutation reveals selective pressure exerted by the bone microenvironment. *Bone*. **78**, 81-86 (2015).
10. Imanishi, H. et al. Mitochondrial DNA mutations regulate metastasis of human breast cancer cells. *PLoS One*. **6** (8), e23401 (2011).
11. Lu, J., Sharma, L. K., Bai, Y. Implications of mitochondrial DNA mutations and mitochondrial dysfunction in tumorigenesis. *Cell Research*. **19** (7), 802-815 (2009).
12. Luo, Y., Ma, J., Lu, W. The significance of mitochondrial dysfunction in cancer. *International Journal of Molecular Sciences*. **21** (16), 5598 (2020).
13. Marco-Brualla, J. et al. Mutations in the ND2 subunit of mitochondrial complex I are sufficient to confer increased tumorigenic and metastatic potential to cancer cells. *Cancers*. **11** (7), 1027 (2019).
14. Schopf, B. et al. OXPHOS remodeling in high-grade prostate cancer involves mtDNA mutations and increased succinate oxidation. *Nature Communications*. **11** (1), 1487 (2020).
15. Yuan, Y. et al. Nonsense and missense mutation of mitochondrial ND6 gene promotes cell migration and invasion in human lung adenocarcinoma. *BMC Cancer*. **15**, 346 (2015).
16. Zielonka, J., Kalyanaraman, B. "ROS-generating mitochondrial DNA mutations can regulate tumor cell metastasis"--a critical commentary. *Free Radicals Biology and Medicine*. **45** (9), 1217-1219 (2008).
17. Welch, D. R., Foster, C., Rigoutsos, I. Roles of mitochondrial genetics in cancer metastasis. *Trends in Cancer*. **8** (12), 1002-1018 (2022).
18. Cavaliere, A., Marchet, S., Di Meo, I., Tiranti, V. An in vitro approach to study mitochondrial dysfunction: A cybrid model. *Journal of Visualized Experiments*. (181), 63452 (2022).
19. King, M. P., Attardi, G. Human cells lacking mtDNA: repopulation with exogenous mitochondria by complementation. *Science*. **246** (4929), 500-503 (1989).
20. Bacman, S. R., Moraes, C. T. Transmitochondrial technology in animal cells. *Methods in Cell Biology*. **80**, 503-524 (2007).
21. Moraes, C. T., Dey, R., Barrientos, A. Transmitochondrial technology in animal cells. *Methods in Cell Biology*. **65**, 397-412 (2001).
22. Acin-Perez, R. et al. Respiratory complex III is required to maintain complex I in mammalian mitochondria. *Molecular Cell*. **13** (6), 805-815 (2004).
23. Bradford, M. M. A rapid and sensitive method for the quantitation of microgram quantities of protein

utilizing the principle of protein-dye binding. *Analytical Biochemistry*. **72**, 248-254 (1976).

24. Bayona-Bafaluy, M. P. et al. Revisiting the mouse mitochondrial DNA sequence. *Nucleic Acids Research*. **31** (18), 5349-5355 (2003).
25. Srinivasan, S., Guha, M., Kashina, A., Avadhani, N. G. Mitochondrial dysfunction and mitochondrial dynamics-The cancer connection. *Biochimica et Biophysica Acta. Bioenergetics*. **1858** (8), 602-614 (2017).
26. Bartoletti-Stella, A. et al. Mitochondrial DNA mutations in oncocytic adnexal lacrimal glands of the conjunctiva. *Archives of Ophthalmology*. **129** (5), 664-666 (2011).
27. Chinnery, P. F., Samuels, D. C., Elson, J., Turnbull, D. M. Accumulation of mitochondrial DNA mutations in ageing, cancer, and mitochondrial disease: is there a common mechanism? *The Lancet*. **360** (9342), 1323-1325 (2002).
28. Copeland, W. C., Wachsman, J. T., Johnson, F. M., Penta, J. S. Mitochondrial DNA alterations in cancer. *Cancer Investigation*. **20** (4), 557-569 (2002).
29. Gasparre, G. et al. Clonal expansion of mutated mitochondrial DNA is associated with tumor formation and complex I deficiency in the benign renal oncocytoma. *Human Molecular Genetics*. **17** (7), 986-995 (2008).
30. Kopinski, P. K., Singh, L. N., Zhang, S., Lott, M. T., Wallace, D. C. Mitochondrial DNA variation and cancer. *Nature Review Cancer*. **21** (7), 431-445 (2021).
31. Pereira, L., Soares, P., Maximo, V., Samuels, D. C. Somatic mitochondrial DNA mutations in cancer escape purifying selection and high pathogenicity mutations lead to the oncocytic phenotype: pathogenicity analysis of reported somatic mtDNA mutations in tumors. *BMC Cancer*. **12**, 53 (2012).
32. Wallace, D. C. Mitochondria and cancer. *Nature Reviews. Cancer*. **12** (10), 685-698 (2012).
33. Hopkins, J. F. et al. Mitochondrial mutations drive prostate cancer aggression. *Nature Communications*. **8** (1), 656 (2017).
34. Weerts, M. J. A., Smid, M., Foekens, J. A., Sleijfer, S., Martens, J. W. M. Mitochondrial RNA expression and single nucleotide variants in association with clinical parameters in primary breast cancers. *Cancers*. **10** (12), 500 (2018).
35. Jimenez-Morales, S., Perez-Amado, C. J., Langley, E., Hidalgo-Miranda, A. Overview of mitochondrial germline variants and mutations in human disease: Focus on breast cancer (Review). *International Journal of Oncology*. **53** (3), 923-936 (2018).
36. Hardie, D. G. AMP-activated/SNF1 protein kinases: conserved guardians of cellular energy. *Nature Reviews Molecular Cell Biology*. **8** (10), 774-785 (2007).
37. Perrone, A. M. et al. Potential for mitochondrial DNA sequencing in the differential diagnosis of gynaecological malignancies. *International Journal of Molecular Sciences*. **19** (7), 2048 (2018).
38. Musicco, C. et al. Mitochondrial dysfunctions in type I endometrial carcinoma: Exploring their role in oncogenesis and tumor progression. *International Journal of Molecular Sciences*. **19** (7), 2076 (2018).
39. Li, N. et al. Dissecting the expression landscape of mitochondrial genes in lung squamous cell carcinoma and lung adenocarcinoma. *Oncology Letters*. **16** (3), 3992-4000 (2018).
40. Kim, H. R. et al. Spectrum of mitochondrial genome instability and implication of mitochondrial haplogroups

in Korean patients with acute myeloid leukemia. *Blood Research*. **53** (3), 240-249 (2018).

41. Tyagi, A. et al. Pattern of mitochondrial D-loop variations and their relation with mitochondrial encoded genes in pediatric acute myeloid leukemia. *Mutation Research*. **810**, 13-18 (2018).
42. Vidone, M. et al. A comprehensive characterization of mitochondrial DNA mutations in glioblastoma multiforme. *The International Journal of Biochemistry & Cell Biology*. **63**, 46-54 (2015).
43. Chatterjee, A., Mambo, E., Sidransky, D. Mitochondrial DNA mutations in human cancer. *Oncogene*. **25** (34), 4663-4674 (2006).
44. Arnold, R. S. et al. An inherited heteroplasmic mutation in mitochondrial gene COI in a patient with prostate cancer alters reactive oxygen, reactive nitrogen and proliferation. *BioMed Research International*. **2013**, 239257 (2013).
45. Petros, J. A. et al. mtDNA mutations increase tumorigenicity in prostate cancer. *Proceedings of the National Academy of Sciences*. **102** (3), 719-724 (2005).
46. Wallace, D. C., Fan, W., Procaccio, V. Mitochondrial energetics and therapeutics. *Annual Review of Pathology*. **5**, 297-348 (2010).
47. Reznik, E. et al. Mitochondrial DNA copy number variation across human cancers. *eLife*. **5**, e10769 (2016).
48. Soler-Agesta, R. et al. PT-112 induces mitochondrial stress and immunogenic cell death, targeting tumor cells with mitochondrial deficiencies. *Cancers*. **14** (16), 3851 (2022).
49. Trounce, I., Wallace, D. C. Production of transmitochondrial mouse cell lines by cybrid rescue of rhodamine-6G pre-treated L-cells. *Somatic Cell and Molecular Genetics*. **22** (1), 81-85 (1996).
50. Pastushenko, I., Blanpain, C. EMT transition states during tumor progression and metastasis. *Trends in Cell Biology*. **29** (3), 212-226 (2019).
51. Pastushenko, I. et al. Identification of the tumour transition states occurring during EMT. *Nature*. **556** (7702), 463-468 (2018).
52. Thiery, J. P., Sleeman, J. P. Complex networks orchestrate epithelial-mesenchymal transitions. *Nature Reviews Molecular Cell Biology*. **7** (2), 131-142 (2006).

cancers

MDPI

Article

PT-112 Induces Mitochondrial Stress and Immunogenic Cell Death, Targeting Tumor Cells with Mitochondrial Deficiencies

Ruth Soler-Agesta [1], Joaquín Marco-Brualla [1], Martha Minjárez-Sáenz [1,2], Christina Y. Yim [3], Marta Martínez-Júlvez [1,2], Matthew R. Price [3], Raquel Moreno-Loshuertos [1], Tyler D. Ames [3], José Jimeno [1,3] and Alberto Anel [1,*]

[1] Department of Biochemistry and Molecular and Cell Biology, Aragón Health Research Institute (IIS-Aragón), University of Zaragoza, 50009 Zaragoza, Spain
[2] Institute for Biocomputation and Physics of Complex Systems, University of Zaragoza, 50018 Zaragoza, Spain
[3] Promontory Therapeutics Inc., New York, NY 10019, USA
* Correspondence: anel@unizar.es; Tel.: +34-976-761279

Simple Summary: PT-112 is a novel pyrophosphate–platinum conjugate under Phase 1/2 clinical development for the treatment of several tumor types. In this study, using mouse tumor cells with well-characterized mitochondrial and metabolic status, we investigated the mechanisms underlying PT-112's cancer cell death effects. Our results showed that cells with defective mitochondria were more sensitive to PT-112 when compared to cells with normal mitochondrial function. Moreover, PT-112 induced tumor cell death in those sensitive cells through non-conventional mechanisms, including increased mitochondrial stress, free radical generation and immunogenic cell death, a form of cell death that elicits an immune response. Taken together, the present findings suggest the potential for predictors of PT-112 sensitivity in the clinical setting on the basis of metabolic function.

Abstract: PT-112 is a novel pyrophosphate–platinum conjugate, with clinical activity reported in advanced pretreated solid tumors. While PT-112 has been shown to induce robust immunogenic cell death (ICD) in vivo but only minimally bind DNA, the molecular mechanism underlying PT-112 target disruption in cancer cells is still under elucidation. The murine L929 in vitro system was used to test whether differential metabolic status alters PT-112's effects, including cell cytotoxicity. The results showed that tumor cells presenting mutations in mitochondrial DNA (mtDNA) (L929dt and $L929^{dt}$ cybrid cells) and reliant on glycolysis for survival were more sensitive to cell death induced by PT-112 compared to the parental and cybrid cells with an intact oxidative phosphorylation (OXPHOS) pathway (L929 and dt^{L929} cybrid cells). The type of cell death induced by PT-112 did not follow the classical apoptotic pathway: the general caspase inhibitor Z-VAD-fmk did not inhibit PT-112-induced cell death, alone or in combination with the necroptosis inhibitor necrostatin-1. Interestingly, PT-112 initiated autophagy in all cell lines, though this process was not complete. Autophagy is known to be associated with an integrated stress response in cancer cells and with subsequent ICD. PT-112 also induced a massive accumulation of mitochondrial reactive oxygen species, as well as changes in mitochondrial polarization—only in the sensitive cells harboring mitochondrial dysfunction—along with calreticulin cell-surface exposure consistent with ICD. PT-112 substantially reduced the amount of mitochondrial CoQ10 in L929 cells, while the basal CoQ10 levels were below our detection limits in L929dt cells, suggesting a potential relationship between a low basal level of CoQ10 and PT-112 sensitivity. Finally, the expression of HIF-1α was much higher in cells sensitive to PT-112 compared to cells with an intact OXPHOS pathway, suggesting potential clinical applications.

Keywords: PT-112; cancer cell death; mitochondrial ROS; CoQ10; immunogenic cell death; ICD; HIF-1α

check for updates

Citation: Soler-Agesta, R.; Marco-Brualla, J.; Minjárez-Sáenz, M.; Yim, C.Y.; Martínez-Júlvez, M.; Price, M.R.; Moreno-Loshuertos, R.; Ames, T.D.; Jimeno, J.; Anel, A. PT-112 Induces Mitochondrial Stress and Immunogenic Cell Death, Targeting Tumor Cells with Mitochondrial Deficiencies. *Cancers* **2022**, *14*, 3851. https://doi.org/10.3390/cancers14163851

Academic Editor: Carmela Fimognari

Received: 23 June 2022
Accepted: 3 August 2022
Published: 9 August 2022

Publisher's Note: MDPI stays neutral with regard to jurisdictional claims in published maps and institutional affiliations.

1. Introduction

PT-112 (R,R-1,2 cyclohexanediamine-pyrosphosphato-platinium (II)) is a novel compound consisting of a stable pyrophosphate conjugated to a diaminocyclohexane-platinum

(Pt) ring [1]. In comparison to traditional platinum-containing agents, it shows substantially reduced DNA binding with minimal acute renal toxicities and neurotoxicity, as shown in early in vitro studies in yeast models, human ovarian cancer cell lines, and in vivo models [2–4]. PT-112 has demonstrated anti-tumor activity in mice bearing various murine and human tumors at sub-toxic doses [2,3,5–7], robust induction of immunogenic cell death (ICD) [7], and systemic biodistribution to multiple tissues and organs, including kidney, lung and liver, with the highest concentrations reached in bone [5]. These observations may be explained at least in part by PT-112's organic pyrophosphate moiety, which is chemically similar to a bisphosphonate. Bisphosphonates can bind to mineral bone surfaces [8] and are generally used in oncology for the management of skeletal complications and/or bone metastases. In addition, some bisphosphonates have been shown to exhibit anti-cancer properties by targeting specific enzymes of the mevalonate pathway [9,10]. Specifically, the nitrogen-containing bisphosphonates inhibit farnesyl pyrophosphate synthase (FPPS), a key enzyme of the mevalonate pathway [11,12].

Preclinical findings with PT-112 provided a rationale for clinical development, and Phase I data reported from the first-in-human study of PT-112 monotherapy in a heavily pretreated population with solid tumors showed favorable tolerability and safety profiles, as well as evidence of efficacy, including prolonged responses and tumor control in different tumor types, such as non-small cell lung cancer, small cell lung cancer and thymoma (ClinicalTrials.gov ID: NCT02266745), [13]. Notably, clinical and serologic responses to the monotherapy in a small sub-population of late-stage, metastatic castration-resistant prostate cancer (mCRPC) patients were observed, and a median overall survival of 15.1 months was reached [13,14]. In addition, in a combination study with PD-L1 immune checkpoint inhibitor avelumab (ClinicalTrials.gov ID: NCT03409458), PT-112 was shown to be feasible with a lack of overlapping toxicities, and preliminary evidence of efficacy included long-lasting objective remissions and tumor control in mCRPC and other solid tumors [13–15]. PT-112 was also shown to have biological activity in mouse models of multiple myeloma [5] and was the subject of a Phase I clinical trial in heavily pretreated multiple myeloma patients (ClinicalTrials.gov ID: NCT03288480), where monotherapy activity has been reported [16]. Phase II studies of PT-112 are currently ongoing.

Along with the progress made in the clinical setting, a major effort has been made in translational studies to discern the mechanisms underlying PT-112 target disruption. In previous work from our laboratory, we characterized the L929dt cell subline derived from the transformed fibroblast cell line L929 [17]. L929dt cells lost matrix attachment and MHC-I expression and showed a lower capacity to generate energy through OXPHOS, as well as decreased respiratory capacity compared to parental L929 cells. These defects correlated with mtDNA mutations in L929dt cells at the *ND2* subunit of complex I and were accompanied by a substantial glycolytic shift and higher in vivo tumorigenic and metastatic potential than the parental cell line. We also demonstrated that mitochondrial mutations are responsible for the aggressive tumor phenotype by generating cybrid cells with L929dt mitochondria in L929 nuclear background ($L929^{dt}$ cells), which reproduced all L929dt properties. Remarkably, cybrid cells with parental L929 mitochondria in the L929dt nuclear background (dt^{L929} cells) recovered the complete parental L929 phenotype [18].

This cellular system, with distinct glycolytic and metabolic phenotypic properties due to defined mitochondrial DNA mutations, was used to explore whether differential metabolic and mitochondrial status alters PT-112-driven effects and cytotoxicity in cells. In addition, we investigated the mechanism underlying cell death induced by PT-112 in this cellular system, connecting to known PT-112 immunogenic cell death potential, and tried to relate it to the expression of specific biomarkers such as HIF-1α.

In the present work, we demonstrate that PT-112 does not kill cells in this L929 panel exclusively by apoptosis or necroptosis but rather by initiating an unresolved autophagy process and causing mitochondrial stress and membrane disruption. Cells that have an intact OXPHOS pathway can cope with this PT-112-induced stress, but in cells that have an extreme glycolytic and hypoxic phenotype as indicated by HIF-1α expression,

exposure to PT-112 is associated with massive mitochondrial ROS generation and cell death. These observations suggest that PT-112's mechanism of action may be selective to cancer metabolic processes, with the potential for clinical applications of PT-112 in metabolically aggressive cancers.

2. Materials and Methods

2.1. Cell Culture

Mouse fibroblast cell lines L929 and L929-derived, "detached" cells (L929dt) were routinely cultured in high glucose DMEM medium with GlutaMAX (Life Technologies, Paisley, UK) supplemented with 10% of fetal calf serum (FCS; Sigma, St. Louis, MO, USA), penicillin (1000 U/mL) and streptomycin (10 mg/mL) (PanBiotech, Aidenbach, Germany) at 37 °C and 5% CO_2 using standard procedures. The cybrid cell lines $L929^{dt}$ and dt^{L929} were obtained as previously described [18] and cultured with the identical medium as parental cells. For L929-ρ^0 cells, complete DMEM medium was also supplemented with pyruvate (100 µg/mL) and uridine (50 µg/mL).

2.2. Cell Viability Assays

Relative cell growth was measured using a modified Mossman method for microplates. Briefly, 3×10^4 cells were seeded per well in a 96-well flat-bottom plate and incubated with increasing concentrations of PT-112 or cisplatin (2, 6 and 10 µM) for 24–72 h at 37 °C. Then, 10 µL of a 5 mg/mL MTT solution was added to each well and incubated for 3 h. During the incubation time, viable cells reduced the MTT solution to insoluble purple formazan crystals, which were subsequently solubilized with isopropanol and 0.05 M HCl mixture, and the absorbance was measured in a microplate reader (Dynatec, Pina de Ebro, Spain). The MTT method in mitochondria-defective cell lines has been used in other studies, as MTT reduction is performed not only by mitochondrial enzymes but also by other cellular oxidoreductases [19,20]. Control cell lines were included in each growth experiment.

2.3. Cytotoxicity Assays and Cell Death Quantification

Cytotoxicity assays were performed as follows: 100 µL aliquots of 3×10^4 cells were seeded per well in a 96-well plate, and 10 µM of PT-112 or cisplatin were added and incubated for 24–72 h at 37 °C. Cell death was analyzed using a FACSCalibur flow cytometer (BD, Biosciences) after incubation with annexin-V-FITC and 7-AAD (BD Biosciences, Madrid, Spain) in annexin binding buffer (140 mM NaCl, 2.5 mM $CaCl_2$, 10 mM HEPES/NaOH, pH 7.4) for 10 min.

2.4. ROS Production and Mitochondrial Membrane Potential Measurement

Total ROS production and mitochondrial membrane potential were simultaneously measured using a FACScalibur flow cytometer (BD Biosciences). Pretreated cells with PT-112 were incubated with $DiOC_6$ at 20 nM (Molecular Probes, Madrid, Spain) and DHE at 2 µM (Molecular Probes, Madrid, Spain) for 30 min at 37 °C. For mitochondria-specific ROS production, cells were incubated with MitoSOX™ (5 µM, ThermoFisher, Rockford, IL, USA) for 30 min at 37 °C.

2.5. Apoptosis and Necroptosis Inhibition Assays

In total, 3×10^4 cells were seeded in a 96-well plate and incubated with a pan-caspase inhibitor Z-VAD-fmk (50 µM, MedChem Express, Monmouth Junction, NJ, USA) and/or RIPK-1 inhibitor necrostatin-1 (30 µM, MedChem Express, Monmouth Junction, NJ, USA) for 1 h. Next, cells were treated with 10 µM of PT-112 and incubated for 48 h at 37 °C. Both inhibitors were refreshed in their corresponding well after 24 h. Finally, cell death was assessed using flow cytometry after incubation with annexin-V-FITC and 7-AAD for 10 min.

2.6. Analysis of Caspase-3 Activation

Caspase-3 activation was measured using a FITC-labelled antibody against cleaved caspase-3 (BD Pharmingen™, Madrid, Spain). Cells pretreated with 10 μM of PT-112 were fixed with 4% paraformaldehyde solution for 15 min at 4 °C. Then, cells were washed with PBS buffer, permeabilized using a 0.1% saponin dilution supplemented with 5% fetal bovine serum and incubated for 15 min at room temperature (RT). After washing them, samples were incubated with the antibody for 30 min at RT and analyzed by flow cytometry.

2.7. Cyto-ID® Analysis and Autophagosome Formation Measurement

For autophagy analysis, the autophagosome formation after treatment with PT-112 was evaluated using a Cyto-ID® probe (Enzo Life Sciences, Farmingdale, NY, USA). Cells pretreated with 10 μM of PT-112 were incubated with 1 μL of Cyto-ID® dye reagent for 30 min at 37 °C. Subsequently, cells were washed with PBS buffer and analyzed by flow cytometry. For autophagy-positive controls, cells were treated with 1 μM of rapamycin at least 12 h before the analysis.

2.8. Calreticulin (CRT) Surface Expression Measurement

CRT surface expression upon incubation with PT-112 (24–72 h) was analyzed by flow cytometry. Cells treated with PT-112 were incubated with primary rabbit antibody (Abcam, #AB2907) at 1:700 dilution and at 4 °C for 1 h. Then, cells were washed with PBS and incubated simultaneously with secondary goat anti-rabbit IgG antibody conjugated with Alexa Fluor488® (Invitrogen, #A11034) and 7-AAD. To rule out non-specific interactions, untreated cells were incubated only with secondary antibody. 7-AAD-positive cells were excluded from the analysis.

2.9. Immunoblot Analysis

A total of 5×10^6 cells were lysed with 100 μL of 1× lysis buffer (1% Triton-X-100; 150 mM NaCl; 50 mM Tris/HCl pH 7,6; 10% *v/v* glycerol; 1 mM EDTA; 1 mM sodium orthovanadate; 10 mM sodium pyrophosphate; 10 μg/mL leupeptin; 10 mM sodium fluoride; 1 mM methyl phenyl sulfide, Sigma, St. Louis, MO, USA) for 30 min on ice. The mixture was ultra-centrifugated at 12,000 rpm for 20 min at 4 °C. The protein concentration in the supernatant was analyzed using the BCA assay (Thermo Fisher, Rockford, IL, USA) and was mixed with 3× lysis buffer (SDS 3% *v/v*; 150 mM Tris/HCl; 0.3 mM sodium molybdate; 30% *v/v* glycerol; 30 mM sodium pyrophosphate; 30 mM sodium fluoride; 0.06% *p/v* bromophenol blue; 30% *v/v* 2-mercaptoethanol, all purchased from Sigma, St. Louis, MO, USA). Protein separation was performed using SDS-PAGE (6% or 12% polyacrylamide gel), and proteins were transferred to nitrocellulose membranes using a semi-dry electro-transfer (GE Healthcare, Chicago, IL, USA). Membranes were blocked with TBS-T buffer (10 mM Tris/HCl, pH 8.0; 120 mM NaCl; 0.1% Tween-20, 0.1 g/L thimerosal, Sigma, St. Louis, MO, USA) containing 5% skimmed milk. Protein detection was performed by western blot using specific antibodies against p62 (Santa Cruz, SC-28359), LC3BI/II (Sigma, L7543) and HIF-1α (Novus, NB100–479) that were incubated overnight at 4 °C in agitation. Anti-rabbit or anti-mouse secondary antibodies labeled with peroxidase (Sigma, A9044) were incubated for 1 h at RT. Blots were analyzed with Pierce ELC Western Blotting Substrate (Thermo Scientific, Rockford, IL, USA) using an Amersham Imager 680 (GE Healthcare Life Sciences). Protein expression was quantified by densitometry using ImageJ software. β-actin or tubulin levels were used as a reference to normalize data (Cell Signaling, 3700).

2.10. Coenzyme Q Quantification

Mitochondria were isolated from cultured cell lines as previously described [21] with small modifications [22]. A mitochondrial pellet was immediately frozen in liquid nitrogen under anaerobic conditions. Then, lipids extraction and CoQ determination were performed as described previously [23]. Briefly, mitochondrial samples (0.6 mg of mitochondrial

protein for each measurement) were lysed with 1% SDS and vortexed for 1 min. Then, a mixture of ethanol:2-propanol (95:5) was added and the samples vortexed again for 1 min. To recover CoQ, 5 mL of hexane was added, and the samples were centrifuged at 1000× *g* for 5 min at 4 °C. The upper phases from two extractions were recovered and dried using a rotary evaporator. Lipid extracts were suspended in 1 mL ethanol, dried in a speed-vac and stored at −20 °C. Samples were resuspended in a suitable volume of ethanol prior to HPLC injection. Lipid components were separated with an Alliance HPLC system (Waters) equipped with a 2707 autosampler and 2996 photodiode array detector, with HSST3 column (4.6 × 150 mm, 3.5 µm, Waters), preceded by a pre-column (4.6 × 20 mm, 3.5 µm, Waters), with a flow rate of 1 mL/min and a mobile phase containing 40:60 methanol/2-propanol. Commercial CoQ10 (Sigma) was used as an internal standard to detect the CoQ10 peak in the samples.

2.11. Statistical Analysis and Data Processing

Statistical analysis was performed using GraphPad Prism8 (GraphPad Software Inc., San Diego, CA, USA). For quantitative variables, results are shown as mean ± standard deviation (SD). Statistical significance was evaluated using Student's *t*-test, and differences were considered significant when $p < 0.05$. Data obtained by flow cytometry were analyzed using FlowJo 10.0.7 (Tree star Inc., San Francisco, CA, USA).

3. Results

3.1. Cell Growth Inhibition by PT-112 and Cisplatin in L929, L929dt and Cybrid Cells

First, we compared the sensitivity of L929, L929dt and cybrid cells to PT-112 and to cisplatin, a Pt-based chemotherapeutic agent whose mechanism of action is known to involve DNA damage and apoptosis induction [24]. All cell lines were treated with increasing concentrations of PT-112 or cisplatin (2, 6 and 10 µM) and incubated for 24–72 h at 37 °C. The concentrations used are compatible with active levels achieved during well-tolerated in vivo experiments [13,14]. Cell growth was assessed by the MTT reduction method. As shown in the upper panel of Figure 1, PT-112 inhibited cell growth in a time-dependent manner, as a clear decrease in cell growth was not observed until 48 h of exposure. We also observed that the cell lines with mtDNA mutations, L929dt and the $L929^{dt}$ cybrid, were noticeably more sensitive to PT-112 than L929 cells and the dt^{L929} cybrid. This difference was statistically significant at 48 h and was more pronounced at 72 h, where the growth of glycolytic cells was inhibited by around 80% at the highest concentration. On the contrary, limited growth inhibition was observed in the OXPHOS-competent L929 and dt^{L929} cybrid cells at 48 h (i.e., <40% inhibition at the higher concentration used), and the degree of inhibition did not further increase with increased exposure time.

For cisplatin treatments (Figure 1, bottom panel), we observed a significant effect on cell growth starting at 24 h. At 48 h, cisplatin inhibited the growth of all cell lines, with no statistically significant differences among them, contrary to those observed for PT-112. At 72 h, cisplatin-induced effects on growth were more pronounced in the glycolytic cells, although dose-dependent effects were also seen in the non-glycolytic cell lines (i.e., 95% inhibition in L929dt and $L929^{dt}$ cells and 70% inhibition in L929 and dt^{L929} cells at 10 µM cisplatin).

These data demonstrate that PT-112 has a marked selectivity for tumor cells with defective mitochondria (i.e., those exhibiting a glycolytic phenotype), suggesting a relationship between PT-112 sensitivity and the metabolic status of tumor cells.

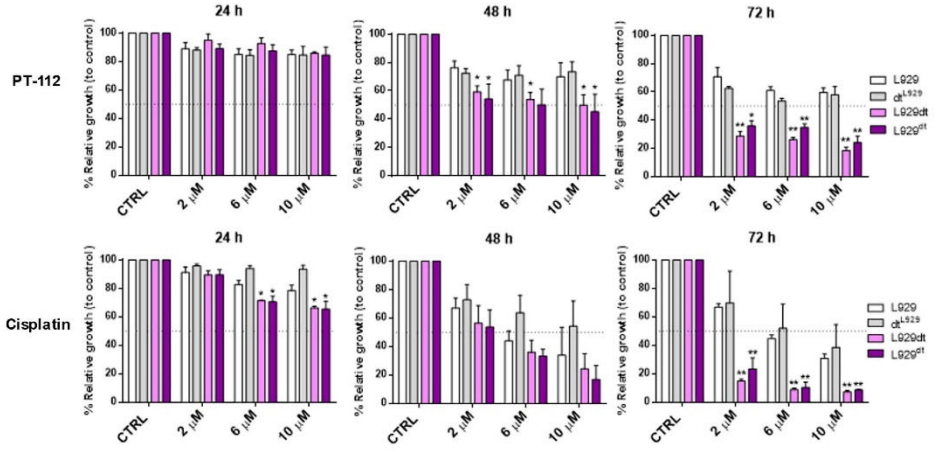

Figure 1. Cell growth analysis after treatment with PT-112 or cisplatin, as indicated. Cells were treated with increasing concentrations of PT-112 or cisplatin, incubated for 24–72 h, and cell growth was measured by the MTT assay. Results were expressed as the percentage of relative growth compared to control, untreated cells (CTRL) ± SD of at least 2 independent experiments performed in duplicate. Statistical significance represents those values in which cell growth inhibition by the drugs was higher in a given cell type as compared with parental L929 cells. *, $p < 0.05$; **, $p < 0.01$.

3.2. Cytotoxic Effect of PT-112 and Cisplatin in L929, L929dt and Cybrid Cells and Caspase-3 Activation by PT-112 in Sensitive Cells

To characterize cell death induction by PT-112 and cisplatin, cells were incubated with 10 μM of PT-112 or cisplatin for 24, 48 or 72 h, and at the end of the incubation, cells were stained with annexin-V-FITC and 7-AAD and analyzed by flow cytometry. The results showed that cisplatin induced cell death in all cell lines, especially after long-time drug exposure (Figure 2). In contrast, PT-112 was cytotoxic only in glycolytic cells, consistent with the differential sensitivity observed in Figure 1 (Figure 2). In cisplatin-induced cell death, the apoptotic cell population (annexin-V^+, 7-AAD) was observed in all cell lines, albeit cell death was induced more rapidly in the more glycolytic cells (Figure 2B, bar sections colored in black). On the contrary, this population was not appreciably observed at any time point in sensitive L929dt and $L929^{dt}$ cells treated with PT-112. Dead cells (annexin-V^+, 7-AAD^+) were detected at an early time point, and the population increased with time (Figure 2B, bar sections colored in white). Finally, at longer exposure times, both glycolytic cell lines showed a population that is positive for 7-AAD and negative for annexin-V staining, typical of necrotic cell death (Figure 2B, bar sections colored in grey). Taken together, these results clearly demonstrate that PT-112 has a distinct mechanism of action from cisplatin and differential sensitivity to the glycolytic phenotype driven by mtDNA mutations.

To further investigate if and how PT-112 cell death related to the induction of apoptosis in sensitive cells, we analyzed the effect of PT-112 on caspase-3 activation, the main apoptotic executioner. We used a FITC-labelled anti-caspase-3 antibody specific for cleaved, active caspase-3 that can be measured by flow cytometry. As shown in Figure 3A, the levels of active caspase-3 clearly increased in a time-dependent manner in L929dt and $L929^{dt}$ cells sensitive to PT-112-induced cell death. To further investigate the implications of caspase-3 activation in this process, we tested the ability of the general pan-caspase inhibitor Z-VAD-fmk and/or the necroptosis inhibitor necrostatin-1 to prevent cell death induced by PT-112 (Figure 3B). Cells were stained simultaneously with annexin-V-FITC and 7-AAD, and the percentage of the different populations was analyzed by flow cytometry.

We observed, in agreement with the results presented in Figure 2A, that PT-112 induced a direct accumulation of double positive (i.e., dead) cells. Z-VAD-fmk, necrostatin-1 or their combination did not inhibit cell death, and the double positive population remained the dominant group in all cases. In fact, cells were more sensitive to PT-112 treatment in the presence of Z-VAD-fmk. Co-incubation with necrostatin-1 prevented this Z-VAD-fmk-induced increase in sensitivity, though this effect was only significant in L929dt cells. These data indicate that neither apoptosis nor necroptosis were the main mechanisms of cell death induced by PT-112 in these cell lines, while a small necroptotic component is observed only if caspases are inhibited. This is reminiscent of other cell death inducers such as TNF-α, specifically in L929 cells [25].

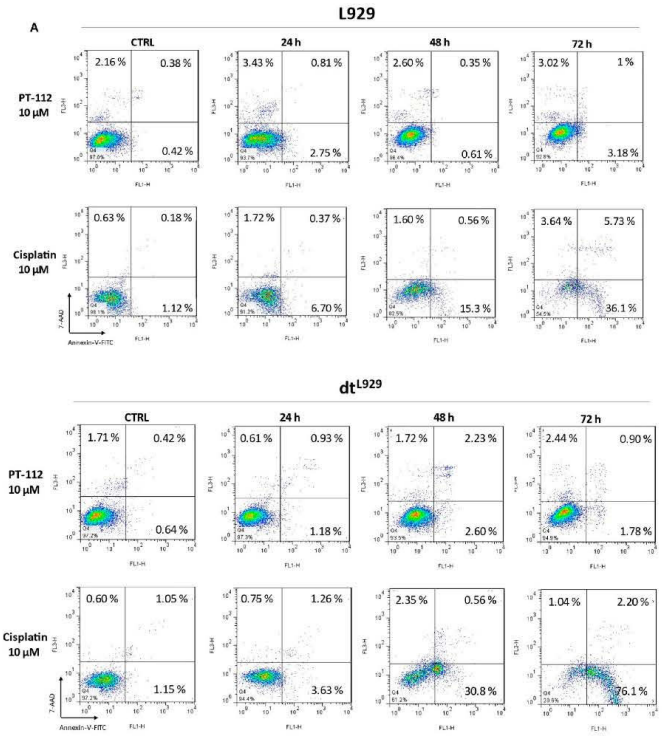

Figure 2. *Cont.*

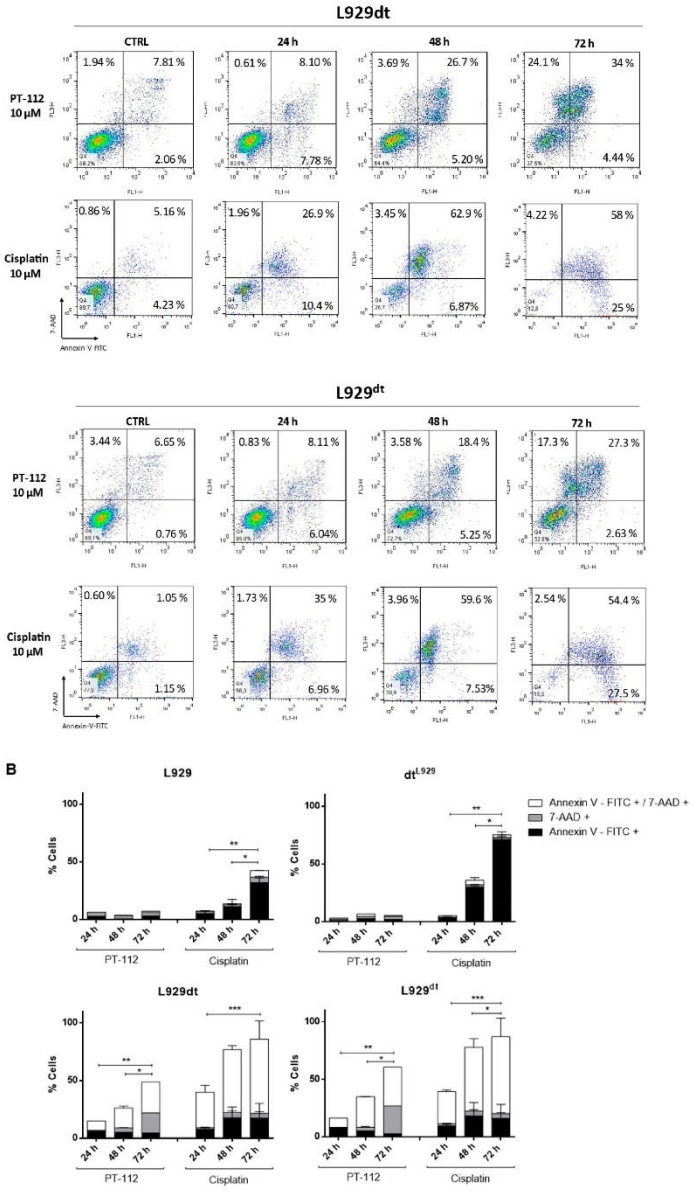

Figure 2. Cytotoxicity of PT-112 or cisplatin. Parental L929, L929dt and cybrids cells were incubated with 10 µM of PT-112 or cisplatin for 24, 48 and 72 h. Then, cells were simultaneously stained with annexin-V-FITC and 7-AAD and analyzed by flow cytometry. (**A**) Dot plots represent the staining evolution of the treated cell population compared to the control. (**B**) Graph bars correspond to a graphical representation of obtained data reporting cell percentage in each quadrant of dot plots. Results are shown as mean ± SD of at least 2 independent experiments performed in duplicate. *, $p < 0.05$; **, $p < 0.01$; ***, $p < 0.001$.

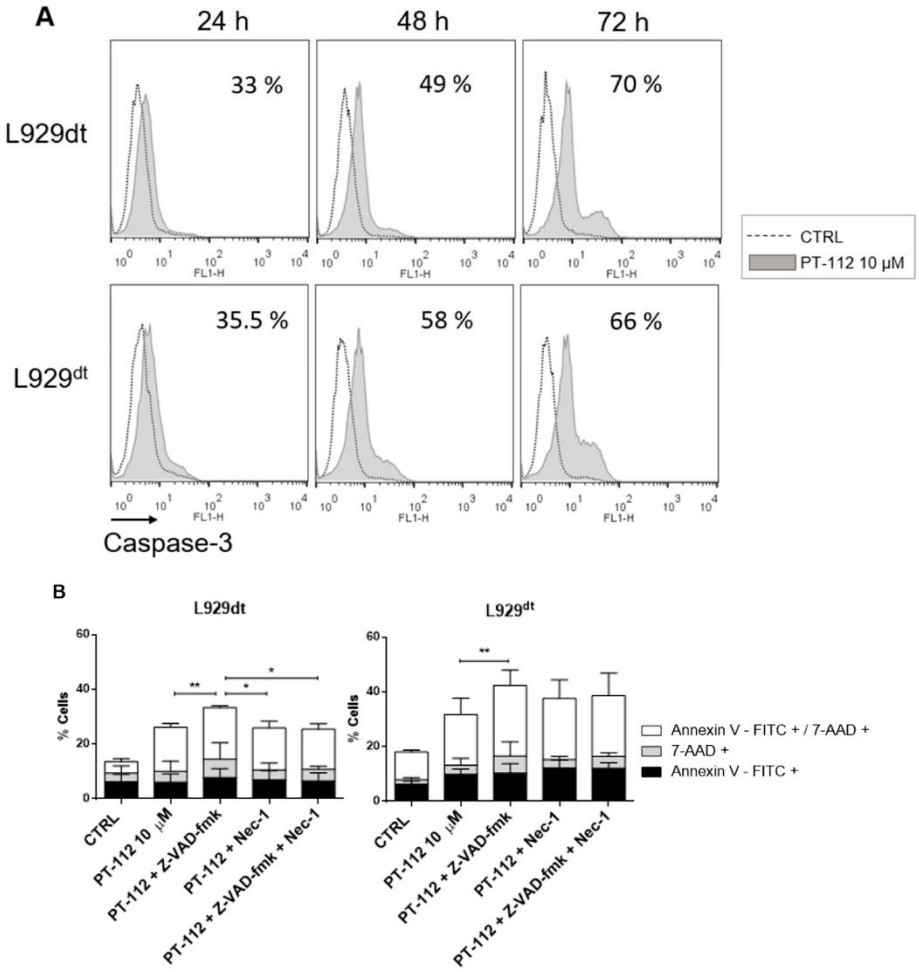

Figure 3. Caspase-3 activation by PT-112 and effect of apoptosis and necroptosis inhibitors. (**A**) Levels of caspase-3 activation upon treatment with PT-112. 3×10^4 cells were treated with 10 µM of PT-112 for 24–72 h. Then, cells were incubated with anti-cleaved caspase-3 labelled with FITC dye and analyzed by flow cytometry. The numbers in each box represent the percentage of cleaved caspase-3 compared to untreated cells. (**B**) Cytotoxicity analysis of PT-112 combined with Z-VAD-fmk and/or necrostatin-1 inhibitors. Cells were pretreated for 1 h with or without pan-caspase or/and necroptosis inhibitors and then, incubated with 10 µM of PT-112 for 48 h. Flow cytometry analysis was performed using annexin-V-FITC and 7-AAD staining. Results are shown as mean ± SD of 3 independent experiments performed in duplicate. Statistical significance is depicted in the graphics. *, $p < 0.05$; **, $p < 0.01$.

3.3. PT-112 Induces Autophagosome Formation

After observing that PT-112 was not reliant on apoptosis or necroptosis (Figures 2 and 3), we tested the possibility that it could induce autophagy. The initiation of autophagy was analyzed using the Cyto-ID® method that allows detection of intracellular autophagosome formation by flow cytometry. As shown in Figure 4, PT-112 clearly induced autophagosome formation in all cell lines at 48 h of PT-112 treatment. At 72 h, autophagosome formation decreased in L929dt and L929^{dt} cells, possibly due to the induction of cell death. On the contrary, in L929 and dt^{L929} cells, autophagosome formation was maintained at 72 h (Figure 4A,B). Of note, we observed that L929dt and L929^{dt} cells were more sensitive to autophagy induction by rapamycin than L929 and dt^{L929} cells (Figure 4A). To further investigate the activation of autophagy upon PT-112 treatment, we analyzed expression levels of p62 and the conversion of LC3BI to LC3BII, known indicators of autophagy induction. The results showed a tendency towards the conversion of LC3BI to LC3BII in L929, and especially in dt^{L929} cells, and a gradual accumulation of p62 (Figure 4C). In L929dt and L929^{dt} cells, we did not observe significant changes in p62 levels, while a rapid reduction in LC3BI levels was observed after drug treatment and accompanied by the appearance of faint LC3BII bands. The Cyto-ID® results, the most sensitive method to detect autophagosome formation [26], and the LC3B data demonstrate that PT-112 initiates the autophagy process. However, the absence of p62 reduction or degradation indicates this process did not reach completion.

The observation of cells on the microscope after treatment with PT-112 showed abundant brilliant spots inside the cytoplasm of all four cell lines, which may correspond to autophagosomes. In addition, in L929dt and L929^{dt} cells sensitive to cell death, induction by small, uniform PT-112 cell debris was also detected (Figure S1).

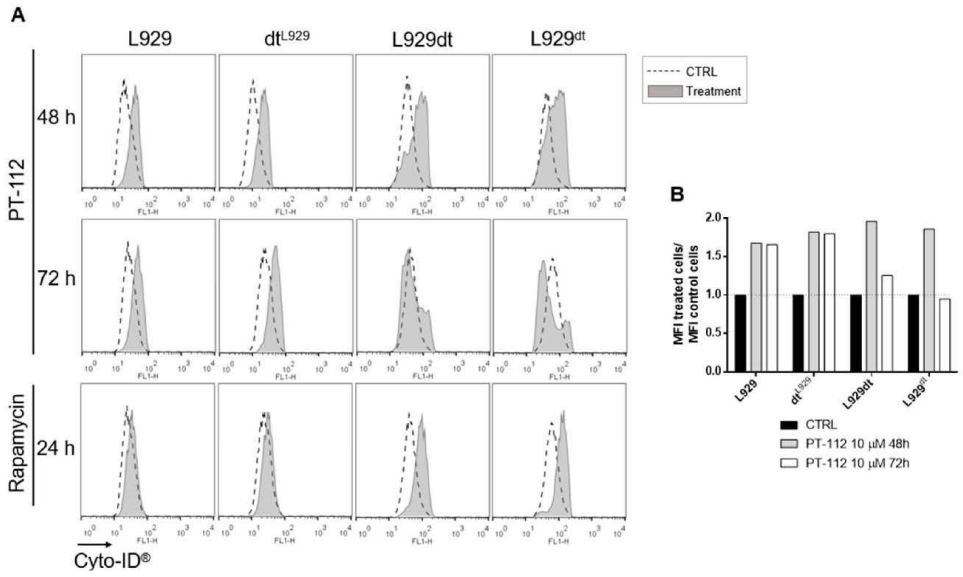

Figure 4. *Cont.*

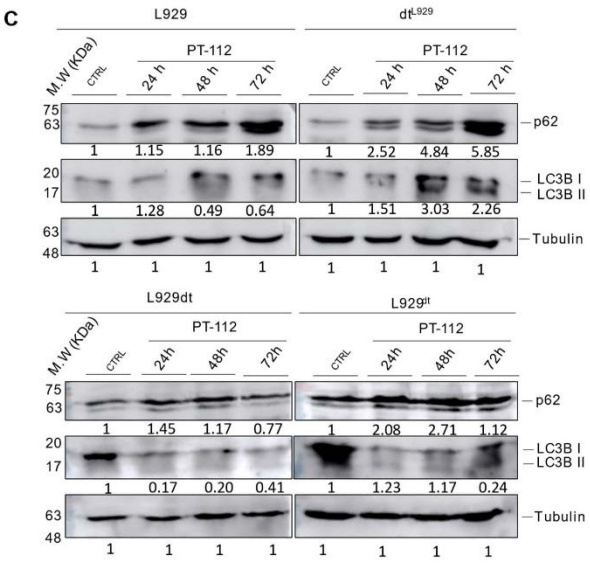

Figure 4. PT-112 induces the initiation of autophagy. (**A**) Analysis of autophagosome formation. Cells were incubated with 10 μM of PT-112 for 48–72 h. The autophagosome formation was analyzed by flow cytometry using the Cyto-ID® method. (**B**) Graphical representation of data obtained with Cyto-ID® analysis. Mean fluorescence intensity (MFI) of treated cells compared to untreated cells is shown. (**C**) Expression levels of p62 and LC3BI/II upon PT-112 treatment. Tubulin was used as a control of protein load. The uncropped blots are shown in Figure S3.

3.4. PT-112 Affects Mitochondrial Membrane Potential and Induces Massive Mitochondrial Reactive Oxygen Species (ROS) Generation in Sensitive Cells

One typical event related to the activation of the mitochondrial apoptotic pathway is the loss of mitochondrial membrane potential (ΔΨm) [27]. Hence, we analyzed the effect of PT-112 on ΔΨm using $DiOC_6$ (3) staining and flow cytometry. As shown in Figure 5, while ΔΨm did not experience any change during the 72 h incubation with PT-112 in L929 and $dt^{I.929}$ cells, a significant change was observed in the PT-112 sensitive, glycolytic cells. Remarkably, ΔΨm increased in these cells upon PT-112 treatment, showing the appearance of a cell population with hyperpolarized mitochondria at 48 h, simultaneously accompanied by a population that partially lost ΔΨm. Both populations were detected at 72 h, but with a larger fraction of cells showing a loss of ΔΨm.

Next, we studied the effects of PT-112 exposure on ROS production. First, we performed a time-course determination of total ROS generation by detection of 2HE oxidation by flow cytometry. As shown in Figure 6A, we observed a moderate increase in total ROS production in a time-dependent manner in all cell lines tested, reaching maximum levels between 48 and 72 h. L929 and $dt^{I.929}$ cells showed similar levels of total ROS production to L929dt and $L929^{dt}$ cells after 72 h of exposure, but the rate of increase in ROS levels was faster in the latter, sensitive cell types. To further delineate these effects, we determined specific mitochondrial ROS (mtROS) production upon PT-112 treatment using the MitoSOX™ reagent. As shown in Figure 6B,C, mtROS production was massively increased in sensitive cells after treatment with PT-112, while little to no change was observed in insensitive L929 or $dt^{I.929}$ cells, suggesting that this event may be related to cell death induced by PT-112.

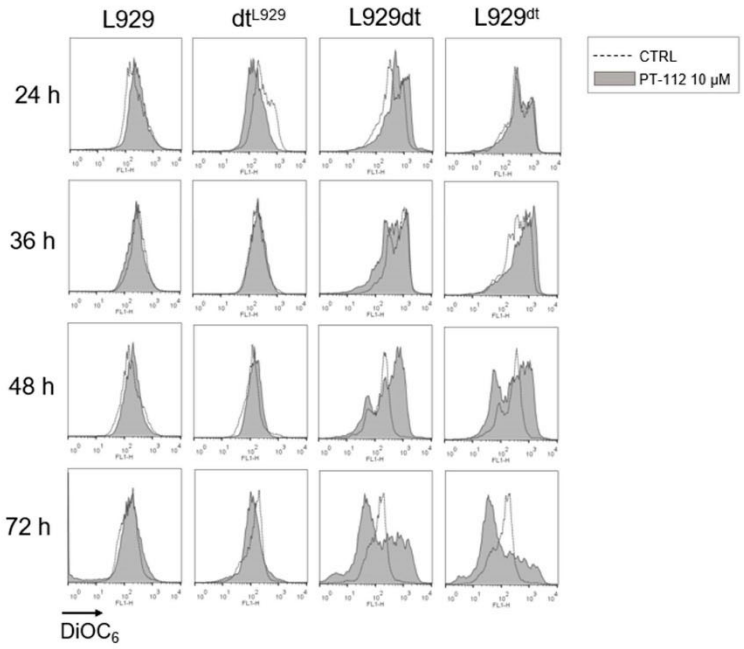

Figure 5. Analysis of mitochondrial membrane potential (ΔΨm) upon treatment with PT-112 at different incubation times. A total of 3×10^4 cells were incubated with 10 µM of PT-112 for 24, 36, 48 and 72 h at 37 °C. Changes in ΔΨm were determined by staining with $DiOC_6$ and analyzed by flow cytometry. As shown in the legend, dotted histograms correspond to fluorescence values of untreated cells, and grey-colored histograms correspond to those of treated cells.

Next, we attempted to further investigate the causality of ROS generation in the cell death process induced by PT-112. Since PT-112-induced ROS generation seems to be concentrated in mitochondria, we used the mitochondria-specific ROS scavenger, MitoTEMPO. As shown in Figure 7A, MitoTEMPO was able to almost completely abolish mitochondrial superoxide generation induced by the potent mitochondrial complex III inhibitor, antimycin A. PT-112 induced a higher amount of mitochondrial superoxide anion compared to antimycin A, and co-incubation with MitoTEMPO resulted in a limited reduction in mitochondrial ROS (Figure 7B). A reduction in PT-112-induced L929dt cell death was also observed when co-incubated with mitoTEMPO and was statistically significant after 72 h (Figure 7C). These data suggest that mitochondrial ROS generation is implicated in PT-112-induced cell death, although it is experimentally difficult to prevent ROS formation in order to finitely determine causality by chemical means.

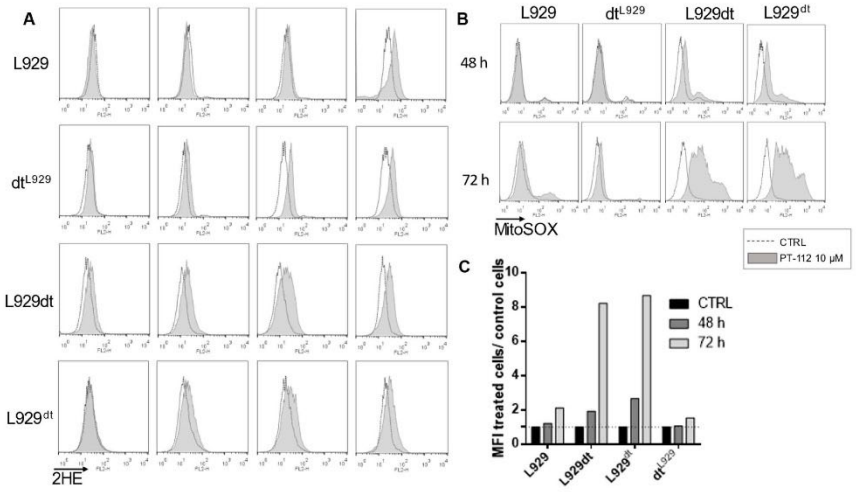

Figure 6. Analysis of total and specific mitochondrial ROS production upon treatment with PT-112 at different incubation times. (**A**) A total of 3×10^4 cells were incubated with 10 μM of PT-112 for 24, 36, 48 and 72 h at 37 °C. Total ROS production was determined by staining with 2HE and flow cytometry. (**B**) Specific mitochondrial ROS production after incubation with 10 μM of PT-112. Cells were stained with a mitochondrial superoxide indicator MitoSOX™ for 15 min at 37 °C, in darkness. The fluorescence intensity values of treated cells compared to control cells (CTRL) were determined by flow cytometry. As shown in the legend, dotted histograms correspond to the fluorescence of untreated cells, and grey-colored histograms correspond to the fluorescence values of treated cells. (**C**) Graphical representation of data obtained in Figure 6B. Data are shown as MFI of treated cells compared to untreated cells.

As an alternative approach, we decided to use L929-ρ^0 cells. ρ^0 cells are devoid of mtDNA by prolonged exposure to ethidium bromide and are unable to perform OXPHOS or generate mitochondrial ROS; although, upon specific treatments (such as with perforin/granzyme B), they can generate ROS from extra-mitochondrial sources [17,28]. We tested the growth inhibition effect of PT-112 and cisplatin on these L929-ρ^0 cells in order to assess whether the complete absence of mitochondrial function would affect PT-112 sensitivity.

As shown in Figure 8, while cisplatin inhibited the growth of these cells, PT-112 scarcely affected their growth rate at any concentration or time of incubation. In addition, while PT-112 did not robustly induce cell death in parental L929 cells (Figure 2), it did inhibit the growth of these cells to some extent (Figure 1), contrasting with the lack of effects on the growth of L929-ρ^0 cells. These differences in PT-112 effects between L929 and the L929-ρ^0 cells are not due to differences in the basal growth rate of these two types of cells. These data suggest that the effects on mitochondria play a large role in the PT-112 mechanism of action, potentially mediated via mtROS generation.

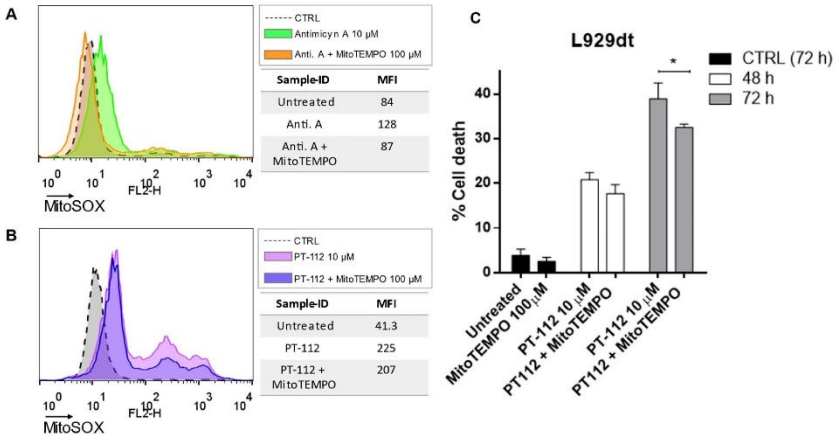

Figure 7. Partial inhibition of PT-112-induced mtROS generation and cell death in L929dt cells by the mtROS scavenger MitoTempo. A total of 3×10^4 cells were seeded in a 96-well plate in phenol red-free medium and some wells were incubated with 100 µM of MitoTEMPO for 2 h. Then, 10 µM of antimycin A or PT-112 were added and incubated for 48 or 72 h, respectively. (**A**,**B**) mtROS levels were measured using MitoSOX™ staining after treatment with either (**A**) antimycin A or (**B**) PT-112. (**C**) Cell death induced by PT-112 in the presence or absence of MitoTEMPO after 48 or 72 h was evaluated by flow cytometry using annexin-V-FITC and 7-AAD staining. Results are shown as mean ± SD of at least 2 independent experiments performed in duplicate. * $p < 0.05$.

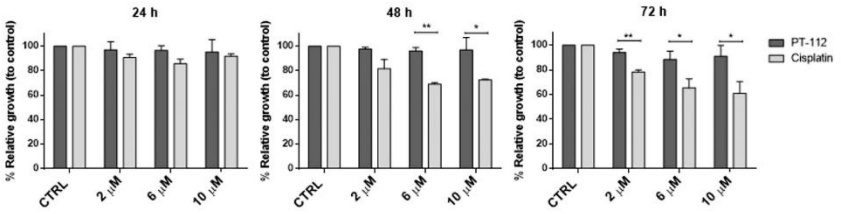

Figure 8. Cell growth analysis after treatment of L929-ρ^0 cells with PT-112 or cisplatin. Cells were treated with increasing concentrations of PT-112 or cisplatin, incubated for 24–72 h, and relative growth was measured by MTT assay. Results correspond to the percentage of relative growth compared to untreated, control cells (CTRL). Results are shown as mean ± SD of at least 2 independent experiments performed in duplicate. * $p < 0.05$, ** $p < 0.01$.

3.5. Effect of PT-112 on Mitochondrial CoQ10 Levels

The mevalonate pathway not only provides farnesyl or geranylgeranyl units for protein post-translational modifications but also provides longer prenyl groups for the final steps of Coenzyme Q synthesis, generating coenzyme Q9, Q10 or longer ubiquinone derivatives [29,30]. In all these steps of the mevalonate pathway, pyrophosphate derivatives are central to enzyme activity, and we speculated that it is possible PT-112 could act on these enzymes through its pyrophosphate moiety. Hence, we decided to study the possible effect of PT-112 on CoQ10 levels, analyzed by HPLC determination in mitochondrial lipid extracts. We first optimized the method of detection using commercial CoQ10. We confirmed the purity of commercial CoQ10 and determined its absorbance peak at 274.9 nm (Figure S2, right panel). We then determined the retention time of pure CoQ10 in the HLPC column to be used in the analysis of cell samples, obtaining a retention time of 7.749 min (Figure S2,

left panel). When we analyzed mitochondrial lipid extracts using this HPLC column, we observed that PT-112 substantially reduced the amount of CoQ10 in L929 mitochondria (Figure 9). However, these cells, which are OXPHOS-competent, were not sensitive to PT-112-induced cell death, although their growth was inhibited by 40% after 72 h of exposure (see Figure 1). In L929dt cells that are sensitive to PT-112-induced cell death, the basal amount of CoQ10 was below detection.

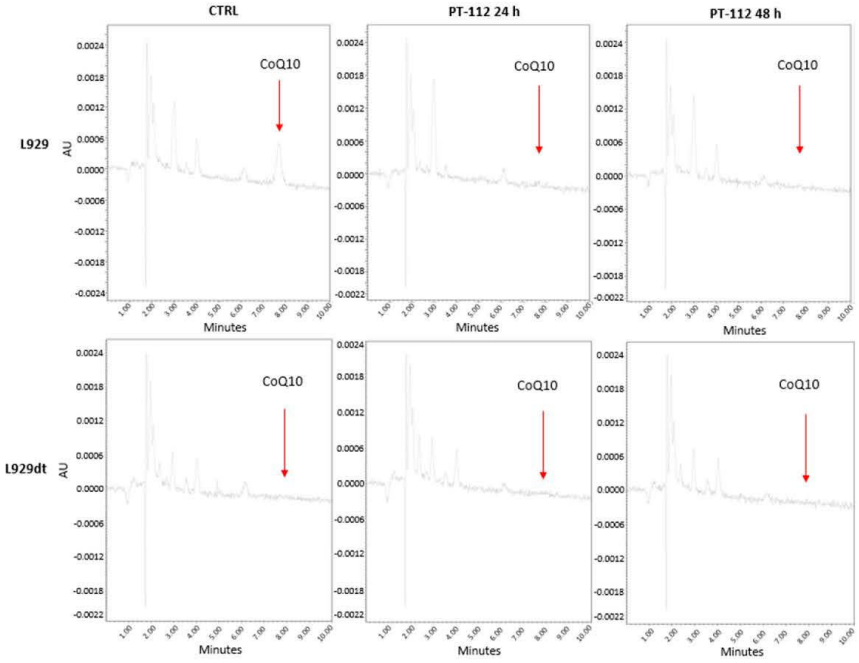

Figure 9. HLPC determination of mitochondrial CoQ10 amounts on L929 or L929dt cells after treatment with PT-112. The mitochondrial lipid fraction of 20×10^6 cells (L929 or L929dt), treated with 10 µM PT-112 for 24 or 48 h was extracted. Untreated cells (CTRL) were also included. CoQ10 levels were determined by HPLC methodology (see Materials and Methods). Commercial CoQ10 was used as a positive control (see Figure S2). Representative plots are shown.

3.6. PT-112 Induces CRT Exposure on the Surface of Sensitive Cells

PT-112 has been shown to induce ICD, characterized by CRT exposure on the cell membrane, together with emission of other danger signals in several types of tumor cells [7]. Hence, we tested whether PT-112 would induce ICD in sensitive L929dt and L929^{dt} cells. As shown in Figure 10, PT-112 induced CRT exposure on the surface of both cell lines. In addition, the level of CRT exposure increased with time of treatment. This finding, together with the spreading of cell debris observed upon PT-112 treatment as shown in Figure S1, demonstrates the high immunogenic potential of PT-112-induced cell death in this cellular system.

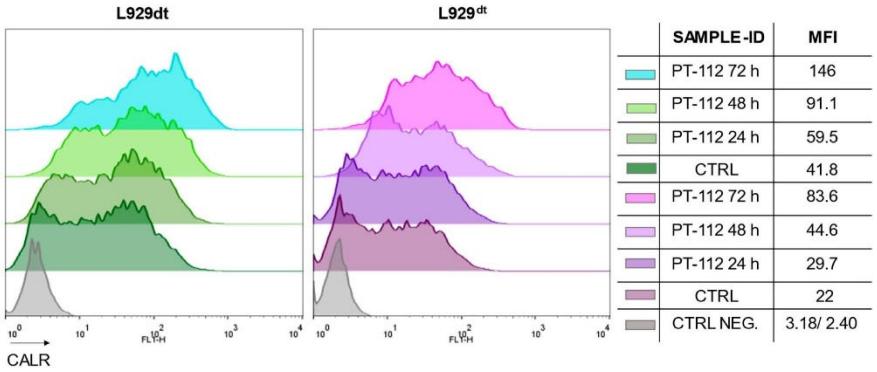

Figure 10. CRT exposure upon PT-112 treatment. Representative plots are shown. CRT exposure was analyzed in L929dt or L929^{dt} cells upon treatment with 10 μM PT-112 for the time indicated. Grey histograms correspond to the labeling with the secondary antibody alone and are considered as negative controls (CTRL NEG.), while control labelings correspond to the basal labeling of untreated cells (CTRL). Representative plots are shown.

3.7. Cells Sensitive to PT-112 Express High Levels of HIF-1α

L929dt and L929^{dt} cells favor glycolysis for ATP production due to their defective mitochondria associated with mtDNA mutations, as described [18]. Since HIF-1α is a transcription factor that regulates the expression of key genes implicated in glycolysis [31], we decided to further investigate the relationship between the metabolic profile of L929dt and L929^{dt} cells and basal HIF-1α expression in our cellular models and any changes observed after treatment with PT-112. As shown in Figure 11, we demonstrated that even in the presence of oxygen, L929dt and L929^{dt} cells expressed elevated levels of HIF-1α compared to L929 and dt^{L929} cells (around a 12-fold increase compared with parental L929 cells). PT-112 did not substantially affect expression levels of HIF-1α across all cell lines, yet higher baseline expression was found in those cells more sensitive to PT-112. These data suggest that sensitivity to PT-112 could be closely related to HIF-1α expression and could have prognostic and clinical applications.

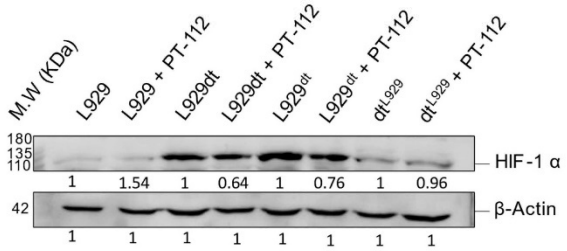

Cell line	HIF 1 -α expression (comparedto L929)
L929	1
L929dt	11.43
L929^{dt}	12.31
dt^{L929}	3.99

Figure 11. Analysis of HIF-1α expression levels in the presence or absence of PT-112. Cells were incubated with 10 μM of PT-112 for 72 h. Cell lysates were resolved in an SDS-PAGE 6% polyacrylamide gel, and proteins were transferred to nitrocellulose membrane and incubated with a specific antibody against HIF-1α. β-actin was used as a control of the protein loaded. The table shows the percentage of protein expression in basal conditions compared to parental L929 cells. The uncropped blots are shown in Figure S3.

4. Discussion

PT-112 presents the intriguing possibility that an anti-cancer agent with a platinum chiral center may operate through a mechanism of action that is selective to cancer metabolic processes, specifically mitochondrial dysfunction. In contrast to the canonical understanding of the cell death mechanism of approved platinum salts, it has been shown previously that PT-112 minimally binds nuclear DNA [1,4]. Structurally, PT-112 is unique because it contains a pyrophosphate moiety, which among other attributes contributes to a marked osteotropism, something that the closest structural analog, oxaliplatin, does not share [1].

Beyond osteotropism, however, based upon the data presented herein, it is possible that PT-112's pyrophosphate component may, in fact, be associated with its cell death mechanisms, including effects on cancer metabolic pathways. Examples of active anabolic pathways in tumor cells are the pentose phosphate pathway, needed for the synthesis of DNA and RNA nucleotides [32], and the mevalonate pathway, needed for the de novo synthesis of sterols and geranyls [33]. Farnesyl and geranylgeranyl backbones are required for the post-translational modification of relevant proteins in signaling, such as Ras [30], and also for the synthesis of mitochondrial coenzyme Q derivatives [29]. Notably, both pathways involve pyrophosphates for specific enzyme activities. This subject matter has not been deeply studied in the field of cancer treatment, perhaps because there are no approved drugs that contain pyrophosphate groups. Potential pyrophosphate-driven effects could include an increase in PT-112 uptake by tumor cells that are especially metabolically active and dependent on the mevalonate or the pentose phosphate pathway and/or PT-112 more directly affecting those pathways. Further studies will be needed to test these hypotheses.

L929dt and $L929^{dt}$ cybrid cells present mutations in mtDNA, causing a shift towards a glycolytic phenotype. These cells were especially sensitive to cell death induced by PT-112 while tumor cells with an intact OXPHOS pathway (L929 and dt^{L929} cybrid cells) were shown to be less sensitive to PT-112 and, strikingly, to lack a dose-response. In contrast, the classical Pt-containing drug cisplatin induced cell death and a dose-response across all the cell lines, irrespective of their metabolic and mitochondrial status. In addition, while cisplatin follows the canonical apoptotic pathway used by many chemotherapeutic drugs such as doxorubicin [27,34], PT-112 does not appear to comply with this canonical pathway, rather showing hints of necrotic cell death. Moreover, while PT-112 activates caspase-3 at the same time as cell death, the general caspase inhibitor Z-VAD-fmk does not inhibit PT-112-induced cell death, alone or in combination with the necroptosis inhibitor necrostatin-1. On the other hand, PT-112 induced the initiation of autophagy in all cell lines, detected by the Cyto-ID® method and by an increase in the LC3BII/LC3BI ratio, although it appears that the autophagy process was not completed, as evidenced by the lack of p62 degradation.

The observed difference in PT-112 sensitivity based on the baseline metabolic and mitochondrial mutational status of the L929 model cells led us to investigate the possibility that PT-112 cell death effects could themselves involve mitochondrial pathways. Indeed, PT-112 induced ROS in all cells tested, regardless of their sensitivity to cell death induction, although ROS appeared more rapidly in more sensitive cells. Importantly, when this analysis was restricted to the detection of mtROS, only the PT-112-sensitive, OXPHOS deficient cells showed a massive mtROS accumulation. We demonstrated partial protection from PT-112-induced cell death in sensitive cells by the use of the mitochondria-restricted ROS scavenger MitoTEMPO. Moreover, we have shown that L929-ρ^0 cells, devoid of mtDNA and unable to perform OXPHOS or to generate mtROS [17], were less sensitive to PT-112-induced growth inhibition versus the parental L929 cell line. These data point to the observed massive mitochondrial ROS generation as an important event in PT-112-induced cell death. It should be noted that, although L929-ρ^0 cells are an extreme and unnatural case of the glycolytic phenotype, their inability to generate mitochondrial ROS makes them highly resistant to PT-112, reinforcing the importance of this biochemical event in PT-112-induced cell death. On the other hand, this observation indicates that in our experimental system, the sensitivity to PT-112 is associated more specifically with the

presence of defective mitochondria that generate ROS upon stress and not generally with every glycolytic phenotype.

PT-112 also affected mitochondrial membrane potential ($\Delta\Psi m$) in sensitive cells, albeit in an unexpected way. After short incubation times with PT-112 (24–36 h), an initial mitochondrial hyperpolarization was observed. At later time points (48 h), two cell populations were detected: one with hyperpolarized mitochondria and another one that showed loss of $\Delta\Psi m$. At 72 h, when cell death notably increased in response to PT-112, the population with a loss of membrane polarization predominated.

Based on the literature surrounding bisphosphonates [35,36] and the structural similarity between bisphosphonates and pyrophosphates, it is possible that PT-112 could act directly on enzymes of the mevalonate pathway, such as farnesyltransferase or geranylgeranyl transferase. Increases in farnesyltransferase expression activity have been reported in prostate cancer patients, correlating with poor prognosis [37], and PT-112 has shown some efficacy signals in late-stage mCRPC, either alone [13] or in combination with PD-L1 immune checkpoint inhibition [14]. In support of such a hypothesis, we note that Qiu et al. [36] have developed $[Pt(en)]_2ZL$, a complex which conjugates the bisphosphonate zoledronic acid with Pt^{2+} ions and demonstrated that it prevented the prenylation of small G proteins through inhibition of the mevalonate pathway.

The mevalonate pathway not only provides farnesyl or geranylgeranyl units for protein post-translational modifications but also provides longer prenyl groups for the final steps of Coenzyme Q synthesis, generating coenzyme Q9, Q10 or longer ubiquinone derivatives [29,30]. In all these steps of the mevalonate pathway, pyrophosphate derivatives are important for enzymatic activities, and PT-112 could act on these enzymes through its pyrophosphate moiety. We have demonstrated that PT-112 substantially reduced the amount of CoQ10 in L929 mitochondria. Although L929 cells, which are OXPHOS-competent, are not sensitive to PT-112-induced cell death, their growth is substantially reduced by the drug, and this could be related to this CoQ10 depletion. In L929dt cells that are sensitive to PT-112-induced cell death, the basal amount of CoQ10 is much lower than in L929 cells (i.e., below the detection level). The low amount of CoQ10 in these cells, as well as the mtDNA mutations in complex I components, could explain the massive accumulation of mitochondrial ROS observed upon PT-112 treatment, the resulting non-apoptotic form of cell death, and evidence of ICD. Additional studies will be needed to better understand the relevance of CoQ10 in PT-112's anti-cancer activity and explore if these effects originate from effects on the mevalonate or other biological pathways.

Our data point to a cell death mechanism in which PT-112 would not kill cells by apoptosis nor by necroptosis but rather by inducing the initiation of an unresolved autophagy process, possibly leading to ER stress, together with the above-mentioned massive mtROS generation. It is also interesting to note that autophagy processes, normally not related to cell death, are associated with immunogenic signals and damage-associated molecular pattern (DAMP) emission [38]. In line with this conceptual approach, we demonstrated that PT-112 induces CRT exposure in sensitive L929dt and $L929^{dt}$ cells, a *bona fide* marker of ICD. These data correlate with prior work in vitro and in vivo showing that PT-112 causes ICD [7].

Finally, we demonstrate that the expression of HIF-1α is higher in cells that are sensitive to PT-112 compared to cells with an intact OXPHOS pathway. HIF-1α is the master regulator of the glycolytic phenotype and is caused by hypoxia or by aerobic glycolysis observed in many tumor cells [31]. Our data indicate that this relationship is conserved in our cellular model, in which the glycolytic phenotype originates from defective mitochondrial function due to mtDNA mutations [18]. In addition, low levels of CoQ10, as detected in L929dt cells at the basal state, have been recently correlated with high HIF-1α expression and stabilization [39]. Based on these observations, HIF1-α expression may be associated with differential sensitivity to PT-112, warranting further studies to explore future clinical applications.

5. Conclusions

PT-112 is a novel pyrophosphate-Pt conjugate with favorable safety profiles and evidence of efficacy in Phase I clinical trials. Using the L929 murine in vitro model system, we demonstrated that tumor cells presenting mtDNA mutations and the resulting glycolytic phenotypes (L929dt and $L929^{dt}$ cybrid cells) were more sensitive to cell death induced by PT-112 compared to the parental and cybrid cells with an intact OXPHOS pathway (L929 and dt^{L929} cybrid cells). PT-112 caused an incomplete autophagic process, along with massive accumulation of mtROS. PT-112 also reduced the amount of mitochondrial CoQ10 in L929 cells, while the basal CoQ10 levels were below our detection limits in L929dt cells, suggesting a potential relationship between a low basal level of CoQ10 and PT-112 sensitivity. In addition, PT-112 induced CRT exposure in sensitive L929dt and $L929^{dt}$ cells, consistent with ICD. Finally, the expression of HIF-1α was much higher in glycolytic cells sensitive to PT-112 compared to cells with an intact OXPHOS pathway. Taken together, these findings suggest the selectivity of PT-112 to differential metabolic statuses of cancer cells, with the potential for clinical applications of PT-112 in metabolically aggressive cancers.

6. Patents

The use of PT-112 to treat cancer is protected by US patent 9,688,709, registered on 27 June 2017, and an application has been submitted pertaining to the identification of PT-112-sensitive cancer cells on the basis of glycolytic features (international application number PCT/US2021/055907).

Supplementary Materials: The following supporting information can be downloaded at: https://www.mdpi.com/article/10.3390/cancers14163851/s1, Figure S1: Cell morphology after PT-112 treatment. Figure S2: HPLC chromatogram and absorbance spectrum of commercial CoQ10. Figure S3: Uncropped blots shown in the Figures of the manuscript.

Author Contributions: M.R.P., R.M.-L., T.D.A., J.J. and A.A. conceptualization; T.D.A., J.J. and A.A., data curation; R.S.-A., C.Y.Y., T.D.A. and A.A. formal analysis; M.R.P. funding acquisition; R.S.-A., J.M.-B., M.M.-S., M.M.-J. and R.M.-L. investigation; M.M.-J., R.M.-L. and C.Y.Y. methodology; M.R.P. and A.A. project administration; M.M.-J., R.M.-L. and A.A. resources; M.R.P., T.D.A. and A.A. supervision; R.S.-A. and A.A. writing—original draft; J.M.-B., C.Y.Y., M.M.-J., M.R.P., R.M.-L., T.D.A. and J.J. writing—review and editing. All authors have read and agreed to the published version of the manuscript.

Funding: This work was mainly supported by Promontory Therapeutics Inc. through the contract 2019/0715 with OTRI from the University of Zaragoza. R.S.-A. was supported by this contract. This research was also partially supported by project PID2019-105128RB-I00 financed by MCIN/AEI/10.13039/501100011033/ and "FEDER Una manera de hacer Europa".

Institutional Review Board Statement: Not applicable.

Informed Consent Statement: Not applicable.

Data Availability Statement: The datasets generated and/or analyzed during the current study are available from the corresponding authors on reasonable request.

Conflicts of Interest: J.J. is a former employee of Promontory Therapeutics and currently serves on the Scientific Advisory Board in a non-remunerated capacity. M.R.P., T.D.A. and C.Y.Y. are Promontory Therapeutics employees. J.J., M.R.P., T.D.A. and C.Y.Y. All own Promontory Therapeutics stocks and/or stock options.

References

1. Bose, R.; Maurmann, L.; Mishur, R.; Yasui, L.; Gupta, S.; Grayburn, W.; Hofstetter, H.; Salley, T. Non-DNA-binding platinum anticancer agents: Cytotoxic activities of platinum-phosphato complexes towards human ovarian cancer cells. *Proc. Natl. Acad. Sci. USA* **2008**, *105*, 18314–18319. [CrossRef]
2. Ames, T.; Slusher, B.; Wozniak, K.; Takase, Y.; Shimizu, H.; Kanada-Sonobe, R.; Kerns, W.; Fong, K.; Pourquier, P.; Nishibata-Kobayashi, K.; et al. Findings across pre-clinical models in the development of PT-112, a novel investigational platinum-pyrophosphate anti-cancer agent. *Eur. J. Cancer* **2016**, *69*, S153. [CrossRef]
3. Bose, R.; Moghaddas, S.; Belkacemi, L.; Tripathi, S.; Adams, N.; Majmudar, P.; McCall, K.; Dezvareh, H.; Nislow, C. Absence of activation of DNA repair genes and excellent efficacy of phosphaplatins against human ovarian cancers: Implications to treat resistant cancers. *J. Med. Chem.* **2015**, *58*, 8387–8401. [CrossRef]
4. Corte-Rodriguez, M.; Espina, M.; Sierra, L.; Blanco, E.; Ames, T.; Montes-Bayon, M.; Sanz-Medel, A. Quantitative evaluation of cellular uptake, DNA incorporation and adduct formation in cisplatin sensitive and resistant cell lines: Comparison of different Pt-containing drugs. *Biochem. Pharmacol.* **2015**, *98*, 69–77. [CrossRef]
5. Ames, T.; Sharik, M.; Rather, G.; Hochart, G.; Bonnel, D.; Linehan, S.; Stauber, J.; Wing, R.; Jimeno, J.; Medina, D.; et al. Translational research of PT-112, a clinical agent in advanced phase i development: Evident bone tropism, synergy in vitro with bortezomib and lenalidomide, and potent efficacy in the Vk*MYC mouse model of multiple myeloma. *Blood* **2017**, *130*, 1797.
6. Moghaddas, S.; Majmudar, P.; Marin, R.; Dezvareh, H.; Qi, C.; Soans, E.; Bose, R. Phosphaplatins, next generation platinum antitumor agents: A paradigm shift in designing and defining molecular targets. *Inorg. Chim. Acta* **2012**, *393*, 173–181. [CrossRef]
7. Yamazaki, T.; Buqué, A.; Ames, T.; Galluzzi, L. PT-112 induces immunogenic cell death and synergizes with immune checkpoint blockers in mouse tumor models. *OncoImmunology* **2020**, *9*, e1721810. [CrossRef]
8. Russell, R.; Watts, N.; Ebetino, F.; Rogers, M. Mechanisms of action of bisphosphonates: Similarities and differences and their potential influence on clinical efficacy. *Osteoporos. Int.* **2008**, *19*, 733–759. [CrossRef]
9. Kobayashi, Y.; Kashima, H.; Rahmanto, Y.; Banno, K.; Yu, Y.; Matoba, Y.; Watanabe, K.; Iijima, M.; Takeda, T.; Kunitomi, H.; et al. Drug repositioning of mevalonate pathway inhibitors as antitumor agents for ovarian cancer. *Oncotarget* **2017**, *8*, 72147–72156. [CrossRef]
10. Rogers, M.; Crockett, J.; Coxon, F.; Mönkkönen, J. Biochemical and molecular mechanisms of action of bisphosphonates. *Bone* **2011**, *49*, 34–41. [CrossRef]
11. Clézardin, P.; Benzaïd, I.; Croucher, P. Bisphosphonates in preclinical bone oncology. *Bone* **2011**, *49*, 66–70. [CrossRef] [PubMed]
12. van Beek, E.; Pieterman, E.; Cohen, L.; Löwik, C.; Papapoulos, S. Farnesyl Pyrophosphate Synthase Is the Molecular Target of Nitrogen-Containing Bisphosphonates. *Biochem. Biophys. Res. Commun.* **1999**, *264*, 108–111. [CrossRef] [PubMed]
13. Karp, D.; Camidge, D.; Infante, J.; Ames, T.; Jimeno, J.; Bryce, A. A well-tolerated novel immunogenic cell death (ICD) inducer with activity in advanced solid tumors. *Ann. Oncol.* **2018**, *29*, viii143. [CrossRef]
14. Bryce, A.; Dronca, R.; Costello, B.; Infante, J.; Ames, T.; Jimeno, J.; Karp, D. PT-112 in advanced metastatic castrate-resistant prostate cancer (mCRPC), as monotherapy or in combination with PD-L1 inhibitor avelumab: Findings from two phase I studies. *J. Clin. Oncol.* **2020**, *2020*, 38. [CrossRef]
15. Karp, D.; Dronca, R.; Camidge, R.; Costello, B.; Mansfield, A.; Ames, T.; Jimeno, J.; Bryce, A. Phase Ib dose escalation study of novel immunogenic cell death (ICD) inducer PT-112 plus PD-L1 inhibitor avelumab in solid tumours. *Ann. Oncol.* **2020**, *31*, S708. [CrossRef]
16. Kourelis, T.; Ailawadhi, S.; Vogl, D.; Cooper, D.; Ames, T.; Yim, C.; Price, M.; Jimeno, J.; Bergsagel, P. A Phase I Dose Escalation Study of PT-112 in Patients with Relapsed or Refractory Multiple Myeloma. *Blood* **2020**, *136* (Suppl. 1), 9–10. [CrossRef]
17. Catalán, E.; Charni, S.; Jaime, P.; Aguiló, J.; Enríquez, J.; Naval, J.; Pardo, J.; Villalba, M.; Anel, A. MHC-I modulation due to changes in tumor cell metabolism regulates tumor sensitivity to CTL and NK cells. *OncoImmunology* **2015**, *4*, e985924. [CrossRef]
18. Marco-Brualla, J.; Al-Wasaby, S.; Soler, R.; Romanos, E.; Conde, B.; Justo-Méndez, R.; Enríquez, J.; Fernández-Silva, P.; Martínez-Lostao, L.; Villalba, M.; et al. Mutations in the ND2 subunit of mitochondrial complex I are sufficient to confer increased tumorigenic and metastatic potential to cancer cells. *Cancers* **2019**, *11*, 1027. [CrossRef]
19. Gamen, S.; Anel, A.; Montoya, J.; Marzo, I.; Piñeiro, A.; Naval, J. mtDNA depleted U937 cells are sensitive to TNF- and Fas-induced cytotoxicity. *FEBS Lett.* **1995**, *376*, 15–18. [CrossRef]
20. Loveland, B.E.; Johns, T.G.; Mackay, I.R.; Vaillant, F.; Wang, Z.X.; Hertzog, P.J. Validation of the MTT dye assay for enumeration of cells in proliferative and antiproliferative assays. *Biochem. Int.* **1992**, *27*, 501–510.
21. Schagger, H.; Pfeiffer, K. Supercomplexes in the respiratory chains of yeast and mammalian mitochondria. *Embo J.* **2000**, *19*, 1777–1783. [CrossRef]
22. Acín-Pérez, R.; Fernández-Silva, P.; Peleato, M.; Pérez-Martos, A.; Enriquez, J. Respiratory active mitochondrial supercomplexes. *Mol. Cell* **2008**, *32*, 529–539. [CrossRef]
23. Brea-Calvo, G.; Rodríguez-Hernández, A.; Fernández-Ayala, D.; Navas, P.; Sánchez-Alcázar, J. Chemotherapy induces an increase in coenzyme Q10 levels in cancer cell lines. *Free Radic. Biol. Med.* **2006**, *40*, 1293–1302. [CrossRef]
24. Barry, M.; Behnke, C.; Eastman, A. Activation of Programmed Cell Death (Apoptosis) by Cisplatin, Other Anticancer Drugs, Toxins and Hyperthermia. *Biochem. Pharmacol.* **1990**, *40*, 2353–2362. [CrossRef]

25. Vercammen, D.; Beyaert, R.; Denecker, G.; Goossens, V.; Van Loo, G.; Declercq, W.; Grooten, J.; Fiers, W.; Vandenabeele, P. Inhibition of caspases increases the sensitivity of L929 cells to necrosis mediated by tumor necrosis factor. *J. Exp. Med.* **1998**, *187*, 1477–1485. [CrossRef]
26. Chan, L.; Shen, D.; Wilkinson, A.; Patton, W.; Lai, N.; Chan, E.; Kuksin, D.; Lin, B.; Qiu, J. A novel image-based cytometry method for autophagy detection in living cells. *Autophagy* **2012**, *8*, 1371–1382. [CrossRef]
27. Gamen, S.; Anel, A.; Pérez-Galán, P.; Lasierra, P.; Johnson, D.; Piñeiro, A.; Naval, J. Doxorubicin treatment activates a Z-VAD-sensitive caspase, which causes $\Delta\Psi_m$ loss, caspase-9 activity, and apoptosis in Jurkat cells. *Exp. Cell Res.* **2000**, *258*, 223–235. [CrossRef]
28. Aguiló, J.I.; Anel, A.; Catalán, E.; Sebastián, A.; Acín-Pérez, R.; Naval, J.; Wallich, R.; Simon, M.M.; Pardo, J. Granzyme B of cytotoxic T cells induces extramitochondrial reactive oxygen species production via caspase-dependent NADPH oxidase activation. *Immunol. Cell Biol.* **2010**, *88*, 545–554. [CrossRef]
29. Gruenbacher, G.; Thurnher, M. Mevalonate metabolism governs cancer immune surveillance. *OncoImmunology* **2017**, *6*, e1342917. [CrossRef]
30. Tricarico, P.; Crovella, S.; Celsi, F. Mevalonate Pathway Blockade, Mitochondrial Dysfunction and Autophagy: A Possible Link. *Int. J. Mol. Sci.* **2015**, *16*, 16067–16084. [CrossRef]
31. Semenza, G. HIF-1: Upstream and downstream of cancer metabolism. *Curr. Opin. Genet. Dev.* **2010**, *20*, 51–56. [CrossRef]
32. Patra, K.; Hay, N. The pentose phosphate pathway and cancer. *Trends Biochem. Sci.* **2014**, *39*, 347–354. [CrossRef]
33. Bathaie, S.; Ashrafi, M.; Azizian, M.; Tamanoi, F. Mevalonate Pathway and Human Cancers. *Curr. Mol. Pharmacol.* **2017**, *10*, 77–85.
34. Antoku, K.; Liu, Z.; Johnson, D. Inhibition of caspase proteases by CrmA enhances the resistance of human leukemic cells to multiple chemotherapeutic agents. *Leukemia* **1997**, *11*, 1665–1672. [CrossRef]
35. Farrell, K.; Karpeisky, A.; Thamm, D.; Zinnen, S. Bisphosphonate conjugation for bone specific drug targeting. *Bone Rep.* **2017**, *9*, 47–60. [CrossRef]
36. Qiu, L.; Yang, H.; Lv, G.; Li, K.; Liu, G.; Wang, W.; Wang, S.; Zhao, X.; Xie, M.; Lin, J. Insights into the mevalonate pathway in the anticancer effect of a platinum complex on human gastric cancer cells. *Eur. J. Pharmacol.* **2017**, *810*, 120–127. [CrossRef]
37. Todenhöfer, T.; Hennenlotter, J.; Kühs, U.; Gerber, V.; Gakis, G.; Vogel, U.; Aufderklamm, S.; Merseburger, A.; Knapp, J.; Stenzl, A.; et al. Altered expression of farnesyl pyrophosphate synthase in prostate cancer: Evidence for a role of the mevalonate pathway in disease progression? *World J. Urol.* **2013**, *31*, 345–350. [CrossRef]
38. Kepp, O.; Kroemer, G. Autophagy induction by thiostrepton for the improvement of anticancer therapy. *Autophagy* **2020**, *16*, 1166–1167. [CrossRef]
39. Liparulo, I.; Bergamini, C.; Bortolus, M.; Calonghi, N.; Gasparre, G.; Kurelac, I.; Masin, L.; Rizzardi, N.; Rugolo, M.; Wang, W.; et al. Coenzyme Q biosynthesis inhibition induces HIF-1α stabilization and metabolic switch toward glycolysis. *FEBS J.* **2021**, *288*, 1956–1974. [CrossRef]

5.CHAPTER II: Mitochondrial effects on human prostate cancer cells

Cancer Cell-Selective Induction of Mitochondrial Stress and Immunogenic Cell Death by PT-112 in Human Prostate Cell Lines

Soler-Agesta, R.[1], Moreno-Loshuertos, R.[1], Yim, C.Y.[2], Congenie, M. T.[2], Ames, T.D.[2], Johnson, H.L.[3], Stossi, F.[3], Marco-Brualla, J.[1], Junquera, C.[4], Martínez-De-Mena, R.[5], Enríquez, J.A.[5], Price, M.R.[2], Jimeno, J.[1,2], Anel, A.[1]

[1] University of Zaragoza/Aragón Health Research Institute (IIS-Aragón), Biochemistry and Molecular and Cell Biology, Zaragoza, Spain

[2] Promontory Therapeutics Inc., New York, NY, USA.

[3] Baylor College of Medicine, Integrated Microscopy Core, Houston, TX, USA.

[4] Anatomy and Human Histology Department, Faculty of Medicine, University of Zaragoza/IIS-Aragón.

[5] Carlos III National Center for Cardiovascular Research, Madrid, Spain.

Abstract

PT-112 is a novel immunogenic small molecule currently under Phase 2 clinical development, including in metastatic castration-resistant prostate cancer (mCRPC), an immunologically cold and heterogeneous disease state in need of novel therapeutic approaches. PT-112 has been shown to cause ribosomal biogenesis inhibition and organelle stress followed by immunogenic cell death (ICD) in cancer cells, culminating in anticancer immunity. In addition, clinical evidence of PT-112-driven immune effects has been observed in patient immunoprofiling. Given the unmet need for immune-based therapies in prostate cancer, along with a Phase I study (NCT#02266745) showing PT-112 activity in mCRPC patients, we investigated PT-112 effects in a panel of human prostate cancer cell lines. PT-112 demonstrated cancer cell selectivity, inhibiting cell growth and leading to cell death in prostate cancer cells without affecting non-tumorigenic epithelial prostate cell line RWPE-1 at the concentrations tested. PT-112 also caused caspase-3 activation, as well as stress features in mitochondria including ROS generation, compromised membrane integrity, altered respiration, and morphological changes. Moreover, PT-112 induced damage-associated

molecular pattern (DAMP) release, the first demonstration of ICD in human cancer cell lines, in addition to autophagy initiation across the panel. Taken together, PT-112 caused selective stress, growth inhibition and death in human prostate cancer cell lines. Our data provide additional insight into mitochondrial stress and ICD in response to PT-112. PT-112 immunogenicity could have clinical applications and is currently under investigation in a Phase 2 mCRPC study.

Background

Prostate cancer is the second leading cause of cancer-associated death among men, with an estimated 34,700 deaths per year in the United States [1]. Over 1.4 million men were diagnosed with the disease in 2020, making it one of the most frequently occurring malignancies leading to mortality in men worldwide [2]. Despite recent improvements in prostate cancer treatment, the development of new therapies is a persistent clinical challenge, as current standard-of-care (SOC) regimens such as chemotherapy (e.g., docetaxel or cabazitaxel) and androgen-deprivation therapy exhibit toxicity and/or a high incidence of acquired resistance [3-7], and there is an unclear treatment paradigm as disease continues to progress. This is particularly true in late-line mCRPC patients who have already received chemotherapy, hormone therapy and/or recently approved lutetium-177 and have limited treatment options [8-10]. Additionally, precision medicine approaches, while resulting in regulatory approval of PARP inhibitors, are generally indicated for 11-13% of the mCRPC population harboring BRCA1/2 mutations [11-13]. Recently, immune checkpoint inhibitor-based approaches have been successfully used across several different cancer types [14, 15]. However, these agents have not demonstrated robust clinical activity in prostate cancer, with several large Phase 3 studies terminated, or resulting in negative results, likely due to the immunologically cold nature of disease resulting in reduced activity of CTLA-4 and PD-1 inhibitors [16-19]. Taken together, there is a high unmet need for novel agents capable of anticancer immune activation, particularly in the late-line setting [8-10, 16, 17].

PT-112 is a novel, immunogenic small molecule currently under Phase 2 clinical development, including in late-line mCRPC [20, 21]. Preliminary evidence of safety, efficacy and clinical benefit in mCRPC was observed in monotherapy and in combination with anti-PD-L1 in two prior dose escalation trials with PT-112 [22-25]. Recent findings have shown evidence of ribosome biogenesis inhibition and nucleolar stress by PT-112 in human cancer cell lines [26]. These early molecular effects, together with organelle stress observed in mitochondria and endoplasmic reticulum in murine cells [27-29] likely contribute to the immunogenicity of PT-112; in preclinical models, it induces immunogenic cell death (ICD) via damage-

associated molecular pattern (DAMP) release, recruits immune effector cells in the tumor environment, and synergizes with immune checkpoint inhibitors [30]. Immune effects of PT-112 have recently been demonstrated in a Phase 2 study in patients with thymic epithelial tumors [31, 32].

In addition, PT-112 is distributed to multiple tissues and organs, including kidney, lung and liver, with the highest concentrations found in bone, likely driven by the pyrophosphate moiety [33]. This suggests PT-112 may provide benefit to patients with prostate cancer, a population with a high incidence of bone metastases [34] and where immune checkpoint inhibitors have not been demonstrated to be effective, highlighting a need for novel immune-based therapies.

Our previous studies using L929 mouse tumor cell lines with well-characterized metabolic features showed mitochondrial stress induced by PT-112, as demonstrated by mitochondrial reactive oxygen species (mtROS) accumulation and changes in the mitochondrial membrane potential [28]. These PT-112-induced effects, along with cell death, were more pronounced in cell lines with mitochondrial DNA mutations, dependence on glycolysis for survival, and higher in vivo tumorigenic and metastatic potential [35]. These data suggested the relevance of mitochondria to PT-112-induced cell death.

Mitochondria are essential organelles as a hub for metabolic, bioenergetic, redox, and apoptotic signaling pathways, and thus play a key role in tumor cell proliferation [36]. Mitochondrial stress has been shown to facilitate pro-tumorigenic metabolic reprogramming in malignant cells, and basal levels of mtROS are commonly higher in cancer compared to healthy cells [37-39]. However, driving mitochondrial stress and mtROS levels beyond a certain threshold can lead to unmanageable oxidative stress and ultimately cell death [36, 38]. These observations suggest that novel therapeutic approaches harnessing the unique metabolic profile of cancer cells can promote antitumor activity and cancer cell death through the induction of a mitochondrial stress response.

Given PT-112 activity observed in prostate cancer patients, as well as previously reported mitochondrial stress induction by PT-112 in mouse tumor cells, we explored PT-112-induced effects in a panel of human prostate cell lines. Here, we report: 1) cancer cell selectivity; 2) cell death characterization; 3) mitochondrial stress features such as mtROS generation, compromised membrane integrity and changes in morphology; 4) ICD induction via DAMP release; and lastly, 5) evidence of autophagy. Together, this work aims to advance the understanding of a key organelle stress contributing to PT-112's activity and its resulting anticancer immunity in prostate cancer.

Methods

Cell Culture. Human prostate cell lines were maintained according to ATCC recommendations. PC-3, DU-145, and VCap were cultured in high glucose DMEM medium with GlutaMAX (Life Technologies, Paisley, UK). LNCap and 22Rv1 were cultured in RPMI 1640 medium (Life Technologies, Paisley, UK). LNCap-C4 and LNCap-C4-2 were cultured in a mixture of DMEM: F12 (4:1) supplemented with biotin (4.9 ng/ml), adenine (251.8 ng/ml), insulin (0.1 ng/ml), and transferrin (88.6 ng/ml). RWPE-1 (immortalized, non-tumorigenic human prostate cell line) was cultured in Keratinocyte-SFM supplemented with EGF human recombinant (5 ng/mL) and bovine pituitary extract (50 µg/mL) (Gibco, Grand Island, NY, USA). All cell culture media used for prostate cancer cell lines were supplemented with 10% fetal calf serum, penicillin (1000 U/mL) and streptomycin (10 mg/mL) (PanBiotech, Aidenbach, Germany). Cells were incubated at 37°C and 5% CO2 using standard procedures. PC3, LNCap, VCap, and RWPE-1 cell lines were kindly provided by Dr. M. Jesús Vicent from CIPF, Valencia, while DU-145, LNCap C4, LNCap C4-2 and 22Rv1 cell lines were a kind gift of Dr. Santiago Ramón y Cajal from Hospital Vall d'Hebron (Barcelona).

Cell Viability Assays. Relative cell growth in response to PT-112 compared to control, untreated cells was measured using Mossman's method (i.e., MTT assay). Briefly, 2104 cells were seeded per well in a 96-well flat-bottom plate and incubated with increasing concentrations of PT-112 (2, 6, and 10 µM) for 24-72 hours (h) at 37°C. Subsequently, 10 µL of a 5 mg/mL MTT solution was added to each well and incubated for 3 h at 37ºC. During incubation, viable cells reduced the MTT solution to insoluble purple formazan crystals, which were then solubilized with a mixture of isopropanol and 0.05 M HCl. Finally, absorbance was measured by a microplate reader (Dynatec, Pina de Ebro, Spain).

Cytotoxicity Assays and Cell Death Quantification. Cytotoxicity induced by PT-112 was measured as follows: $2x10^4$ cells were seeded per well in a 96-well plate and incubated with increasing concentrations of PT-112 (2, 6, and 10 µM) for 24-72 h at 37°C. Cell death in untreated and treated cells was analyzed by flow cytometry using a FACSCalibur flow cytometer (BD Biosciences, Madrid, Spain) after simultaneous incubation with annexin-V-FITC and 7-AAD (BD Biosciences, Madrid, Spain) in annexin binding buffer (140 mM NaCl, 2.5 mM CaCl2, 10mM HEPES/NaOH, pH 7.4) for 10 minutes (min).

Analysis of Caspase-3 Activation. Caspase-3 activation was measured using a FITC-labelled antibody against cleaved caspase-3 (BD Pharmingen™, Madrid, Spain). For this purpose, 1x105 LNCap-C4 and DU-145 cells pretreated with 10 µM of PT-112 for 24-72 h were fixed with 4% paraformaldehyde solution for 15 min at 4°C. Then, cells were washed with PBS buffer, permeabilized using a 0.1% saponin dilution supplemented

with 5% fetal bovine serum and incubated for 15 min at room temperature (RT). After washing, samples were incubated with the antibody for 30 min at RT and analyzed by flow cytometry using a FACSCalibur flow cytometer (BD Biosciences, Madrid, Spain).

Cell Morphology Assessments. $2x10^4$ cells (DU-145, LNCap, or PC-3) were treated with or without 10 µM of PT-112 for 72 h Images were taken using an inverted microscope (Nikon Eclipse TE300). For cell morphology assessments using transmission electron microscopy (TEM), refer to Transmission Electron Microscopy (TEM).

Apoptosis and Necroptosis Inhibition Assays. $2x10^4$ cells (LNCap-C4 and DU-145) were seeded in a 96-well plate and incubated with pan-caspase inhibitor Z-VAD-fmk (50 µM; MedChem Express, New Jersey, USA) and/or RIPK-1 inhibitor necrostatin-1 (30 µM; MedChem Express, New Jersey, USA) for 1 h. Cells were then treated with 10 µM of PT-112 and incubated for 48 h at 37°C. Both inhibitors were refreshed in their corresponding wells after 24 h. Finally, cell death was assessed via flow cytometry using a FACSCalibur flow cytometer (BD Biosciences, Madrid, Spain) after 10 min incubation with annexin-V-FITC and 7-AAD (Sigma, Madrid, Spain) in annexin binding buffer (140 mM NaCl, 2.5 mM CaCl2, 10mM HEPES/NaOH, pH 7.4).

Mitochondrial ROS (mtROS), Mitochondrial Mass and Mitochondrial Membrane Potential Measurements. Total mtROS production, mitochondrial mass, and mitochondrial membrane potential were each measured using a FACSCalibur flow cytometer (BD Biosciences, Madrid, Spain) in prostate cells with or without 10 µM PT-112 for 24-72 h. For mtROS production and mitochondrial mass, cells were incubated at 37°C with 5 µM MitoSOX™ (ThermoFisher, Rockford, IL, USA) for 30 min or 300 nM MitoTracker™ green staining (Invitrogen) for 15 min, respectively. To measure alterations in mitochondrial membrane potential, DU-145 and LNCap-C4 cells were simultaneously incubated with 20 nM TMRE (Molecular Probes, Madrid, Spain) and annexin-V-DYE-634 (Sigma, Madrid, Spain) for 30 min at 37°C.

Confocal fluorescence microscopy was used to visualize mitochondrial membrane polarization. 2 x 103 cells (LNCap and DU-145) per well were plated in an optical plastic bottom 384-well plate (Aurora Microplates, Scottsdale, AZ, USA) and, after overnight attachment, treated with control buffer or 25 µM PT-112 for 72 h. Cells were then stained live with Hoechst 33342 (ThermoFisher, Rockford, IL, USA #62249, 1:5000 dilution) and either TMRE (ThermoFisher, Rockford, IL, USA #T669, 1:1000 dilution) or JC-1 (ThermoFisher, Rockford, IL, USA #T3168, 1:1000 dilution) for 30 min. Next, cells were imaged on a Yokogawa CV8000 high-throughput spinning disk confocal using a 20x/1.0 water objective capturing a 10 µm z-stack in 9 fields of view per condition. Images were then projected at maximum intensity for

quantification. Image analysis was performed using the CellPathfinder software (Yokogawa, Sugar Land, TX, USA). Briefly, nuclei were identified using the Hoechst channel, followed by a dilation step to include the mitochondrial signal ("virtual cell") from where intensity-based measurements were extracted. The experiment was repeated three independent times with four technical replicates per biological replicate.

OXPHOS Performance and Metabolism Measurements. Oxygen consumption rate (OCR) measurements of 30,000 LNCap-C4 cells treated with or without 10 µM PT-112 for 24 h were performed using the Seahorse XF Cell Mito Stress Test Kit and the XF96 Extracellular Flux Analyzer (Seahorse Biosciences, Lexington, MA, USA). Cells were incubated in Seahorse media (1mM pyruvate, 2mM glutamine, 1M glucose at pH 7.4) for 30 min at 37ºC without CO2. According to the manufacturer's instructions, OCR was measured in basal conditions and after sequential addition of oligomycin (CV inhibitor), FCCP (respiration and ATP synthesis uncoupler), and rotenone + antimycin A (AA + Rot, CI and CIII inhibitors, respectively). OCR data were normalized to the number of viable cells as determined by the CyQuant Cell Proliferation Assay (Thermo Fisher, Rockford, IL, USA).

Energy maps were constructed using the XF96 Extracellular Flux Analyzer (Seahorse Biosciences, Lexington, MA, USA) per the manufacturer's instructions. The energetic phenotype of LNCap-C4 cells was determined based on measurements of OCR and extracellular acidification rate (ECAR) indicative of OXPHOS and glycolysis, respectively, in untreated, control cells and following 10 µM PT-112 treatment for 24 h.

Mitochondria Purification. Mitochondria were purified as previously described [40]. Briefly, $2x10^7$ cells were centrifuged, washed twice with PBS, and frozen at -80°C for 24 h. Pellets were resuspended in a volume of a hypotonic buffer (MOPS 10mM, saccharose 83 mM, pH 7.2) equal to 7 the cell pellet volume and incubated on ice for 2 min. Samples were then homogenized using a Potter-Dounce homogenizer with a Teflon piston, and 8 to 10 strokes were performed. After adding an equal volume of a hypertonic buffer (MOPS 30 mM, 250 mM, pH 7.2), the samples were centrifuged at 1000 x g for 5 min at 4°C, and only the supernatants were centrifuged again at 11000 x g for 2 min at 4°C. Finally, mitochondria-containing pellets were washed with media A (Tris 10 mM, EDTA 1 mM, saccharose 0.32 M, pH 7).

Protein Extraction. A total of $5x10^6$ cells were lysed with 100 µL of lysis buffer (1% Triton-X-100, 150 mM NaCl, 50 mM Tris/HCl pH 7.6, 10% v/v glycerol, 1 mM EDTA, 1 mM sodium orthovanadate, 10 mM sodium pyrophosphate, 10 µg/mL leupeptin, 10 mM sodium fluoride, 1 mM methyl phenyl sulfide; Sigma, St. Louis, MO, USA) for 30 min on ice. The mixture was ultra-centrifugated at 12000 rpm for 20 min at 4°C. The

supernatant was analyzed using the BCA assay (Thermo Fisher, Rockford, IL, USA) for determining protein concentration and mixed with 3x loading buffer (SDS 3% v/v, 150 mM Tris/HCl, 0.3 mM sodium molybdate, 30% v/v glycerol, 30 mM sodium pyrophosphate, 30 mM sodium fluoride, 0.06% p/v bromophenol blue, 30% v/v 2-mercaptoethanol; Sigma, St. Louis, MO, USA).

Blue Native Electrophoresis and Immunoblot Analysis. Separation of respiratory complex (CI, CII, CIII, CIV and CV) and supercomplex (SC) proteins in mitochondrial extracts was performed using blue native electrophoresis in a gel gradient according to the published methodology [41, 42]. Briefly, samples were loaded in NativePAGE™ 3-12% Bis-Tris Gel (Invitrogen, Waltham, MA, USA) and run at 100 V for the first 30 min, then at 300 V and 15 mA for the next 3 h. For protein separation of protein extracts, SDS-PAGE (6% and 12% polyacrylamide gel) was used.

Following either method, proteins were transferred to PVDF membranes using semi-dry electrotransfer (GE Healthcare, Chicago, IL, USA). Membranes were blocked with TBS-T buffer (Tris/HCl 10mM, pH 8; NaCl 0.12 M; Tween-20 0.1%, thimerosal 0.1 g/L; Sigma, St. Louis, MO, USA) containing 5% skimmed milk. Protein detection was performed by immunoblot using specific antibodies (Invitrogen, Waltham, MA, USA) against the individual complexes of the mitochondrial electron transport chain: CI (anti-NDUFA9; #459100), CII (anti-SDHA; #459200), CIII (anti-Uqcrc1; #459140), CIV (anti-COI; 459600), and CV (anti-α-F1-ATPase; #459240). Other proteins detected by immunoblot were p62 (Santa Cruz, Dallas, TX, USA, #SC-28359), LC3BI/II (Sigma, Madrid, Spain, #L7543) and HIF-1α (Novus, Littleton, CO, USA, #NB100–479). Primary antibodies were incubated overnight at 4°C in agitation. Afterwards, anti-mouse (Sigma, Madrid, Spain, #A9044) or anti-rabbit (Sigma, Madrid, Spain, #A9169) secondary antibodies labeled with peroxidase were incubated for 1 h at RT. Blots were analyzed with Pierce ELC Western Blotting Substrate (Thermo Scientific, Rockford, IL, USA) using Amersham Imager 680 (GE Healthcare Life Sciences, Chicago, IL, USA). Protein expression was quantified by densitometry using ImageJ software. β actin levels were used as a reference to normalize data (Cell Signaling, Danvers, MA, USA, 3700).

Enzymatic Activity Analysis of Respiratory Complexes. Purified mitochondria from DU-145 cells treated with or without 10 µM PT-112 for 24 h were used to assess enzymatic activity of respiratory complexes via spectrophotometric quantification as previously described [43]. Briefly, activity of individual complexes and supercomplexes was measured using a spectrophotometer (Fisher Scientific; Alcobendas, Spain) based on the following: CI (NADH-dehydrogenase) activity via oxidation of NADH at 340 nm, CII (succinate dehydrogenase) activity via reduction of 2,6'dichlorophenolindophenol at 600 nm, CIV (cytochrome c

oxidase) activity via oxidation of cytochrome c at 550 nm, CI+III (NADH cytochrome c oxido-reductase) via reduction of cytochrome c at 550 nm when NADH is added, and CII+III (succinate cytochrome c oxido-reductase) activity via reduction of cytochrome c at 550 nm when succinate is added.

Transmission Electron Microscopy (TEM). Samples for TEM were prepared as follows: 5□104 DU-145 cells were seeded overnight in an 8-well NuncTM Lab-Tek® Chamber Slide™ (Thermo, Rockford, IL, USA). Cells were treated with 10 µM PT-112 for 1, 6, 24 and 48 h, and after incubation, the medium was removed. Cells were carefully washed 3x for 2 min with 0.1 M PBS at RT and a solution containing 2.5% glutaraldehyde in 0.1 M phosphate buffer (PB; Na2HPO4 + NaH2PO4 4:1, pH 7.4) was added. The chamber slide was then incubated at 37°C for 5 min. The glutaraldehyde solution was refreshed, and the chamber slide was again incubated for additional 2 h at 4°C. It was subsequently washed 4x (5 min each) with 0.1 M PB before adding a solution of 0.05% NaN3 in 0.1 M PB and storing the chamber slide at 4°C. For the fixation process, samples were washed 5x (5 min each) with PBS and incubated with 2% OsO4 in PB for 1 h. Next, 3 washes (5 min each) with cold distilled water were performed and samples were dehydrated with increasing concentrations of ethanol (30%, 50% and 70%) before staining with 2% uranyl acetate in 70% ethanol for 2 h 30 min. Samples were dehydrated a second time with increasing concentrations of ethanol (70%, 96%, 100%), gradually included in resin, transferred to a 100% epoxy resin, and incubated overnight. The next day, 3 changes of epoxy resin were performed (30 min each), and samples were embedded in the molds with epoxy resin and dried in the oven for 48-72 h at 70°C. Finally, ultrafine 50 nm cuts were performed and stained with Reynol's solution. Images were taken using a transmission electron microscope (JEOL 1010) at 80 kV.

DAMP Emission. ATP secretion was quantified using the luciferase-based ENLITEN ATP Assay (Promega) per the manufacturer's recommendations via a fluorometer (Biotek) using the supernatant of cells treated with or without 10 µM PT-112 collected at 48 h. Calreticulin exposure on the cell surface upon incubation with or without 10 µM PT-112 (48 h) was analyzed by flow cytometry using the Attune NxT flow cytometer (Thermo Fisher Scientific; Branchburg, NJ, USA). Following treatment, cells were washed and stained with Zombie Aqua™ Fixable Viability Kit (BioLegend, San Diego, CA, USA) for 15 min. Subsequently, cells were washed with PBS and incubated with the calreticulin (D3E6) XP® rabbit monoclonal antibody PE Conjugate (Cell Signaling, Danvers, MA, USA, #19780S) in PBS + 0.5 % BSA (FACs buffer) for 25 min at 4°C in the dark. Afterwards, cells were washed with FACs buffer and fixed (eBioscience™ Intracellular Fixation & Permeabilization Buffer Set, Invitrogen, Carlsbad, CA, USA) for 30 min at 4°C in the dark. Then, the supernatant was discarded by centrifugation and cells were incubated with the permeabilization buffer

(eBioscience™ Intracellular Fixation & Permeabilization Buffer Set, Invitrogen, Carlsbad, CA, USA) for 5 min. Finally, the supernatant was discarded again by centrifugation and cells were resuspended in FACs buffer for its subsequent analysis. Zombie Aqua™ positive cells (i.e., dead cells) were excluded from the analysis.

Cyto-ID® Analysis and Autophagosome Formation Measurement. For autophagy analysis, the autophagosome formation after treatment with PT-112 was evaluated using a Cyto-ID® probe (Enzo Life Sciences, Farmingdale, NY, USA). Cells treated with or without 10 µM of PT-112 for 48-72 h were incubated with 1 µL of Cyto-ID® dye for 30 min at 37°C. Subsequently, cells were washed with PBS and analyzed by flow cytometry via a FACSCalibur flow cytometer (BD Biosciences, Madrid, Spain).

Statistical Analysis and Data Processing. Statistical analysis was performed using GraphPad Prism (GraphPad Software Inc.). For quantitative variables, results are shown as mean ± standard error of the mean (SEM). Statistical significance was evaluated using Student's t-test and two-way ANOVA uncorrected Fisher's LSD. Differences were considered significant when $p < 0.05$. Data obtained by flow cytometry were analyzed using FlowJo 10.0.7 (Tree Star Inc., Ashland, OR, USA).

Results

PT-112 selectively inhibits cell growth and causes cell death in prostate cancer cells, but not in non-tumorigenic epithelial prostate cells

We tested differential sensitivity to PT-112 in vitro across a panel of human prostate cancer cell lines (LNCap, LNCap-C4, LNCap-C4-2, DU-145, 22Rv1, VCap, PC-3) and the non-tumorigenic prostate cell line (RWPE-1). First, we evaluated the ability of PT-112 to inhibit cell growth at increasing concentrations (2, 6, 10 µM) and incubation times (24, 48 and 72 h) via the MTT assay. Selected PT-112 concentrations represent clinically relevant doses successfully used in previous in vivo experiments [23, 44].

PT-112 inhibited cell growth of prostate cancer cell lines with varying degrees, without appreciably affecting that of the non-tumorigenic cell line RWPE-1 (Figure 1). In addition, cell death induced by PT-112 was analyzed by flow cytometry using annexin-V-FITC and 7-AAD staining, as described in our previous report using murine fibroblast tumor cell lines [28]. Consistent with the growth inhibition data, PT-112 caused cancer cell death while healthy RWPE-1 cells were largely unaffected after 48-72 h PT-112 treatment (Figure 2). Overall, PT-112 was broadly active across the prostate cancer cell lines tested, while sparing benign prostate cells, demonstrating PT-112 cancer cell selectivity.

Our previous work performed in the L929 murine tumorigenic cellular system showed that cells with mitochondrial dysfunction expressed higher levels of HIF-1α and were more sensitive to PT-112 compared to cells with an intact OXPHOS pathway [28]. To explore this potential relationship between HIF-1α expression and PT-112 sensitivity in the human prostate cell line panel, we analyzed IC50s (determined by the relative 50% inhibition concentration at 72 h of PT-112 treatment in Figure 1) and basal HIF-1α protein expression levels using western blot. Non-tumoral RWPE-1 cells exhibited the lowest HIF-1α expression, while LNCap-C4, the most sensitive prostate cancer cell line to PT-112, had the highest level of HIF-1α expression (Supplementary Figure 1). However, not all cell lines in the panel followed this trend, making a relationship between PT-112 sensitivity and HIF-1α levels unclear.

PT-112 induces caspase-3 activation

Next, we further explored PT-112-induced cell death in select cell lines. DU-145 cells treated with PT-112 followed by simultaneous staining with annexin-V-FITC and 7-AAD were analyzed by flow cytometry. We observed a prominent apoptotic population (annexin-V+/7-AAD-) in response to PT-112 at 48 h (29.8%) and 72 h (44.1%), with an eventual increase in double-positive stained (i.e., dead) cells (annexin-V+/7-AAD+) at 72 h, potentially indicative of secondary necrosis (Figure 3A).

Given the emergence of the apoptotic population in response to PT-112, we next analyzed the activation of an apoptosis effector, caspase-3. Caspase-3 activation in LNCap-C4 and DU-145 cells treated with PT-112 for 24, 48, and 72 h was measured by flow cytometry using an antibody specific for cleaved caspase-3. As shown in Figure 3B, the levels of cleaved caspase-3 increased in a time-dependent manner upon PT-112 treatment, reaching as high as 85% and 100% caspase-3 activation at 72 h compared to control in LNCap-C4 and DU-145 cells, respectively. Moreover, PT-112-treated cells showed features of cells undergoing apoptosis, such as plasma membrane blebbing, as well as nuclear and cell fragmentation in apoptotic bodies (Figure 3C).

To further investigate cell death in PT-112-treated cells, we pretreated LNCap-C4 and DU-145 with the pan-caspase inhibitor, Z-VAD-fmk, and/or the RIPK-dependent necroptosis inhibitor, necrostatin-1. In DU-145, we observed inhibition of PT-112-induced cell death with Z-VAD-fmk (where % cell death was comparable to that of untreated cells), and to a lesser degree with necrostatin-1. In LNCap-C4, only Z-VAD-fmk caused a significant decrease in cell death following PT-112 treatment. Co-pretreatment of both inhibitors versus Z-VAD-fmk alone resulted in a comparable reduction in cell death in response to PT-112

(Figure 3D). Together, these results suggest that the mechanism underlying PT-112-induced cell death in these human prostate cancer cell lines at least in part involves caspase-mediated apoptosis.

PT-112 induces mitochondrial stress

Based on our previous work illustrating PT-112 sensitivity in the transformed murine fibroblast cell lines with mitochondrial deficiencies [28], we investigated different mitochondrial parameters in human prostate cancer cells treated with PT-112. As shown in Figure 4A, 10 µM PT-112 treatment for 48-72 h increased mtROS production in all cancer cell lines, but not in the healthy prostate cell line RWPE-1, in line with the selective growth inhibition and cytotoxicity data in Figures 1 and 2. Notably, LNCap-C4 and DU-145 cells exhibited pronounced increases in mtROS levels compared to untreated cells after 72 h PT-112 treatment (Figure 4B). Again, PT-112 was broadly active, inducing mitochondrial stress across the cancer cell lines, which exhibit varying basal mitochondrial features (Supplementary Figure 2A). Furthermore, PT-112 induced a significant increase in mitochondrial mass at 48 h and 72 h (Figure 4C).

Next, we analyzed the effect of PT-112 on mitochondrial membrane potential (Δψm) in DU-145 and LNCap-C4 cells by flow cytometry using double TMRE and annexin-V-DYE-634 staining, allowing for simultaneous quantification of Δψm and cell death, respectively. In both cell lines, PT-112 decreased Δψm at 48 h and 72 h of incubation in a time-dependent manner (Figure 5A). Interestingly, in LNCaP-C4, this decrease in Δψm was accompanied by cell death (see Q1) starting at 48 h of PT-112 treatment. In contrast, DU-145 exhibited a cell population that was positive for annexin-V-DYE-634, but still had normal Δψm (see Q2), and it was only at 72 h that cells began losing their Δψm.

We further investigated the effects of PT-112 on Δψm using confocal fluorescence microscopy to visualize mitochondrial membrane polarization. LNCap and DU145 cells were treated with vehicle or 25 µM PT-112 for 72 h and stained with the nuclei marker Hoechst and a mitochondrial marker, either TMRE or JC-1. TMRE staining intensity indicates the degree of mitochondrial membrane polarization, while a red-to-green shift in the JC-1 staining indicates a reduction in mitochondrial membrane potential. In both cell lines, clear evidence of mitochondrial membrane depolarization was observed, as indicated by diminished TMRE intensity and by the green shift in the JC-1 stain (Figure 5B). Together, these results demonstrate that PT-112 reduces mitochondrial membrane polarization, contributing to mitochondrial dysfunction.

PT-112 alters mitochondrial respiration

We next evaluated the effects of PT-112 on mitochondrial respiration and the activity of respiratory complexes in the electron transport chain (ETC). We analyzed the oxygen consumption rate (OCR) and the extracellular acidification rate (ECAR) after 24 h of PT-112 treatment in LNCap-C4, indicating the rates of respiration and glycolysis, respectively. Using cellular respiration modulators oligomycin, FCCP, and rotenone/antimycin A, we assessed key parameters related to mitochondrial respiration and observed compromised mitochondrial function in PT-112-treated cells compared to untreated cells (Figure 6A). Specifically, relative to control cells, PT-112 caused reductions in 1) basal respiration, 2) ATP-linked oxygen consumption (as shown by the reduction in the OCR upon oligomycin addition), and 3) the spare respiratory capacity (SRC) (as shown by the increase in the OCR relative to basal respiration upon FCCP addition) (Figure 6A and 6B), all of which point to mitochondrial dysfunction [45, 46]. In addition, we generated "energy maps" to compare shifts in cellular metabolic programs in response to PT-112. In line with the results above, PT-112 decreased oxygen consumption (Figure 6C). Interestingly, PT-112 simultaneously reduced glycolysis as indicated by a decrease in ECAR, shifting cells from being "energetic" (i.e. utilizing OXPHOS and glycolysis) to "quiescent" (i.e. utilizing both metabolic pathways to a lesser degree), indicative of reductions in ATP across these two major pathways.

Additionally, we characterized the basal protein expression of respiratory complexes and supercomplexes within the ETC in the cell line panel, which showed differential metabolic phenotypes (Supplementary Figure 2B). We further investigated respiratory complexes in DU-145. The activity of specific complexes (CI, CII and CIV) and supercomplexes (CI+CIII and CII+CIII) was measured after PT-112 treatment via spectrophotometric quantification in mitochondrial extracts and compared to untreated control cells. PT-112 treatment for 24 h significantly reduced the activity of CI and CIV, as well as increased the activity of supercomplexes involving CIII, with no notable effects on CII (Figure 6D). Given that CIII respiratory complexes contribute to ROS production [47, 48], this increase in the activity of CIII-containing supercomplexes in response to PT-112 may explain mtROS generation (see Figure 4).

PT-112 causes morphological changes in mitochondria

In order to further assess the effects of PT-112 on mitochondria, we analyzed cell and organelle morphology of DU-145 treated with PT-112 via TEM at different time points. Overall, after brief exposure as short as 1 h, PT-112 caused changes in mitochondrial morphology, electron density, and size; modifications to and loss of cristae; and breakage of mitochondrial membranes, and these effects became more pronounced

over time (Figure 7). Moreover, autophagic vacuole formation was observed, especially in the vicinity of mitochondria, suggesting an active mitochondrial autophagic process, or mitophagy [49], in response to PT-112. In addition to mitochondrial morphological changes, evidence of increased cytoplasmic complexity and features of apoptosis were seen, as expected.

PT-112 induces DAMP release associated with ICD

Given the immunogenic properties of PT-112 demonstrated in mouse in vitro and in vivo models [24, 28, 30, 44], we tested the ability of PT-112 to induce DAMP emission in human prostate cancer cell lines. We assessed ATP release and calreticulin (CRT) exposure on the cell surface, both of which are important immunostimulatory DAMPs essential for ICD [50]. Consistent with the prior findings, PT-112 caused ATP release in LNCap, 22Rv1 and DU-145 (Figure 8A). On the other hand, CRT exposure was clearly detected in DU-145, but not in LNCap-C4 or 22Rv1 cells (Figure 8B). These data indicate that not all DAMPs are necessary for ICD induction, and that the spectrum of DAMP release is cell-specific.

ICD has been linked to autophagy [51], and we previously reported the initiation of autophagy by PT-112 in transformed murine fibroblast cell lines [28]. This is consistent with the evidence of PT-112-induced mitophagy observed via TEM in Figure 7. Based on these data, we set out to investigate autophagosome formation using the Cyto-ID® method, as well as LC3B-I to LC3B-II conversion and p62 degradation as markers of autophagy initiation and completion, respectively.

As shown in Figure 9A, PT-112 induced autophagosome formation across the tested cell lines, demonstrating autophagy initiation as early as 24 h of treatment. Most cell lines had reduced autophagosome formation at 72 h relative to the 24 h time point, and in some cases the levels dropped below those seen in control cells. These changes are likely due to the presence of apoptotic and/or dying cells at these later time points, as shown in Figure 2. In contrast, PC-3 exhibited increasing autophagosome formation over time, which may in part be explained by the lower degree of cell death in response to PT-112 (i.e., more non-apoptotic cells measured in the assay) in comparison to the other cancer cell lines.

We then further explored autophagy in two cell lines, LNCap and PC-3, demonstrating a different pattern for autophagy activation in response to PT-112. In LNCap cells, upon PT-112 treatment, we observed the conversion of LC3B-I to LC3B-II, along with the reduction in the total expression levels of both proteins. Similarly, a gradual decrease in p62 expression was observed in a time-dependent manner (Figure 9B). These results demonstrate the initiation of active autophagy by PT-112, followed by protein

degradation at the end of the process. In contrast, while PC-3 cells exhibited a clear conversion of LC3B-I to LC3B-II in response to PT-112, we observed no changes in total protein levels, along with gradual accumulation of p62 over time. These data point to the initiation of autophagy by PT-112 in PC-3, but p62 accumulation instead of degradation indicates that this process did not reach completion, at least within 72 h. This is suggestive of a differential autophagic flux in PC-3 cells, again perhaps relating to the lower degree of PT-112-induced cell death compared to other cell lines at 72h (Figure 2). Nevertheless, PT-112 clearly activates autophagy in prostate cancer cells, as indicated by increases in autophagosome formation and LC3B-I-to-LC3B-II conversion.

Discussion

This is the first demonstration of PT-112's broad preclinical anticancer effects as well as its ability to induce ICD and mitochondrial stress in human prostate cancer cells, in line with clinical evidence of PT-112 activity observed in mCRPC patients [22, 23]. Specifically, using a panel of human prostate cancer cell lines, the present study demonstrates the ability of PT-112 to 1) cause growth inhibition and death in cancer cells without affecting non-tumorigenic epithelial prostate cells, 2) promote mitochondrial stress in cancer cells, as evidenced by mtROS generation and disruptions in mitochondrial membrane potential, respiration, and morphology, 3) activate autophagy, and lastly, 4) induce ICD.

The selective growth inhibition and cytotoxicity, as well as mitochondrial stress induction by PT-112 observed in prostate cancer cells, but not in non-tumorigenic prostate cells, was consistent with our prior data in the murine L929 system, where those cell lines with a higher degree of in vivo tumorigenicity and metastatic potential exhibited a higher sensitivity to PT-112 [28, 35]. This selectivity may explain PT-112's general safety and tolerability observed in clinical studies [21, 24, 25, 31, 32, 52]. It is interesting to note that PT-112 was active across different prostate cancer cell lines exhibiting varying basal mitochondrial features and mutational status, suggesting broad clinical application in prostate cancer, especially the late-line setting where the disease is highly heterogeneous [3-5, 53].

Moreover, the evidence of apoptosis and ICD in PT-112-treated cells raises an intriguing question of how these distinct types of cell death could be observed simultaneously. Caspase-3-dependent apoptosis was previously thought to be an immunologically silent event; however, there is emerging evidence that it neither precludes ICD nor contradicts evidence of anticancer immunity [54]. Apoptotic cells can release DAMPs and ultimately undergo ICD in certain conditions [54]. It is interesting to note that, in contrast to what was observed here in human prostate cancer cells, PT-112-induced cell death in murine L929-derived

cell lines did not rely on the activity of caspase-3. Nevertheless, evidence of ICD induction via DAMP release was clearly observed in both L929-derived and human prostate cancer cell lines [28]. This suggests that while varying cell death mechanisms are possible, the ability of PT-112 to induce ICD remains consistent across all the cell lines tested and may be a more universal feature of PT-112's mechanism.

Our findings clearly demonstrate that PT-112 causes mitochondrial stress and DAMP release in prostate cancer cells. Given the link between these two events reported in the literature, it is plausible that these effects observed in PT-112-treated cells may be directly related, contributing to an anticancer immune response. For example, upon mitochondrial stress and damage, mitochondria have been shown to promote not only mtROS generation, but also release of ICD-associated DAMPs such as ATP and HMGB1 [55, 56].

Our data also show the ability of PT-112 to affect autophagic flux (e.g. autophagosome formation, autophagic degradation of proteins etc.), which may stem from mitochondrial stress, given mitochondria are the major source of ROS required for autophagy induction [51, 57, 58]. Additionally, recent studies have reported a link between the initiation of autophagy and the release of ATP, promoting ICD [51, 59]. Increased extracellular ATP can also lead to cancer cell death by contributing to mitochondrial membrane damage and caspase-3-dependent apoptosis in tumor cells [51], suggesting bidirectionality and/or crosstalk in this process. While the precise mechanisms through which mitochondrial stress leads to ICD in response to PT-112 are to be investigated, it is likely that PT-112-driven mitochondrial stress contributes to ICD induction via mtROS generation and DAMP release, the latter of which can be further stimulated upon autophagy initiation.

Lastly, this work reinforces the ability of PT-112 to induce organelle stress, adding to the recent finding that PT-112 caused ribosome biogenesis inhibition and nucleolar stress as early as 6 to 8 h post-treatment in vitro [26]. These events have been reported to contribute to downstream organelle stresses, including mitochondrial stress. During nucleolar stress, nucleolar proteins such as NPM1 translocate to the nucleoplasm and interact with mitochondrial proteins, causing mitochondrial stress and release of mitochondrial DNA (mtDNA) into the cytosol, potentially activating the innate immune system via cGAS/STING [60-64]. Interestingly, mtDNA release has been observed in PT-112-treated cancer cells [27]. Disrupted ribosome biogenesis has also been shown to upregulate autophagy [65], which is linked to ICD as described above, and can have broad impacts on protein translation that likely plays a role in driving organelle stress. Moreover, this disruption could explain PT-112's selectivity to cancer cells observed here.

Cancer cells have increased demand for ribosome biogenesis in the nucleolus compared to normal cells due to high proliferation rates and associated need for protein generation [66, 67], potentially rendering them more sensitive to ribosome biogenesis disruption by PT-112.

Conclusions

In the evolving treatment landscape of mCRPC, there remains a need for novel therapies with anticancer immune effects. PT-112 is a promising small molecule with a mechanism of action selective to cancer cells, causing organelle stress and ICD. Taken together, our data provide additional insight into mitochondrial stress and ICD in response to PT-112 and how these effects culminate in anticancer immunity. PT-112 immunogenicity could in part explain previous clinical observation of durable responses extending beyond the treatment duration [24] and immune effects demonstrated in a small cohort of human patients [31, 32]. In addition, the broad activity of PT-112 in prostate cancer cells coupled with its differentiated mechanism from the current standards of care could help address the high unmet need in late-line mCRPC. PT-112 monotherapy is currently under investigation in a Phase 2 study with mCRPC patients who have exhausted SOC options [20]. Future work will aim to further characterize and identify key components facilitating PT-112-induced mitochondrial stress and exploring connections with ICD and ribosome biogenesis inhibition.

Acknowledgements

This work was mainly supported by Promontory Therapeutics Inc., and it was also partially supported by project PID2019-105128RB-I00 financed by MCIN/AEI/655 10.13039/501100011033/ and "FEDER Una manera de hacer Europa". The work of RSA was supported by the grant from the Asociación Española Contra el Cáncer (AECC) PRDAR21487SOLE

The authors would like to acknowledge Dr. Santiago Ramón y Cajal and Anna Santamaría, Vall d'Hebron Institute of Oncology, Barcelona; Dr. Mª Jesús Vicent, Centro de Investigación Príncipe Felipe, Valencia, for prostate cancer cell lines and the use of Servicio General de Apoyo a la Investigación-SAI at Universidad de Zaragoza.

Figures and legends

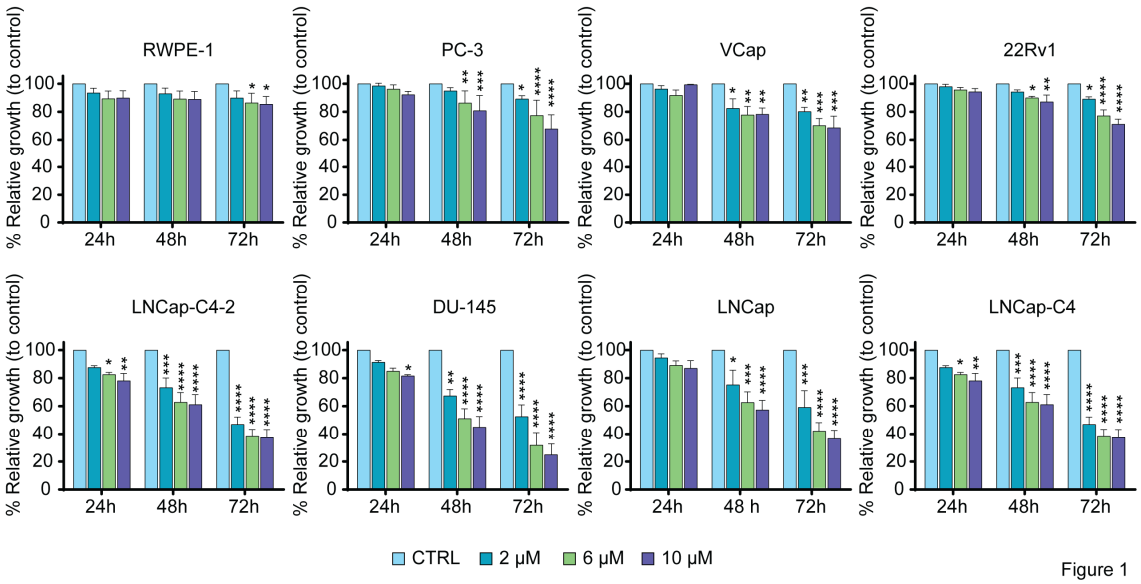

Figure 1. Relative cell growth (%) upon PT-112 treatment compared to untreated control (CTRL) cells. Cell lines were incubated with increasing concentrations of PT-112 (2, 6, and 10 µM) for 24-72 h. Cell growth was measured by the MTT assay. Results are shown as a mean ± SEM of at least 2 independent experiments performed in duplicate. * $p \leq 0.05$, ** $p \leq 0.01$, *** $p \leq 0.001$, **** $p \leq 0.0001$.

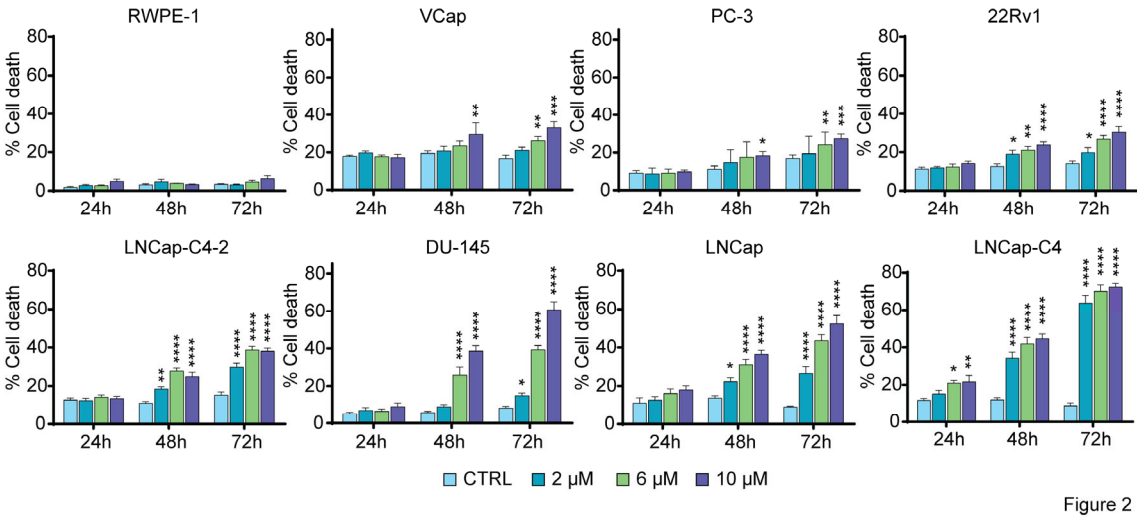

Figure 2. Relative cell death (%) upon PT-112 treatment compared to untreated control (CTRL) cells. Cells were incubated with increasing concentrations of PT-112 (2, 6, and 10 µM) for 24-72 h. Cells were then simultaneously stained with annexin-V-FITC and 7-AAD and analyzed by flow cytometry. Results are shown as mean ± SEM of at least 2 independent experiments performed in duplicate. * $p \leq 0.05$, ** $p \leq 0.01$, *** $p \leq 0.001$, **** $p \leq 0.0001$.

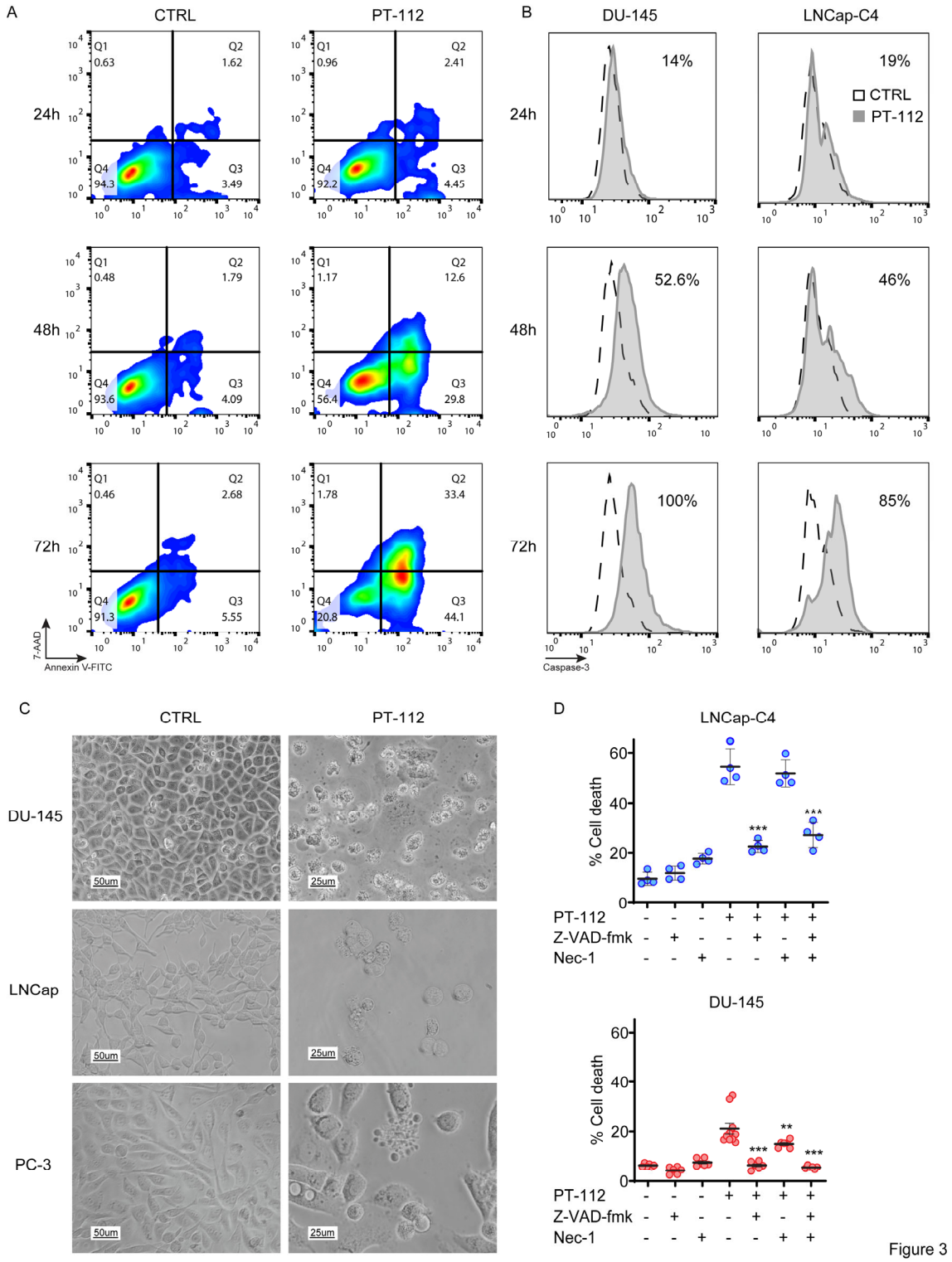

Figure 3

Figure 3. Characterization of cell death induced by PT-112 in human prostate cancer cells. (A) Dot-plots represent the 7-AAD and annexin-V-FITC staining evolution of DU-145 cells treated with 10 µM PT-112 for 24-72 h compared to untreated control (CTRL) cells. (B) Levels of caspase-3 activation upon PT-112

treatment in LNCap-C4 and DU-145. Cells were treated with 10 µM of PT-112 for 24-72 h, incubated with anti-cleaved caspase-3 labeled with FITC dye, and analyzed by flow cytometry. The numbers in each box represent the percentage of cleaved caspase-3 compared to untreated control (CTRL) cells. (C) Representative images of cells treated with 10 µM PT-112 for 72 h were taken using an inverted microscope. (D) Effects of Z-VAD-fmk and/or necrostatin-1 (Nec-1) inhibitors on PT-112-induced-cell death. Cells were pretreated for 1 h with or without pan-caspase and/or necroptosis inhibitors and incubated with 10 µM of PT-112 for 48 h. Flow cytometry analysis was performed using annexin-V-FITC and 7-AAD staining. Results are shown as mean ± SEM of at least 2 independent experiments performed in duplicate. Statistical significance compared to cells treated with PT-112 only is depicted in the graphics. ** $p \leq 0.01$, *** $p \leq 0.001$.

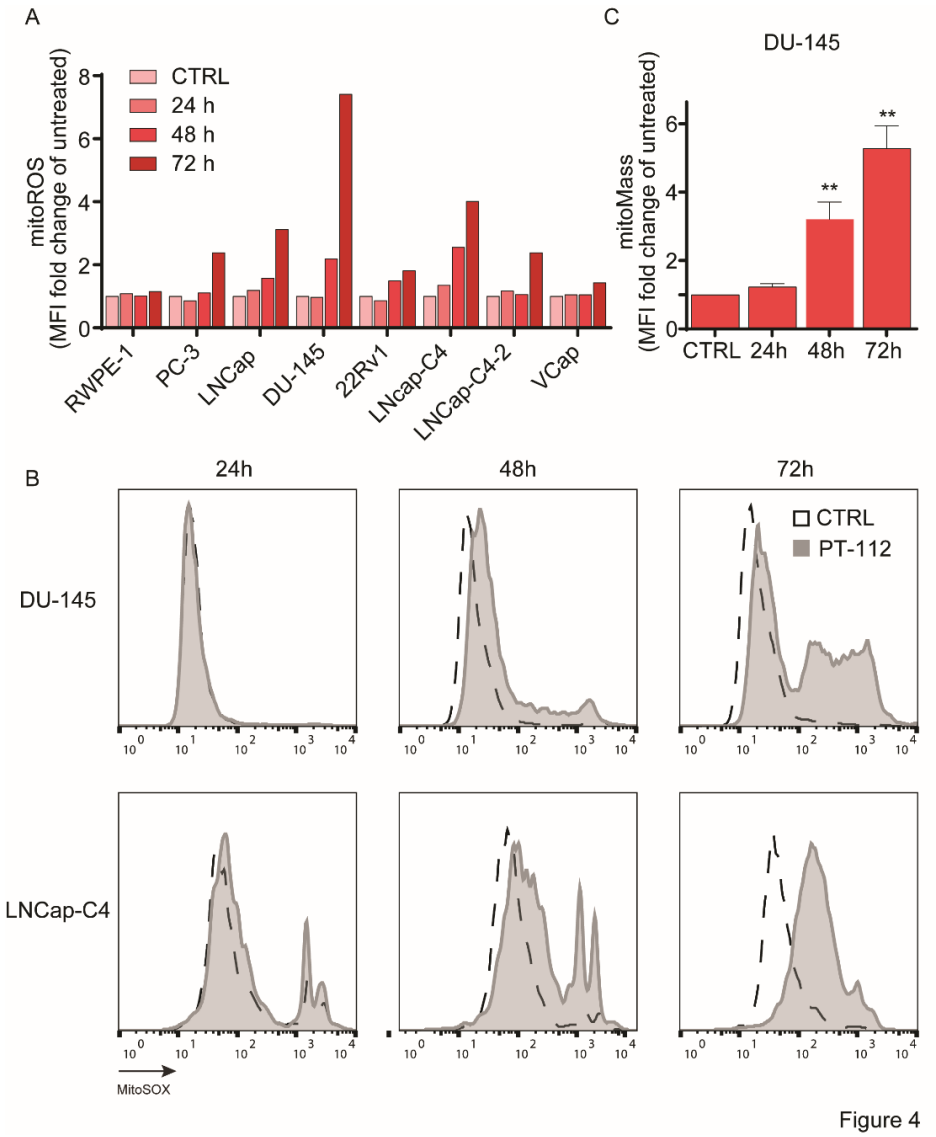

Figure 4

Figure 4. Effects of PT-112 on mtROS production and mitochondrial mass in human prostate cancer cell lines. (A) mtROS levels in cells treated with 10 µM PT-112 for 24-72 h were analyzed by flow cytometry

using MitoSOX™ labeling. Graph bars correspond to mean fluorescence intensity (MFI) normalized to untreated control (CTRL) cells. (B) Representative histograms showing mtROS production in DU-145 and LNCap-C4. Dotted histograms correspond to the fluorescence of untreated control (CTRL) cells, and gray-colored histograms correspond to the fluorescence values of treated cells. (C) Mitochondrial mass (mitoMass) was measured by flow cytometry using MitoTracker™ Green in DU-145 upon 10 µM PT-112 incubation for 24, 48, and 72 h. Graph bars correspond to mean fluorescence intensity (MFI) normalized to CTRL. Results are shown as mean ± SEM from 3 independent experiments. ** $p \leq 0.01$.

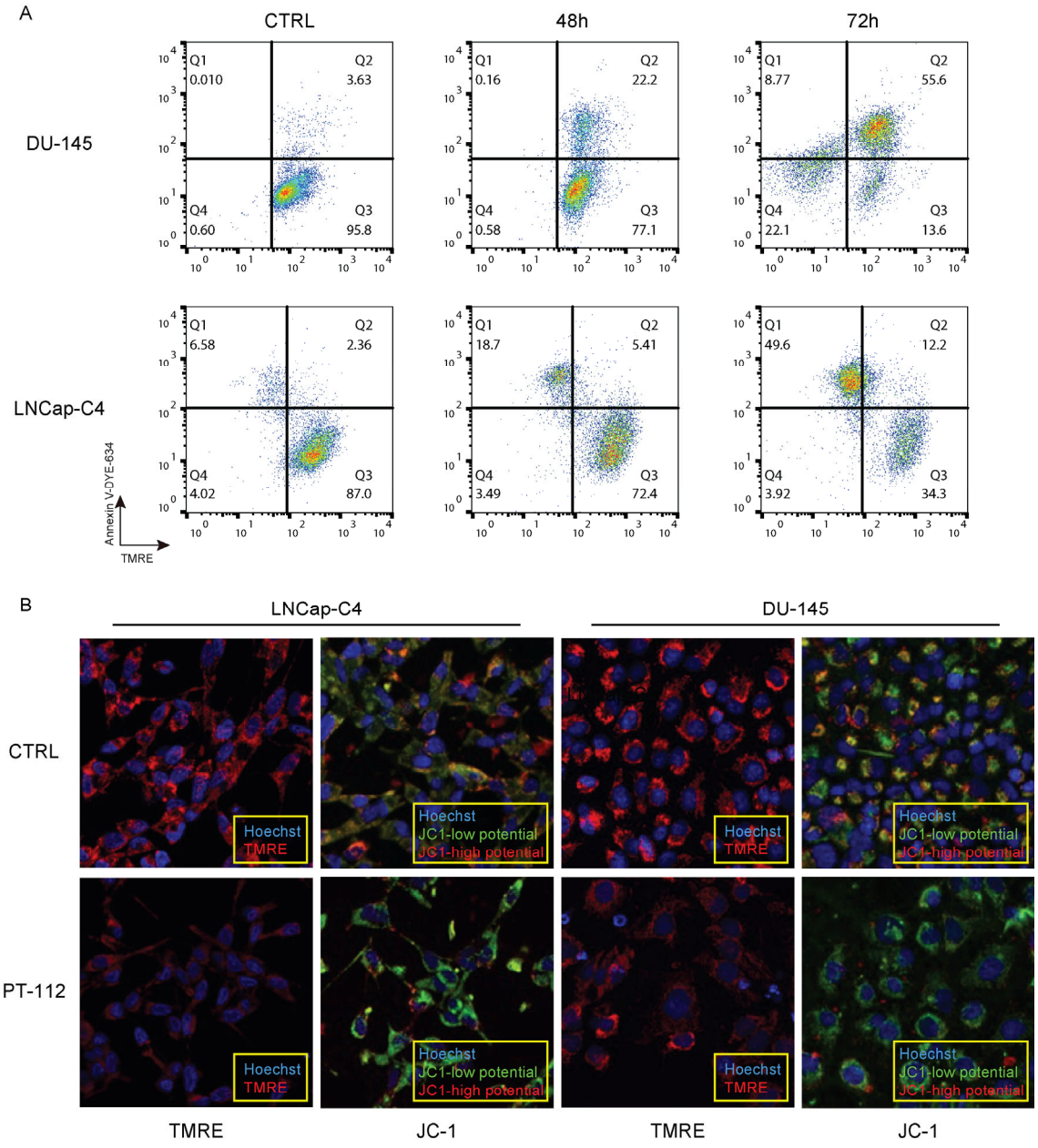

Figure 5

Figure 5. Effects of PT-112 on mitochondrial membrane potential ($\Delta\psi_m$) in human prostate cancer cell lines. (A) Mitochondrial membrane potential was monitored by flow cytometry using simultaneous TMRE and annexin-V-DYE-634 staining in DU-145 and LNCaP-C4 treated with 10 µM PT-112 for 48 h and 72 h. The series of dot plots show the staining evolution of the treated cell population compared to the control (CTRL). (B) Confocal fluorescence microscopy images correspond to mitochondrial staining of LNCap and DU-145 cell lines with TMRE or JC-1, with or without 25 µM PT-112 treatment for 72 h. Nuclei were stained in blue using Hoechst dye.

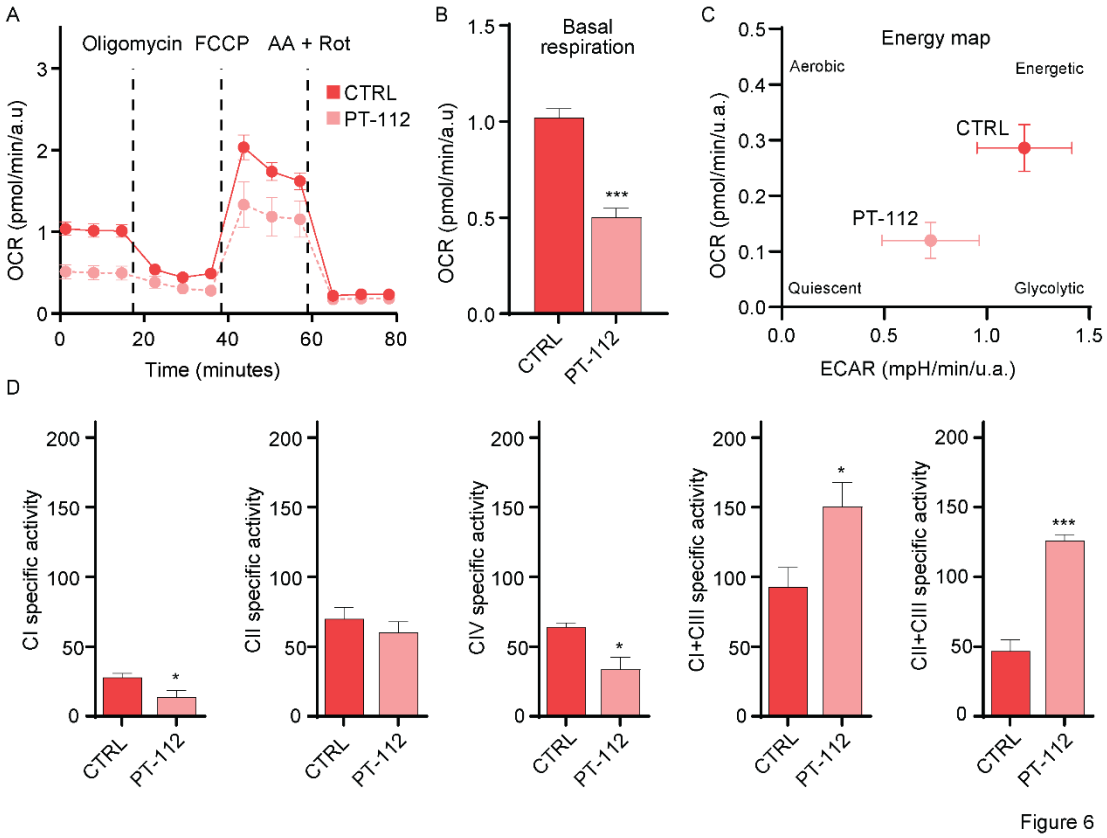

Figure 6. Effects of PT-112 on mitochondrial respiration and activity of respiratory complexes and supercomplexes in the ETC. (A) OCR and ECAR were measured in LNCap-C4 cells treated with vehicle (CTRL) or 10 µM PT-112 for 24 h. Dotted vertical lines indicate administration of injections of the specified cellular respiration modulators at different time points, such that basal respiration (i.e. OCR prior to oligomycin injection), ATP-linked oxygen consumption (the difference between basal OCR and oligomycin-inhibited OCR) and spare respiratory capacity (the difference between FCCP-induced maximal OCR and basal OCR) were investigated. Results are expressed as mean ± SEM at each time point. (B) Graph bars quantifying basal respiration measured in Figure 6A. Results are expressed as mean ± SEM. *** $p \leq 0.001$. (C) Energy map plotting OCR (indicative of OXPHOS) vs. ECAR (indicative of glycolysis) for cells treated with vehicle (CTRL) or 10 µM PT-112 for 24 h. Four relative bioenergetic phenotypes (aerobic vs. glycolytic and energetic vs. quiescent) are labeled. Note that the axes for OCR in (A) and (C) utilize arbitrary units (a.u.), and thus

are not comparable. (D) Bar graphs show the activity of respiratory complexes and supercomplexes in DU-145 cells treated with 10 µM PT-112 for 24 h. Results are expressed as mean ± SEM. * p ≤ 0.05, *** p ≤ 0.001.

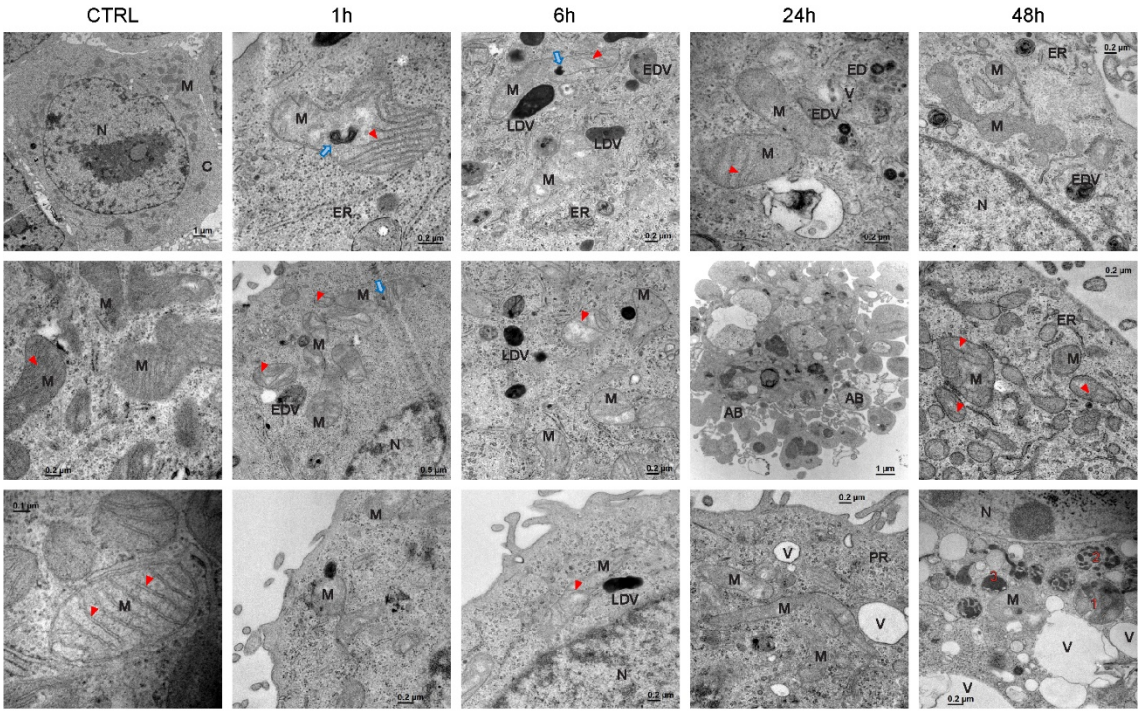

Figure 7

Figure 7. Effects of PT-112 on cell and organelle morphology in DU-145 cells treated with vehicle (CTRL) or 10 µM PT-112 for 1, 6, 24 and 48 h. Representative TEM images at the indicated resolution are shown. Letters and symbols indicate the following. **Red arrows:** mitochondria cristae, **blue arrows:** accumulation of degraded membranes inside the mitochondrial matrix, **PR**: Polyribosome, **C**: Cytoplasm, **M**: Mitochondria, **N**: Nucleus, **AB**: Apoptotic Body, **EDV**: Early Degradation Vesicle (secondary lysosome), **LDV**: Late Degradation Vesicle (late lysosome), **ER**: Endoplasmic Reticulum, **V**: low electron density vacuole.

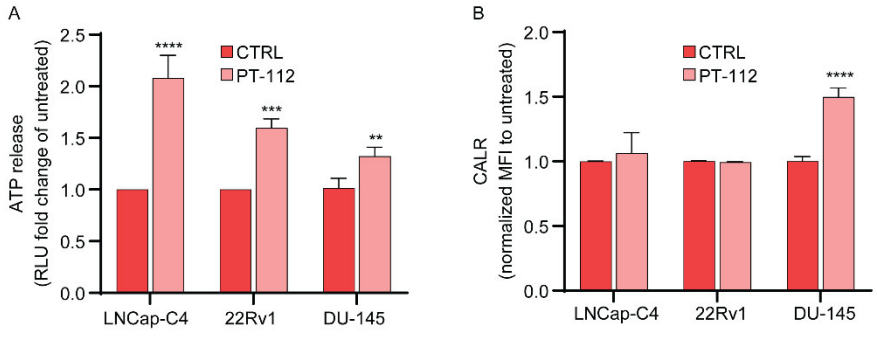

Figure 8

White numbers in the right bottom image (48h time) illustrate sequential stages of a possible mitophagy process.

Figure 8. DAMP emission induced by PT-112 in human prostate cancer cell lines. (A) ATP release and (B) calreticulin exposure upon 10 µM PT-112 treatment for 48 h. Bar graphs show relative measurement for each parameter normalized to untreated control (CTRL) samples. Results are expressed as mean ± SEM from 2 independent experiments. RLU: relative light units. * $p \leq 0.05$, *** $p \leq 0.001$, *** $p \leq 0.001$.

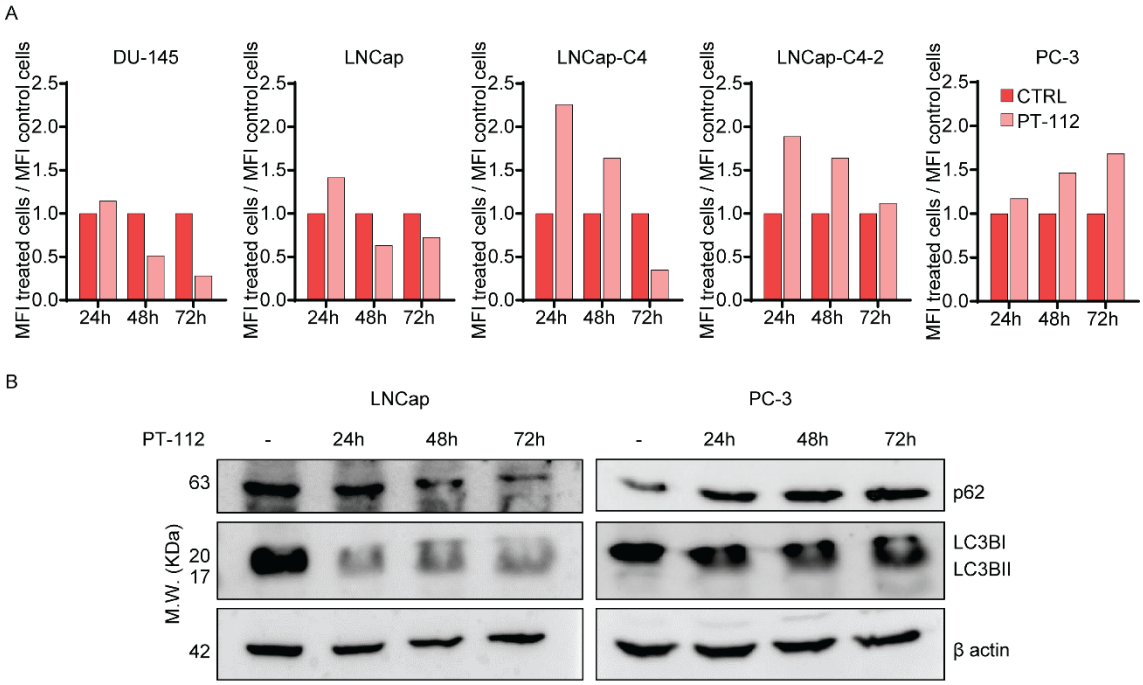

Figure 9

Figure 9. Autophagy induction by PT-112. (A) Analysis of autophagosome formation. Cells were incubated with 10 µM of PT-112 for 24–72 h. The autophagosome formation was analyzed by flow cytometry using the Cyto-ID® method. Bars represent the mean fluorescence intensity (MFI) of treated cells compared to untreated control cells (CTRL). (B) Analysis of p62 and LC3BI/II expression levels upon 10 µM of PT-112 treatment. β actin was used as a control of protein loaded.

Supplementary Material

A

Cell line	IC_{50} (μM)	HIF-1α expression
PC-3	>10	1.06
DU-145	2.15	1.65
VCap	>10	0.27
22Rv1	>10	0.58
LNCap	2.66	0.90
LNCap-C4	1.32	1.74
LNCap-C4-2	1.88	1.30
RWPE-1	-	0.09

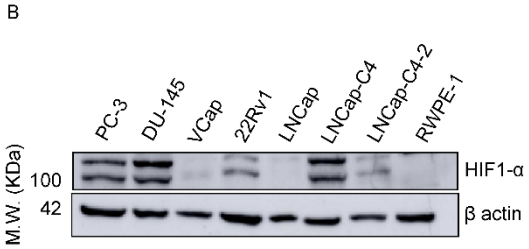

S. Figure 1

Supplementary Figure 1. Relationship between HIF-1α protein expression levels and PT-112 sensitivity. (A) Levels of HIF-1α expression were analyzed by western blot in prostate cancer cell lines and non-tumorigenic RWPE-1 cells. B actin was used as a control for protein loading. (B) IC_{50} values were calculated from 72 h cell growth inhibition experiments (Figure 1).

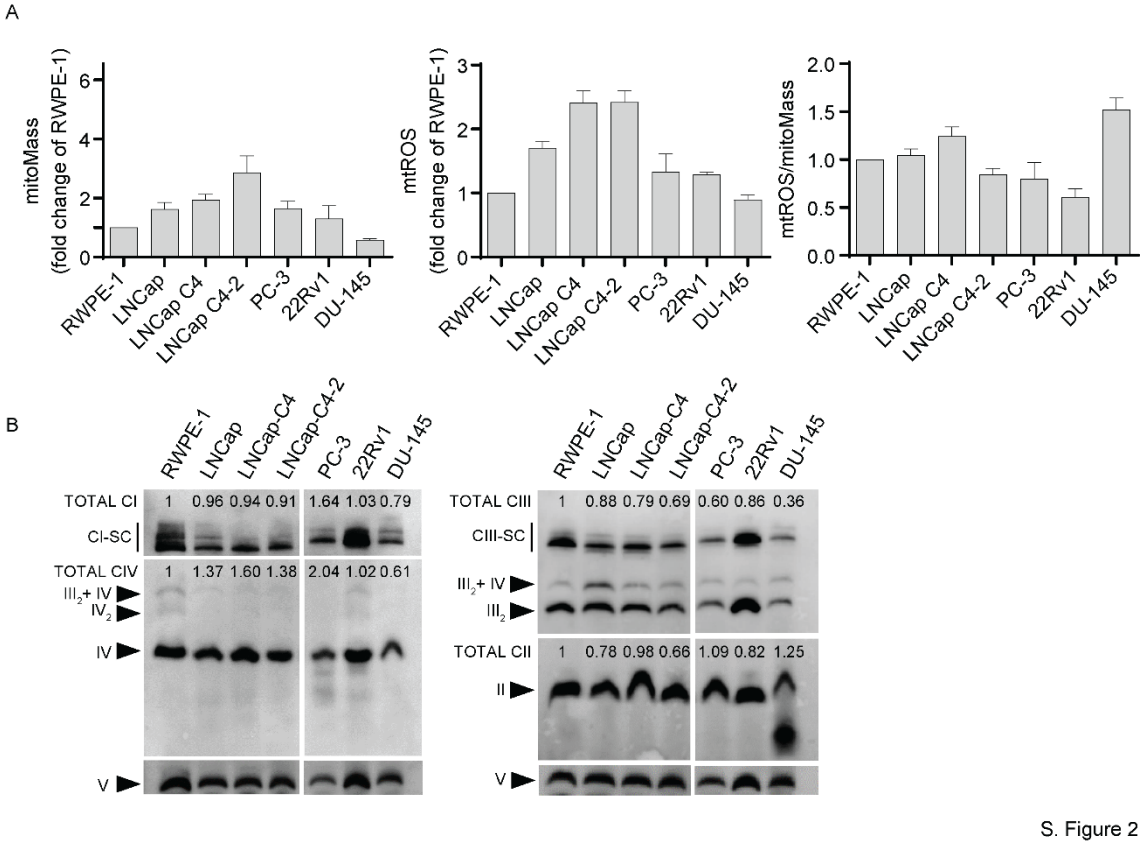

S. Figure 2

Supplementary Figure 2. Basal mitochondrial characterization of human prostate cancer cell lines and the non-tumorigenic prostate cell line RWPE-1. (A) Graph bars correspond to mean fluorescence intensity (MFI) normalized to the non-tumorigenic cell line RWPE-1. The ratio of mtROS levels to mitochondrial mass was

calculated and normalized to that of RWPE-1. Results are shown as a mean ± SEM of at least 3 experiments. (B) Protein expression of respiratory complexes and supercomplexes (SCs) was first normalized to Complex V then compared to healthy prostate cell line RWPE-1. The numbers represent the summed expression level of the indicated complex protein found as a monomer or within a SC. Complex and SC composition are annotated in the figure, with unresolved SC bands labeled as CI-SC (left) and CIII-SC (right).

References

1. Siegel R, Miller K, Wagle N, Jemal A: Cancer statistics, 2023. CA Cancer J Clin 2023, 73:17-48.

2. Sung H, Ferlay J, Siegel R, Laversanne M, Soerjomataram I, Jemal A, Bray F: Global Cancer Statistics 2020: GLOBOCAN Estimates of Incidence and Mortality Worldwide for 36 Cancers in 185 Countries. CA Cancer J Clin 2021, 71:209-249.

3. Buck S, Koolen S, Mathijssen R, de Wit R, van Soest R: Cross-resistance and drug sequence in prostate cancer. Drug Resist Update 2021, 56:100761.

4. Galletti G, Leach B, Lam L, Tagawa S: Mechanisms of resistance to systemic therapy in metastatic castration-resistant prostate cancer. Cancer Treat Rev 2017, 57:16-27.

5. Hwang C: Overcoming docetaxel resistance in prostate cancer: a perspective review. Ther Adv Med Oncol 2012, 4:329-340.

6. Parker C, Castro E, Fizazi K, Heidenreich A, Ost P, Procopio G, Tombal N, Gillessen S, al e: Prostate cancer: ESMO Clinical Practice Guidelines for diagnosis, treatment and follow-up. Ann Oncol 2020, 31:1119-1134.

7. Sandhu S, Moore C, Chiong E, Beltran H, Bristow R, Williams S: Prostate cancer. Lancet 2021, 398:1075-1090.

8. Chazan G, Anton A, Wong S, Shapiro J, Weickhardt A, Azad A, Kwan E, Spain L, Gunjur A, Torres J et al: Beyond cabazitaxel: Late line treatments in metastatic castration resistant prostate cancer: A retrospective multicentre analysis. Asian-Pacific J Clin Oncol 2022, 18:642-649.

9. Turco F, Gillessen S, Cathomas R, Buttiglioero C, Vogl U: Treatment Landscape for Patients with Castration-Resistant Prostate Cancer: Patient Selection and Unmet Clinical Needs Res Rep Urol 2022, 14:339-350.

10. Shore N, Ionescu-Ittu R, Laliberté F, Yang L, Lejeune D, Yu L, Duh M, Mahendran M, Kim J, Ghote S: Beyond Frontline Therapy with Abiraterone and Enzalutamide in Metastatic Castration-Resistant Prostate Cancer: A Real-World US Study. Clin Genit Cancer 2021, 19:480-490.

11. Valsecchi A, Dionisio R, Panepinto O, Paparo J, Palicelli A, Vignani F, Di Maio M: Frequency of Germline and Somatic BRCA1 and BRCA2 Mutations in Prostate Cancer: An Updated Systematic Review and Meta-Analysis. Cancers 2023, 15:2435.

12. Lukashchuk N, Barnicle A, Adelman C, Armenia J, Kang J, Barrett J, Harrington E: Impact of DNA damage repair alterations on prostate cancer progression and metastasis Front Oncol 2023, 26:1162644.

13. Al-Akhras A, Chehade C, Narang A, Swami U: PARP Inhibitors in Metastatic Castration-Resistant Prostate Cancer: Unraveling the Therapeutic Landscape Life 2024, 14:198.

14.Sanmamed MF, Chen L: A Paradigm Shift in Cancer Immunotherapy: From Enhancement to Normalization. Cell 2018, 175:313-326.

15.Sharma P, Allison J: The future of immune checkpoint therapy. Science 2015, 348:56-61.

16. Cha H, Lee J, Ponnazhagan S: Revisiting Immunotherapy: A Focus on Prostate Cancer. Cancer Res 2020, 80:1615-1623.

17. Runcie K, Dallos M: Prostate Cancer Immunotherapy—Finally in From the Cold?. Curr Oncol Rep 2021, 23:88.

18. Serrano-Del Valle A, Naval J, Anel A, Marzo I: Novel Forms of Immunomodulation for Cancer Therapy. . Trends Cancer 2020, 6:518-532.

19. Lanka S, Zorko N, Antonarakis E, Barata P: Metastatic Castration-Resistant Prostate Cancer, Immune Checkpoint Inhibitors, and Beyond Curr Oncol 2023, 30:4246-4256.

20. Bryce A, Karp D, Tagawa S, Nordquist L, Rathkopf D, Adra N, Dorff T, Baeck J, O'Donnell J, Ames T et al: A phase 2 study of immunogenic cell death inducer PT-112 in patients with metastatic castration-resistant prostate cancer. J Clin Oncol 2023, 41(Suppl 6):TPS292.

21. Imbimbo M, Ghisoni E, Mulvey A, Bouchaab H, Mederos-Alfonso N, Karp D, Camidge D, Mansfield A, Yim C, Ames T et al: A phase IIa study of the novel immunogenic cell death (ICD) inducer PT-112 plus avelumab ("PAVE") in advanced non-small cell lung cancer (NSCLC) patients Immuno-Oncol Thechnol 2022, 16(Suppl 1):125P.

22. Bryce A, Dronca R, Costello B, Aparicio A, Subudhi S, O'Donnell J, Jimeno J, Yim C, Price M, Karp D: A phase 1b study of novel immunogenic cell death inducer PT-112 plus PD-L1 inhibitor avelumab in metastatic castrate-resistant prostate cancer (mCRPC) patients. . J Clin Oncol 2021, 39:e17025.

23. Bryce A, Dronca R, Costello B, Infante J, Ames T, Jimeno J, Karp D: PT-112 in advanced metastatic castrate-resistant prostate cancer (mCRPC), as monotherapy or in combination with PD-L1 inhibitor avelumab: findings from two phase I studies. J Clin Oncol 2020, 2020:38.

24. Karp D, Camidge D, Infante J, Ames T, Price M, Jimeno J, Bryce A: Phase I study of PT-112, a novel pyrophosphateplatinum immunogenic cell death inducer, in advanced solid tumours. Lancet eClinMed 2022, 49:101430.

25. Karp D, Dronca R, Camidge R, Costello B, Mansfield A, Ames T, Jimeno J, Bryce A: Phase Ib dose escalation study of novel immunogenic cell death (ICD) inducer PT-112 plus PD-L1 inhibitor avelumab in solid tumours. Ann Oncol 2020, 31:S708.

26. Yim C, MT C, Johnson H, Mancini M, Stossi F, Mancini M, Azofeifa J, Price M, Baeck J, Ames T: PT-112, a novel immunogenic cell death (ICD) inducer, causes nucleolar stress leading to ribosomal biogenesis inhibition in cancer cells. AACR-NCU-EORTC International Conference Poster C128 2023.

27. Soler-Agesta R, Guilbaud E, Sato A, Yamazaki T, Yim C, Congenie M, Price M, Ames T, Anel A, Galluzzi L: Molecular mechanisms of immunogenic cell death driven by PT-112. J Immunother Cancer 2023, 11:doi: 10.1136/jitc-2023-SITC2023.1106

28. Soler-Agesta R, Marco-Brualla J, Minjárez-Sáenz M, Yim C, Martínez-Júlvez M, Price M, Moreno-Loshuertos R, Ames T, Jimeno J, Anel A: PT-112 Induces Mitochondrial Stress and Immunogenic Cell Death, Targeting Tumor Cells with Mitochondrial Deficiencies. Cancers 2022, 14:3851.

29. Yamazaki T, Galluzzi L, Yim C, Ames T: Immunologically relevant effects of PT-112 on cancer cell mitochondria. J Immunother Cancer 2022, 10 (Suppl 2):A1160.

30. Yamazaki T, Buqué A, Ames T, Galluzzi L: PT-112 induces immunogenic cell death and synergizes with immune checkpoint blockers in mouse tumor models. OncoImmunol 2020, 9:e1721810.

31. McAdams M, Swift S, Donahue R, Celades C, Tsai Y, Bingham M, Szabo E, Zhao C, Sansone S, Choradia N et al: Preliminary efficacy, safety, and immunomodulatory effects of PT-112 from a phase 2 proof of concept study in patients with thymic epithelial tumors. J Clin Oncol 2023, 41, supplementS:e20647.

32. McAdams M, Swift S, Donahue R, Celades C, Tsai Y, Bingham M, Szabo E, Zhao C, Sansone S, Feierabend C et al: Phase 2 Clinical Trial of PT-112 in Patients with Thymic Epithelial Tumors. Mediastinum 2023, 7:AB016.

33. Ames T, Sharik M, Rather G, Hochart G, Bonnel D, Linehan S, Stauber J, Wing R, Jimeno J, Medina D et al: Translational research of PT-112, a clinical agent in advanced phase i development: evident bone tropism, synergy in vitro with bortezomib and lenalidomide, and potent efficacy in the Vk*MYC mouse model of multiple myeloma. Blood 2017, 130:1797.

34. Nishimura K: Management of bone metastasis in prostate cancer. . J Bone Miner Metab 2023, 41:317-326.

35. Marco-Brualla J, Al-Wasaby S, Soler R, Romanos E, Conde B, Justo-Méndez R, Enríquez J, Fernández-Silva P, Martínez-Lostao L, Villalba M et al: Mutations in the ND2 subunit of mitochondrial complex I are sufficient to confer increased tumorigenic and metastatic potential to cancer cells. Cancers 2019, 11(7):1027.

36. Dong L, Neuzil J: Targeting mitochondria as an anticancer strategy Cancer Commun 2019, 39:63.

37. Sainero-Alcolado L, Liaño-Pons J, Ruiz-Pérez M, Arsenian-Henriksson M: Targeting mitochondrial metabolism for precision medicine in cancer Cell Death Differ 2022, 29:1304-1317.

38. Lee Y, Park D, Chae Y: Role of Mitochondrial Stress Response in Cancer Progression Cells 2022, 11:771.

39. Jin P, Jiang J, Zhou L, Huang Z, Nice E, Huang C, Fu L: Mitochondrial adaptation in cancer drug resistance: prevalence, mechanisms, and management J Hematol Oncol 2022, 15:97.

40. Onukwufor J, Berry B, Wojtovich A: Physiologic Implications of Reactive Oxygen Species Production by Mitochondrial Complex I Reverse Electron Transport. Antioxidants 2019, 8:285.

41. Acín-Pérez R, Fernández-Silva P, Peleato M, Pérez-Martos A, Enriquez J: Respiratory active mitochondrial supercomplexes. Mol Cell 2008, 32:529-539.

42. Schagger H, Pfeiffer K: Supercomplexes in the respiratory chains of yeast and mammalian mitochondria. Embo J 2000, 19(8):1777-1783.

43. Lapuente-Brun E, Moreno-Loshuertos R, Acín-Pérez R, Latorre-Pellicer A, Colás C, Balsa E, Perales-Clemente E, Quirós P, Calvo E, Rodríguez-Hernández M et al: Supercomplex assembly determines electron flux in the mitochondrial electron transport chain. Science 2013, 340:1567-1570.

44. Karp D, Camidge D, Infante J, Ames T, Jimeno J, Bryce A: A well-tolerated novel immunogenic cell death (ICD) inducer with activity in advanced solid tumors. Ann Oncol 2018, 29:viii143.

45. Marchetti P, Fovez Q, Germain N, Khamari R, Kluza J: Mitochondrial spare respiratory capacity: Mechanisms, regulation, and significance in non-transformed and cancer cells. FASEB J 2020, 34:13106-13124.

46. Hill B, Benavides G, Lancaster J, Ballinger S, Dell'Italia L, Jianhua Z, VM D-U: Integration of cellular bioenergetics with mitochondrial quality control and autophagy Biol Chem 2012, 393:1485-1512.

47. Chen Q, Vazquez E, Moghaddas S, Hoppel C, Lesnefsky E: Production of Reactive Oxygen Species by Mitochondria. CENTRAL ROLE OF COMPLEX III. J Biol Chem 2003, 278:36027-36031.

48. Nakamura H, Takada K: Reactive oxygen species in cancer: Current findings and future directions. Cancer Sci 2021, 112:3945-3952.

49. Lee S, Son J, Lee J, Cheong H: Unraveling the Intricacies of Autophagy and Mitophagy: Implications in Cancer Biology Cells 2023, 12:2742.

50. Serrano-Del Valle A, Anel A, Naval J, Marzo I: Immunogenic Cell Death and Immunotherapy of Multiple Myeloma. Front Cell Dev Biol 2019, 7:50.

51. Gupta G, Borgium K, Chen H: Immunogenic Cell Death: A Step Ahead of Autophagy in Cancer Therapy. . J Cancer Immunol 2021, 3:47-59.

52. Kourelis T, Ailawadhi S, Vogl D, Cooper D, Ames T, Yim C, Price M, Jimeno J, Bergsagel P: A Phase I Dose Escalation Study of PT-112 in Patients with Relapsed or Refractory Multiple Myeloma. Blood 2020, 136. Suppl 1:10.1182/blood-2020-134916.

53. Tang D: Understanding and targeting prostate cancer cell heterogeneity and plasticity Semin Cancer Biol 2022, 82:68-93.

54. Galluzzi L, Kepp O, Hett E, Kroemer G, Marincola F: Immunogenic cell death in cancer: concept and therapeutic implications. J Transl Med 2023, 21:162.

55. Song Y, Zhou Y, Zhou X: The role of mitophagy in innate immune responses triggered by mitochondrial stress. Cell Commun Signal 2020, 18:186.

56. Vringer E, Tait S: Mitochondria and cell death-associated inflammation Cell Death Differ 2022, 30:304-312.

57. Filomeni G, De Zio D, Cecconi F: Oxidative stress and autophagy: the clash between damage and metabolic needs Cell Death Differ 2015, 22:377-388.

58. Roca-Agujetas V, de Dios C, Lestón L, Marí M, Morales A, Colell A: Recent Insights into the Mitochondrial Role in Autophagy and Its Regulation by Oxidative Stress Oxid Med Cell Longev 2019, 2019:3809308.

59. Galluzzi L, Kepp O, Hett E, Kroemer G, Marincola F: Immunogenci cell death in cancer: concept and therapeutic implications. J Transl Med 2023.

60. Yamazaki T, Kirchmair A, Sato A, Buqué A, Rybstein M, Petroni G, Bloy N, Finotello F, Stafford L, Navarro Manzano E et al: Mitochondrial DNA drives abscopal responses to radiation that are inhibited by autophagy. Nature Immunol 2020, 21:1160-1171.

61. Wang Z, Gall J, Bonegio R, Havasi A, Illanes K, Schwartz J, Borkan S: Nucleophosmin, a critical Bax cofactor in ischemia-induced cell death Mol Cell Biol 2013, 33:1916-1924.

62. Maehama T, Nishio M, Otani J, Mak T, Suzuki A: Nucleolar stress: Molecular mechanisms and related human diseases Cancer Sci 2023, 114:2078-2086.

63. Kim J, Kim H, Chung J: Molecular mechanisms of mitochondrial DNA release and activation of the cGAS-STING pathway Exp Mol Med 2023, 55:510-519.

64. Kwon J, Bakhoum S: The Cytosolic DNA-Sensing cGAS-STING Pathway in Cancer Cancer Discov 2020, 10:26-39.

65. Pfister A: Emerging Role of the Nucleolar Stress Response in Autophagy Front Cell Neurosci 2019, 13:156.

66. Quin J, Devlin J, Cameron D, Hannan K, Pearson R, Hannan R: Targeting the nucleolus for cancer intervention. Biochim Biophys Acta 2014, 1842:802-816.

67. Gilles A, Frechin L, Natchiar K, Biondani G, von Loeffelholz O, Holvec S, Malaval J, Winum J, Klaholz B, Peyron J: Targeting the Human 80S Ribosome in Cancer: From Structure to Function and Drug Design for Innovative Adjuvant Therapeutic Strategies Cells 2020, 9:629.

6.CHAPTER III: Mitochondrial implications on ICD

Mitochondrial involvement in the cytotoxicity and immunogenicity of PT-112

Ruth Soler-Agesta[1,2], Manuel Beltrán-Visiedo[1], Ai Sato[1], Emma Guilbaud[1], Christina Yim[2], Tyler D. Ames[2] and Lorenzo Galluzzi[1,3,4,*]

[1]Department of Radiation Oncology, Weill Cornell Medical College, New York, NY, USA; [2]Promontory Therapeutics, New York, NY, USA; [3]Caryl and Israel Englander Institute for Precision Medicine, New York, NY, USA; [4]Sandra and Edward Meyer Cancer Center, New York, NY, USA.

*Correspondence to Lorenzo Galluzzi (deadoc80@gmail.com)

Keywords: CGAS; $CD8^+$ cytotoxic T lymphocytes; dendritic cells; immune checkpoint inhibitors; mtDNA; PD-1.

Abstract

PT-112 is a novel immunotherapeutic agent with promising clinical activity in patients with a variety of solid tumors. Mechanistically, PT-112 has been shown to kill malignant cells while eliciting the emission of endogenous adjuvant-like signals commonly known as damage-associated molecular patterns (DAMPs), which promote the recognition of cancer cell death as immunogenic. In line with this notion, PT-112 has been shown to positively interact with immune checkpoint inhibitors in preclinical models of mammary and colorectal carcinoma. Mitochondrial outer membrane permeabilization (MOMP) as mediated by BCL2 associated X, apoptosis regulator (BAX) and BCL2 antagonist/killer 1 (BAK1) and antagonized by BCL2, apoptosis regulator (BCL2) and BCL2-like 1 (BCL2L1, best known as BCL-X_L) has been shown to regulate both the cytotoxicity and immunostimulatory potential of various anticancer agents. Here, we harnessed mouse mammary carcinoma TS/A cells bearing genetic alterations that affect the molecular machinery for MOMP to demonstrate that while the overtly cytotoxic effects of PT-112 and hence the short-term release of the cell death-related DAMP high mobility group box 1 (HMGB1) involves MOMP, its cytostatic activity does not. Along similar lines, MOMP defects failed to alter the ability of PT-112 to elicit the immunogenic cell death (ICD)-associated exposure of calreticulin (CALR) on the outer leaflet of the plasma membrane, as well as the secretion of type I interferon (IFN). That said, the absence of BAX and BAK1 considerably limited MHC Class I exposure in TS/A cells, overall pointing to partial involvement of MOMP in the immunogenicity of PT-112-driven cell death.

Introduction

PT-112 is a novel immunotherapeutic agent with promising single-agent clinical activity in patients affected by advanced solid tumors of different origin (Karp et al., 2022), including (but not limited to) castration-resistant prostate cancer (Alan Haruo Bryce et al., 2021; Bryce et al., 2020) and thymic epithelial tumors (M. McAdams et al., 2023). In line with this notion, PT-112 has been shown to efficiently arrest the proliferation and kill a wide panel of human and mouse cancer cell lines (Ames et al., 2016), with a mechanism of action that appears to involve ribosomal biogenesis inhibition (C. Y. Yim et al., 2023) coupled to mitochondrial stress (Agesta et al., 2022; Soler-Agesta, Ames, et al., 2022; Soler-Agesta, Marco-Brualla, et al., 2022b). Importantly, PT-112 has also been demonstrated to elicit a type of cell death that (in immunocompetent hosts) can elicit the activation of adaptive anticancer immune responses associated with an active effector phase (Yamazaki et al., 2019; T. Yamazaki, A. Buqué, et al., 2020), i.e., immunogenic cell death (ICD) (Pan et al., 2024). Accordingly, PT-112 appears to positively cooperates with various immune checkpoint inhibitors (ICIs) in the control of syngeneic mouse tumor models (T. Yamazaki, A. Buqué, et al., 2020). Moreover, two Phase I clinical trials testing PT-112 in combination with an ICI specific for CD274 (best known as PD-L1) documents promising activity in patients with castration-resistant prostate cancer (A. H. Bryce et al., 2021).

Of note, the ability of cancer cells to release endogenous molecules with adjuvant-like activity as they succumb to perturbations of homeostasis that cannot be resolved by core mechanisms of adaptation like the integrated stress response (ISR) or autophagy (Lorenzo Galluzzi, Takahiro Yamazaki, et al., 2018) is critical for cell death to be perceived as immunogenic (Kroemer et al., 2022). These molecules are commonly referred to damage-associated molecular patterns (DAMPs) and include calreticulin (CALR), which is exposed on the surface of cancer cells undergoing ICD, as well as ATP and high-mobility group box 1 (HGMB1), which are release therefrom (Fucikova et al., 2021; Kepp et al., 2021; Kroemer et al., 2022). Moreover, the activation of adaptive immunity by dying cells generally involves their ability to secrete immunostimulatory cytokines like type I interferon (IFN), a process that (at least in some settings) results from mitochondrial damage and the consequent release of mitochondrial DNA (mtDNA) in the cytosol, culminating with the activation of cyclic GMP-AMP synthase (CGAS) (Marchi et al., 2023; T. Yamazaki, A. Kirchmair, et al., 2020). Finally, the effector phase of antigen-specific anticancer immune responses as elicited by ICD requires that target cells present antigenic determinants on their surface in complex with MHC Class I molecules to enabling recognition and elimination by $CD8^+$ cytotoxic T lymphocytes (CTLs) (Jhunjhunwala et al., 2021; Yang et al., 2023) .

Mitochondrial outer membrane permeabilization (MOMP) as elicited by BCL2 associated X, apoptosis regulator (BAX) and BCL2 antagonist/killer 1 (BAK1) and antagonized by BCL2, apoptosis regulator (BCL2) and BCL2-like 1 (BCL2L1, best known as BCL-X_L) has been involved not only in the ability of multiple anticancer agents to kill malignant cells (Bock & Tait, 2020; Tait & Green, 2010), but also in their capacity to elicit the secretion of type I IFN via the mtDNA-dependent activation of CGAS (McArthur et al., 2018; Riley et al., 2018; Takahiro Yamazaki et al., 2020). Here, we harnessed mouse hormone receptor (HR)-positive T/SA cells (De Giovanni et al., 2019) to demonstrate that while MOMP is involved in the acute cytotoxic effects of PT-112, genetic alterations in core components of the MOMP machinery generally fail to alter its antiproliferative and immunostimulatory activity.

Materials and Methods

Chemicals and cell culture. TS/A cells (SCC177) were obtained from Millipore Sigma and maintained in culture as per manufacturer's recommendations. Wild-type (WT) TS/A and TS/A-derived clones were routinely cultured at 37 °C under 5 % of CO_2 in DMEM containing 1 mM sodium pyruvate, 1mM HEPES buffer, 4.5 g/L glucose (Corning®) and supplemented with 10% fetal bovine serum (GeminiBio), 100 µg/mL streptomycin sulfate, 100 U/mL penicillin sodium and 290 µg/mL L-glutamine (Gibco™).

CRISPR/Cas9. TS/A cells were transfected with a commercial control CRISPR-cas9 plasmid (CRISPR06-1EA, Sigma Aldrich) or customized CRISPR-cas9 plasmids based on CRISPR06-1EA targeting *Bak1*, *Bax*, *Bcl2*, *Bcl2l1* (Sigma Aldrich), harnessing the TransIT-CRISPR as per manufacturer protocol. After transfection, individual GFP-expressing cells were sorted into 96-well plates using a FACS Symphony S6 Sorter (BD Biosciences) for expansion and immunoblotting validation.

Immunoblotting. Immunoblotting was performed according to conventional procedures (Takahiro Yamazaki et al., 2020) with primary antibodies specific for BAK1 (#12105, Cell Signaling Technology, 1:500), BAX (#2772, Cell Signaling Technology, 1:1,000), BCL2 (#3498, Cell Signaling Technology, 1:500), BCL-X_L (#2764, Cell Signaling Technology, 1:500) and ACTB1 (#3700, Cell Signaling Technology, 1:2,000) as a loading control. After washing and incubation with horseradish peroxidase-conjugated anti-rabbit (#NA934, GE Healthcare Life Sciences, 1:5,000) or anti-mouse secondary antibodies (#NA931, GE Healthcare Life Sciences, 1:5,000), the SuperSignal West Femto Maximum Sensitivity Substrate (#34094, Thermo Fisher) was employed to visualize protein expression on an Azure 600 Imaging System operated by Azure capture v. 1.9.0.0406 (Azure Biosystems).

Cell number and cell death. Cell number and cell death were evaluated by flow cytometry using the Attune NxT flow cytometer (Thermo Fisher Scientific) upon staining with 0.5 µg/mL 4',6-diamidino-2-phenylindole (DAPI, Sigma-Aldrich).

Clonogenic assays. Seven days after treatment initiation colonies were fixed with 70% ethanol and stained with 0.1% crystal violet (Electron Microscopy Sciences), according to conventional procedures (Serrano-Mendioroz et al., 2023). Colonies were manually counted with the eCountTM Colony counter (Heathrow Scientific).

Mitochondrial parameters. Mitochondrial membrane potential and mitochondrial mass were analyzed by flow cytometry using the Attune NxT flow cytometer (Thermo Fisher Scientific) upon staining with 100 nM MitoTracker™ Deep Red FM (Invitrogen™), 150 nM of MitoTracker™ Green FM (Invitrogen™), and 0.5 µg/mL DAPI (Sigma-Aldrich), which was used as a vital dye.

DAMP emission. HMGB1, and type I IFN release were quantified with the HMGB1 express ELISA Kit (Tecan), and the IFN-β ELISA kit, High Sensitivity (PBL Assay Science), respectively, as per manufacturer's recommendations. Sample absorbance at 450 nm was measured on a FlexStation 3 Multi-Mode Microplate Reader operated by SoftMaxPro v.5.4.6 (Molecular Devices LLC). Absolute quantification was calculated based on standard curves with $R^2 \geq 0.99$.

MHC-I and CRT surface expression. Cells were washed with PBS and stained with Zombie Aqua™ Fixable Viability Kit (BioLegend) for 15 min. Subsequently, cells were washed and incubated with the Calreticulin (D3E6) XP® rabbit monoclonal antibody PE Conjugate (#19780S, Cell Signaling, 0.5 µL/sample) and PE anti-mouse H-2 Antibody anti-H-2- M1/42 (#125505, BioLegend, 1 µL/sample) in 0.5% BSA in PBS (FACS buffer) for 25 min at 4°C in the dark. Then, cells were washed and fixed with eBioscience™ Intracellular Fixation & Permeabilization Buffer Set (Invitrogen) for 30 min at 4°C in the dark, incubated with the permeabilization buffer eBioscience™ Intracellular Fixation & Permeabilization Buffer Set (Invitrogen) for 5 min, washed and resuspended in FACS buffer for analysis by flow cytometry (Attune NxT flow cytometer, Thermo Fisher Scientific). Zombie Aqua™ positive cells (*i.e.*, dead cells) were excluded from the analysis.

Immunofluorescence microscopy. For cytosolic dsDNA analysis, cells growing on glass coverslips were fixed with 4% paraformaldehyde (#sc-281692, Santa Cruz Biotechnology), plasma membrane was permeabilized with 0.1% Tween20 and 0.01% Triton X-100 in PBS followed by incubation with specific dsDNA primary antibody (#ab27156, Abcam, 1:1,000). Cells were next washed with 0.1% Tween20 in PBS and incubated with Goat Anti-Mouse IgG H&L (Alexa Fluor® 488) preadsorbed (#ab150117, Abcam). Finally, samples were

washed and mounted on slides with Hoechst 33342-containing ProLong Glass Antifade Mountant (Thermo Fisher Scientific).

Images were acquired with an EVOS FL Imaging System operated by embedded software v.1.4 (Rev 26059) (Thermo Fisher Scientific). Quantitative dsDNA analyses were performed on ≥10 randomly selected images per condition. Briefly, blue (nuclear) and green (dsDNA) levels were normalized with a LUT file optimized for each sample set on Photoshop v. 25.7.0 (Adobe), followed by the identification of nuclear and cytoplasmic regions of interest, which were quantified for the presence and relative localization of dsDNA spots above a predefined threshold size (to account for background noise) with Cell Profiler v. 4.2.1 (Broad Institute). All steps were performed with commands that are publicly available at https://cellprofiler.org/ (Sato et al., 2022; Sato et al., 2021).

Data processing and statistical analysis. Prism v. 10 (GraphPad) and Excel 2021 (Microsoft) were used for data processing, plotting and statistical analysis. Illustrator 2020 (Adobe) was used for figure preparation. Otherwise noted, for statistical analysis, two-way ANOVA and uncorrected Fisher's LSD were applied in comparisons involving two or more groups. For samples not following a Gaussian distribution, statistical significance was assessed by Wilcoxon test. Unless otherwise noted, all experiments were performed at least in three independent replicates.

Results

Antiproliferative and cytotoxic effects. To investigate the involvement of the molecular machinery for MOMP in in the anticancer activity of PT-112, we harnessed the CRISPR/Cas9 technology to establish multiple mouse HR^+ mammary carcinoma TS/A cell clones lacking *Bax* plus *Bak1*, or *Bcl2* plus *Bcl2l1* (**Suppl. Fig. 1A**) and tested their sensitivity to the antiproliferative and cytotoxic effects of PT-112. In line with previous findings (Ames et al., 2016), exposing control TS/A cells to 20 µM or 40 µM PT-112 resulted in a pronounced proliferative arrest (**Fig. 1A**) coupled with a dose-dependent accumulation of dead cells (**Fig. 1B**), as assessed by enumerating cell number by flow cytometry in the presence of a DAPI, which selectively stains dead cells (Galluzzi et al., 2009). Of note, while the ability of PT-112 to kill TS/A cells was exacerbated in *Bcl2*$^{-/-}$*Bcl2l1*$^{-/-}$ TS/A cell clones and compromised in *Bax*$^{-/-}$*Bak1*$^{-/-}$ TS/A cell clones (**Fig. 1B**), its antiproliferative potential was not altered by genetic perturbations affecting MOMP (**Fig. 1A**). These findings were corroborated by conventional clonogenic assays (Serrano-Mendioroz et al., 2023) (**Fig. 1C**). Interestingly, cell death as driven by PT-112 in control TS/A cells was accompanied by a dose-dependent increase in total mitochondrial mass (**Fig. 1D**), but considerably less so in mitochondrial transmembrane

potential ($\Delta\psi_m$) (**Fig. 1E**), as assessed by flow cytometry upon staining with the mass- and $\Delta\psi_m$-sensitive probes MitoTracker™ Green FM and MitoTracker™ Deep Red FM, respectively, resulting in relative mitochondrial depolarization (**Fig. 1F**). The increase in mitochondrial mass elicited by PT-112 was exacerbated in *Bcl2*$^{-/-}$*Bcl2l1*$^{-/-}$ TS/A cell clones and reduced in *Bax*$^{-/-}$*Bak1*$^{-/-}$ TS/A cell clones (**Fig. 1D**), the latter of which also exhibited improved mitochondrial polarization as compared to control TS/A cells (**Fig. 1E**). In this setting, *Bcl2*$^{-/-}$*Bcl2l1*$^{-/-}$ TS/A cell clones were more sensitive to relative mitochondrial depolarization as elicited by PT-112, while their *Bax*$^{-/-}$*Bak1*$^{-/-}$ counterparts responded to PT-112 with relative mitochondrial hyperpolarization (**Fig. 1F**), which is in line with (1) the role of MOMP and consequent mitochondrial depolarization in apoptotic cell death (Vitale et al., 2023), and (2) the differential sensitivity of *Bcl2*$^{-/-}$*Bcl2l1*$^{-/-}$ and *Bax*$^{-/-}$*Bak1*$^{-/-}$ TS/A cell clones to PT-112 induced cell death (**Fig. 1B**).

Taken together, these findings indicates that PT-112 exerts antiproliferative effects independent of mitochondrial apoptosis but mediates overt cytotoxicity through BAX- and BAK1-dependent MOMP.

DAMP emission. We next focused on the impact of the MOMP machinery on the ability of PT-112 to promote the release of ICD-relevant DAMPs and modulate the visibility of cancer cells to $CD8^+$ CTLs (Galluzzi et al., 2024). The relative mitochondrial depolarization promoted by PT-112 in TS/A cells (**Fig. 1F**) was accompanied by the dose-independent accumulation of cytosolic double-stranded DNA (dsDNA) (**Fig. 2A, B**), which is known to drive type I IFN secretion (Marchi et al., 2023). Accordingly, TS/A cells exposed to PT-112 secreted approximately two-fold more interferon beta 1 (IFNB1) in their supernatant than their control counterparts (**Fig. 2C**). However, while the absence of BAX and BAK1 completely abrogated cytosolic dsDNA accumulation as elicited in TS/A cells by PT-112 (**Fig. 2A, B**), it failed to influence type I IFN secretion (**Fig. 2C**). Of note, the *Bcl2*$^{-/-}$*Bcl2l1*$^{-/-}$ phenotype had little effects on the ability of PT-112 to promote cytosolic dsDNA accumulation (**Fig. 2A,B**) and type I IFN release (**Fig. 2C**), potentially suggesting the (at least partial) involvement of alternative mechanisms of mitochondrial permeabilization, *e.g.*, the mitochondrial permeability transition (MPT) (Bonora et al., 2022) or an accrued reliance of TS/A cells on another antiapoptotic protein of the BCL2 family to preserve mitochondrial integrity, namely MCL1 apoptosis regulator, BCL2 family member (MCL1) (Vitale et al., 2023).

As previously demonstrated with higher PT-112 doses (T. Yamazaki, A. Buqué, et al., 2020), WT TS/A cells exposed to 20 μM or 40 μM PT-112 for 48 hours exposed CALR on the outer leaflet of the plasma membrane, with non-significant differences across doses (**Fig. 3A**), an immunogenic effect that was not influence by the *Bax*$^{-/-}$*Bak1*$^{-/-}$ or the *Bcl2*$^{-/-}$*Bcl2l1*$^{-/-}$ genotype (**Fig. 3A**). These findings are in line with the notion that CALR exposure in malignant cells undergoing ICD involves the ISR, and notably its

pathognomonic inactivating phosphorylation of eukaryotic translation initiation factor 2 subunit alpha (EIF2S1, best known as eIF2α), but not MOMP (Galluzzi et al., 2024).

At odds with previous findings obtained with ~100 μM PT-112 (T. Yamazaki, A. Buqué, et al., 2020), WT TS/A cells treated *in vitro* with 20 μM or 40 μM PT-112 for 48 hours did not release significant amounts of HMGB1 in the culture supernatant (**Fig. 3B**). Conversely, the concomitant absence of BCL2 and BCL-X_L enabled abundant HMGB1 secretion by TS/A cell clones responding to PT-112, which is in line with the accrued cytotoxic response of these cells (**Fig. 1D**). *Bax*$^{-/-}$*Bak1*$^{-/-}$ TS/A cell clones exposed to 40 μM PT-112 for 48 hours exhibited significant reduced HMGB1 release as compared to their similarly treated WT counterpart, although the magnitude of this effect was minimal (**Fig. 3B**). Most likely, such a marginal effect was due to the lack of HGMB1 release in WT TS/A cells.

Finally, TS/A cells exposed to 20 μM or 40 μM PT-112 for 48 hours exhibited a nearly 2-fold upregulation in surface-expose MHC Class I molecules as compared to their untreated counterparts (**Fig. 3C**). Intriguingly, this was not affected by the co-deletion of *Bcl2* and *Bcl2l1* but was significantly limited by the concomitant absence of BAX and BAK1 (**Fig. 3C**), potentially suggesting a role for cytosolic dsDNA accumulation (but not type I IFN signaling) (**Fig. 2B, C**) in this process.

Altogether, our findings point to a partial involvement of the molecular machinery for MOMP in the cytotoxic and immunogenic activity of PT-112 in TS/A cells.

Discussion

In summary, the molecular machinery for MOMP appears to be dispensable for the antiproliferative effects that PT-112 exerts on mouse HR$^+$ mammary carcinoma TS/A cells, but to be involved in its overt cytotoxic effects and associated release of the immunostimulatory DAMP HMGB1 in the culture supernatant. Moreover, MOMP seems to influence, at least in part, the ability of PT-112 to promote the upregulation of MHC Class I molecules on the outer leaflet of the plasma membrane, but not the ICD-associated exposure of CALR.

Thus, while these findings have been obtained with a single cell line and hence must be recapitulated in other cellular systems, MOMP may influence (at least in part) the ability of PT-112 to elicit *bona fide* ICD associated with immunological protection in gold-standard prophylactic vaccination assays (Fucikova et al., 2020), a possibility that we are currently investigating. Moreover, while the concomitant absence of BAX and BAK1 limited the cytosolic accumulation of dsDNA and the upregulation of MHC Class I molecules on the TS/A cell surface as elicited by PT-112, the co-deletion of *Bcl2* and *Bcl2l1* had little effects

on these processes (**Fig. 2B and 3B**). These finding may indicate that TS/A cells either are particularly dependent on MCL1 for the preservation of mitochondrial integrity under stressful conditions (Vitale et al., 2023) or respond to PT-112 with the MPT, a MOMP-related but not completely overlapping mechanism of mitochondrial permeabilization (Bonora et al., 2022). Thus, it will be interesting to test the antiproliferative, cytotoxic and immunostimulatory effects of PT-112 in *Bcl2*$^{-/-}$*Bcl2l1*$^{-/-}$ TS/A cells also exposed to an MCL1-specific inhibitor such as ABBV-467 (Yuda et al., 2023) or an MPT inhibitor such as cyclosporin A (CsA) (Bonora et al., 2022).

That said, activation of apoptotic caspases as elicited by widespread MOMP has been associated with multipronged immunosuppressive effects including suppressed type I IFN signaling in a variety of settings (Rodriguez-Ruiz et al., 2019; Anthony Rongvaux et al., 2014; White et al., 2014). At least hypothetically, this may also explain why *Bcl2*$^{-/-}$*Bcl2l1*$^{-/-}$ TS/A cells (which are more prone to activate caspases as compared to their WT counterparts) failed to exhibit superior type I IFN secretion. Finally, while *Bax*$^{-/-}$*Bak1*$^{-/-}$ TS/A cells exhibited limited PT-112-driven cytosolic dsDNA accumulation as compared to their WT counterparts (**Fig. 2B**), the concomitant absence of BAX and BAK1 failed to affect PT-112-drive type I IFN secretion, potentially pointing to extramitochondrial nucleic acids (notably nuclear DNA or RNA species) as potential drivers of the latter process. Additional work is required to clarify this possibility.

Despite this and other unknown, the molecular machinery for MOMP appears to be partially involved in the immunogenicity of PT-112, suggesting that (at least in some settings), pharmacologically compromising the mitochondrial checkpoint (Yamazaki & Galluzzi, 2020) may boost the ability of PT-112 to elicit therapeutically relevant anticancer immunity.

Competing Interests. CY and TDA are full-time employees of Promontory Therapeutics. LG is/has been holding research contracts with Lytix Biopharma, Promontory and Onxeo, has received consulting/advisory honoraria from Boehringer Ingelheim, AstraZeneca, OmniSEQ, Onxeo, The Longevity Labs, Inzen, Imvax, Sotio, Promontory, Noxopharm, EduCom, and the Luke Heller TECPR2 Foundation, and holds Promontory stock options. All other authors have no conflicts to declare.

Acknowledgements. RS-A has been partially supported by Promontory Therapeutics. LG is/has been supported (as a PI unless otherwise indicated) by one R01 grant from the NIH/NCI (#CA271915), by two Breakthrough Level 2 grants from the US DoD BCRP (#BC180476P1, #BC210945), by a grant from the STARR Cancer Consortium (#I16-0064), by a Transformative Breast Cancer Consortium Grant from the US DoD BCRP (#W81XWH2120034, PI: Formenti), by a U54 grant from NIH/NCI (#CA274291, PI: Deasy, Formenti,

Weichselbaum), by the 2019 Laura Ziskin Prize in Translational Research (#ZP-6177, PI: Formenti) from the Stand Up to Cancer (SU2C), by a Mantle Cell Lymphoma Research Initiative (MCL-RI, PI: Chen-Kiang) grant from the Leukemia and Lymphoma Society (LLS), by a Rapid Response Grant from the Functional Genomics Initiative (New York, US), by a pre-SPORE grant (PI: Demaria, Formenti) and a Clinical Trials Innovation Grant from the Sandra and Edward Meyer Cancer Center (New York, US); by startup funds from the Dept. of Radiation Oncology at Weill Cornell Medicine (New York, US), by industrial collaborations with Lytix Biopharma (Oslo, Norway), Promontory (New York, US) and Onxeo (Paris, France), as well as by donations from Promontory (New York, US), the Luke Heller TECPR2 Foundation (Boston, US), Sotio a.s. (Prague, Czech Republic), Lytix Biopharma (Oslo, Norway), Onxeo (Paris, France), Ricerchiamo (Brescia, Italy), and Noxopharm (Chatswood, Australia).

Author contributions. TDA and LG conceived the study. RS-A and MB-V performed most experimental assessments with technical help from AI and Emma Guilbaud. LG wrote the first version of the manuscript with input from all authors. All authors approve the submitted version of the article.

Figures and legends

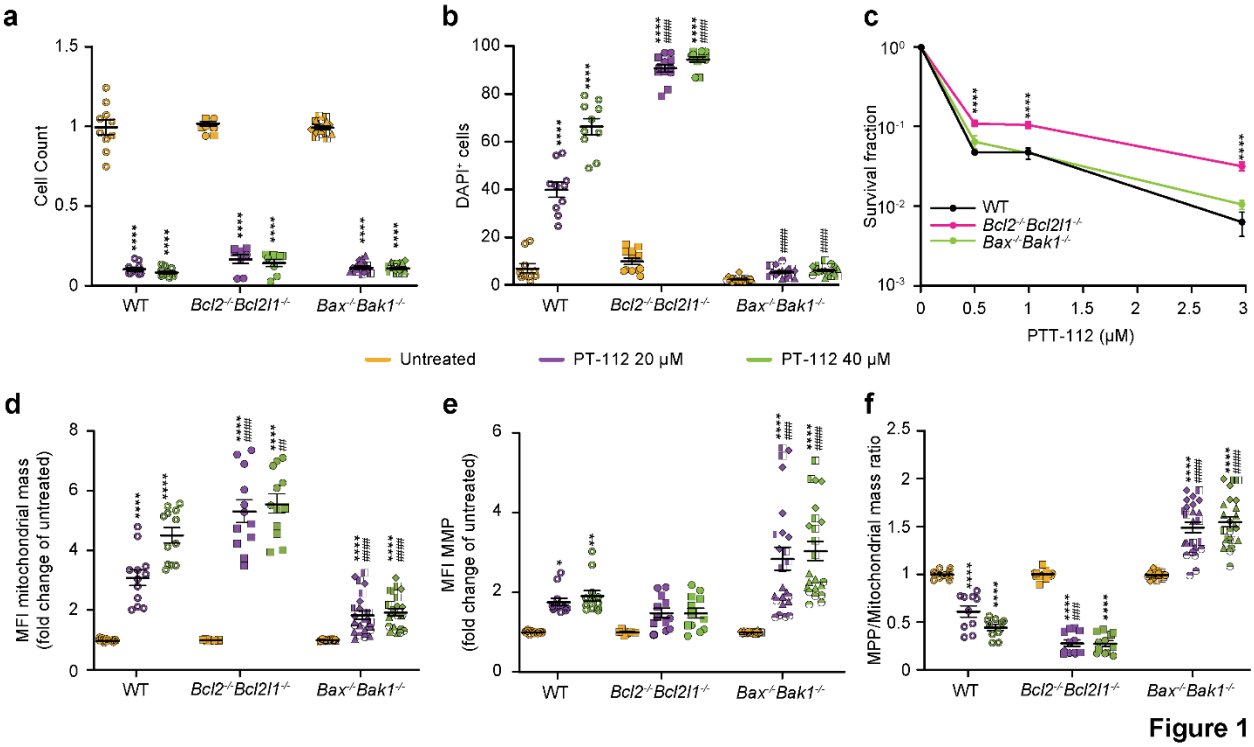

Figure 1

Figure 1. PT-112 represses cancer cell proliferation and induces Bax and Bak-dependent cell death associated with mitochondrial stress. TS/A WT and genetically modified *Bcl2*$^{-/-}$*Bcl2l1*$^{-/-}$ and *Bax*$^{-/-}$*Bak*$^{-/-}$ cells were treated with 20 µM or 40 µM of PT-112 and incubated for 72 h. (**a**) Normalized cell number and (**b**) percentage of DAPI $^{+}$ cells (death cells) was evaluated by flow cytometry using DAPI staining. (**c**) Residual clonogenic potential of cells exposed to 0.5 µM, 1 µM and 3 µM PT-112 and allowed to generate colonies for 7 d. Results are represented as the mean ± SEM of 6 biological duplicates from at least, 3 independent experiments. **** p<0.0001, compared to TS/A WT for each individual concentration (paired two-tailed Student's *t*-test). (**d**) Changes in mitochondrial membrane potential (MMP) and (**e**) mitochondrial mass were evaluated by flow cytometry in the indicated concentrations of PT-112 for 72 h. Data are represented as the mean fluorescence intensity (MFI) normalized to MFI of untreated cells of the same genotype. (**f**) MMP and mitochondrial mass MFI ratio. In **a**, **b**, **e,** and **f** results are represented as the mean ± SEM of 2 biological duplicates from 3 independent experiments. **** p<0.0001, ** p<0.01, * p<0.05, compared to untreated cells of the same genotype. #### p<0.0001, ### p<0.001, ## p<0.01, compared to TS/A cells treated with the same dose of PT-112 (two-way ANOVA). Symbols represents different cell clones with same genotype.

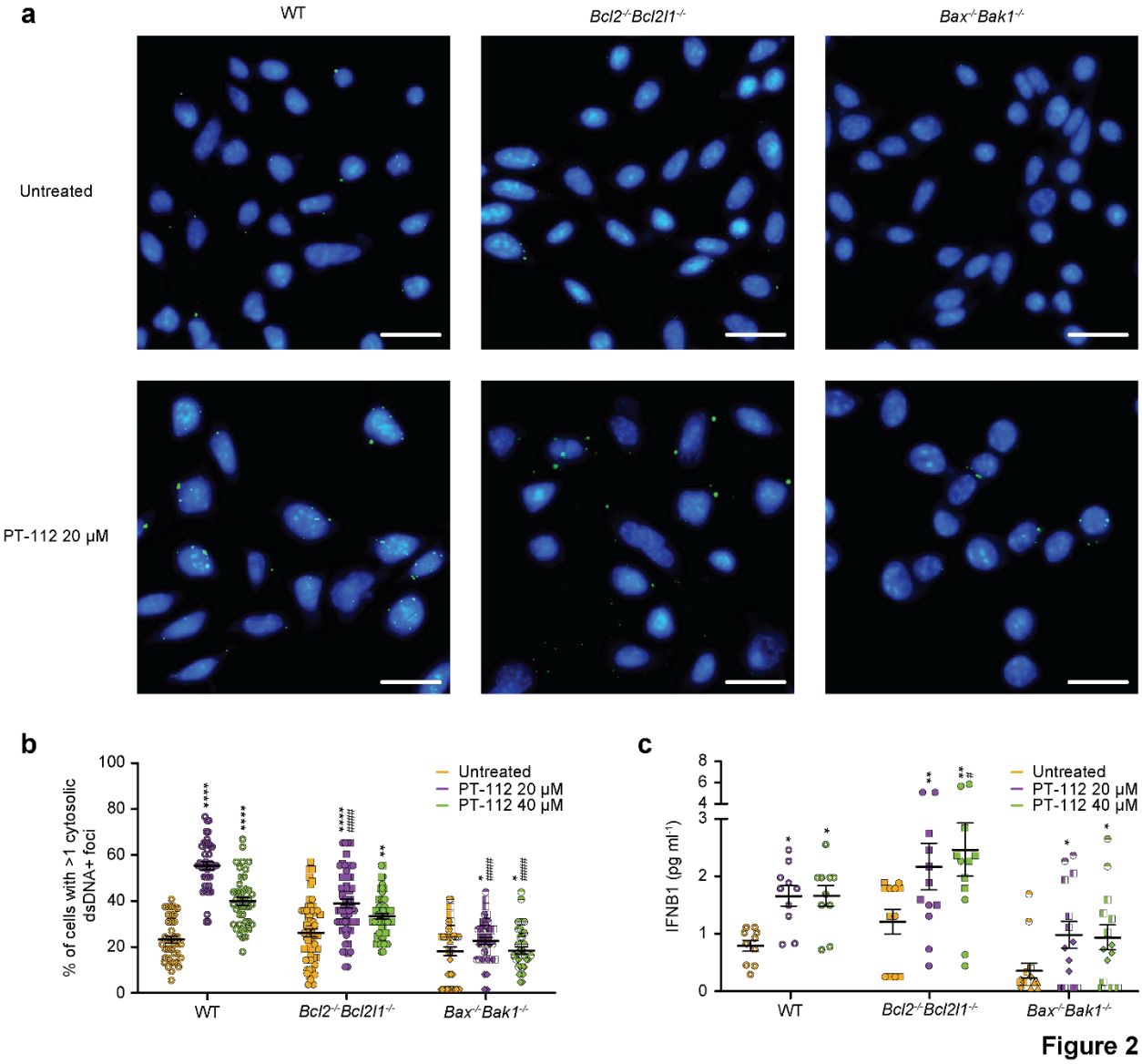

Figure 2. PT-112 induces MOMP-dependent cytosolic dsDNA accumulation and type I IFN production. (**a**, **b**) Automated image analysis of cytosolic dsDNA accumulation in TS/A WT and genetically modified *Bcl2*$^{-/-}$*Bcl2l1*$^{-/-}$ and *Bax*$^{-/-}$*Bak*$^{-/-}$ cells upon 48 h of incubation with 20 µM or 40 µM PT-112 were assessed by immunofluorescence using a dsDNA-specific antibody. (**a**) Representative images (scale bar, 20 µm) and (**b**) quantitative results are represented as the mean ± SEM of 2 independent experiments (two-way ANOVA). (**c**) IFNB1 levels in the supernatant of TS/A WT and genetically modified *Bcl2*$^{-/-}$*Bcl2l1*$^{-/-}$ and *Bax*$^{-/-}$*Bak*$^{-/-}$ cells upon 24 h of incubation with 20 µM or 40 µM PT-112. Results are represented as the mean ± SEM of 2 biological duplicates from 3 independent experiments (paired two-tailed Student's *t*-test). **** p<0.0001, ** p<0.01, * p<0.05, compared to untreated cells of the same genotype. #### p<0.0001, # p<0.05,

compared to TS/A cells treated with the same dose of PT-112. Symbols represents different cell clones with same genotype.

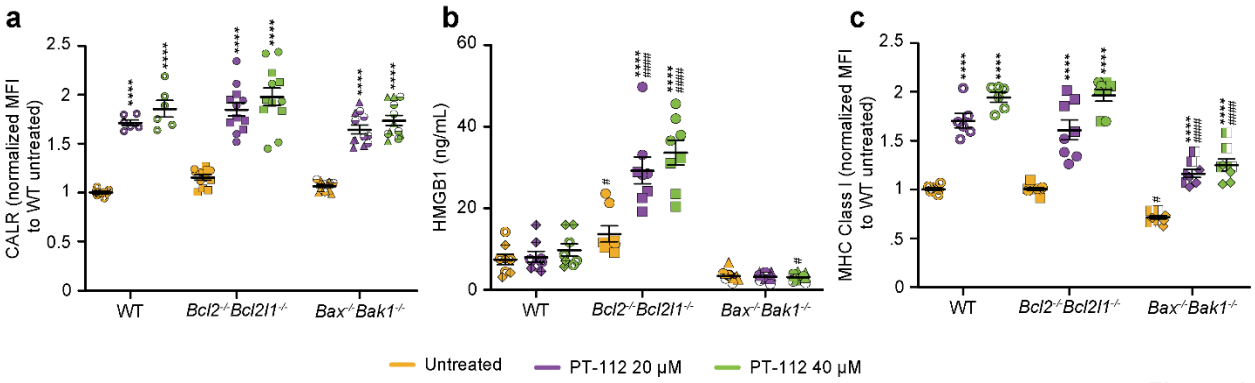

Figure 3

Figure 3. PT-112 elicits signals of ICD and increases MHC class I exposure. TS/A WT and genetically modified *Bcl2*$^{-/-}$*Bcl2l1*$^{-/-}$ and *Bax*$^{-/-}$*Bak*$^{-/-}$ cells were treated for 48 h with 20 µM or 40 µM PT-112. (**a**) Ecto-calreticulin levels (CALR) were analyzed by flow cytometry using specific labelled anti-CALR antibody. Results are represented as the MFI normalized to MFI of WT untreated cells. (**b**) HMGB1 amounts in the supernatant. (**c**) Levels of MHC class I cell-surface exposure were analyzed by flow cytometry using specific labelled anti-MHC-I antibody. Results are represented as the MFI normalized to MFI of WT untreated cells. Data shown corresponds to the mean ± SEM of 2 biological duplicates from 3 independent experiments. In **a**, **c**, zombie aqua positive cells (death cells) were excluded from the analysis. **** p<0.0001, compared to untreated cells of the same genotype. #### p<0.0001, ## p<0.01, compared to TS/A cells treated with the same dose of PT-112 (two-way ANOVA). Symbols represents different cell clones with same genotype.

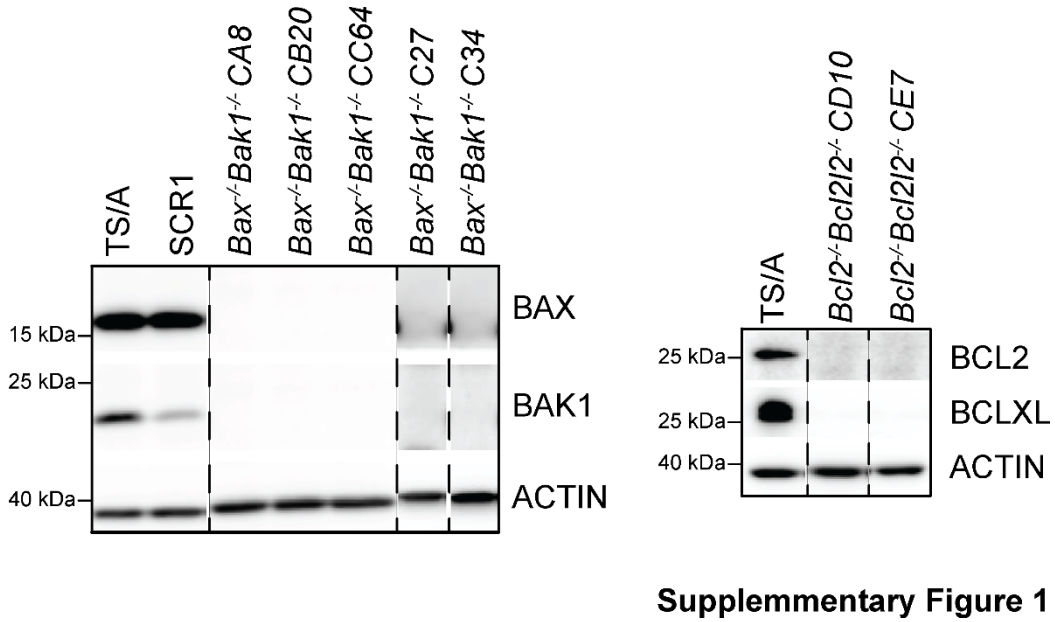

Supplemmentary Figure 1

Suppl. Fig. 1. Validation of *Bcl2*$^{-/-}$*Bcl2l1*$^{-/-}$ and *Bax*$^{-/-}$*Bak*$^{-/-}$ cell clones. Absence of BCL2, BCL2L1, BAX and BAK proteins in cell lysates from different clones was validated by Western blot technique.

References

Agesta, R. S., Moreno-Loshuertos, R., Marco-Brualla, J., Junquera, C., De Mena, R. M., Enríquez, J. A., Yim, C. Y., Price, M. R., Ames, T. D., Jimeno, J., & Anel, A. (2022). Characterization of differential metabolic phenotypes and PT-112-induced mitochondrial effects in human prostate cancer cells [Meeting Abstract]. European Journal of Cancer, 174, S39-S39. <Go to ISI>://WOS:000876973400096

Ames, T., Slusher, B., Wozniak, K., Takase, Y., Shimizu, H., Nishibata-Kobayashi, K., Kanada-Sonobe, R. M., Kerns, W., Fong, K. L., Pourquier, P., Gongora, C., Jimeno, J., & Chatterjee, D. (2016). Findings across pre-clinical models in the development of PT-112, a novel investigational platinum-pyrophosphate anti-cancer agent [Meeting Abstract]. European Journal of Cancer, 69, S153-S153. https://doi.org/10.1016/s0959-8049(16)33054-4

Bock, F. J., & Tait, S. W. G. (2020). Mitochondria as multifaceted regulators of cell death. Nat Rev Mol Cell Biol, 21(2), 85-100. https://doi.org/10.1038/s41580-019-0173-8

Bonora, M., Giorgi, C., & Pinton, P. (2022). Molecular mechanisms and consequences of mitochondrial permeability transition. Nat Rev Mol Cell Biol, 23(4), 266-285. https://doi.org/10.1038/s41580-021-00433-y

Bryce, A. H., Dronca, R. S., Costello, B. A., Aparicio, A., Subudhi, S. K., O'Donnell, J. F., Jimeno, J., Yim, C. Y., Ames, T. D., Price, M., & Karp, D. D. (2021). A phase 1b study of novel immunogenic cell death inducer PT-112 plus PD-L1 inhibitor avelumab in metastatic castrate-resistant prostate cancer (mCRPC) patients. Journal of Clinical Oncology, 39(15_suppl), e17025-e17025. https://doi.org/10.1200/JCO.2021.39.15_suppl.e17025

Bryce, A. H., Dronca, R. S., Costello, B. A., Aparicio, A., Subudhi, S. K., O'Donnell, J. F., Jimeno, J., Yim, C. Y., Ames, T. D., Price, M., & Karp, D. D. (2021). A phase 1b study of novel immunogenic cell death inducer PT-112 plus PD-L1 inhibitor avelumab in metastatic castrate-resistant prostate cancer (mCRPC) patients [Meeting Abstract]. Journal of Clinical Oncology, 39(15), 3. https://doi.org/10.1200/JCO.2021.39.15_suppl.e17025

Bryce, A. H., Dronca, R. S., Costello, B. A., Infante, J. R., Ames, T. D., Jimeno, J., & Karp, D. D. (2020). PT-112 in advanced metastatic castrate-resistant prostate cancer (mCRPC), as monotherapy or in combination with PD-L1 inhibitor avelumab: Findings from two phase I studies. Journal of Clinical Oncology, 38(6_suppl), 83-83. https://doi.org/10.1200/JCO.2020.38.6_suppl.83

De Giovanni, C., Nicoletti, G., Landuzzi, L., Palladini, A., Lollini, P. L., & Nanni, P. (2019). Bioprofiling TS/A Murine Mammary Cancer for a Functional Precision Experimental Model. Cancers (Basel), 11(12). https://doi.org/10.3390/cancers11121889

Fucikova, J., Kepp, O., Kasikova, L., Petroni, G., Yamazaki, T., Liu, P., Zhao, L., Spisek, R., Kroemer, G., & Galluzzi, L. (2020). Detection of immunogenic cell death and its relevance for cancer therapy. Cell Death & Disease, 11(11), 1013. https://doi.org/10.1038/s41419-020-03221-2

Fucikova, J., Spisek, R., Kroemer, G., & Galluzzi, L. (2021). Calreticulin and cancer. Cell Research, 31(1), 5-16. https://doi.org/10.1038/s41422-020-0383-9

Galluzzi, L., Aaronson, S. A., Abrams, J., Alnemri, E. S., Andrews, D. W., Baehrecke, E. H., Bazan, N. G., Blagosklonny, M. V., Blomgren, K., Borner, C., Bredesen, D. E., Brenner, C., Castedo, M., Cidlowski, J. A., Ciechanover, A., Cohen, G. M., De Laurenzi, V., De Maria, R., Deshmukh, M., . . . Kroemer, G. (2009). Guidelines for the use and interpretation of assays for monitoring cell death in higher eukaryotes. Cell Death Differ, 16(8), 1093-1107. https://doi.org/10.1038/cdd.2009.44

Galluzzi, L., Guilbaud, E., Schmidt, D., Kroemer, G., & Marincola, F. M. (2024). Targeting immunogenic cell stress and death for cancer therapy. Nat Rev Drug Discov, 23(6), 445-460. https://doi.org/10.1038/s41573-024-00920-9

Galluzzi, L., Yamazaki, T., & Kroemer, G. (2018). Linking cellular stress responses to systemic homeostasis. Nature Reviews Molecular Cell Biology, 19(11), 731-745. https://doi.org/10.1038/s41580-018-0068-0

Jhunjhunwala, S., Hammer, C., & Delamarre, L. (2021). Antigen presentation in cancer: insights into tumour immunogenicity and immune evasion. Nature Reviews Cancer, 21(5), 298-312. https://doi.org/10.1038/s41568-021-00339-z

Karp, D. D., Camidge, D. R., Infante, J. R., Ames, T. D., Price, M. R., Jimeno, J., & Bryce, A. H. (2022). Phase I study of PT-112, a novel pyrophosphate-platinum immunogenic cell death inducer, in advanced solid tumours. EClinicalMedicine, 49, 101430. https://doi.org/10.1016/j.eclinm.2022.101430

Kepp, O., Bezu, L., Yamazaki, T., Di Virgilio, F., Smyth, M. J., Kroemer, G., & Galluzzi, L. (2021). ATP and cancer immunosurveillance. Embo j, 40(13), e108130. https://doi.org/10.15252/embj.2021108130

Kroemer, G., Galassi, C., Zitvogel, L., & Galluzzi, L. (2022). Immunogenic cell stress and death. Nature Immunology, 23(4), 487-500. https://doi.org/10.1038/s41590-022-01132-2

Marchi, S., Guilbaud, E., Tait, S. W. G., Yamazaki, T., & Galluzzi, L. (2023). Mitochondrial control of inflammation. Nat Rev Immunol, 23(3), 159-173. https://doi.org/10.1038/s41577-022-00760-x

McAdams, M., Swift, S., Donahue, R. N., Celades, C., Tsai, Y. T., Bingham, M., Szabo, E., Zhao, C., Sansone, S., Choradia, N., Shelat, M., O'Donnell, J. F., Ames, T. D., Raphael, B., Steinberg, S. M., Gulley, J. L., Schlom, J., & Rajan, A. (2023). Preliminary efficacy, safety, and immunomodulatory effects of PT-112 from a phase 2 proof of concept study in patients (pts) with thymic epithelial tumors (TETs) [Meeting Abstract]. Journal of Clinical Oncology, 41(16), 1. <Go to ISI>://WOS:001053772004757

McArthur, K., Whitehead, L. W., Heddleston, J. M., Li, L., Padman, B. S., Oorschot, V., Geoghegan, N. D., Chappaz, S., Davidson, S., San Chin, H., Lane, R. M., Dramicanin, M., Saunders, T. L., Sugiana, C., Lessene, R., Osellame, L. D., Chew, T. L., Dewson, G., Lazarou, M., . . . Kile, B. T. (2018). BAK/BAX macropores facilitate mitochondrial herniation and mtDNA efflux during apoptosis. Science, 359(6378). https://doi.org/10.1126/science.aao6047

Pan, H., Liu, P., Zhao, L., Pan, Y., Mao, M., Kroemer, G., & Kepp, O. (2024). Immunogenic cell stress and death in the treatment of cancer. Semin Cell Dev Biol, 156, 11-21. https://doi.org/10.1016/j.semcdb.2023.10.007

Riley, J. S., Quarato, G., Cloix, C., Lopez, J., O'Prey, J., Pearson, M., Chapman, J., Sesaki, H., Carlin, L. M., Passos, J. F., Wheeler, A. P., Oberst, A., Ryan, K. M., & Tait, S. W. (2018). Mitochondrial inner membrane

permeabilisation enables mtDNA release during apoptosis. Embo j, 37(17). https://doi.org/10.15252/embj.201899238

Rodriguez-Ruiz, M. E., Buqué, A., Hensler, M., Chen, J., Bloy, N., Petroni, G., Sato, A., Yamazaki, T., Fucikova, J., & Galluzzi, L. (2019). Apoptotic caspases inhibit abscopal responses to radiation and identify a new prognostic biomarker for breast cancer patients. OncoImmunology, 8(11), e1655964. https://doi.org/10.1080/2162402x.2019.1655964

Rongvaux, A., Jackson, R., Harman, Christian C. D., Li, T., West, A. P., de Zoete, Marcel R., Wu, Y., Yordy, B., Lakhani, Saquib A., Kuan, C.-Y., Taniguchi, T., Shadel, Gerald S., Chen, Zhijian J., Iwasaki, A., & Flavell, Richard A. (2014). Apoptotic Caspases Prevent the Induction of Type I Interferons by Mitochondrial DNA. Cell, 159(7), 1563-1577. https://doi.org/https://doi.org/10.1016/j.cell.2014.11.037

Sato, A., Bloy, N., Galassi, C., Jiménez-Cortegana, C., Klapp, V., Aretz, A., Guilbaud, E., Yamazaki, T., Petroni, G., Galluzzi, L., & Buqué, A. (2022). Quantification of cytosolic DNA species by immunofluorescence microscopy and automated image analysis. Methods Cell Biol, 172, 115-134. https://doi.org/10.1016/bs.mcb.2022.05.004

Sato, A., Buque, A., Yamazaki, T., Bloy, N., Petroni, G., & Galluzzi, L. (2021). Immunofluorescence microscopy-based assessment of cytosolic DNA accumulation in mammalian cells. STAR protocols, 2(2), 100488. https://doi.org/10.1016/j.xpro.2021.100488

Serrano-Mendioroz, I., Garate-Soraluze, E., & Rodriguez-Ruiz, M. E. (2023). A simple method to assess clonogenic survival of irradiated cancer cells. Methods Cell Biol, 174, 127-136. https://doi.org/10.1016/bs.mcb.2022.08.002

Soler-Agesta, R., Ames, T. D., Price, M., Jimeno, J., Yim, C. Y., Moreno-Loshuertos, R., & Anel, A. (2022). PT-112 induces potent mitochondrial stress and immunogenic cell death in human prostate cancer cell lines [Meeting Abstract]. Cancer Research, 82(12), 2. <Go to ISI>://WOS:000892509505402

Soler-Agesta, R., Marco-Brualla, J., Minjárez-Sáenz, M., Yim, C. Y., Martínez-Júlvez, M., Price, M. R., Moreno-Loshuertos, R., Ames, T. D., Jimeno, J., & Anel, A. (2022). PT-112 Induces Mitochondrial Stress and Immunogenic Cell Death, Targeting Tumor Cells with Mitochondrial Deficiencies [Article]. Cancers, 14(16), 21, Article 3851. https://doi.org/10.3390/cancers14163851

Tait, S. W. G., & Green, D. R. (2010). Mitochondria and cell death: outer membrane permeabilization and beyond. Nature reviews. Molecular cell biology, 11(9), 621-632. https://doi.org/10.1038/nrm2952

Vitale, I., Pietrocola, F., Guilbaud, E., Aaronson, S. A., Abrams, J. M., Adam, D., Agostini, M., Agostinis, P., Alnemri, E. S., Altucci, L., Amelio, I., Andrews, D. W., Aqeilan, R. I., Arama, E., Baehrecke, E. H., Balachandran, S., Bano, D., Barlev, N. A., Bartek, J., . . . Galluzzi, L. (2023). Apoptotic cell death in disease—Current understanding of the NCCD 2023. Cell Death & Differentiation, 30(5), 1097-1154. https://doi.org/10.1038/s41418-023-01153-w

White, M. J., McArthur, K., Metcalf, D., Lane, R. M., Cambier, J. C., Herold, M. J., van Delft, M. F., Bedoui, S., Lessene, G., Ritchie, M. E., Huang, D. C., & Kile, B. T. (2014). Apoptotic caspases suppress mtDNA-induced STING-mediated type I IFN production. Cell, 159(7), 1549-1562. https://doi.org/10.1016/j.cell.2014.11.036

Yamazaki, T., Ames, T. D., & Galluzzi, L. (2019). Potent induction of immunogenic cell death by PT-112 [Meeting Abstract]. Cancer Immunology Research, 7(2), 2. https://doi.org/10.1158/2326-6074.Cricimteatiaacr18-b199

Yamazaki, T., Buqué, A., Ames, T. D., & Galluzzi, L. (2020). PT-112 induces immunogenic cell death and synergizes with immune checkpoint blockers in mouse tumor models. OncoImmunology, 9(1), 1721810. https://doi.org/10.1080/2162402x.2020.1721810

Yamazaki, T., & Galluzzi, L. (2020). Mitochondrial control of innate immune signaling by irradiated cancer cells. OncoImmunology, 9(1), 1797292. https://doi.org/10.1080/2162402x.2020.1797292

Yamazaki, T., Kirchmair, A., Sato, A., Buqué, A., Rybstein, M., Petroni, G., Bloy, N., Finotello, F., Stafford, L., Navarro Manzano, E., Ayala de la Peña, F., García-Martínez, E., Formenti, S. C., Trajanoski, Z., & Galluzzi, L. (2020). Mitochondrial DNA drives abscopal responses to radiation that are inhibited by autophagy. Nat Immunol, 21(10), 1160-1171. https://doi.org/10.1038/s41590-020-0751-0

Yamazaki, T., Kirchmair, A., Sato, A., Buqué, A., Rybstein, M., Petroni, G., Bloy, N., Finotello, F., Stafford, L., Navarro Manzano, E., Ayala de la Peña, F., García-Martínez, E., Formenti, S. C., Trajanoski, Z., & Galluzzi, L. (2020). Mitochondrial DNA drives abscopal responses to radiation that are inhibited by autophagy. Nature Immunology, 21(10), 1160-1171. https://doi.org/10.1038/s41590-020-0751-0

Yang, K., Halima, A., & Chan, T. A. (2023). Antigen presentation in cancer - mechanisms and clinical implications for immunotherapy. Nat Rev Clin Oncol, 20(9), 604-623. https://doi.org/10.1038/s41571-023-00789-4

Yim, C. Y., Congenie, M. T., Johnson, H. L., Mancini, M. G., Stossi, F., Mancini, M. A., Azofeifa, J., Price, M. R., Baeck, J., & Ames, T. D. (2023). PT-112, a novel immunogenic cell death inducer, causes ribosomal biogenesis inhibition and organelle stress in cancer cells [Meeting Abstract]. Molecular Cancer Therapeutics, 22(12), 2. https://doi.org/10.1158/1535-7163.Targ-23-c128

Yuda, J., Will, C., Phillips, D. C., Abraham, L., Alvey, C., Avigdor, A., Buck, W., Besenhofer, L., Boghaert, E., Cheng, D., Cojocari, D., Doyle, K., Hansen, T. M., Huang, K., Johnson, E. F., Judd, A. S., Judge, R. A., Kalvass, J. C., Kunzer, A., . . . Souers, A. J. (2023). Selective MCL-1 inhibitor ABBV-467 is efficacious in tumor models but is associated with cardiac troponin increases in patients. Commun Med (Lond), 3(1), 154. https://doi.org/10.1038/s43856-023-00380-z

GENERAL DISCUSSION

“Only those who attempt the absurd can achieve the impossible”

-Albert Einstein-

7.General discussion

PT-112 is a small platinum molecule conjugated to a pyrophosphate currently in clinical trials for solid tumors including mCRPC. From a structural point of view, PT-112 seems to be *unique* in its class as it contains a pyrophosphate moiety that attributes to it a marked affinity for bone tissue, something that the closest chemical analog oxaliplatin does not share. Accordingly, the initiation of this work was driven by the scientific premise that a chemotherapeutic platinum agent with a chemical structure such as PT-112 could establish novel intracellular interactions compared to their traditional platinum salts analogs. In part, PT-112 chemical nature appeals to a traditional bisphosphonate whose clinical administration is indicated to manage bone-related pathologies (Russell et al., 2008). For instance, heterocyclic nitrogen-containing bisphosphonates such as zoledronic acid are known to inhibit the enzyme farnesyl pyrophosphate synthase (FPPS) of the mevalonate pathway, preventing bone resorption by osteoclasts (Jahnke et al., 2010). In relation to this, Qiu and colleagues have reported the synthesis of a zoledronic acid-platinum complex $[Pt(en)]_2ZL$, that demonstrated anticancer effects on human gastric cancer cells SGC7901. This effect was mediated by preventing the prenylation of small G proteins, possibly through inhibition of the enzymes of the mevalonate pathway (Qiu et al., 2017).

Similarly, in this work we hypothesize that alterations in the nature of the ligands in platinum complexes such as the addition of the pyrophosphate moiety found in PT-112's chemical structure, could have profound implications for its primary mechanism of action, conferring it more affinity for other intracellular molecules rather than DNA, as it has been previously described (Bose et al., 2008; Bruno et al., 2017).

Oxaliplatin is the FDA-approved platinum compound with the closest chemical structure to PT-112. Indeed, oxaliplatin and PT-112 share a large part of their structures as both contain the diaminocyclohexane (DACH) carrier ligand, that is conjugated to an oxalate group in the case of oxaliplatin and replaced by an inorganic pyrophosphate in the case of PT-112. In line with this, one of the first *in vitro* works carried out with this compound demonstrated that both oxaliplatin and PT-112 display reduced affinity for DNA when compared with the platinum analog cisplatin (Corte-Rodríguez et al., 2015). According to the results obtained from that work, the measurement of platinum (Pt) incorporation in A549 cells exposed to cisplatin, oxaliplatin and PT-112 revealed that cells receiving oxaliplatin showed lower levels of Pt per gram of cell than cells treated with cisplatin, and below 1 µg per gram of cell in the case of PT-112 administration, which resulted to be the lowest amount of Pt measurement among all the treatments. Furthermore, DNA

samples extracted from A549 cells previously exposed to oxaliplatin showed around 40 % to 84 % less Pt accumulation compared to the ones treated with the same doses of cisplatin. Interestingly, in A549 cells, Pt levels found in DNA samples upon PT-112 exposure revealed to be close to the baseline. Similar experiments carried out with ovarian A2780 cancer cells have detected comparable and low amounts of Pt associated to DNA in samples treated with oxaliplatin or PT-112.

Pointing out the similarities evidenced between both compounds, recent data obtained from Yim and colleagues showed that PT-112 induces ribosome biogenesis stress (Christina Y. Yim et al., 2023), akin to what it has been described to induce oxaliplatin (Bruno et al., 2017). Despite some of the close characteristics observed, during the work carried out by Corte-Rodríguez in A2780 cells that have acquired resistance to cisplatin, they demonstrated that PT-112 seems not to be affected by the same resistance mechanism than cisplatin or oxaliplatin. This observation could be in line to what has been reported in the clinic, since a substantial number of patients resistant to oxaliplatin have shown clinical benefits after PT-112 administration (Karp et al., 2022).

Regarding the data obtained in this doctoral Thesis, the transmitochondrial cybrid generation tool that has been improved in part by our research group (Marco-Brualla et al., 2019; Soler-Agesta et al., 2023), made possible to demonstrate for the first time that PT-112 is especially cytotoxic in cells harboring mitochondrial DNA mutations (L929dt and $L929^{dt}$ cybrid cells) while cancer cells with an intact OXPHOS pathway (L929 and dt^{L929} cybrid cells) were not sensitive to cell death at the doses tested, although cell growth was affected. Certainly, the technique employed to generate $L929^{dt}$ and dt^{L929} cybrid cells was fundamental for the validation of our initial working hypothesis which postulated that PT-112 mechanism of action would involve mitochondrial/metabolic pathways. Furthermore, PT-112's selectivity towards cells with mtDNA mutations was also corroborated by demonstrating that the same cellular system treated with the same dose of cisplatin did not display signs of this selectivity (Soler-Agesta, Marco-Brualla, et al., 2022a).

Regarding the study on the type of cell death induced by PT-112, the first results obtained in the L929dt cellular system suggested that PT-112 does not induce apoptosis but show hints of necrotic cell death. These findings were in part supported by the experiments combining the pan caspase inhibitor Z-VAD-fmk and PT-112. While PT-112 seems to activate CASP3 at the same time as cell death is taking place, the general caspase inhibitor Z-VAD-fmk were not able to prevent PT-112-induced cell death in this cellular system, alone or in combination with the necroptosis inhibitor necrostatin-1. Opposed to this, the results obtained in human prostate cancer cells DU-145 and LNCap-C4 demonstrated that Z-VAD-fmk is able to block most of cell death induced by the drug, supporting the idea that PT-112 is in fact able to induce

apoptosis. The contradiction between the results obtained between these two cellular systems could be explained by the fact that L929 system lacks CASP8, with tumor necrosis-α inducing rather necroptosis and not apoptosis, especially when caspases are inhibited (Vercammen, Beyaert, et al., 1998). In line with this concept, experiments performed with the model of adenocarcinoma TS/A demonstrated that the absence of BAK1 and BAX proteins protected TS/A cells from PT-112-induced cell death, at least the first 72h of incubation, confirming that the main mechanism by which PT-112 induces cell death is through the activation of the mitochondrial apoptosis pathway mediated by BAK1/BAX oligomerization. Supporting this idea, CASP3, the main effector of apoptosis, has been shown to be activated by PT-112 in all the models employed in this work.

Moreover, data obtained in human prostate cell lines showed that PT-112 displays cancer cell cytotoxicity across different prostate cancer cell lines -exhibiting variations in mitochondrial features and mutational status- but not in non-tumorigenic prostate cells, at least, at the doses tested. This selectivity may explain PT-112's general safety and tolerability observed in clinical studies (Imbimbo et al., 2022; Karp et al., 2022; Kourelis et al., 2020; Meredith McAdams et al., 2023). It is interesting to note that PT-112 was active in cells widely differing in their genotype, suggesting broad clinical application in prostate cancer, especially the late-line setting where the disease is highly heterogeneous (Buck et al., 2021; Galletti et al., 2017; Hwang, 2012; Tang, 2022).

In line with the first experiments performed in the murine model L929dt with PT-112, the observed differences in PT-112 sensitivity based on the metabolic and mitochondrial mutational status compelled us to investigate the possibility that PT-112 mechanism of action could involve mitochondrial pathways. Undoubtedly, the results obtained described for the first time that PT-112 induces severe mitochondrial stress by increasing the production of mitochondrial ROS, disturbing the mitochondrial membrane potential, and increasing the mitochondrial mass. Particularly, mitochondrial ROS production was noticeable in all cell models used in this work and appeared to be more pronounced in cells that were more sensitive to PT-112-induced cell death. Moreover, mitochondrial mass measurements revealed an increase of the mitochondrial mass after PT-112 exposure, that were higher in the case of sensitive cells and less marked in cells resistant to PT-112 such as observed in TS/A BAK1/BAX KO cells. Furthermore, the measurement of the functionality and OXPHOS activity in human prostate cancer cells after PT-112 exposure suggests that PT-112 alters the functioning of the electron transport chain by modulating the association and activity of respiratory complexes and supercomplexes. In fact, it has been reported that PT-112 increases the complex III-combined activities (II+III and I+III) and the assembly of CIII-containing

supercomplexes, revealing that PT-112 is forcing the OXPHOS machinery and increasing the electron flux. As it has been discussed, our data indicate that PT-112 mainly induces cell death through the BAK1 and BAX-dependent mitochondrial apoptotic pathway which is known to be linked to the release of cytochrome c and subsequent caspase activation. In this scenario, it seems plausible that the release of cytochrome c during the initiation of the intrinsic apoptotic pathway could be one of the reasons for the increase of mitochondrial ROS production observed, which is especially elevated in cells with mitochondrial dysfunctions. Certainly, the absence of cytochrome c during the dismantling of mitochondria associated to cell death process would cause an interruption in the electron flux from complex III to complex IV. Since it has been demonstrated that PT-112 increases the activity of complex III containing supercomplexes, the release of cytochrome c would cause the accumulation of free electrons into the intermembrane space being more prone to react with oxygen, generating free radicals and pushing the system to produce excessive ROS. In addition, Seahorse measurements in human prostate cancer LNCap-C4 cells exposed to PT-112 for 24h indicated a reduction in oxygen consumption rate as well as a decrease in oxygen consumption directly linked to ATP production. These results point to a possible dysfunction of the electron transport chain that would plausibly explain the rearrangement of the respiratory supercomplexes in order to maximize the respiration function when mitochondrial damage is happening.

Due to the mitochondrial effects observed as well as the chemical similarities between PT-112 and nitrogen-bisphosphonates described above, it was raised the possibility that PT-112 could be affecting the activity of enzymes of the mevalonate pathway. In this connection, we analyzed mitochondrial coenzyme Q10 (CoQ_{10}) levels whose chemical precursors are generated in different steps of the mevalonate pathway. Preliminary results showed a reduction of CoQ_{10} upon PT-112 treatment in L929 parental cells while in L929dt cells basal CoQ_{10} levels were undetectable and no effect of PT-112 could be observed. These data did not demonstrate the implication of a reduction in CoQ_{10} in PT-112-induce cell death, since only L929dt, but no L929 cells, were sensitive to cell death induced by this agent. Subsequent experiments carried out with human DU-145 cells, sensitive to PT-112-induced cell death, demonstrated that in fact PT-112 stimulates the production of CoQ_{10} (data not shown), in agreement with the observed increase in mitochondrial mass, as previously discussed.

Regarding the contribution of mitochondrial ROS in the cell death process induced by PT-112, in this work it has been demonstrated that L929 cells devoid of mtDNA -known as rho cero (ρ^0) cells- that are unable to generate mtROS (Catalán et al., 2015) due to their inability to perform OXPHOS, display a reduced sensitivity to cell growth inhibition induced by PT-112 when compared with the parental L929 cell line.

These results reinforced the significance of this biochemical event during PT-112-induced cell death process and the special relevance of the presence of defective mitochondria able to generate ROS upon stress. According with the mitochondrial aspects that seem to be involved in PT-112 mechanism of action, images taken with the transmission electron microscope (TEM) clearly show a process of mitochondrial damage taking place in prostate cancer DU-145 cells that were exposed to PT-112 at different times. Interestingly, PT-112 appears to induce changes in the morphology, number of cristae and size of the mitochondria even at early incubation time points. In addition, treated cells showed an increase in the complexity of their cytoplasm as indicated by the formation of numerous vacuoles containing organelles and membranes in process of degradation. Moreover, in most of the TEM samples analyzed, vacuoles were detected at the vicinity of damaged mitochondria, some of them already enclosed in the vesicles for its subsequent digestion. Accordingly, it has been demonstrated that PT-112 induces signs of autophagy activation. Despite in this work it has not been specifically analyzed mitophagy, TEM images would suggest that mitophagy would be taking place. Altogether, data seems to indicate that damaging mitochondria by an excessive ROS production could lead to the activation of the autophagy machinery to promote damaged organelle clearance. Accordingly, increase in mitochondrial biogenesis and autophagy activation could be interpreted as a pro-survival mechanism put in place for cancer cells to cope with mitochondrial damage induced by PT-112.

Furthermore, the activation of autophagy observed could be also directly linked with PT-112's ability to induce immunogenic cell death (ICD; (Michaud et al., 2011). According to previous studies, autophagic processes are known to be associated with immunogenic signals and the release of damage-associated molecular patterns (DAMPs) (Oliver Kepp & Guido Kroemer, 2020). In line with this conceptual approach, previous work has demonstrated that PT-112 induces HMGB1 release, ATP secretion and CALR exposure (T. Yamazaki, A. Buqué, et al., 2020). Accordingly, in the present work we corroborated that PT-112 induces ATP secretion and CALR exposure in all the cell models employed as well as the release of HMGB1 in TS/A cells lines. Overall, this data suggests that while varying cancer cell types, the ability of PT-112 to promote ICD remains consistent and comes across a universal feature of PT-112's mechanism of action.

Over the last years, more and more works have started documenting the connection between mitochondria, ICD, and the activation of the immune system (Marchi et al., 2023; Vringer & Tait, 2023). In line with this, the results obtained in the TS/A cell model showed that PT-112 increases the amount of cytosolic dsDNA in WT and TS/A BCL2/BCLXL KO cells, a feature that was substantially prevented in TS/A

BAK1/BAX KO cells, suggesting that it would be mostly from mitochondrial origin. According to the capacity of dsDNA in the cytosol to stimulate type I IFN secretion mediated by the cGAS/STING pathway (Yamazaki & Galluzzi, 2020), we showed that PT-112 increases type I IFN secretion in all cells included in the TS/A cell model, following a similar tendency as cytosolic dsDNA quantification. Despite lacking data from TS/A ρ^0 cells, all the results presented point to mitochondria as a relevant component intervening in PT-112's capacity to induce antitumor immune responses.

Interestingly, we show for the first time in this work the ability of PT-112 to increase MHC class I (MHC-I) expression in the surface of TS/A cells, an increase that was similar in WT and BCL2/BCLXL KO cells but less pronounced in BAK1/BAX KO cells. These results clearly indicate PT-112's capacity to modulate the anti-tumor immune response. Accordingly, MHC-I surface expression is known to be regulated by the autocrine type I IFN secretion observed along the treatment. In addition, in several works MHC-I expression has also been described to be modulated by the mitochondrial electron transport chain (Catalán et al., 2015; Mangalhara et al., 2023). This could connect the mitochondrial damage induced by PT-112 with the increase in MHC-I expression detected. Yet, further experiments need to be done to validate this hypothesis.

Given the link between ICD and mitochondria reported in the literature, on one hand, it is plausible that the effects observed in PT-112-treated cells may directly contribute to the anticancer immune responses observed in the clinic (Karp et al., 2022). For example, upon mitochondrial stress and damage, mitochondria have been shown to promote not only mtROS generation but also the release of ICD-associated DAMPs (Gupta et al., 2021; Vringer & Tait, 2023).

On the other hand, based on the evidence of the capacity of PT-112 to induce caspase activation and ICD, it raises an intriguing question of how these events can be observed simultaneously. Certainly, caspase-dependent apoptosis has been described to be an immunologically silent event (A. Rongvaux et al., 2014; White et al., 2014). Nevertheless, the role of caspases in this context is still a matter of debate. There is emerging evidence that caspase activation neither precludes ICD nor contradicts evidence of anticancer immunity (Serrano-Del Valle et al., 2019). Indeed, it has been described that apoptosis induced by specific agents is also associated with DAMPs release and ICD induction (Martins et al., 2014a).

Overall, this work reinforces the ability of PT-112 to induce organelle stress, in line with the recent finding that demonstrates that PT-112 causes ribosome biogenesis inhibition and nucleolar stress *in vitro* (Christina Y. Yim et al., 2023). Positively, these events have been reported to contribute to downstream

mitochondrial stress. During nucleolar stress, nucleolar proteins such as NPM1 can translocate to the nucleoplasm and interact with mitochondrial proteins, causing mitochondrial stress and release of mitochondrial DNA (mtDNA) into the cytosol (Kwon & Bakhoum, 2020; Mackenzie et al., 2017), as it has been evidenced in this work for PT-112. In addition, disrupted ribosome biogenesis has also been shown to upregulate autophagy (Pfister, 2019) which is linked to ICD, as described above. Moreover, this disruption could explain in part PT-112's selectivity for highly proliferative cancer cells since having an increased demand of protein synthesis, they would potentially be more sensitive to ribosome biogenesis disruption by PT-112.

Altogether, PT-112 appears to be a promising small molecule for cancer treatment with very unique characteristics not only in its mechanism of action but also for being the first platinum compound in clinical stage showing bone affinity. The data provided by this work add new insights into mitochondrial stress and ICD in response to PT-112 and how these effects can culminate in anticancer immunity. Over the course of this Doctoral Thesis it has been demonstrated PT-112's broad preclinical anticancer effects as well as its ability to induce ICD and mitochondrial stress, especially relevant in human prostate cancer cells, in line with clinical evidence of PT-112 activity observed in mCRPC patients (Alan Haruo Bryce et al., 2021; Bryce et al., 2020). All the data obtained about PT-112 immunogenicity could in part explain previous observation of durable clinical responses (Karp et al., 2022). However, more work is needed to characterize and identify key components involved in PT-112-induced mitochondrial stress and exploring connections with ICD and ribosome biogenesis inhibition.

CONCLUSIONS/CONCLUSIONES

"The toughest climbs will let you to the best views"

-Vanessa Gendoma-

8.1 Conclusions

The results obtained in this work have allowed us to reach the following conclusions:

1. The mitochondrial status of cancer cells appears to be relevant in the mechanism of action of PT-112 as it is observed to selectively induce cell death in cancer cells with mitochondrial dysfunctions.
2. PT-112 shows selectivity for cancer cells at clinically relevant doses. This was demonstrated by the ability of PT-112 to cause growth inhibition and cell death in human prostate cancer cells without affecting non-tumorigenic epithelial prostate cells at the doses tested.
3. PT-112 induces mitochondrial apoptosis dependent of BAK1 and BAX and CASP3 activation with the exception of the L929dt model which display a rather necrotic cell death phenotype.
4. PT-112 induces mitochondrial stress in cancer cells, as evidenced by an increase of mtROS generation, disruptions in mitochondrial membrane potential and increase in mitochondrial mass.
5. PT-112 induces mitochondrial damage and reorganization of the ETC as observed by a decrease in the oxygen consumption rate, changes in the activity and reorganization of the respiratory supercomplexes as well as deleterious effects in mitochondrial morphology.
6. PT-112 increases the amount of cytosolic dsDNA which is partially dependent on BAK1 and BAX expression.
7. PT-112 stimulates de production of type I IFN which is in part regulated by BAK1 and BAX expression.
8. PT-112 displays the capacity to modulate immune responses as it has been observed to increase the expression of MHC-I molecules on the surface of cancer cells, as well as the release of DAMPs such as ATP, HMGB1 or CALR exposure.
9. PT-112 activates autophagy which can be related to the hints of immunogenic cell death observed.

8.2 Conclusiones

Los resultados obtenidos en este trabajo nos han permitido llegar a las siguientes conclusiones:

1. El estado mitocondrial de las células cancerosas parece ser relevante en el mecanismo de acción de PT-112, ya que se ha observado que dicha droga induce selectivamente la muerte en células con disfunciones mitocondriales.
2. PT-112 muestra cierta selectividad por las células tumorales a dosis que son clínicamente relevantes. Esto se demostró a través de la capacidad de PT-112 para inhibir el crecimiento e inducir muerte en células de cáncer de próstata humano sin afectar a las células epiteliales no tumorales RWPE-1, al menos a las dosis ensayadas.
3. PT-112 induce apoptosis mitocondrial dependiente de BAK1 y BAX mediante la activación de la CASP3, exceptuando en el modelo celular L929dt, que en su lugar muestra un fenotipo de muerte similar al necrótico.
4. PT-112 induce estrés mitocondrial en las células tumorales asociado a un aumento en la producción de ROS mitocondriales, alteraciones en el potencial de membrana mitocondrial, así como en el aumento de la masa mitocondrial.
5. PT-112 induce daño mitocondrial y promueve la reorganización de la cadena de transporte electrónico tal y como sugiere la disminución en el consumo de oxígeno, el cambio en la actividad y ensamblaje de los supercomplejos respiratorios, así como los cambios patogénicos asociados a la morfología mitocondrial.
6. PT-112 incrementa la cantidad de ADN de doble hebra en el citosol, cuya acumulación es parcialmente dependiente de la expresión de BAK1 y BAX.
7. PT-112 estimula la producción de interferón de tipo I que está parcialmente regulada por la expresión de BAK1 y BAX.
8. PT-112 tendría la capacidad de modular la respuesta inmune a través del aumento de la expresión de moléculas MHC-I en la superficie de las células cancerosas, así por el aumento en la liberación de patrones moleculares asociados a daño como son la liberación de ATP, la secreción de HMGB1 y la exposición de calreticulina.
9. PT-112 activa la autofagia la cual podría estar relacionada con los signos relacionados con la muerte celular inmunogénica detectados.

BIBLIOGRAPHY

“Think before you speak. Read before you think”

-Franz Lebowitz-

9.Bibliography

Acín-Pérez, R., Fernández-Silva, P., Peleato, M. L., Pérez-Martos, A., & Enriquez, J. A. (2008). Respiratory Active Mitochondrial Supercomplexes. *Molecular Cell*, *32*(4), 529-539. https://doi.org/https://doi.org/10.1016/j.molcel.2008.10.021

Adams, K. L., & Palmer, J. D. (2003). Evolution of mitochondrial gene content: gene loss and transfer to the nucleus. *Mol Phylogenet Evol*, *29*(3), 380-395. https://doi.org/10.1016/s1055-7903(03)00194-5

Agalliu, I., Gern, R., Leanza, S., & Burk, R. D. (2009). Associations of high-grade prostate cancer with BRCA1 and BRCA2 founder mutations. *Clin Cancer Res*, *15*(3), 1112-1120. https://doi.org/10.1158/1078-0432.Ccr-08-1822

Agesta, R. S., Moreno-Loshuertos, R., Marco-Brualla, J., Junquera, C., De Mena, R. M., Enríquez, J. A., Yim, C. Y., Price, M. R., Ames, T. D., Jimeno, J., & Anel, A. (2022). Characterization of differential metabolic phenotypes and PT-112-induced mitochondrial effects in human prostate cancer cells [Meeting Abstract]. *European Journal of Cancer*, *174*, S39-S39. <Go to ISI>://WOS:000876973400096

Ahmadi, E., Wang, S., Gouran-Savadkoohi, M., Douvi, G., Isfahanian, N., Tsakiridis, N., Faught, B. E., Cutz, J. C., Sur, M., Chawla, S., Pond, G. R., Steinberg, G. R., Brown, I., & Tsakiridis, T. (2023). Prostate-Specific Membrane Antigen (PSMA) Expression Predicts Need for Early Treatment in Prostate Cancer Patients Managed with Active Surveillance. *Int J Mol Sci*, *24*(22). https://doi.org/10.3390/ijms242216022

Ahn, C. S., & Metallo, C. M. (2015). Mitochondria as biosynthetic factories for cancer proliferation. *Cancer Metab*, *3*(1), 1. https://doi.org/10.1186/s40170-015-0128-2

Ahn, J., Xia, T., Konno, H., Konno, K., Ruiz, P., & Barber, G. N. (2014). Inflammation-driven carcinogenesis is mediated through STING. *Nature Communications*, *5*(1), 5166. https://doi.org/10.1038/ncomms6166

Allende-Vega, N., Marco Brualla, J., Falvo, P., Alexia, C., Constantinides, M., de Maudave, A. F., Coenon, L., Gitenay, D., Mitola, G., Massa, P., Orecchioni, S., Bertolini, F., Marzo, I., Anel, A., & Villalba, M. (2022). Metformin sensitizes leukemic cells to cytotoxic lymphocytes by increasing expression of intercellular adhesion molecule-1 (ICAM-1). *Sci Rep*, *12*(1), 1341. https://doi.org/10.1038/s41598-022-05470-x

Almuradova, E., Seyyar, M., Arak, H., Tamer, F., Kefeli, U., Koca, S., Sen, E., Telli, T. A., Karatas, F., Gokmen, I., Turhal, N. S., Sakalar, T., Ayhan, M., Ekinci, F., Hafizoglu, E., Kahraman, S., Kesen, O., Unal, C., Alan, O., . . . Gokmen, E. (2024). The real-world outcomes of Lutetium-177 PSMA-617 radioligand therapy in metastatic castration-resistant prostate cancer: Turkish Oncology Group multicenter study. *Int J Cancer*, *154*(4), 692-700. https://doi.org/10.1002/ijc.34749

Alur, M., Nguyen, M. M., Eggener, S. E., Jiang, F., Dadras, S. S., Stern, J., Kimm, S., Roehl, K., Kozlowski, J., Pins, M., Michalak, M., Dhir, R., & Wang, Z. (2009). Suppressive roles of calreticulin in prostate cancer growth and metastasis. *Am J Pathol*, *175*(2), 882-890. https://doi.org/10.2353/ajpath.2009.080417

American Cancer Society. (2024). *What Is Prostate Cancer?* Retrieved April 28, 2024 from https://www.cancer.org/cancer/types/prostate-cancer/about/what-is-prostate-cancer.html

Ames, T., Slusher, B., Wozniak, K., Takase, Y., Shimizu, H., Nishibata-Kobayashi, K., Kanada-Sonobe, R. M., Kerns, W., Fong, K. L., Pourquier, P., Gongora, C., Jimeno, J., & Chatterjee, D. (2016). Findings across pre-clinical models in the development of PT-112, a novel investigational platinum-

pyrophosphate anti-cancer agent [Meeting Abstract]. *European Journal of Cancer*, *69*, S153-S153. https://doi.org/10.1016/s0959-8049(16)33054-4

Ames, T. D., Sharik, M. E., Rather, G. M., Hochart, G., Bonnel, D., Linehan, S., Stauber, J., Wing, R. A., Jimeno, J. J., Medina, D., Bertino, J. R., Chesi, M., & Bergsagel, P. L. (2017). Translational Research of PT-112, a Clinical Agent in Advanced Phase I Development: Evident Bone Tropism, Synergy In Vitro with Bortezomib and Lenalidomide , and Potent Efficacy in the Vk*MYC Mouse Model of Multiple Myeloma. *Blood*, *130*, 1797. https://doi.org/https://doi.org/10.1182/blood.V130.Suppl_1.1797.1797

Anderson, S., Bankier, A. T., Barrell, B. G., de Bruijn, M. H., Coulson, A. R., Drouin, J., Eperon, I. C., Nierlich, D. P., Roe, B. A., Sanger, F., Schreier, P. H., Smith, A. J., Staden, R., & Young, I. G. (1981). Sequence and organization of the human mitochondrial genome. *Nature*, *290*(5806), 457-465. https://doi.org/10.1038/290457a0

André, F., Ciruelos, E., Rubovszky, G., Campone, M., Loibl, S., Rugo, H. S., Iwata, H., Conte, P., Mayer, I. A., Kaufman, B., Yamashita, T., Lu, Y.-S., Inoue, K., Takahashi, M., Pápai, Z., Longin, A.-S., Mills, D., Wilke, C., Hirawat, S., & Juric, D. (2019). Alpelisib for PIK3CA-Mutated, Hormone Receptor–Positive Advanced Breast Cancer. *New England Journal of Medicine*, *380*(20), 1929-1940. https://doi.org/doi:10.1056/NEJMoa1813904

Andrews, P. A., & Albright, K. D. (1992). Mitochondrial defects in cis-diamminedichloroplatinum(II)-resistant human ovarian carcinoma cells. *Cancer Res*, *52*(7), 1895-1901.

Andrews, R. M., Kubacka, I., Chinnery, P. F., Lightowlers, R. N., Turnbull, D. M., & Howell, N. (1999). Reanalysis and revision of the Cambridge reference sequence for human mitochondrial DNA. *Nature Genetics*, *23*(2), 147-147. https://doi.org/10.1038/13779

Anel, A., Martínez-Lorenzo, M. J., Schmitt-Verhulst, A. M., & Boyer, C. (1997). Influence on CD8 of TCR/CD3-generated signals in CTL clones and CTL precursor cells. *J Immunol*, *158*(1), 19-28.

Apostolova, P., & Pearce, E. L. (2022). Lactic acid and lactate: revisiting the physiological roles in the tumor microenvironment. *Trends Immunol*, *43*(12), 969-977. https://doi.org/10.1016/j.it.2022.10.005

Apps, M. G., Choi, E. H. Y., & Wheate, N. J. (2015). The state-of-play and future of platinum drugs. *Endocrine-Related Cancer*, *22*(4), R219-R233. https://doi.org/10.1530/erc-15-0237

Araki, K., & Miyoshi, Y. (2018). Mechanism of resistance to endocrine therapy in breast cancer: the important role of PI3K/Akt/mTOR in estrogen receptor-positive, HER2-negative breast cancer. *Breast Cancer*, *25*(4), 392-401. https://doi.org/10.1007/s12282-017-0812-x

Arnold, R. S., Sun, C. Q., Richards, J. C., Grigoriev, G., Coleman, I. M., Nelson, P. S., Hsieh, C. L., Lee, J. K., Xu, Z., Rogatko, A., Osunkoya, A. O., Zayzafoon, M., Chung, L., & Petros, J. A. (2009). Mitochondrial DNA mutation stimulates prostate cancer growth in bone stromal environment. *Prostate*, *69*(1), 1-11. https://doi.org/10.1002/pros.20854

Attard, G., Parker, C., Eeles, R. A., Schröder, F., Tomlins, S. A., Tannock, I., Drake, C. G., & de Bono, J. S. (2016). Prostate cancer. *The Lancet*, *387*(10013), 70-82. https://doi.org/https://doi.org/10.1016/S0140-6736(14)61947-4

Au-Yeung, S. C. F., Pang, P. S. K., & Ho, Y.-p. (2006). Innovative platinum derived anticancer agents – risk or opportunity? *Nature Reviews Drug Discovery*, *5*(9), 800-800. https://doi.org/10.1038/nrd1691-c1

Bacman, S. R., Nissanka, N., & Moraes, C. T. (2020). Chapter 18 - Cybrid technology. In L. A. Pon & E. A. Schon (Eds.), *Methods in Cell Biology* (Vol. 155, pp. 415-439). Academic Press. https://doi.org/https://doi.org/10.1016/bs.mcb.2019.11.025

Bader, D. A., & McGuire, S. E. (2020). Tumour metabolism and its unique properties in prostate adenocarcinoma. *Nature Reviews Urology*, *17*(4), 214-231. https://doi.org/10.1038/s41585-020-0288-x

Bagnoli, M., Canevari, S., & Mezzanzanica, D. (2010). Cellular FLICE-inhibitory protein (c-FLIP) signalling: a key regulator of receptor-mediated apoptosis in physiologic context and in cancer. *Int J Biochem Cell Biol*, *42*(2), 210-213. https://doi.org/10.1016/j.biocel.2009.11.015

Bakhoum, S. F., Ngo, B., Laughney, A. M., Cavallo, J.-A., Murphy, C. J., Ly, P., Shah, P., Sriram, R. K., Watkins, T. B. K., Taunk, N. K., Duran, M., Pauli, C., Shaw, C., Chadalavada, K., Rajasekhar, V. K., Genovese, G., Venkatesan, S., Birkbak, N. J., McGranahan, N., . . . Cantley, L. C. (2018). Chromosomal instability drives metastasis through a cytosolic DNA response. *Nature*, *553*(7689), 467-472. https://doi.org/10.1038/nature25432

Bakhoum, S. F., Ngo, B., Laughney, A. M., Cavallo, J. A., Murphy, C. J., Ly, P., Shah, P., Sriram, R. K., Watkins, T. B. K., Taunk, N. K., Duran, M., Pauli, C., Shaw, C., Chadalavada, K., Rajasekhar, V. K., Genovese, G., Venkatesan, S., Birkbak, N. J., McGranahan, N., . . . Cantley, L. C. (2018). Chromosomal instability drives metastasis through a cytosolic DNA response. *Nature*, *553*(7689), 467-472. https://doi.org/10.1038/nature25432

Bao, X., Zhang, J., Huang, G., Yan, J., Xu, C., Dou, Z., Sun, C., & Zhang, H. (2021). The crosstalk between HIFs and mitochondrial dysfunctions in cancer development. *Cell Death & Disease*, *12*(2), 215. https://doi.org/10.1038/s41419-021-03505-1

Baracco, E. E., Petrazzuolo, A., & Kroemer, G. (2019). Chapter Five - Assessment of annexin A1 release during immunogenic cell death. In L. Galluzzi & N.-P. Rudqvist (Eds.), *Methods in Enzymology* (Vol. 629, pp. 71-79). Academic Press. https://doi.org/https://doi.org/10.1016/bs.mie.2019.06.010

Barron, E. S., & Huggins, C. (1946). The metabolism of the prostate; transamination and citric acid. *J Urol*, *55*, 385-390. https://doi.org/10.1016/s0022-5347(17)69926-9

Bedoui, S., Herold, M. J., & Strasser, A. (2020). Emerging connectivity of programmed cell death pathways and its physiological implications. *Nature Reviews Molecular Cell Biology*, *21*(11), 678-695. https://doi.org/10.1038/s41580-020-0270-8

Bezu, L., Sauvat, A., Humeau, J., Gomes-da-Silva, L. C., Iribarren, K., Forveille, S., Garcia, P., Zhao, L., Liu, P., Zitvogel, L., Senovilla, L., Kepp, O., & Kroemer, G. (2018). eIF2α phosphorylation is pathognomonic for immunogenic cell death. *Cell Death Differ*, *25*(8), 1375-1393. https://doi.org/10.1038/s41418-017-0044-9

Bhutia, S. K., Mukhopadhyay, S., Sinha, N., Das, D. N., Panda, P. K., Patra, S. K., Maiti, T. K., Mandal, M., Dent, P., Wang, X. Y., Das, S. K., Sarkar, D., & Fisher, P. B. (2013). Autophagy: cancer's friend or foe? *Adv Cancer Res*, *118*, 61-95. https://doi.org/10.1016/b978-0-12-407173-5.00003-0

Birch-Machin, M. A., & Turnbull, D. M. (2001). Assaying mitochondrial respiratory complex activity in mitochondria isolated from human cells and tissues. *Methods Cell Biol*, *65*, 97-117. https://doi.org/10.1016/s0091-679x(01)65006-4

Birner, P., Schindl, M., Obermair, A., Plank, C., Breitenecker, G., & Oberhuber, G. (2000). Overexpression of hypoxia-inducible factor 1alpha is a marker for an unfavorable prognosis in early-stage invasive cervical cancer. *Cancer Res*, *60*(17), 4693-4696.

Blachère, N. E., Darnell, R. B., & Albert, M. L. (2005). Apoptotic cells deliver processed antigen to dendritic cells for cross-presentation. *PLoS Biol*, *3*(6), e185. https://doi.org/10.1371/journal.pbio.0030185

Blasco, M. A. (2005). Telomeres and human disease: ageing, cancer and beyond. *Nature Reviews Genetics*, *6*(8), 611-622. https://doi.org/10.1038/nrg1656

BOATRIGHT, Kelly M., DEIS, C., DENAULT, J.-B., SUTHERLIN, Daniel P., & SALVESEN, Guy S. (2004). Activation of caspases-8 and -10 by FLIPL. *Biochemical Journal*, *382*(2), 651-657. https://doi.org/10.1042/bj20040809

Bock, F. J., & Tait, S. W. G. (2020). Mitochondria as multifaceted regulators of cell death. *Nat Rev Mol Cell Biol*, *21*(2), 85-100. https://doi.org/10.1038/s41580-019-0173-8

Bonaldi, T., Talamo, F., Scaffidi, P., Ferrera, D., Porto, A., Bachi, A., Rubartelli, A., Agresti, A., & Bianchi, M. E. (2003). Monocytic cells hyperacetylate chromatin protein HMGB1 to redirect it towards secretion. *Embo j*, *22*(20), 5551-5560. https://doi.org/10.1093/emboj/cdg516

Bonora, M., Giorgi, C., & Pinton, P. (2022). Molecular mechanisms and consequences of mitochondrial permeability transition. *Nat Rev Mol Cell Biol*, *23*(4), 266-285. https://doi.org/10.1038/s41580-021-00433-y

Bonora, M., Wieckowski, M. R., Sinclair, D. A., Kroemer, G., Pinton, P., & Galluzzi, L. (2019). Targeting mitochondria for cardiovascular disorders: therapeutic potential and obstacles. *Nature Reviews Cardiology*, *16*(1), 33-55. https://doi.org/10.1038/s41569-018-0074-0

Bos, R., van der Groep, P., Greijer, A. E., Shvarts, A., Meijer, S., Pinedo, H. M., Semenza, G. L., van Diest, P. J., & van der Wall, E. (2003). Levels of hypoxia-inducible factor-1alpha independently predict prognosis in patients with lymph node negative breast carcinoma. *Cancer*, *97*(6), 1573-1581. https://doi.org/10.1002/cncr.11246

Bose, R. N., Maurmann, L., Mishur, R. J., Yasui, L., Gupta, S., Grayburn, W. S., Hofstetter, H., & Salley, T. (2008). Non-DNA-binding platinum anticancer agents: Cytotoxic activities of platinum–phosphato complexes towards human ovarian cancer cells. *Proceedings of the National Academy of Sciences*, *105*(47), 18314-18319. https://doi.org/doi:10.1073/pnas.0803094105

Brandon, M., Baldi, P., & Wallace, D. C. (2006). Mitochondrial mutations in cancer. *Oncogene*, *25*(34), 4647-4662. https://doi.org/10.1038/sj.onc.1209607

Brea-Calvo, G., Rodríguez-Hernández, Á., Fernández-Ayala, D. J. M., Navas, P., & Sánchez-Alcázar, J. A. (2006). Chemotherapy induces an increase in coenzyme Q10 levels in cancer cell lines. *Free Radical Biology and Medicine*, *40*(8), 1293-1302. https://doi.org/https://doi.org/10.1016/j.freeradbiomed.2005.11.014

Brough, D., & Rothwell, N. J. (2007). Caspase-1-dependent processing of pro-interleukin-1β is cytosolic and precedes cell death. *Journal of Cell Science*, *120*(5), 772-781. https://doi.org/10.1242/jcs.03377

Brunet, J.-F., Denizot, F., Luciani, M.-F., Roux-Dosseto, M., Suzan, M., Mattei, M.-G., & Golstein, P. (1987). A new member of the immunoglobulin superfamily—CTLA-4. *Nature*, *328*(6127), 267-270. https://doi.org/10.1038/328267a0

Bruno, P. M., Liu, Y., Park, G. Y., Murai, J., Koch, C. E., Eisen, T. J., Pritchard, J. R., Pommier, Y., Lippard, S. J., & Hemann, M. T. (2017). A subset of platinum-containing chemotherapeutic agents kills cells by inducing ribosome biogenesis stress. *Nat Med*, *23*(4), 461-471. https://doi.org/10.1038/nm.4291

Bryce, A. H., Dronca, R. S., Costello, B. A., Aparicio, A., Subudhi, S. K., O'Donnell, J. F., Jimeno, J., Yim, C. Y., Ames, T. D., Price, M., & Karp, D. D. (2021). A phase 1b study of novel immunogenic cell death inducer PT-112 plus PD-L1 inhibitor avelumab in metastatic castrate-resistant prostate cancer (mCRPC) patients [Meeting Abstract]. *Journal of Clinical Oncology*, *39*(15), 3. https://doi.org/10.1200/JCO.2021.39.15_suppl.e17025

Bryce, A. H., Dronca, R. S., Costello, B. A., Aparicio, A., Subudhi, S. K., O'Donnell, J. F., Jimeno, J., Yim, C. Y., Ames, T. D., Price, M., & Karp, D. D. (2021). A phase 1b study of novel immunogenic cell death inducer PT-112 plus PD-L1 inhibitor avelumab in metastatic castrate-resistant prostate cancer (mCRPC) patients. *Journal of Clinical Oncology*, *39*(15_suppl), e17025-e17025. https://doi.org/10.1200/JCO.2021.39.15_suppl.e17025

Bryce, A. H., Dronca, R. S., Costello, B. A., Infante, J. R., Ames, T. D., Jimeno, J., & Karp, D. D. (2020). PT-112 in advanced metastatic castrate-resistant prostate cancer (mCRPC), as monotherapy or in combination with PD-L1 inhibitor avelumab: Findings from two phase I studies. *Journal of Clinical Oncology*, *38*(6_suppl), 83-83. https://doi.org/10.1200/JCO.2020.38.6_suppl.83

Bryce, A. H., Karp, D. D., Tagawa, S. T., Nordquist, L. T., Rathkopf, D. E., Adra, N., Dorff, T. B., Baeck, J., O'Donnell, J. F., Ames, T. D., Yim, C. Y., Price, M., & Scher, H. I. (2023). A phase 2 study of immunogenic cell death inducer PT-112 in patients with metastatic castration-resistant prostate cancer. *Journal of Clinical Oncology*, *41*(6_suppl), TPS292-TPS292. https://doi.org/10.1200/JCO.2023.41.6_suppl.TPS292

Buck, S. A. J., Koolen, S. L. W., Mathijssen, R. H. J., de Wit, R., & van Soest, R. J. (2021). Cross-resistance and drug sequence in prostate cancer. *Drug Resist Updat*, *56*, 100761. https://doi.org/10.1016/j.drup.2021.100761

Cancer Research UK. (2024a). *Symptoms of metastasic prostate cancer*. Retrieved April 28, 2024 from https://www.cancerresearchuk.org/about-cancer/prostate-cancer/metastatic-cancer/symptoms

Cancer Research UK. (2024b). *Treatment for prostate cancer*. Retrieved April 28, 2024 from https://www.cancerresearchuk.org/about-cancer/prostate-cancer/treatment

Carneiro, B. A., & El-Deiry, W. S. (2020). Targeting apoptosis in cancer therapy. *Nat Rev Clin Oncol*, *17*(7), 395-417. https://doi.org/10.1038/s41571-020-0341-y

Carver, B. S., Chapinski, C., Wongvipat, J., Hieronymus, H., Chen, Y., Chandarlapaty, S., Arora, V. K., Le, C., Koutcher, J., Scher, H., Scardino, P. T., Rosen, N., & Sawyers, C. L. (2011). Reciprocal feedback regulation of PI3K and androgen receptor signaling in PTEN-deficient prostate cancer. *Cancer Cell*, *19*(5), 575-586. https://doi.org/10.1016/j.ccr.2011.04.008

Casares, N., Pequignot, M. O., Tesniere, A., Ghiringhelli, F., Roux, S., Chaput, N., Schmitt, E., Hamai, A., Hervas-Stubbs, S., Obeid, M., Coutant, F., Métivier, D., Pichard, E., Aucouturier, P., Pierron, G., Garrido, C., Zitvogel, L., & Kroemer, G. (2005). Caspase-dependent immunogenicity of doxorubicin-induced tumor cell death. *J Exp Med*, *202*(12), 1691-1701. https://doi.org/10.1084/jem.20050915

Catalán, E., Charni, S., Jaime, P., Aguiló, J. I., Enríquez, J. A., Naval, J., Pardo, J., Villalba, M., & Anel, A. (2015). MHC-I modulation due to changes in tumor cell metabolism regulates tumor sensitivity to CTL and NK cells. *OncoImmunology*, *4*(1), e985924. https://doi.org/10.4161/2162402X.2014.985924

Cavalli, L. R., Varella-Garcia, M., & Liang, B. C. (1997). Diminished tumorigenic phenotype after depletion of mitochondrial DNA. *Cell Growth Differ*, *8*(11), 1189-1198.

Certo, M., Moore, V. D. G., Nishino, M., Wei, G., Korsmeyer, S., Armstrong, S. A., & Letai, A. (2006). Mitochondria primed by death signals determine cellular addiction to antiapoptotic BCL-2 family members. *Cancer Cell*, *9*(5), 351-365. https://doi.org/https://doi.org/10.1016/j.ccr.2006.03.027

Chang, J. Y., Yi, H.-S., Kim, H.-W., & Shong, M. (2017). Dysregulation of mitophagy in carcinogenesis and tumor progression. *Biochimica et Biophysica Acta (BBA) - Bioenergetics*, *1858*(8), 633-640. https://doi.org/https://doi.org/10.1016/j.bbabio.2016.12.008

Chang, X., Bian, M., Liu, L., Yang, J., Yang, Z., Wang, Z., Lu, Y., & Liu, W. (2023). Induction of immunogenic cell death by novel platinum-based anticancer agents. *Pharmacological Research*, *187*, 106556. https://doi.org/https://doi.org/10.1016/j.phrs.2022.106556

Charni, S., de Bettignies, G., Rathore, M. G., Aguiló, J. I., van den Elsen, P. J., Haouzi, D., Hipskind, R. A., Enriquez, J. A., Sanchez-Beato, M., Pardo, J., Anel, A., & Villalba, M. (2010). Oxidative phosphorylation induces de novo expression of the MHC class I in tumor cells through the ERK5 pathway. *J Immunol*, *185*(6), 3498-3503. https://doi.org/10.4049/jimmunol.1001250

Chen, C., Liu, Y., Lu, C., Cross, J. R., Morris, J. P. t., Shroff, A. S., Ward, P. S., Bradner, J. E., Thompson, C., & Lowe, S. W. (2013). Cancer-associated IDH2 mutants drive an acute myeloid leukemia that is susceptible to Brd4 inhibition. *Genes Dev*, *27*(18), 1974-1985. https://doi.org/10.1101/gad.226613.113

Chen, J., Ren, Y., Gui, C., Zhao, M., Wu, X., Mao, K., Li, W., & Zou, F. (2018). Phosphorylation of Parkin at serine 131 by p38 MAPK promotes mitochondrial dysfunction and neuronal death in mutant

A53T α-synuclein model of Parkinson's disease. *Cell Death & Disease*, *9*(6), 700. https://doi.org/10.1038/s41419-018-0722-7

Chen, J. Z., Gokden, N., Greene, G. F., Mukunyadzi, P., & Kadlubar, F. F. (2002). Extensive somatic mitochondrial mutations in primary prostate cancer using laser capture microdissection. *Cancer Res*, *62*(22), 6470-6474.

Chen, Q., Boire, A., Jin, X., Valiente, M., Er, E. E., Lopez-Soto, A., Jacob, L., Patwa, R., Shah, H., Xu, K., Cross, J. R., & Massagué, J. (2016). Carcinoma-astrocyte gap junctions promote brain metastasis by cGAMP transfer. *Nature*, *533*(7604), 493-498. https://doi.org/10.1038/nature18268

Chen, R., Kang, R., & Tang, D. (2022). The mechanism of HMGB1 secretion and release. *Experimental & Molecular Medicine*, *54*(2), 91-102. https://doi.org/10.1038/s12276-022-00736-w

Chen, W., Frank, M. E., Jin, W., & Wahl, S. M. (2001). TGF-beta released by apoptotic T cells contributes to an immunosuppressive milieu. *Immunity*, *14*(6), 715-725. https://doi.org/10.1016/s1074-7613(01)00147-9

Chen, X., Fosco, D., Kline, D. E., & Kline, J. (2017). Calreticulin promotes immunity and type I interferon-dependent survival in mice with acute myeloid leukemia. *OncoImmunology*, *6*(4), e1278332. https://doi.org/10.1080/2162402x.2016.1278332

Chen, X. S., Li, L. Y., Guan, Y. D., Yang, J. M., & Cheng, Y. (2016). Anticancer strategies based on the metabolic profile of tumor cells: therapeutic targeting of the Warburg effect. *Acta Pharmacol Sin*, *37*(8), 1013-1019. https://doi.org/10.1038/aps.2016.47

Chinnery, P. F., Johnson, M. A., Wardell, T. M., Singh-Kler, R., Hayes, C., Brown, D. T., Taylor, R. W., Bindoff, L. A., & Turnbull, D. M. (2000). The epidemiology of pathogenic mitochondrial DNA mutations. *Ann Neurol*, *48*(2), 188-193.

Chinnery, P. F., Samuels, D. C., Elson, J., & Turnbull, D. M. (2002). Accumulation of mitochondrial DNA mutations in ageing, cancer, and mitochondrial disease: is there a common mechanism? *Lancet*, *360*(9342), 1323-1325. https://doi.org/10.1016/s0140-6736(02)11310-9

Chonghaile, T. N., Sarosiek, K. A., Vo, T.-T., Ryan, J. A., Tammareddi, A., Moore, V. D. G., Deng, J., Anderson, K. C., Richardson, P., Tai, Y.-T., Mitsiades, C. S., Matulonis, U. A., Drapkin, R., Stone, R., DeAngelo, D. J., McConkey, D. J., Sallan, S. E., Silverman, L., Hirsch, M. S., . . . Letai, A. (2011). Pretreatment Mitochondrial Priming Correlates with Clinical Response to Cytotoxic Chemotherapy. *Science*, *334*(6059), 1129-1133. https://doi.org/doi:10.1126/science.1206727

Chu, C. T., Ji, J., Dagda, R. K., Jiang, J. F., Tyurina, Y. Y., Kapralov, A. A., Tyurin, V. A., Yanamala, N., Shrivastava, I. H., Mohammadyani, D., Wang, K. Z. Q., Zhu, J., Klein-Seetharaman, J., Balasubramanian, K., Amoscato, A. A., Borisenko, G., Huang, Z., Gusdon, A. M., Cheikhi, A., . . . Kagan, V. E. (2013). Cardiolipin externalization to the outer mitochondrial membrane acts as an elimination signal for mitophagy in neuronal cells. *Nat Cell Biol*, *15*(10), 1197-1205. https://doi.org/10.1038/ncb2837

Coffelt, S. B., Kersten, K., Doornebal, C. W., Weiden, J., Vrijland, K., Hau, C.-S., Verstegen, N. J. M., Ciampricotti, M., Hawinkels, L. J. A. C., Jonkers, J., & de Visser, K. E. (2015). IL-17-producing γδ T cells and neutrophils conspire to promote breast cancer metastasis. *Nature*, *522*(7556), 345-348. https://doi.org/10.1038/nature14282

Collins, A. C., Cai, H., Li, T., Franco, L. H., Li, X. D., Nair, V. R., Scharn, C. R., Stamm, C. E., Levine, B., Chen, Z. J., & Shiloh, M. U. (2015). Cyclic GMP-AMP Synthase Is an Innate Immune DNA Sensor for Mycobacterium tuberculosis. *Cell Host Microbe*, *17*(6), 820-828. https://doi.org/10.1016/j.chom.2015.05.005

Comprehensive molecular portraits of human breast tumours. (2012). *Nature*, *490*(7418), 61-70. https://doi.org/10.1038/nature11412

Conlon, J., Burdette, D. L., Sharma, S., Bhat, N., Thompson, M., Jiang, Z., Rathinam, V. A., Monks, B., Jin, T., Xiao, T. S., Vogel, S. N., Vance, R. E., & Fitzgerald, K. A. (2013). Mouse, but not human STING,

binds and signals in response to the vascular disrupting agent 5,6-dimethylxanthenone-4-acetic acid. *J Immunol*, *190*(10), 5216-5225. https://doi.org/10.4049/jimmunol.1300097

Corte-Rodríguez, M., Espina, M., Sierra, L. M., Blanco, E., Ames, T., Montes-Bayón, M., & Sanz-Medel, A. (2015). Quantitative evaluation of cellular uptake, DNA incorporation and adduct formation in cisplatin sensitive and resistant cell lines: Comparison of different Pt-containing drugs. *Biochemical Pharmacology*, *98*(1), 69-77. https://doi.org/https://doi.org/10.1016/j.bcp.2015.08.112

Cosentino, K., Hertlein, V., Jenner, A., Dellmann, T., Gojkovic, M., Peña-Blanco, A., Dadsena, S., Wajngarten, N., Danial, J. S. H., Thevathasan, J. V., Mund, M., Ries, J., & Garcia-Saez, A. J. (2022). The interplay between BAX and BAK tunes apoptotic pore growth to control mitochondrial-DNA-mediated inflammation. *Mol Cell*, *82*(5), 933-949.e939. https://doi.org/10.1016/j.molcel.2022.01.008

Costa-Mattioli, M., & Walter, P. (2020). The integrated stress response: From mechanism to disease. *Science*, *368*(6489), eaat5314. https://doi.org/doi:10.1126/science.aat5314

Costello, L. C., & Franklin, R. B. (1981). Aconitase activity, citrate oxidation, and zinc inhibition in rat ventral prostate. *Enzyme*, *26*(6), 281-287. https://doi.org/10.1159/000459195

Costello, L. C., & Franklin, R. B. (1991). Concepts of citrate production and secretion by prostate: 2. Hormonal relationships in normal and neoplastic prostate. *Prostate*, *19*(3), 181-205. https://doi.org/10.1002/pros.2990190302

Costello, L. C., & Franklin, R. B. (1994). Bioenergetic theory of prostate malignancy. *Prostate*, *25*(3), 162-166. https://doi.org/10.1002/pros.2990250308

Costello, L. C., & Franklin, R. B. (1998). Novel role of zinc in the regulation of prostate citrate metabolism and its implications in prostate cancer. *Prostate*, *35*(4), 285-296. https://doi.org/10.1002/(sici)1097-0045(19980601)35:4<285::aid-pros8>3.0.co;2-f

Costello, L. C., Liu, Y., Franklin, R. B., & Kennedy, M. C. (1997). Zinc Inhibition of Mitochondrial Aconitase and Its Importance in Citrate Metabolism of Prostate Epithelial Cells*. *Journal of Biological Chemistry*, *272*(46), 28875-28881. https://doi.org/https://doi.org/10.1074/jbc.272.46.28875

Costello, L. C., Liu, Y., Zou, J., & Franklin, R. B. (2000). Mitochondrial aconitase gene expression is regulated by testosterone and prolactin in prostate epithelial cells. *Prostate*, *42*(3), 196-202. https://doi.org/10.1002/(sici)1097-0045(20000215)42:3<196::aid-pros5>3.0.co;2-8

Cox, A., Dunning, A. M., Garcia-Closas, M., Balasubramanian, S., Reed, M. W., Pooley, K. A., Scollen, S., Baynes, C., Ponder, B. A., Chanock, S., Lissowska, J., Brinton, L., Peplonska, B., Southey, M. C., Hopper, J. L., McCredie, M. R., Giles, G. G., Fletcher, O., Johnson, N., . . . Easton, D. F. (2007). A common coding variant in CASP8 is associated with breast cancer risk. *Nat Genet*, *39*(3), 352-358. https://doi.org/10.1038/ng1981

Cruz-Bermúdez, A., Vallejo, C. G., Vicente-Blanco, R. J., Gallardo, M. E., Fernández-Moreno, M., Quintanilla, M., & Garesse, R. (2015). Enhanced tumorigenicity by mitochondrial DNA mild mutations. *Oncotarget*, *6*(15), 13628-13643. https://doi.org/10.18632/oncotarget.3698

Cucolo, L., & Minn, A. J. (2015). Getting Tumor Dendritic Cells to Engage the Dead. *Cancer Cell*, *28*(6), 685-687. https://doi.org/https://doi.org/10.1016/j.ccell.2015.11.009

Cullen, K. J., Yang, Z., Schumaker, L., & Guo, Z. (2007). Mitochondria as a critical target of the chemotheraputic agent cisplatin in head and neck cancer. *J Bioenerg Biomembr*, *39*(1), 43-50. https://doi.org/10.1007/s10863-006-9059-5

Darmon, A. J., Nicholson, D. W., & Bleackley, R. C. (1995). Activation of the apoptotic protease CPP32 by cytotoxic T-cell-derived granzyme B. *Nature*, *377*(6548), 446-448. https://doi.org/10.1038/377446a0

De Giovanni, C., Nicoletti, G., Landuzzi, L., Palladini, A., Lollini, P. L., & Nanni, P. (2019). Bioprofiling TS/A Murine Mammary Cancer for a Functional Precision Experimental Model. *Cancers (Basel)*, *11*(12). https://doi.org/10.3390/cancers11121889

de Mey, S., Dufait, I., Jiang, H., Corbet, C., Wang, H., Van De Gucht, M., Kerkhove, L., Law, K. L., Vandenplas, H., Gevaert, T., Feron, O., & De Ridder, M. (2020). Dichloroacetate Radiosensitizes Hypoxic Breast Cancer Cells. *Int J Mol Sci*, *21*(24). https://doi.org/10.3390/ijms21249367

de Weerd, N. A., Vivian, J. P., Nguyen, T. K., Mangan, N. E., Gould, J. A., Braniff, S. J., Zaker-Tabrizi, L., Fung, K. Y., Forster, S. C., Beddoe, T., Reid, H. H., Rossjohn, J., & Hertzog, P. J. (2013). Structural basis of a unique interferon-β signaling axis mediated via the receptor IFNAR1. *Nat Immunol*, *14*(9), 901-907. https://doi.org/10.1038/ni.2667

DeBerardinis, R. J., & Chandel, N. S. (2020). We need to talk about the Warburg effect. *Nat Metab*, *2*(2), 127-129. https://doi.org/10.1038/s42255-020-0172-2

DeBerardinis, R. J., & Chandel, N. S. (2020). We need to talk about the Warburg effect. *Nature Metabolism*, *2*(2), 127-129. https://doi.org/10.1038/s42255-020-0172-2

Del Cid, N., Jeffery, E., Rizvi, S. M., Stamper, E., Peters, L. R., Brown, W. C., Provoda, C., & Raghavan, M. (2010). Modes of calreticulin recruitment to the major histocompatibility complex class I assembly pathway. *J Biol Chem*, *285*(7), 4520-4535. https://doi.org/10.1074/jbc.M109.085407

Del Gaizo Moore, V., & Letai, A. (2013). BH3 profiling--measuring integrated function of the mitochondrial apoptotic pathway to predict cell fate decisions. *Cancer Lett*, *332*(2), 202-205. https://doi.org/10.1016/j.canlet.2011.12.021

Del Prete, A., Salvi, V., Soriani, A., Laffranchi, M., Sozio, F., Bosisio, D., & Sozzani, S. (2023). Dendritic cell subsets in cancer immunity and tumor antigen sensing. *Cellular & Molecular Immunology*, *20*(5), 432-447. https://doi.org/10.1038/s41423-023-00990-6

Deng, L., Liang, H., Xu, M., Yang, X., Burnette, B., Arina, A., Li, X. D., Mauceri, H., Beckett, M., Darga, T., Huang, X., Gajewski, T. F., Chen, Z. J., Fu, Y. X., & Weichselbaum, R. R. (2014). STING-Dependent Cytosolic DNA Sensing Promotes Radiation-Induced Type I Interferon-Dependent Antitumor Immunity in Immunogenic Tumors. *Immunity*, *41*(5), 843-852. https://doi.org/10.1016/j.immuni.2014.10.019

Desagher, S., & Martinou, J. C. (2000). Mitochondria as the central control point of apoptosis. *Trends Cell Biol*, *10*(9), 369-377. https://doi.org/10.1016/s0962-8924(00)01803-1

Desouki, M. M., Geradts, J., Milon, B., Franklin, R. B., & Costello, L. C. (2007). hZip2 and hZip3 zinc transporters are down regulated in human prostate adenocarcinomatous glands. *Mol Cancer*, *6*, 37. https://doi.org/10.1186/1476-4598-6-37

Devasia, T. P., Mariotto, A. B., Nyame, Y. A., & Etzioni, R. (2023). Estimating the Number of Men Living with Metastatic Prostate Cancer in the United States. *Cancer Epidemiology, Biomarkers & Prevention*, *32*(5), 659-665. https://doi.org/10.1158/1055-9965.Epi-22-1038

Deveraux, Q. L., Takahashi, R., Salvesen, G. S., & Reed, J. C. (1997). X-linked IAP is a direct inhibitor of cell-death proteases. *Nature*, *388*(6639), 300-304. https://doi.org/10.1038/40901

Dewan, M. Z., Galloway, A. E., Kawashima, N., Dewyngaert, J. K., Babb, J. S., Formenti, S. C., & Demaria, S. (2009). Fractionated but not single-dose radiotherapy induces an immune-mediated abscopal effect when combined with anti-CTLA-4 antibody. *Clin Cancer Res*, *15*(17), 5379-5388. https://doi.org/10.1158/1078-0432.Ccr-09-0265

Diepstraten, S. T., Anderson, M. A., Czabotar, P. E., Lessene, G., Strasser, A., & Kelly, G. L. (2022). The manipulation of apoptosis for cancer therapy using BH3-mimetic drugs. *Nature Reviews Cancer*, *22*(1), 45-64. https://doi.org/10.1038/s41568-021-00407-4

Ding, M., Dong, Q., Liu, Z., Liu, Z., Qu, Y., Li, X., Huo, C., Jia, X., Fu, F., & Wang, X. (2017). Inhibition of dynamin-related protein 1 protects against myocardial ischemia-reperfusion injury in diabetic mice. *Cardiovasc Diabetol*, *16*(1), 19. https://doi.org/10.1186/s12933-017-0501-2

Donehower, L. A., Harvey, M., Slagle, B. L., McArthur, M. J., Montgomery, C. A., Jr., Butel, J. S., & Bradley, A. (1992). Mice deficient for p53 are developmentally normal but susceptible to spontaneous tumours. *Nature*, *356*(6366), 215-221. https://doi.org/10.1038/356215a0

Dougé, A., El Ghazzi, N., Lemal, R., & Rouzaire, P. (2024). Adoptive T Cell Therapy in Solid Tumors: State-of-the Art, Current Challenges, and Upcoming Improvements. *Molecular Cancer Therapeutics*, *23*(3), 272-284. https://doi.org/10.1158/1535-7163.Mct-23-0310

Dunbar, E. M., Coats, B. S., Shroads, A. L., Langaee, T., Lew, A., Forder, J. R., Shuster, J. J., Wagner, D. A., & Stacpoole, P. W. (2014). Phase 1 trial of dichloroacetate (DCA) in adults with recurrent malignant brain tumors. *Invest New Drugs*, *32*(3), 452-464. https://doi.org/10.1007/s10637-013-0047-4

Dunn, G. P., Bruce, A. T., Ikeda, H., Old, L. J., & Schreiber, R. D. (2002). Cancer immunoediting: from immunosurveillance to tumor escape. *Nat Immunol*, *3*(11), 991-998. https://doi.org/10.1038/ni1102-991

Elliott, M. R., Chekeni, F. B., Trampont, P. C., Lazarowski, E. R., Kadl, A., Walk, S. F., Park, D., Woodson, R. I., Ostankovich, M., Sharma, P., Lysiak, J. J., Harden, T. K., Leitinger, N., & Ravichandran, K. S. (2009). Nucleotides released by apoptotic cells act as a find-me signal to promote phagocytic clearance. *Nature*, *461*(7261), 282-286. https://doi.org/10.1038/nature08296

Elmore, S. (2007). Apoptosis: a review of programmed cell death. *Toxicol Pathol*, *35*(4), 495-516. https://doi.org/10.1080/01926230701320337

Engelman, J. A., Luo, J., & Cantley, L. C. (2006). The evolution of phosphatidylinositol 3-kinases as regulators of growth and metabolism. *Nat Rev Genet*, *7*(8), 606-619. https://doi.org/10.1038/nrg1879

Enríquez, J. A. (2016). Supramolecular Organization of Respiratory Complexes. *Annual Review of Physiology*, *78*(Volume 78, 2016), 533-561. https://doi.org/https://doi.org/10.1146/annurev-physiol-021115-105031

Eskelinen, E. L. (2011). The dual role of autophagy in cancer. *Curr Opin Pharmacol*, *11*(4), 294-300. https://doi.org/10.1016/j.coph.2011.03.009

Evan, G., & Littlewood, T. (1998). A matter of life and cell death [Review]. *Science*, *281*(5381), 1317-1322. https://doi.org/10.1126/science.281.5381.1317

Fadok, V. A., Bratton, D. L., Frasch, S. C., Warner, M. L., & Henson, P. M. (1998). The role of phosphatidylserine in recognition of apoptotic cells by phagocytes. *Cell Death & Differentiation*, *5*(7), 551-562. https://doi.org/10.1038/sj.cdd.4400404

Fan, Z., Beresford, P. J., Oh, D. Y., Zhang, D., & Lieberman, J. (2003). Tumor suppressor NM23-H1 is a granzyme A-activated DNase during CTL-mediated apoptosis, and the nucleosome assembly protein SET is its inhibitor. *Cell*, *112*(5), 659-672. https://doi.org/10.1016/s0092-8674(03)00150-8

Fang, E. F., Hou, Y., Palikaras, K., Adriaanse, B. A., Kerr, J. S., Yang, B., Lautrup, S., Hasan-Olive, M. M., Caponio, D., Dan, X., Rocktäschel, P., Croteau, D. L., Akbari, M., Greig, N. H., Fladby, T., Nilsen, H., Cader, M. Z., Mattson, M. P., Tavernarakis, N., & Bohr, V. A. (2019). Mitophagy inhibits amyloid-β and tau pathology and reverses cognitive deficits in models of Alzheimer's disease. *Nature Neuroscience*, *22*(3), 401-412. https://doi.org/10.1038/s41593-018-0332-9

Fares, J., Fares, M. Y., Khachfe, H. H., Salhab, H. A., & Fares, Y. (2020). Molecular principles of metastasis: a hallmark of cancer revisited. *Signal Transduction and Targeted Therapy*, *5*(1), 28. https://doi.org/10.1038/s41392-020-0134-x

FDA. (2024). *Novel Drug Approvals for 2019*. Retrieved April 28, 2024 from https://www.fda.gov/drugs/novel-drug-approvals-fda/novel-drug-approvals-2019

Ferrara, N., & Kerbel, R. S. (2005). Angiogenesis as a therapeutic target. *Nature*, *438*(7070), 967-974. https://doi.org/10.1038/nature04483

Ferretti, S., Mercinelli, C., Marandino, L., Litterio, G., Marchioni, M., & Schips, L. (2023). Metastatic Castration-Resistant Prostate Cancer: Insights on Current Therapy and Promising Experimental Drugs. *Res Rep Urol*, *15*, 243-259. https://doi.org/10.2147/rru.S385257

Fink, S. L., & Cookson, B. T. (2006). Caspase-1-dependent pore formation during pyroptosis leads to osmotic lysis of infected host macrophages. *Cellular Microbiology*, *8*(11), 1812-1825. https://doi.org/https://doi.org/10.1111/j.1462-5822.2006.00751.x

Finlay, C. A., Hinds, P. W., & Levine, A. J. (1989). The p53 proto-oncogene can act as a suppressor of transformation. *Cell*, *57*(7), 1083-1093. https://doi.org/https://doi.org/10.1016/0092-8674(89)90045-7

Finn, O. J. (2018). A Believer's Overview of Cancer Immunosurveillance and Immunotherapy. *The Journal of Immunology*, *200*(2), 385-391. https://doi.org/10.4049/jimmunol.1701302

Flanagan, S. P. (1966). 'Nude', a new hairless gene with pleiotropic effects in the mouse. *Genetical Research*, *8*(3), 295-309. https://doi.org/10.1017/S0016672300010168

Follain, G., Osmani, N., Azevedo, A. S., Allio, G., Mercier, L., Karreman, M. A., Solecki, G., Garcia Leòn, M. J., Lefebvre, O., Fekonja, N., Hille, C., Chabannes, V., Dollé, G., Metivet, T., Hovsepian, F. D., Prudhomme, C., Pichot, A., Paul, N., Carapito, R., . . . Goetz, J. G. (2018). Hemodynamic Forces Tune the Arrest, Adhesion, and Extravasation of Circulating Tumor Cells. *Developmental Cell*, *45*(1), 33-52.e12. https://doi.org/https://doi.org/10.1016/j.devcel.2018.02.015

Follo, C., Cheng, Y., Richards, W. G., Bueno, R., & Broaddus, V. C. (2019). Autophagy facilitates the release of immunogenic signals following chemotherapy in 3D models of mesothelioma. *Molecular Carcinogenesis*, *58*(10), 1754-1769. https://doi.org/https://doi.org/10.1002/mc.23050

François-Martin, H., Lardy-Cléaud, A., Pistilli, B., Levy, C., Diéras, V., Frenel, J. S., Guiu, S., Mouret-Reynier, M. A., Mailliez, A., Eymard, J. C., Petit, T., Ung, M., Desmoulins, I., Augereau, P., Bachelot, T., Uwer, L., Debled, M., Ferrero, J. M., Clatot, F., . . . Cottu, P. (2023). Long-Term Results with Everolimus in Advanced Hormone Receptor Positive Breast Cancer in a Multicenter National Real-World Observational Study. *Cancers (Basel)*, *15*(4). https://doi.org/10.3390/cancers15041191

Frenette, C. T., Morelli, G., Shiffman, M. L., Frederick, R. T., Rubin, R. A., Fallon, M. B., Cheng, J. T., Cave, M., Khaderi, S. A., Massoud, O., Pyrsopoulos, N., Park, J. S., Robinson, J. M., Yamashita, M., Spada, A. P., Chan, J. L., & Hagerty, D. T. (2019). Emricasan Improves Liver Function in Patients With Cirrhosis and High Model for End-Stage Liver Disease Scores Compared With Placebo. *Clin Gastroenterol Hepatol*, *17*(4), 774-783.e774. https://doi.org/10.1016/j.cgh.2018.06.012

Fucikova, J., Becht, E., Iribarren, K., Goc, J., Remark, R., Damotte, D., Alifano, M., Devi, P., Biton, J., Germain, C., Lupo, A., Fridman, W. H., Dieu-Nosjean, M. C., Kroemer, G., Sautès-Fridman, C., & Cremer, I. (2016). Calreticulin Expression in Human Non-Small Cell Lung Cancers Correlates with Increased Accumulation of Antitumor Immune Cells and Favorable Prognosis. *Cancer Res*, *76*(7), 1746-1756. https://doi.org/10.1158/0008-5472.Can-15-1142

Fucikova, J., Kepp, O., Kasikova, L., Petroni, G., Yamazaki, T., Liu, P., Zhao, L., Spisek, R., Kroemer, G., & Galluzzi, L. (2020). Detection of immunogenic cell death and its relevance for cancer therapy. *Cell Death & Disease*, *11*(11), 1013. https://doi.org/10.1038/s41419-020-03221-2

Fucikova, J., Spisek, R., Kroemer, G., & Galluzzi, L. (2021). Calreticulin and cancer. *Cell Research*, *31*(1), 5-16. https://doi.org/10.1038/s41422-020-0383-9

Fuertes, M. B., Kacha, A. K., Kline, J., Woo, S. R., Kranz, D. M., Murphy, K. M., & Gajewski, T. F. (2011). Host type I IFN signals are required for antitumor CD8+ T cell responses through CD8{alpha}+ dendritic cells. *J Exp Med*, *208*(10), 2005-2016. https://doi.org/10.1084/jem.20101159

Fulda, S. (2009). Tumor resistance to apoptosis. *International Journal of Cancer*, *124*(3), 511-515. https://doi.org/https://doi.org/10.1002/ijc.24064

Gallagher, D. J., Gaudet, M. M., Pal, P., Kirchhoff, T., Balistreri, L., Vora, K., Bhatia, J., Stadler, Z., Fine, S. W., Reuter, V., Zelefsky, M., Morris, M. J., Scher, H. I., Klein, R. J., Norton, L., Eastham, J. A.,

Scardino, P. T., Robson, M. E., & Offit, K. (2010). Germline BRCA mutations denote a clinicopathologic subset of prostate cancer. *Clin Cancer Res*, *16*(7), 2115-2121. https://doi.org/10.1158/1078-0432.Ccr-09-2871

Galletti, G., Leach, B. I., Lam, L., & Tagawa, S. T. (2017). Mechanisms of resistance to systemic therapy in metastatic castration-resistant prostate cancer. *Cancer Treat Rev*, *57*, 16-27. https://doi.org/10.1016/j.ctrv.2017.04.008

Galluzzi, L., Aaronson, S. A., Abrams, J., Alnemri, E. S., Andrews, D. W., Baehrecke, E. H., Bazan, N. G., Blagosklonny, M. V., Blomgren, K., Borner, C., Bredesen, D. E., Brenner, C., Castedo, M., Cidlowski, J. A., Ciechanover, A., Cohen, G. M., De Laurenzi, V., De Maria, R., Deshmukh, M., . . . Kroemer, G. (2009). Guidelines for the use and interpretation of assays for monitoring cell death in higher eukaryotes. *Cell Death Differ*, *16*(8), 1093-1107. https://doi.org/10.1038/cdd.2009.44

Galluzzi, L., Baehrecke, E. H., Ballabio, A., Boya, P., Bravo‐San Pedro, J. M., Cecconi, F., Choi, A. M., Chu, C. T., Codogno, P., Colombo, M. I., Cuervo, A. M., Debnath, J., Deretic, V., Dikic, I., Eskelinen, E. L., Fimia, G. M., Fulda, S., Gewirtz, D. A., Green, D. R., . . . Kroemer, G. (2017). Molecular definitions of autophagy and related processes. *The EMBO Journal*, *36*(13), 1811-1836. https://doi.org/https://doi.org/10.15252/embj.201796697

Galluzzi, L., Buqué, A., Kepp, O., Zitvogel, L., & Kroemer, G. (2017). Immunogenic cell death in cancer and infectious disease. *Nature Reviews Immunology*, *17*(2), 97-111. https://doi.org/10.1038/nri.2016.107

Galluzzi, L., Guilbaud, E., Schmidt, D., Kroemer, G., & Marincola, F. M. (2024). Targeting immunogenic cell stress and death for cancer therapy. *Nat Rev Drug Discov*, *23*(6), 445-460. https://doi.org/10.1038/s41573-024-00920-9

Galluzzi, L., Humeau, J., Buqué, A., Zitvogel, L., & Kroemer, G. (2020). Immunostimulation with chemotherapy in the era of immune checkpoint inhibitors. *Nature Reviews Clinical Oncology*, *17*(12), 725-741. https://doi.org/10.1038/s41571-020-0413-z

Galluzzi, L., Morselli, E., Kepp, O., Vitale, I., Rigoni, A., Vacchelli, E., Michaud, M., Zischka, H., Castedo, M., & Kroemer, G. (2010). Mitochondrial gateways to cancer. *Mol Aspects Med*, *31*(1), 1-20. https://doi.org/10.1016/j.mam.2009.08.002

Galluzzi, L., Vitale, I., Aaronson, S. A., Abrams, J. M., Adam, D., Agostinis, P., Alnemri, E. S., Altucci, L., Amelio, I., Andrews, D. W., Annicchiarico-Petruzzelli, M., Antonov, A. V., Arama, E., Baehrecke, E. H., Barlev, N. A., Bazan, N. G., Bernassola, F., Bertrand, M. J. M., Bianchi, K., . . . Kroemer, G. (2018). Molecular mechanisms of cell death: recommendations of the Nomenclature Committee on Cell Death 2018. *Cell Death Differ*, *25*(3), 486-541. https://doi.org/10.1038/s41418-017-0012-4

Galluzzi, L., Vitale, I., Aaronson, S. A., Abrams, J. M., Adam, D., Agostinis, P., Alnemri, E. S., Altucci, L., Amelio, I., Andrews, D. W., Annicchiarico-Petruzzelli, M., Antonov, A. V., Arama, E., Baehrecke, E. H., Barlev, N. A., Bazan, N. G., Bernassola, F., Bertrand, M. J. M., Bianchi, K., . . . Kroemer, G. (2018). Molecular mechanisms of cell death: recommendations of the Nomenclature Committee on Cell Death 2018. *Cell Death & Differentiation*, *25*(3), 486-541. https://doi.org/10.1038/s41418-017-0012-4

Galluzzi, L., Vitale, I., Warren, S., Adjemian, S., Agostinis, P., Martinez, A. B., Chan, T. A., Coukos, G., Demaria, S., Deutsch, E., Draganov, D., Edelson, R. L., Formenti, S. C., Fucikova, J., Gabriele, L., Gaipl, U. S., Gameiro, S. R., Garg, A. D., Golden, E., . . . Marincola, F. M. (2020). Consensus guidelines for the definition, detection and interpretation of immunogenic cell death. *J Immunother Cancer*, *8*(1). https://doi.org/10.1136/jitc-2019-000337

Galluzzi, L., Yamazaki, T., & Kroemer, G. (2018). Linking cellular stress responses to systemic homeostasis. *Nature Reviews Molecular Cell Biology*, *19*(11), 731-745. https://doi.org/10.1038/s41580-018-0068-0

Galon, J., & Lanzi, A. (2020). Immunoscore and its introduction in clinical practice. *Q J Nucl Med Mol Imaging*, *64*(2), 152-161. https://doi.org/10.23736/s1824-4785.20.03249-5

Gan, Z. Y., Callegari, S., Cobbold, S. A., Cotton, T. R., Mlodzianoski, M. J., Schubert, A. F., Geoghegan, N. D., Rogers, K. L., Leis, A., Dewson, G., Glukhova, A., & Komander, D. (2022). Activation mechanism of PINK1. *Nature*, *602*(7896), 328-335. https://doi.org/10.1038/s41586-021-04340-2

Gandhi, J., Afridi, A., Vatsia, S., Joshi, G., Joshi, G., Kaplan, S. A., Smith, N. L., & Khan, S. A. (2018). The molecular biology of prostate cancer: current understanding and clinical implications. *Prostate Cancer and Prostatic Diseases*, *21*(1), 22-36. https://doi.org/10.1038/s41391-017-0023-8

Gao, Y., Herndon, J. M., Zhang, H., Griffith, T. S., & Ferguson, T. A. (1998). Antiinflammatory effects of CD95 ligand (FasL)-induced apoptosis. *J Exp Med*, *188*(5), 887-896. https://doi.org/10.1084/jem.188.5.887

Gardella, S., Andrei, C., Ferrera, D., Lotti, L. V., Torrisi, M. R., Bianchi, M. E., & Rubartelli, A. (2002). The nuclear protein HMGB1 is secreted by monocytes via a non‐classical, vesicle‐mediated secretory pathway. *EMBO reports*, *3*(10), 995-1001. https://doi.org/https://doi.org/10.1093/embo-reports/kvf198

Garrido, F., Cabrera, T., & Aptsiauri, N. (2010). "Hard" and "soft" lesions underlying the HLA class I alterations in cancer cells: implications for immunotherapy. *Int J Cancer*, *127*(2), 249-256. https://doi.org/10.1002/ijc.25270

Gavilondo, J., Fernandez, A., Castillo, R., & Lage, A. (1982). Neoplastic progression evidenced in the L929 cell system. I. Selection of tumorigenic and metastasizing cell variants. *Neoplasma*, *29*(3), 269-279.

Gerke, V., Creutz, C. E., & Moss, S. E. (2005). Annexins: linking Ca2+ signalling to membrane dynamics. *Nature Reviews Molecular Cell Biology*, *6*(6), 449-461. https://doi.org/10.1038/nrm1661

Gerstberger, S., Jiang, Q., & Ganesh, K. (2023). Metastasis. *Cell*, *186*(8), 1564-1579. https://doi.org/https://doi.org/10.1016/j.cell.2023.03.003

Ghanavat, M., Shahrouzian, M., Deris Zayeri, Z., Banihashemi, S., Kazemi, S. M., & Saki, N. (2021). Digging deeper through glucose metabolism and its regulators in cancer and metastasis. *Life Sci*, *264*, 118603. https://doi.org/10.1016/j.lfs.2020.118603

Ghiringhelli, F., Apetoh, L., Tesniere, A., Aymeric, L., Ma, Y., Ortiz, C., Vermaelen, K., Panaretakis, T., Mignot, G., Ullrich, E., Perfettini, J. L., Schlemmer, F., Tasdemir, E., Uhl, M., Génin, P., Civas, A., Ryffel, B., Kanellopoulos, J., Tschopp, J., . . . Zitvogel, L. (2009). Activation of the NLRP3 inflammasome in dendritic cells induces IL-1beta-dependent adaptive immunity against tumors. *Nat Med*, *15*(10), 1170-1178. https://doi.org/10.1038/nm.2028

Ghosh, P., Vidal, C., Dey, S., & Zhang, L. (2020). Mitochondria Targeting as an Effective Strategy for Cancer Therapy. *Int J Mol Sci*, *21*(9). https://doi.org/10.3390/ijms21093363

Giampazolias, E., & Tait, S. W. (2016). Mitochondria and the hallmarks of cancer. *Febs j*, *283*(5), 803-814. https://doi.org/10.1111/febs.13603

Giampazolias, E., Zunino, B., Dhayade, S., Bock, F., Cloix, C., Cao, K., Roca, A., Lopez, J., Ichim, G., Proïcs, E., Rubio-Patiño, C., Fort, L., Yatim, N., Woodham, E., Orozco, S., Taraborrelli, L., Peltzer, N., Lecis, D., Machesky, L., . . . Tait, S. W. G. (2017). Mitochondrial permeabilization engages NF-κB-dependent anti-tumour activity under caspase deficiency. *Nat Cell Biol*, *19*(9), 1116-1129. https://doi.org/10.1038/ncb3596

Gillett, C., Fantl, V., Smith, R., Fisher, C., Bartek, J., Dickson, C., Barnes, D., & Peters, G. (1994). Amplification and overexpression of cyclin D1 in breast cancer detected by immunohistochemical staining. *Cancer Res*, *54*(7), 1812-1817.

Gimm, O., Armanios, M., Dziema, H., Neumann, H. P., & Eng, C. (2000). Somatic and occult germ-line mutations in SDHD, a mitochondrial complex II gene, in nonfamilial pheochromocytoma. *Cancer Res*, *60*(24), 6822-6825.

Glück, S., Guey, B., Gulen, M. F., Wolter, K., Kang, T. W., Schmacke, N. A., Bridgeman, A., Rehwinkel, J., Zender, L., & Ablasser, A. (2017). Innate immune sensing of cytosolic chromatin fragments through cGAS promotes senescence. *Nat Cell Biol*, *19*(9), 1061-1070. https://doi.org/10.1038/ncb3586

Glytsou, C., Chen, X., Zacharioudakis, E., Al-Santli, W., Zhou, H., Nadorp, B., Lee, S., Lasry, A., Sun, Z., Papaioannou, D., Cammer, M., Wang, K., Zal, T., Zal, M. A., Carter, B. Z., Ishizawa, J., Tibes, R., Tsirigos, A., Andreeff, M., . . . Aifantis, I. (2023). Mitophagy Promotes Resistance to BH3 Mimetics in Acute Myeloid Leukemia. *Cancer Discovery*, *13*(7), 1656-1677. https://doi.org/10.1158/2159-8290.Cd-22-0601

Golden, E. B., Pellicciotta, I., Demaria, S., Barcellos-Hoff, M. H., & Formenti, S. C. (2012). The convergence of radiation and immunogenic cell death signaling pathways. *Front Oncol*, *2*, 88. https://doi.org/10.3389/fonc.2012.00088

Gómez-Zaera, M., Abril, J., González, L., Aguiló, F., Condom, E., Nadal, M., & Nunes, V. (2006). Identification of somatic and germline mitochondrial DNA sequence variants in prostate cancer patients. *Mutat Res*, *595*(1-2), 42-51. https://doi.org/10.1016/j.mrfmmm.2005.10.012

Gonzalo, Ó., Benedi, A., Vela, L., Anel, A., Naval, J., & Marzo, I. (2023). Study of the Bcl-2 Interactome by BiFC Reveals Differences in the Activation Mechanism of Bax and Bak. *Cells*, *12*(5). https://doi.org/10.3390/cells12050800

Goodwin, G. H., & Johns, E. W. (1973). Isolation and characterisation of two calf-thymus chromatin non-histone proteins with high contents of acidic and basic amino acids. *Eur J Biochem*, *40*(1), 215-219. https://doi.org/10.1111/j.1432-1033.1973.tb03188.x

Gradishar, W. J., Moran, M. S., Abraham, J., Aft, R., Agnese, D., Allison, K. H., Blair, S. L., Burstein, H. J., Dang, C., Elias, A. D., Giordano, S. H., Goetz, M. P., Goldstein, L. J., Hurvitz, S. A., Isakoff, S. J., Jankowitz, R. C., Javid, S. H., Krishnamurthy, J., Leitch, M., . . . Kumar, R. (2021). NCCN Guidelines® Insights: Breast Cancer, Version 4.2021. *J Natl Compr Canc Netw*, *19*(5), 484-493. https://doi.org/10.6004/jnccn.2021.0023

Grakoui, A., Bromley, S. K., Sumen, C., Davis, M. M., Shaw, A. S., Allen, P. M., & Dustin, M. L. (1999). The Immunological Synapse: A Molecular Machine Controlling T Cell Activation. *Science*, *285*(5425), 221-227. https://doi.org/doi:10.1126/science.285.5425.221

Grasso, D., Zampieri, L. X., Capelôa, T., Van de Velde, J. A., & Sonveaux, P. (2020). Mitochondria in cancer. *Cell Stress*, *4*(6), 114-146. https://doi.org/10.15698/cst2020.06.221

Green, D. R., Ferguson, T., Zitvogel, L., & Kroemer, G. (2009). Immunogenic and tolerogenic cell death. *Nat Rev Immunol*, *9*(5), 353-363. https://doi.org/10.1038/nri2545

Green, J. P., Yu, S., Martín-Sánchez, F., Pelegrin, P., Lopez-Castejon, G., Lawrence, C. B., & Brough, D. (2018). Chloride regulates dynamic NLRP3-dependent ASC oligomerization and inflammasome priming. *Proc Natl Acad Sci U S A*, *115*(40), E9371-e9380. https://doi.org/10.1073/pnas.1812744115

Greiner, J. W., Hand, P. H., Noguchi, P., Fisher, P. B., Pestka, S., & Schlom, J. (1984). Enhanced expression of surface tumor-associated antigens on human breast and colon tumor cells after recombinant human leukocyte alpha-interferon treatment. *Cancer Res*, *44*(8), 3208-3214.

Guermonprez, P., Valladeau, J., Zitvogel, L., Théry, C., & Amigorena, S. (2002). Antigen presentation and T cell stimulation by dendritic cells. *Annu Rev Immunol*, *20*, 621-667. https://doi.org/10.1146/annurev.immunol.20.100301.064828

Guerrero-Zotano, A., Mayer, I. A., & Arteaga, C. L. (2016). PI3K/AKT/mTOR: role in breast cancer progression, drug resistance, and treatment. *Cancer Metastasis Rev*, *35*(4), 515-524. https://doi.org/10.1007/s10555-016-9637-x

Guilbaud, E., Kroemer, G., & Galluzzi, L. (2023). Calreticulin exposure orchestrates innate immunosurveillance. *Cancer Cell*, *41*(6), 1014-1016. https://doi.org/https://doi.org/10.1016/j.ccell.2023.04.015

Guo, Z., Yang, X., Sun, F., Jiang, R., Linn, D. E., Chen, H., Chen, H., Kong, X., Melamed, J., Tepper, C. G., Kung, H. J., Brodie, A. M., Edwards, J., & Qiu, Y. (2009). A novel androgen receptor splice variant is up-regulated during prostate cancer progression and promotes androgen depletion-resistant growth. *Cancer Res*, *69*(6), 2305-2313. https://doi.org/10.1158/0008-5472.Can-08-3795

Gupta, G., Borglum, K., & Chen, H. (2021). Immunogenic Cell Death: A Step Ahead of Autophagy in Cancer Therapy. *J Cancer Immunol (Wilmington)*, *3*(1), 47-59. https://doi.org/10.33696/cancerimmunol.3.041

Hall, M. D., Okabe, M., Shen, D. W., Liang, X. J., & Gottesman, M. M. (2008). The role of cellular accumulation in determining sensitivity to platinum-based chemotherapy. *Annu Rev Pharmacol Toxicol*, *48*, 495-535. https://doi.org/10.1146/annurev.pharmtox.48.080907.180426

Hanahan, D. (2022). Hallmarks of Cancer: New Dimensions. *Cancer Discovery*, *12*(1), 31-46. https://doi.org/10.1158/2159-8290.Cd-21-1059

Hanahan, D., & Weinberg, R. A. (2011). Hallmarks of cancer: the next generation. *Cell*, *144*(5), 646-674. https://doi.org/10.1016/j.cell.2011.02.013

Hanahan, D., & Weinberg, Robert A. (2011). Hallmarks of Cancer: The Next Generation. *Cell*, *144*(5), 646-674. https://doi.org/https://doi.org/10.1016/j.cell.2011.02.013

Hardy, M. P., Owczarek, C. M., Jermiin, L. S., Ejdebäck, M., & Hertzog, P. J. (2004). Characterization of the type I interferon locus and identification of novel genes. *Genomics*, *84*(2), 331-345. https://doi.org/https://doi.org/10.1016/j.ygeno.2004.03.003

Harrison, S. A., Goodman, Z., Jabbar, A., Vemulapalli, R., Younes, Z. H., Freilich, B., Sheikh, M. Y., Schattenberg, J. M., Kayali, Z., Zivony, A., Sheikh, A., Garcia-Samaniego, J., Satapathy, S. K., Therapondos, G., Mena, E., Schuppan, D., Robinson, J., Chan, J. L., Hagerty, D. T., & Sanyal, A. J. (2020). A randomized, placebo-controlled trial of emricasan in patients with NASH and F1-F3 fibrosis. *J Hepatol*, *72*(5), 816-827. https://doi.org/10.1016/j.jhep.2019.11.024

He, Y., Wu, J., Dressman, D. C., Iacobuzio-Donahue, C., Markowitz, S. D., Velculescu, V. E., Diaz Jr, L. A., Kinzler, K. W., Vogelstein, B., & Papadopoulos, N. (2010). Heteroplasmic mitochondrial DNA mutations in normal and tumour cells. *Nature*, *464*(7288), 610-614. https://doi.org/10.1038/nature08802

Helmink, B. A., Khan, M. A. W., Hermann, A., Gopalakrishnan, V., & Wargo, J. A. (2019). The microbiome, cancer, and cancer therapy. *Nat Med*, *25*(3), 377-388. https://doi.org/10.1038/s41591-019-0377-7

Hemmi, H., Takeuchi, O., Kawai, T., Kaisho, T., Sato, S., Sanjo, H., Matsumoto, M., Hoshino, K., Wagner, H., Takeda, K., & Akira, S. (2000). A Toll-like receptor recognizes bacterial DNA. *Nature*, *408*(6813), 740-745. https://doi.org/10.1038/35047123

Herberman, R. B., Nunn, M. E., & Lavrin, D. H. (1975). Natural cytotoxic reactivity of mouse lymphoid cells against syngeneic acid allogeneic tumors. I. Distribution of reactivity and specificity. *Int J Cancer*, *16*(2), 216-229. https://doi.org/10.1002/ijc.2910160204

Hermans, K. G., van Marion, R., van Dekken, H., Jenster, G., van Weerden, W. M., & Trapman, J. (2006). TMPRSS2:ERG fusion by translocation or interstitial deletion is highly relevant in androgen-dependent prostate cancer, but is bypassed in late-stage androgen receptor-negative prostate cancer. *Cancer Res*, *66*(22), 10658-10663. https://doi.org/10.1158/0008-5472.Can-06-1871

Hersh, D., Monack, D. M., Smith, M. R., Ghori, N., Falkow, S., & Zychlinsky, A. (1999). The Salmonella invasin SipB induces macrophage apoptosis by binding to caspase-1. *Proceedings of the National Academy of Sciences*, *96*(5), 2396-2401. https://doi.org/doi:10.1073/pnas.96.5.2396

Hetz, C., & Papa, F. R. (2018). The Unfolded Protein Response and Cell Fate Control. *Mol Cell*, *69*(2), 169-181. https://doi.org/10.1016/j.molcel.2017.06.017

Hodi, F. S., O'Day, S. J., McDermott, D. F., Weber, R. W., Sosman, J. A., Haanen, J. B., Gonzalez, R., Robert, C., Schadendorf, D., Hassel, J. C., Akerley, W., Eertwegh, A. J. M. v. d., Lutzky, J., Lorigan, P., Vaubel, J. M., Linette, G. P., Hogg, D., Ottensmeier, C. H., Lebbé, C., . . . Urba, W. J. (2010). Improved Survival with Ipilimumab in Patients with Metastatic Melanoma. *New England Journal of Medicine*, *363*(8), 711-723. https://doi.org/doi:10.1056/NEJMoa1003466

Holicek, P., Guilbaud, E., Klapp, V., Truxova, I., Spisek, R., Galluzzi, L., & Fucikova, J. (2024). Type I interferon and cancer. *Immunological Reviews*, *321*(1), 115-127. https://doi.org/https://doi.org/10.1111/imr.13272

Holzer, A. K., Samimi, G., Katano, K., Naerdemann, W., Lin, X., Safaei, R., & Howell, S. B. (2004). The copper influx transporter human copper transport protein 1 regulates the uptake of cisplatin in human ovarian carcinoma cells. *Mol Pharmacol*, *66*(4), 817-823. https://doi.org/10.1124/mol.104.001198

Hopkins, J. F., Sabelnykova, V. Y., Weischenfeldt, J., Simon, R., Aguiar, J. A., Alkallas, R., Heisler, L. E., Zhang, J., Watson, J. D., Chua, M. L. K., Fraser, M., Favero, F., Lawerenz, C., Plass, C., Sauter, G., McPherson, J. D., van der Kwast, T., Korbel, J., Schlomm, T., . . . Boutros, P. C. (2017). Mitochondrial mutations drive prostate cancer aggression. *Nat Commun*, *8*(1), 656. https://doi.org/10.1038/s41467-017-00377-y

Hopkins, J. F., Sabelnykova, V. Y., Weischenfeldt, J., Simon, R., Aguiar, J. A., Alkallas, R., Heisler, L. E., Zhang, J., Watson, J. D., Chua, M. L. K., Fraser, M., Favero, F., Lawerenz, C., Plass, C., Sauter, G., McPherson, J. D., van der Kwast, T., Korbel, J., Schlomm, T., . . . Boutros, P. C. (2017). Mitochondrial mutations drive prostate cancer aggression. *Nature Communications*, *8*(1), 656. https://doi.org/10.1038/s41467-017-00377-y

Hosios, A. M., Hecht, V. C., Danai, L. V., Johnson, M. O., Rathmell, J. C., Steinhauser, M. L., Manalis, S. R., & Vander Heiden, M. G. (2016). Amino Acids Rather than Glucose Account for the Majority of Cell Mass in Proliferating Mammalian Cells. *Dev Cell*, *36*(5), 540-549. https://doi.org/10.1016/j.devcel.2016.02.012

Howe, C., Garstka, M., Al-Balushi, M., Ghanem, E., Antoniou, A. N., Fritzsche, S., Jankevicius, G., Kontouli, N., Schneeweiss, C., Williams, A., Elliott, T., & Springer, S. (2009). Calreticulin-dependent recycling in the early secretory pathway mediates optimal peptide loading of MHC class I molecules. *Embo j*, *28*(23), 3730-3744. https://doi.org/10.1038/emboj.2009.296

Hsu, W. M., Hsieh, F. J., Jeng, Y. M., Kuo, M. L., Chen, C. N., Lai, D. M., Hsieh, L. J., Wang, B. T., Tsao, P. N., Lee, H., Lin, M. T., Lai, H. S., & Chen, W. J. (2005). Calreticulin expression in neuroblastoma--a novel independent prognostic factor. *Ann Oncol*, *16*(2), 314-321. https://doi.org/10.1093/annonc/mdi062

Huber, V., Camisaschi, C., Berzi, A., Ferro, S., Lugini, L., Triulzi, T., Tuccitto, A., Tagliabue, E., Castelli, C., & Rivoltini, L. (2017). Cancer acidity: An ultimate frontier of tumor immune escape and a novel target of immunomodulation. *Seminars in Cancer Biology*, *43*, 74-89. https://doi.org/https://doi.org/10.1016/j.semcancer.2017.03.001

Hunter, D. J., Kraft, P., Jacobs, K. B., Cox, D. G., Yeager, M., Hankinson, S. E., Wacholder, S., Wang, Z., Welch, R., Hutchinson, A., Wang, J., Yu, K., Chatterjee, N., Orr, N., Willett, W. C., Colditz, G. A., Ziegler, R. G., Berg, C. D., Buys, S. S., . . . Chanock, S. J. (2007). A genome-wide association study identifies alleles in FGFR2 associated with risk of sporadic postmenopausal breast cancer. *Nat Genet*, *39*(7), 870-874. https://doi.org/10.1038/ng2075

Hwang, C. (2012). Overcoming docetaxel resistance in prostate cancer: a perspective review. *Ther Adv Med Oncol*, *4*(6), 329-340. https://doi.org/10.1177/1758834012449685

Hwang, S., Disatnik, M. H., & Mochly-Rosen, D. (2015). Impaired GAPDH-induced mitophagy contributes to the pathology of Huntington's disease. *EMBO Mol Med*, *7*(10), 1307-1326. https://doi.org/10.15252/emmm.201505256

Igney, F. H., & Krammer, P. H. (2002). Death and anti-death: tumour resistance to apoptosis. *Nat Rev Cancer*, *2*(4), 277-288. https://doi.org/10.1038/nrc776

Imbimbo, M., Ghisoni, E., Mulvey, A., Bouchaab, H., Mederos Alfonso, N., Karp, D., Camidge, D. R., Mansfield, A. S., Yim, C. Y., Ames, T. D., Price, M., Baeck, J., O'Donnell, J. F., & Peters, S. (2022). 125P A phase IIa study of the novel immunogenic cell death (ICD) inducer PT-112 plus avelumab ("PAVE") in advanced non-small cell lung cancer (NSCLC) patients (pts). *Immuno-Oncology and Technology*, *16*, 100237. https://doi.org/https://doi.org/10.1016/j.iotech.2022.100237

Inic, Z., Zegarac, M., Inic, M., Markovic, I., Kozomara, Z., Djurisic, I., Inic, I., Pupic, G., & Jancic, S. (2014). Difference between Luminal A and Luminal B Subtypes According to Ki-67, Tumor Size, and Progesterone Receptor Negativity Providing Prognostic Information. *Clin Med Insights Oncol*, *8*, 107-111. https://doi.org/10.4137/cmo.S18006

Isaacs, A., & Lindenmann, J. (1957). Virus interference. I. The interferon. *Proc R Soc Lond B Biol Sci*, *147*(927), 258-267. https://doi.org/10.1098/rspb.1957.0048

Isaacs, A., Lindenmann, J., & Valentine, R. C. (1957). Virus interference. II. Some properties of interferon. *Proc R Soc Lond B Biol Sci*, *147*(927), 268-273. https://doi.org/10.1098/rspb.1957.0049

Ishida, S., Lee, J., Thiele, D. J., & Herskowitz, I. (2002). Uptake of the anticancer drug cisplatin mediated by the copper transporter Ctr1 in yeast and mammals. *Proc Natl Acad Sci U S A*, *99*(22), 14298-14302. https://doi.org/10.1073/pnas.162491399

Ishida, Y., Agata, Y., Shibahara, K., & Honjo, T. (1992). Induced expression of PD - 1, a novel member of the immunoglobulin gene superfamily, upon programmed cell death. *The EMBO Journal*, *11*(11), 3887-3895. https://doi.org/https://doi.org/10.1002/j.1460-2075.1992.tb05481.x

Ishikawa, H., & Barber, G. N. (2008). STING is an endoplasmic reticulum adaptor that facilitates innate immune signalling. *Nature*, *455*(7213), 674-678. https://doi.org/10.1038/nature07317

Ishikawa, K., Takenaga, K., Akimoto, M., Koshikawa, N., Yamaguchi, A., Imanishi, H., Nakada, K., Honma, Y., & Hayashi, J. (2008). ROS-generating mitochondrial DNA mutations can regulate tumor cell metastasis. *Science*, *320*(5876), 661-664. https://doi.org/10.1126/science.1156906

Isonishi, S., Saitou, M., Yasuda, M., & Tanaka, T. (2001). Mitochondria in platinum resistant cells. *Hum Cell*, *14*(3), 203-210.

Jahnke, W., Rondeau, J.-M., Cotesta, S., Marzinzik, A., Pellé, X., Geiser, M., Strauss, A., Götte, M., Bitsch, F., Hemmig, R., Henry, C., Lehmann, S., Glickman, J. F., Roddy, T. P., Stout, S. J., & Green, J. R. (2010). Allosteric non-bisphosphonate FPPS inhibitors identified by fragment-based discovery. *Nature Chemical Biology*, *6*(9), 660-666. https://doi.org/10.1038/nchembio.421

Jamieson, E. R., & Lippard, S. J. (1999). Structure, Recognition, and Processing of Cisplatin-DNA Adducts. *Chem Rev*, *99*(9), 2467-2498. https://doi.org/10.1021/cr980421n

Jarauta, V., Jaime, P., Gonzalo, O., de Miguel, D., Ramírez-Labrada, A., Martínez-Lostao, L., Anel, A., Pardo, J., Marzo, I., & Naval, J. (2016). Inhibition of autophagy with chloroquine potentiates carfilzomib-induced apoptosis in myeloma cells in vitro and in vivo. *Cancer Letters*, *382*(1), 1-10. https://doi.org/https://doi.org/10.1016/j.canlet.2016.08.019

Jayaraman, L., Moorthy, N. C., Murthy, K. G., Manley, J. L., Bustin, M., & Prives, C. (1998). High mobility group protein-1 (HMG-1) is a unique activator of p53. *Genes Dev*, *12*(4), 462-472. https://doi.org/10.1101/gad.12.4.462

Jego, G., Palucka, A. K., Blanck, J. P., Chalouni, C., Pascual, V., & Banchereau, J. (2003). Plasmacytoid dendritic cells induce plasma cell differentiation through type I interferon and interleukin 6. *Immunity*, *19*(2), 225-234. https://doi.org/10.1016/s1074-7613(03)00208-5

Jenson, J., & Chen, Z. J. (2020). Bacteria sting viral invaders. *Nature*, *586*(7829), 363-364. https://doi.org/10.1038/d41586-020-02712-8

Jerónimo, C., Nomoto, S., Caballero, O. L., Usadel, H., Henrique, R., Varzim, G., Oliveira, J., Lopes, C., Fliss, M. S., & Sidransky, D. (2001). Mitochondrial mutations in early stage prostate cancer and bodily fluids. *Oncogene*, *20*(37), 5195-5198. https://doi.org/10.1038/sj.onc.1204646

Jessie, B. C., Sun, C. Q., Irons, H. R., Marshall, F. F., Wallace, D. C., & Petros, J. A. (2001). Accumulation of mitochondrial DNA deletions in the malignant prostate of patients of different ages. *Experimental Gerontology*, *37*(1), 169-174. https://doi.org/https://doi.org/10.1016/S0531-5565(01)00153-X

Jhunjhunwala, S., Hammer, C., & Delamarre, L. (2021). Antigen presentation in cancer: insights into tumour immunogenicity and immune evasion. *Nature Reviews Cancer*, *21*(5), 298-312. https://doi.org/10.1038/s41568-021-00339-z

Jiménez-Loygorri, J. I., Villarejo-Zori, B., Viedma-Poyatos, Á., Zapata-Muñoz, J., Benítez-Fernández, R., Frutos-Lisón, M. D., Tomás-Barberán, F. A., Espín, J. C., Area-Gómez, E., Gomez-Duran, A., & Boya, P. (2024). Mitophagy curtails cytosolic mtDNA-dependent activation of cGAS/STING inflammation during aging. *Nature Communications*, *15*(1), 830. https://doi.org/10.1038/s41467-024-45044-1

Jin, H. S., Suh, H. W., Kim, S. J., & Jo, E. K. (2017). Mitochondrial Control of Innate Immunity and Inflammation. *Immune Netw*, *17*(2), 77-88. https://doi.org/10.4110/in.2017.17.2.77

Johnson, S., Michalak, M., Opas, M., & Eggleton, P. (2001). The ins and outs of calreticulin: from the ER lumen to the extracellular space. *Trends Cell Biol*, *11*(3), 122-129. https://doi.org/10.1016/s0962-8924(01)01926-2

Jordan, V. C. (2003). Tamoxifen: a most unlikely pioneering medicine. *Nature Reviews Drug Discovery*, *2*(3), 205-213. https://doi.org/10.1038/nrd1031

Ju, Y. S., Tubio, J. M., Mifsud, W., Fu, B., Davies, H. R., Ramakrishna, M., Li, Y., Yates, L., Gundem, G., Tarpey, P. S., Behjati, S., Papaemmanuil, E., Martin, S., Fullam, A., Gerstung, M., Nangalia, J., Green, A. R., Caldas, C., Borg, Å., . . . Stratton, M. R. (2015). Frequent somatic transfer of mitochondrial DNA into the nuclear genome of human cancer cells. *Genome Res*, *25*(6), 814-824. https://doi.org/10.1101/gr.190470.115

Junttila, M. R., & Evan, G. I. (2009). p53 — a Jack of all trades but master of none. *Nature Reviews Cancer*, *9*(11), 821-829. https://doi.org/10.1038/nrc2728

Kai, F., Drain, A. P., & Weaver, V. M. (2019). The Extracellular Matrix Modulates the Metastatic Journey. *Developmental Cell*, *49*(3), 332-346. https://doi.org/https://doi.org/10.1016/j.devcel.2019.03.026

Kalinski, P. (2012). Regulation of immune responses by prostaglandin E2. *J Immunol*, *188*(1), 21-28. https://doi.org/10.4049/jimmunol.1101029

Kaloni, D., Diepstraten, S. T., Strasser, A., & Kelly, G. L. (2023). BCL-2 protein family: attractive targets for cancer therapy. *Apoptosis*, *28*(1-2), 20-38. https://doi.org/10.1007/s10495-022-01780-7

Karp, D. D., Camidge, D. R., Infante, J. R., Ames, T. D., Jimeno, J. M., & Bryce, A. H. (2018). 437P - PT-112: A well-tolerated novel immunogenic cell death (ICD) inducer with activity in advanced solid tumors. *Annals of Oncology*, *29*, viii143. https://doi.org/https://doi.org/10.1093/annonc/mdy279.424

Karp, D. D., Camidge, D. R., Infante, J. R., Ames, T. D., Price, M. R., Jimeno, J., & Bryce, A. H. (2022). Phase I study of PT-112, a novel pyrophosphate-platinum immunogenic cell death inducer, in advanced solid tumours. *EClinicalMedicine*, *49*, 101430. https://doi.org/10.1016/j.eclinm.2022.101430

Kauffman, G. B., Pentimalli, R., Doldi , S., & Hall, M. D. (2010). Michele Peyrone (1813–1883), Discoverer of Cisplatin. *Platinum Metals Review*, *54*(4), 250-256. https://doi.org/https://doi.org/10.1595/147106710X534326

Kaur, A., Ecker, B. L., Douglass, S. M., Kugel, C. H., 3rd, Webster, M. R., Almeida, F. V., Somasundaram, R., Hayden, J., Ban, E., Ahmadzadeh, H., Franco-Barraza, J., Shah, N., Mellis, I. A., Keeney, F., Kossenkov, A., Tang, H. Y., Yin, X., Liu, Q., Xu, X., . . . Weeraratna, A. T. (2019). Remodeling of the

Collagen Matrix in Aging Skin Promotes Melanoma Metastasis and Affects Immune Cell Motility. *Cancer Discov*, *9*(1), 64-81. https://doi.org/10.1158/2159-8290.Cd-18-0193

Kaur, J., & Dora, S. (2023). Purinergic signaling: Diverse effects and therapeutic potential in cancer. *Front Oncol*, *13*, 1058371. https://doi.org/10.3389/fonc.2023.1058371

Kaushik, S., & Cuervo, A. M. (2018). The coming of age of chaperone-mediated autophagy. *Nat Rev Mol Cell Biol*, *19*(6), 365-381. https://doi.org/10.1038/s41580-018-0001-6

Ke, F. F. S., Vanyai, H. K., Cowan, A. D., Delbridge, A. R. D., Whitehead, L., Grabow, S., Czabotar, P. E., Voss, A. K., & Strasser, A. (2018). Embryogenesis and Adult Life in the Absence of Intrinsic Apoptosis Effectors BAX, BAK, and BOK. *Cell*, *173*(5), 1217-1230.e1217. https://doi.org/https://doi.org/10.1016/j.cell.2018.04.036

Keefe, D., Shi, L., Feske, S., Massol, R., Navarro, F., Kirchhausen, T., & Lieberman, J. (2005). Perforin Triggers a Plasma Membrane-Repair Response that Facilitates CTL Induction of Apoptosis. *Immunity*, *23*(3), 249-262. https://doi.org/https://doi.org/10.1016/j.immuni.2005.08.001

Kelland, L. R., Sharp, S. Y., O'Neill, C. F., Raynaud, F. I., Beale, P. J., & Judson, I. R. (1999). Mini-review: discovery and development of platinum complexes designed to circumvent cisplatin resistance. *J Inorg Biochem*, *77*(1-2), 111-115.

Kenny, F. S., Hui, R., Musgrove, E. A., Gee, J. M., Blamey, R. W., Nicholson, R. I., Sutherland, R. L., & Robertson, J. F. (1999). Overexpression of cyclin D1 messenger RNA predicts for poor prognosis in estrogen receptor-positive breast cancer. *Clin Cancer Res*, *5*(8), 2069-2076.

Kepp, O., Bezu, L., Yamazaki, T., Di Virgilio, F., Smyth, M. J., Kroemer, G., & Galluzzi, L. (2021). ATP and cancer immunosurveillance. *Embo j*, *40*(13), e108130. https://doi.org/10.15252/embj.2021108130

Kepp, O., & Kroemer, G. (2020). Autophagy induction by thiostrepton for the improvement of anticancer therapy. *Autophagy*, *16*(6), 1166-1167. https://doi.org/10.1080/15548627.2020.1758417

Kepp, O., & Kroemer, G. (2020). A novel platinum-based chemotherapeutic inducing immunogenic cell death. *OncoImmunology*, *9*(1), 1729022. https://doi.org/10.1080/2162402x.2020.1729022

Kerr, J. F. R., Wyllie, A. H., & Currie, A. R. (1972). Apoptosis: A Basic Biological Phenomenon with Wideranging Implications in Tissue Kinetics. *British Journal of Cancer*, *26*(4), 239-257. https://doi.org/10.1038/bjc.1972.33

Khoo, L. T., & Chen, L. Y. (2018). Role of the cGAS–STING pathway in cancer development and oncotherapeutic approaches. *EMBO reports*, *19*(12), e46935. https://doi.org/https://doi.org/10.15252/embr.201846935

Kim, H., Rafiuddin-Shah, M., Tu, H.-C., Jeffers, J. R., Zambetti, G. P., Hsieh, J. J. D., & Cheng, E. H. Y. (2006). Hierarchical regulation of mitochondrion-dependent apoptosis by BCL-2 subfamilies. *Nature Cell Biology*, *8*(12), 1348-1358. https://doi.org/10.1038/ncb1499

Kim, J., Kim, H.-S., & Chung, J. H. (2023). Molecular mechanisms of mitochondrial DNA release and activation of the cGAS-STING pathway. *Experimental & Molecular Medicine*, *55*(3), 510-519. https://doi.org/10.1038/s12276-023-00965-7

Kim, M., Mahmood, M., Reznik, E., & Gammage, P. A. (2022). Mitochondrial DNA is a major source of driver mutations in cancer. *Trends Cancer*, *8*(12), 1046-1059. https://doi.org/10.1016/j.trecan.2022.08.001

King, M. P., & Attardi, G. (1989). Human Cells Lacking mtDNA: Repopulation with Exogenous Mitochondria by Complementation. *Science*, *246*(4929), 500-503. https://doi.org/doi:10.1126/science.2814477

Kleele, T., Rey, T., Winter, J., Zaganelli, S., Mahecic, D., Perreten Lambert, H., Ruberto, F. P., Nemir, M., Wai, T., Pedrazzini, T., & Manley, S. (2021). Distinct fission signatures predict mitochondrial degradation or biogenesis. *Nature*, *593*(7859), 435-439. https://doi.org/10.1038/s41586-021-03510-6

Kleih, M., Böpple, K., Dong, M., Gaißler, A., Heine, S., Olayioye, M. A., Aulitzky, W. E., & Essmann, F. (2019). Direct impact of cisplatin on mitochondria induces ROS production that dictates cell fate of ovarian cancer cells. *Cell Death Dis*, *10*(11), 851. https://doi.org/10.1038/s41419-019-2081-4

Klein, G., Sjogren, H. O., Klein, E., & Hellstrom, K. E. (1960). Demonstration of resistance against methylcholanthrene-induced sarcomas in the primary autochthonous host. *Cancer Res*, *20*, 1561-1572.

Klionsky, D. J., Abdel-Aziz, A. K., Abdelfatah, S., Abdellatif, M., Abdoli, A., Abel, S., Abeliovich, H., Abildgaard, M. H., Abudu, Y. P., Acevedo-Arozena, A., Adamopoulos, I. E., Adeli, K., Adolph, T. E., Adornetto, A., Aflaki, E., Agam, G., Agarwal, A., Aggarwal, B. B., Agnello, M., . . . Tong, C. K. (2021). Guidelines for the use and interpretation of assays for monitoring autophagy (4th edition)(1). *Autophagy*, *17*(1), 1-382. https://doi.org/10.1080/15548627.2020.1797280

Kloss-Brandstätter, A., Schäfer, G., Erhart, G., Hüttenhofer, A., Coassin, S., Seifarth, C., Summerer, M., Bektic, J., Klocker, H., & Kronenberg, F. (2010). Somatic mutations throughout the entire mitochondrial genome are associated with elevated PSA levels in prostate cancer patients. *Am J Hum Genet*, *87*(6), 802-812. https://doi.org/10.1016/j.ajhg.2010.11.001

Komatsu, M., Sumizawa, T., Mutoh, M., Chen, Z. S., Terada, K., Furukawa, T., Yang, X. L., Gao, H., Miura, N., Sugiyama, T., & Akiyama, S. (2000). Copper-transporting P-type adenosine triphosphatase (ATP7B) is associated with cisplatin resistance. *Cancer Res*, *60*(5), 1312-1316.

Kopinski, P. K., Singh, L. N., Zhang, S., Lott, M. T., & Wallace, D. C. (2021). Mitochondrial DNA variation and cancer. *Nat Rev Cancer*, *21*(7), 431-445. https://doi.org/10.1038/s41568-021-00358-w

Kourelis, T., Ailawadhi, S., Vogl, D. T., Cooper, D., Ames, T. D., Yim, C. Y., Price, M. R., Jimeno, J. J., & Bergsagel, P. L. (2020). A Phase I Dose Escalation Study of PT-112 in Patients with Relapsed or Refractory Multiple Myeloma. *Blood*, *136*, 9-10. https://doi.org/https://doi.org/10.1182/blood-2020-134916

Kowaltowski, A. J., & Vercesi, A. E. (1999). Mitochondrial damage induced by conditions of oxidative stress. *Free Radic Biol Med*, *26*(3-4), 463-471. https://doi.org/10.1016/s0891-5849(98)00216-0

Kroemer, G., Chan, T. A., Eggermont, A. M. M., & Galluzzi, L. (2024). Immunosurveillance in clinical cancer management. *CA: A Cancer Journal for Clinicians*, *74*(2), 187-202. https://doi.org/https://doi.org/10.3322/caac.21818

Kroemer, G., Galassi, C., Zitvogel, L., & Galluzzi, L. (2022). Immunogenic cell stress and death. *Nature Immunology*, *23*(4), 487-500. https://doi.org/10.1038/s41590-022-01132-2

Kühlbrandt, W. (2015). Structure and function of mitochondrial membrane protein complexes. *BMC Biology*, *13*(1), 89. https://doi.org/10.1186/s12915-015-0201-x

Kumar, B., Koul, S., Khandrika, L., Meacham, R. B., & Koul, H. K. (2008). Oxidative Stress Is Inherent in Prostate Cancer Cells and Is Required for Aggressive Phenotype. *Cancer Research*, *68*(6), 1777-1785. https://doi.org/10.1158/0008-5472.Can-07-5259

Kwon, J., & Bakhoum, S. F. (2020). The Cytosolic DNA-Sensing cGAS-STING Pathway in Cancer. *Cancer Discov*, *10*(1), 26-39. https://doi.org/10.1158/2159-8290.Cd-19-0761

Lambert, A. W., Pattabiraman, D. R., & Weinberg, R. A. (2017). Emerging Biological Principles of Metastasis. *Cell*, *168*(4), 670-691. https://doi.org/https://doi.org/10.1016/j.cell.2016.11.037

Lane, N., & Martin, W. (2010). The energetics of genome complexity. *Nature*, *467*(7318), 929-934. https://doi.org/10.1038/nature09486

Lapuente-Brun, E., Moreno-Loshuertos, R., Acín-Pérez, R., Latorre-Pellicer, A., Colás, C., Balsa, E., Perales-Clemente, E., Quirós, P. M., Calvo, E., Rodríguez-Hernández, M. A., Navas, P., Cruz, R., Carracedo, Á., López-Otín, C., Pérez-Martos, A., Fernández-Silva, P., Fernández-Vizarra, E., & Enríquez, J. A. (2013). Supercomplex assembly determines electron flux in the mitochondrial electron transport chain. *Science*, *340*(6140), 1567-1570. https://doi.org/10.1126/science.1230381

Latz, E., Schoenemeyer, A., Visintin, A., Fitzgerald, K. A., Monks, B. G., Knetter, C. F., Lien, E., Nilsen, N. J., Espevik, T., & Golenbock, D. T. (2004). TLR9 signals after translocating from the ER to CpG DNA in the lysosome. *Nat Immunol*, *5*(2), 190-198. https://doi.org/10.1038/ni1028

Lauber, K., Bohn, E., Kröber, S. M., Xiao, Y. J., Blumenthal, S. G., Lindemann, R. K., Marini, P., Wiedig, C., Zobywalski, A., Baksh, S., Xu, Y., Autenrieth, I. B., Schulze-Osthoff, K., Belka, C., Stuhler, G., & Wesselborg, S. (2003). Apoptotic cells induce migration of phagocytes via caspase-3-mediated release of a lipid attraction signal. *Cell*, *113*(6), 717-730. https://doi.org/10.1016/s0092-8674(03)00422-7

Le Naour, J., Liu, P., Zhao, L., Adjemian, S., Sztupinszki, Z., Taieb, J., Mulot, C., Silvin, A., Dutertre, C. A., Ginhoux, F., Sauvat, A., Cerrato, G., Castoldi, F., Martins, I., Stoll, G., Paillet, J., Mangane, K., Richter, C., Kepp, O., . . . Kroemer, G. (2021). A TLR3 Ligand Reestablishes Chemotherapeutic Responses in the Context of FPR1 Deficiency. *Cancer Discov*, *11*(2), 408-423. https://doi.org/10.1158/2159-8290.Cd-20-0465

Levine, B., & Kroemer, G. (2019). Biological Functions of Autophagy Genes: A Disease Perspective. *Cell*, *176*(1-2), 11-42. https://doi.org/10.1016/j.cell.2018.09.048

Levy, J. M. M., Towers, C. G., & Thorburn, A. (2017). Targeting autophagy in cancer. *Nature Reviews Cancer*, *17*(9), 528-542. https://doi.org/10.1038/nrc.2017.53

Li, P., Nijhawan, D., Budihardjo, I., Srinivasula, S. M., Ahmad, M., Alnemri, E. S., & Wang, X. (1997). Cytochrome c and dATP-Dependent Formation of Apaf-1/Caspase-9 Complex Initiates an Apoptotic Protease Cascade. *Cell*, *91*(4), 479-489. https://doi.org/https://doi.org/10.1016/S0092-8674(00)80434-1

Li, Z., Wang, Y., Wu, L., Dong, Y., Zhang, J., Chen, F., Xie, W., Huang, J., & Lu, N. (2019). Apurinic endonuclease 1 promotes the cisplatin resistance of lung cancer cells by inducing Parkin-mediated mitophagy. *Oncol Rep*, *42*(6), 2245-2254. https://doi.org/10.3892/or.2019.7345

Liao, P.-C., Bergamini, C., Fato, R., Pon, L. A., & Pallotti, F. (2020). Chapter 1 - Isolation of mitochondria from cells and tissues. In L. A. Pon & E. A. Schon (Eds.), *Methods in Cell Biology* (Vol. 155, pp. 3-31). Academic Press. https://doi.org/https://doi.org/10.1016/bs.mcb.2019.10.002

Liberti, M. V., & Locasale, J. W. (2016). The Warburg Effect: How Does it Benefit Cancer Cells? *Trends in Biochemical Sciences*, *41*(3), 211-218. https://doi.org/https://doi.org/10.1016/j.tibs.2015.12.001

Limagne, E., Nuttin, L., Thibaudin, M., Jacquin, E., Aucagne, R., Bon, M., Revy, S., Barnestein, R., Ballot, E., Truntzer, C., Derangère, V., Fumet, J. D., Latour, C., Rébé, C., Bellaye, P. S., Kaderbhaï, C. G., Spill, A., Collin, B., Callanan, M. B., . . . Ghiringhelli, F. (2022). MEK inhibition overcomes chemoimmunotherapy resistance by inducing CXCL10 in cancer cells. *Cancer Cell*, *40*(2), 136-152.e112. https://doi.org/10.1016/j.ccell.2021.12.009

Lin, M. J., Svensson-Arvelund, J., Lubitz, G. S., Marabelle, A., Melero, I., Brown, B. D., & Brody, J. D. (2022). Cancer vaccines: the next immunotherapy frontier. *Nature Cancer*, *3*(8), 911-926. https://doi.org/10.1038/s43018-022-00418-6

Lindberg, J., Mills, I. G., Klevebring, D., Liu, W., Neiman, M., Xu, J., Wikström, P., Wiklund, P., Wiklund, F., Egevad, L., & Grönberg, H. (2013). The mitochondrial and autosomal mutation landscapes of prostate cancer. *Eur Urol*, *63*(4), 702-708. https://doi.org/10.1016/j.eururo.2012.11.053

Liu, I. J., Zafar, M. B., Lai, Y. H., Segall, G. M., & Terris, M. K. (2001). Fluorodeoxyglucose positron emission tomography studies in diagnosis and staging of clinically organ-confined prostate cancer. *Urology*, *57*(1), 108-111. https://doi.org/10.1016/s0090-4295(00)00896-7

Liu, Q., Li, J., Zheng, H., Yang, S., Hua, Y., Huang, N., Kleeff, J., Liao, Q., & Wu, W. (2023). Adoptive cellular immunotherapy for solid neoplasms beyond CAR-T. *Molecular Cancer*, *22*(1), 28. https://doi.org/10.1186/s12943-023-01735-9

Liu, Y., Franklin, R. B., & Costello, L. C. (1997). Prolactin and testosterone regulation of mitochondrial zinc in prostate epithelial cells. *Prostate*, *30*(1), 26-32. https://doi.org/10.1002/(sici)1097-0045(19970101)30:1<26::aid-pros4>3.0.co;2-j

Liu, Y., Fu, Y., Hu, X., Chen, S., Miao, J., Wang, Y., Zhou, Y., & Zhang, Y. (2020). Caveolin-1 knockdown increases the therapeutic sensitivity of lung cancer to cisplatin-induced apoptosis by repressing Parkin-related mitophagy and activating the ROCK1 pathway. *J Cell Physiol*, *235*(2), 1197-1208. https://doi.org/10.1002/jcp.29033

Livesey, K. M., Kang, R., Vernon, P., Buchser, W., Loughran, P., Watkins, S. C., Zhang, L., Manfredi, J. J., Zeh, H. J., III, Li, L., Lotze, M. T., & Tang, D. (2012). p53/HMGB1 Complexes Regulate Autophagy and Apoptosis. *Cancer Research*, *72*(8), 1996-2005. https://doi.org/10.1158/0008-5472.Can-11-2291

Loblaw, D. A., Perry, J., Chambers, A., & Laperriere, N. J. (2005). Systematic review of the diagnosis and management of malignant extradural spinal cord compression: the Cancer Care Ontario Practice Guidelines Initiative's Neuro-Oncology Disease Site Group. *J Clin Oncol*, *23*(9), 2028-2037. https://doi.org/10.1200/jco.2005.00.067

Lobo-Jarne, T., & Ugalde, C. (2018). Respiratory chain supercomplexes: Structures, function and biogenesis. *Semin Cell Dev Biol*, *76*, 179-190. https://doi.org/10.1016/j.semcdb.2017.07.021

Locasale, J. W., Grassian, A. R., Melman, T., Lyssiotis, C. A., Mattaini, K. R., Bass, A. J., Heffron, G., Metallo, C. M., Muranen, T., Sharfi, H., Sasaki, A. T., Anastasiou, D., Mullarky, E., Vokes, N. I., Sasaki, M., Beroukhim, R., Stephanopoulos, G., Ligon, A. H., Meyerson, M., . . . Vander Heiden, M. G. (2011). Phosphoglycerate dehydrogenase diverts glycolytic flux and contributes to oncogenesis. *Nat Genet*, *43*(9), 869-874. https://doi.org/10.1038/ng.890

Locke, F. L., Filosto, S., Chou, J., Vardhanabhuti, S., Perbost, R., Dreger, P., Hill, B. T., Lee, C., Zinzani, P. L., Kröger, N., López-Guillermo, A., Greinix, H., Zhang, W., Tiwari, G., Budka, J., Marincola, F. M., To, C., Mattie, M., Schupp, M., . . . Galon, J. (2024). Impact of tumor microenvironment on efficacy of anti-CD19 CAR T cell therapy or chemotherapy and transplant in large B cell lymphoma. *Nature Medicine*, *30*(2), 507-518. https://doi.org/10.1038/s41591-023-02754-1

Lord, C. J., & Ashworth, A. (2012). The DNA damage response and cancer therapy. *Nature*, *481*(7381), 287-294. https://doi.org/10.1038/nature10760

Loveland, B. E., Johns, T. G., Mackay, I. R., Vaillant, F., Wang, Z. X., & Hertzog, P. J. (1992). Validation of the MTT dye assay for enumeration of cells in proliferative and antiproliferative assays. *Biochemistry international*, *27*(3), 501-510. http://europepmc.org/abstract/MED/1417886

Lu, C., Klement, J. D., Ibrahim, M. L., Xiao, W., Redd, P. S., Nayak-Kapoor, A., Zhou, G., & Liu, K. (2019). Type I interferon suppresses tumor growth through activating the STAT3-granzyme B pathway in tumor-infiltrating cytotoxic T lymphocytes. *J Immunother Cancer*, *7*(1), 157. https://doi.org/10.1186/s40425-019-0635-8

Lu, C., Venneti, S., Akalin, A., Fang, F., Ward, P. S., Dematteo, R. G., Intlekofer, A. M., Chen, C., Ye, J., Hameed, M., Nafa, K., Agaram, N. P., Cross, J. R., Khanin, R., Mason, C. E., Healey, J. H., Lowe, S. W., Schwartz, G. K., Melnick, A., & Thompson, C. B. (2013). Induction of sarcomas by mutant IDH2. *Genes Dev*, *27*(18), 1986-1998. https://doi.org/10.1101/gad.226753.113

Lu, J., Sharma, L. K., & Bai, Y. (2009). Implications of mitochondrial DNA mutations and mitochondrial dysfunction in tumorigenesis. *Cell Res*, *19*(7), 802-815. https://doi.org/10.1038/cr.2009.69

Luengo, A., Gui, D. Y., & Vander Heiden, M. G. (2017). Targeting Metabolism for Cancer Therapy. *Cell Chem Biol*, *24*(9), 1161-1180. https://doi.org/10.1016/j.chembiol.2017.08.028

Lunt, S. Y., & Vander Heiden, M. G. (2011). Aerobic glycolysis: meeting the metabolic requirements of cell proliferation. *Annu Rev Cell Dev Biol*, *27*, 441-464. https://doi.org/10.1146/annurev-cellbio-092910-154237

Mackenzie, K. J., Carroll, P., Martin, C. A., Murina, O., Fluteau, A., Simpson, D. J., Olova, N., Sutcliffe, H., Rainger, J. K., Leitch, A., Osborn, R. T., Wheeler, A. P., Nowotny, M., Gilbert, N., Chandra, T., Reijns, M. A. M., & Jackson, A. P. (2017). cGAS surveillance of micronuclei links genome instability to innate immunity. *Nature*, *548*(7668), 461-465. https://doi.org/10.1038/nature23449

Makgoba, M. W., Sanders, M. E., Ginther Luce, G. E., Gugel, E. A., Dustin, M. L., Springer, T. A., & Shaw, S. (1988). Functional evidence that intercellular adhesion molecule-1 (ICAM-1) is a ligand for LFA-1-dependent adhesion in T cell-mediated cytotoxicity. *Eur J Immunol*, *18*(4), 637-640. https://doi.org/10.1002/eji.1830180423

Mangalhara, K. C., Varanasi, S. K., Johnson, M. A., Burns, M. J., Rojas, G. R., Esparza Moltó, P. B., Sainz, A. G., Tadepalle, N., Abbott, K. L., Mendiratta, G., Chen, D., Farsakoglu, Y., Kunchok, T., Hoffmann, F. A., Parisi, B., Rincon, M., Vander Heiden, M. G., Bosenberg, M., Hargreaves, D. C., . . . Shadel, G. S. (2023). Manipulating mitochondrial electron flow enhances tumor immunogenicity. *Science*, *381*(6664), 1316-1323. https://doi.org/10.1126/science.abq1053

Marchi, S., Guilbaud, E., Tait, S. W. G., Yamazaki, T., & Galluzzi, L. (2023). Mitochondrial control of inflammation. *Nat Rev Immunol*, *23*(3), 159-173. https://doi.org/10.1038/s41577-022-00760-x

Marco-Brualla, J., Al-Wasaby, S., Soler, R., Romanos, E., Conde, B., Justo-Méndez, R., Enríquez, J. A., Fernández-Silva, P., Martínez-Lostao, L., Villalba, M., Moreno-Loshuertos, R., & Anel, A. (2019). Mutations in the ND2 Subunit of Mitochondrial Complex I Are Sufficient to Confer Increased Tumorigenic and Metastatic Potential to Cancer Cells. *Cancers (Basel)*, *11*(7). https://doi.org/10.3390/cancers11071027

Mariathasan, S., Weiss, D. S., Newton, K., McBride, J., O'Rourke, K., Roose-Girma, M., Lee, W. P., Weinrauch, Y., Monack, D. M., & Dixit, V. M. (2006). Cryopyrin activates the inflammasome in response to toxins and ATP. *Nature*, *440*(7081), 228-232. https://doi.org/10.1038/nature04515

Marrack, P., Kappler, J., & Mitchell, T. (1999). Type I interferons keep activated T cells alive. *J Exp Med*, *189*(3), 521-530. https://doi.org/10.1084/jem.189.3.521

Martelli, L., Di Mario, F., Ragazzi, E., Apostoli, P., Leone, R., Perego, P., & Fumagalli, G. (2006). Different accumulation of cisplatin, oxaliplatin and JM216 in sensitive and cisplatin-resistant human cervical tumour cells. *Biochem Pharmacol*, *72*(6), 693-700. https://doi.org/10.1016/j.bcp.2006.06.008

Martínez-Lorenzo, M. J., Anel, A., Gamen, S., Monle n, I., Lasierra, P., Larrad, L., Piñeiro, A., Alava, M. A., & Naval, J. (1999). Activated human T cells release bioactive Fas ligand and APO2 ligand in microvesicles. *J Immunol*, *163*(3), 1274-1281.

Martínez-Lostao, L., Anel, A., & Pardo, J. (2015). How Do Cytotoxic Lymphocytes Kill Cancer Cells? *Clin Cancer Res*, *21*(22), 5047-5056. https://doi.org/10.1158/1078-0432.Ccr-15-0685

Martínez-Reyes, I., & Chandel, N. S. (2021). Cancer metabolism: looking forward. *Nature Reviews Cancer*, *21*(10), 669-680. https://doi.org/10.1038/s41568-021-00378-6

Martins, I., Michaud, M., Sukkurwala, A. Q., Adjemian, S., Ma, Y., Shen, S., Kepp, O., Menger, L., Vacchelli, E., Galluzzi, L., Zitvogel, L., & Kroemer, G. (2012). Premortem autophagy determines the immunogenicity of chemotherapy-induced cancer cell death. *Autophagy*, *8*(3), 413-415. https://doi.org/10.4161/auto.19009

Martins, I., Wang, Y., Michaud, M., Ma, Y., Sukkurwala, A. Q., Shen, S., Kepp, O., Métivier, D., Galluzzi, L., Perfettini, J. L., Zitvogel, L., & Kroemer, G. (2014a). Molecular mechanisms of ATP secretion during immunogenic cell death. *Cell Death & Differentiation*, *21*(1), 79-91. https://doi.org/10.1038/cdd.2013.75

Martins, I., Wang, Y., Michaud, M., Ma, Y., Sukkurwala, A. Q., Shen, S., Kepp, O., Métivier, D., Galluzzi, L., Perfettini, J. L., Zitvogel, L., & Kroemer, G. (2014b). Molecular mechanisms of ATP secretion during immunogenic cell death. *Cell Death Differ*, *21*(1), 79-91. https://doi.org/10.1038/cdd.2013.75

Masri, S., & Sassone-Corsi, P. (2018). The emerging link between cancer, metabolism, and circadian rhythms. *Nature Medicine*, *24*(12), 1795-1803. https://doi.org/10.1038/s41591-018-0271-8

Massagué, J., & Ganesh, K. (2021). Metastasis-Initiating Cells and Ecosystems. *Cancer Discovery*, *11*(4), 971-994. https://doi.org/10.1158/2159-8290.Cd-21-0010

Massie, C. E., Lynch, A., Ramos-Montoya, A., Boren, J., Stark, R., Fazli, L., Warren, A., Scott, H., Madhu, B., Sharma, N., Bon, H., Zecchini, V., Smith, D. M., Denicola, G. M., Mathews, N., Osborne, M., Hadfield, J., Macarthur, S., Adryan, B., . . . Mills, I. G. (2011). The androgen receptor fuels prostate cancer by regulating central metabolism and biosynthesis. *Embo j*, *30*(13), 2719-2733. https://doi.org/10.1038/emboj.2011.158

McAdams, M., Swift, S., Donahue, R. N., Celades, C., Tsai, Y.-T., Bingham, M. A., Szabó, É., Zhao, C., Sansone, S., Choradia, N., Shelat, M., O'Donnell, J. F., Ames, T. D., Raphael, B., Steinberg, S. M., Gulley, J. L., Schlom, J., & Rajan, A. (2023). Preliminary efficacy, safety, and immunomodulatory effects of PT-112 from a phase 2 proof of concept study in patients (pts) with thymic epithelial tumors (TETs). *Journal of Clinical Oncology*.

McAdams, M., Swift, S., Donahue, R. N., Celades, C., Tsai, Y. T., Bingham, M., Szabo, E., Zhao, C., Sansone, S., Choradia, N., Shelat, M., O'Donnell, J. F., Ames, T. D., Raphael, B., Steinberg, S. M., Gulley, J. L., Schlom, J., & Rajan, A. (2023). Preliminary efficacy, safety, and immunomodulatory effects of PT-112 from a phase 2 proof of concept study in patients (pts) with thymic epithelial tumors (TETs) [Meeting Abstract]. *Journal of Clinical Oncology*, *41*(16), 1. <Go to ISI>://WOS:001053772004757

McArthur, K., Whitehead, L. W., Heddleston, J. M., Li, L., Padman, B. S., Oorschot, V., Geoghegan, N. D., Chappaz, S., Davidson, S., San Chin, H., Lane, R. M., Dramicanin, M., Saunders, T. L., Sugiana, C., Lessene, R., Osellame, L. D., Chew, T. L., Dewson, G., Lazarou, M., . . . Kile, B. T. (2018). BAK/BAX macropores facilitate mitochondrial herniation and mtDNA efflux during apoptosis. *Science*, *359*(6378). https://doi.org/10.1126/science.aao6047

McMenamin, M. E., Soung, P., Perera, S., Kaplan, I., Loda, M., & Sellers, W. R. (1999). Loss of PTEN expression in paraffin-embedded primary prostate cancer correlates with high Gleason score and advanced stage. *Cancer Res*, *59*(17), 4291-4296.

MedChemExpress. (2024). *Imifoplatin* Retrieved April 28, 2024 from https://www.medchemexpress.com/imifoplatin.html?locale=en

Mescher, M. F., Curtsinger, J. M., Agarwal, P., Casey, K. A., Gerner, M., Hammerbeck, C. D., Popescu, F., & Xiao, Z. (2006). Signals required for programming effector and memory development by CD8+ T cells. *Immunol Rev*, *211*, 81-92. https://doi.org/10.1111/j.0105-2896.2006.00382.x

Metkar, S. S., Menaa, C., Pardo, J., Wang, B., Wallich, R., Freudenberg, M., Kim, S., Raja, S. M., Shi, L., Simon, M. M., & Froelich, C. J. (2008). Human and mouse granzyme A induce a proinflammatory cytokine response. *Immunity*, *29*(5), 720-733. https://doi.org/10.1016/j.immuni.2008.08.014

Michaud, M., Martins, I., Sukkurwala, A. Q., Adjemian, S., Ma, Y., Pellegatti, P., Shen, S., Kepp, O., Scoazec, M., Mignot, G., Rello-Varona, S., Tailler, M., Menger, L., Vacchelli, E., Galluzzi, L., Ghiringhelli, F., di Virgilio, F., Zitvogel, L., & Kroemer, G. (2011). Autophagy-dependent anticancer immune responses induced by chemotherapeutic agents in mice. *Science*, *334*(6062), 1573-1577. https://doi.org/10.1126/science.1208347

Miki, Y., Swensen, J., Shattuck-Eidens, D., Futreal, P. A., Harshman, K., Tavtigian, S., Liu, Q., Cochran, C., Bennett, L. M., Ding, W., & et al. (1994). A strong candidate for the breast and ovarian cancer susceptibility gene BRCA1. *Science*, *266*(5182), 66-71. https://doi.org/10.1126/science.7545954

Mizutani, T., Neugebauer, N., Putz, E. M., Moritz, N., Simma, O., Zebedin-Brandl, E., Gotthardt, D., Warsch, W., Eckelhart, E., Kantner, H. P., Kalinke, U., Lienenklaus, S., Weiss, S., Strobl, B., Müller, M., Sexl, V., & Stoiber, D. (2012). Conditional IFNAR1 ablation reveals distinct requirements of Type I IFN signaling for NK cell maturation and tumor surveillance. *OncoImmunology*, *1*(7), 1027-1037. https://doi.org/10.4161/onci.21284

Modi, S., Jacot, W., Yamashita, T., Sohn, J., Vidal, M., Tokunaga, E., Tsurutani, J., Ueno, N. T., Prat, A., Chae, Y. S., Lee, K. S., Niikura, N., Park, Y. H., Xu, B., Wang, X., Gil-Gil, M., Li, W., Pierga, J.-Y., Im, S.-A., . . . Cameron, D. A. (2022). Trastuzumab Deruxtecan in Previously Treated HER2-Low Advanced Breast Cancer. *New England Journal of Medicine*, *387*(1), 9-20. https://doi.org/doi:10.1056/NEJMoa2203690

Moghaddas, S., Majmudar, P., Marin, R., Dezvareh, H., Qi, C., Soans, E., & Bose, R. N. (2012). Phosphaplatins, next generation platinum antitumor agents: A paradigm shift in designing and defining molecular targets. *Inorganica Chimica Acta*, *393*, 173-181. https://doi.org/https://doi.org/10.1016/j.ica.2012.05.040

Monack, D. M., Hersh, D., Ghori, N., Bouley, D., Zychlinsky, A., & Falkow, S. (2000). Salmonella Exploits Caspase-1 to Colonize Peyer's Patches in a Murine Typhoid Model. *Journal of Experimental Medicine*, *192*(2), 249-258. https://doi.org/10.1084/jem.192.2.249

Monks, C. R. F., Freiberg, B. A., Kupfer, H., Sciaky, N., & Kupfer, A. (1998). Three-dimensional segregation of supramolecular activation clusters in T cells. *Nature*, *395*(6697), 82-86. https://doi.org/10.1038/25764

Monleón, I., Martínez-Lorenzo, M. J., Monteagudo, L., Lasierra, P., Taulés, M., Iturralde, M., Piñeiro, A., Larrad, L., Alava, M. A., Naval, J., & Anel, A. (2001). Differential secretion of Fas ligand- or APO2 ligand/TNF-related apoptosis-inducing ligand-carrying microvesicles during activation-induced death of human T cells. *J Immunol*, *167*(12), 6736-6744. https://doi.org/10.4049/jimmunol.167.12.6736

Montoya, J., López-Pérez, M. J., & Ruiz-Pesini, E. (2006). Mitochondrial DNA transcription and diseases: Past, present and future. *Biochimica et Biophysica Acta (BBA) - Bioenergetics*, *1757*(9), 1179-1189. https://doi.org/https://doi.org/10.1016/j.bbabio.2006.03.023

Morais, R., Zinkewich-Péotti, K., Parent, M., Wang, H., Babai, F., & Zollinger, M. (1994). Tumor-forming ability in athymic nude mice of human cell lines devoid of mitochondrial DNA. *Cancer Res*, *54*(14), 3889-3896.

Morinaga, Y., Yanagihara, K., Nakamura, S., Hasegawa, H., Seki, M., Izumikawa, K., Kakeya, H., Yamamoto, Y., Yamada, Y., Kohno, S., & Kamihira, S. (2010). Legionella pneumophila induces cathepsin B-dependent necrotic cell death with releasing high mobility group box1 in macrophages. *Respiratory Research*, *11*(1), 158. https://doi.org/10.1186/1465-9921-11-158

Morrison, L., Loibl, S., & Turner, N. C. (2024). The CDK4/6 inhibitor revolution — a game-changing era for breast cancer treatment. *Nature Reviews Clinical Oncology*, *21*(2), 89-105. https://doi.org/10.1038/s41571-023-00840-4

Mosmann, T. (1983). Rapid colorimetric assay for cellular growth and survival: application to proliferation and cytotoxicity assays. *J Immunol Methods*, *65*(1-2), 55-63. https://doi.org/10.1016/0022-1759(83)90303-4

Muller, P. A. J., & Vousden, K. H. (2013). p53 mutations in cancer. *Nature Cell Biology*, *15*(1), 2-8. https://doi.org/10.1038/ncb2641

Muñoz-Planillo, R., Kuffa, P., Martínez-Colón, G., Smith, B. L., Rajendiran, T. M., & Núñez, G. (2013). K^+ efflux is the common trigger of NLRP3 inflammasome activation by bacterial toxins and particulate matter. *Immunity*, *38*(6), 1142-1153. https://doi.org/10.1016/j.immuni.2013.05.016

Murakami, T., Ockinger, J., Yu, J., Byles, V., McColl, A., Hofer, A. M., & Horng, T. (2012). Critical role for calcium mobilization in activation of the NLRP3 inflammasome. *Proc Natl Acad Sci U S A*, *109*(28), 11282-11287. https://doi.org/10.1073/pnas.1117765109

Murakami, Y., Matsumoto, H., Roh, M., Giani, A., Kataoka, K., Morizane, Y., Kayama, M., Thanos, A., Nakatake, S., Notomi, S., Hisatomi, T., Ikeda, Y., Ishibashi, T., Connor, K. M., Miller, J. W., & Vavvas, D. G. (2014). Programmed necrosis, not apoptosis, is a key mediator of cell loss and

DAMP-mediated inflammation in dsRNA-induced retinal degeneration. *Cell Death Differ*, *21*(2), 270-277. https://doi.org/10.1038/cdd.2013.109

Nagata, S. (1997). Apoptosis by Death Factor. *Cell*, *88*(3), 355-365. https://doi.org/https://doi.org/10.1016/S0092-8674(00)81874-7

Nagate, Y., Ezoe, S., Fujita, J., Okuzaki, D., Motooka, D., Ishibashi, T., Ichii, M., Tanimura, A., Kurashige, M., Morii, E., Fukushima, T., Suehiro, Y., Yokota, T., Shibayama, H., Oritani, K., & Kanakura, Y. (2021). Ectonucleotidase CD39 is highly expressed on ATLL cells and is responsible for their immunosuppressive function. *Leukemia*, *35*(1), 107-118. https://doi.org/10.1038/s41375-020-0788-y

Nakahira, K., Haspel, J. A., Rathinam, V. A. K., Lee, S.-J., Dolinay, T., Lam, H. C., Englert, J. A., Rabinovitch, M., Cernadas, M., Kim, H. P., Fitzgerald, K. A., Ryter, S. W., & Choi, A. M. K. (2011). Autophagy proteins regulate innate immune responses by inhibiting the release of mitochondrial DNA mediated by the NALP3 inflammasome. *Nature Immunology*, *12*(3), 222-230. https://doi.org/10.1038/ni.1980

Newton, K., & Manning, G. (2016). Necroptosis and Inflammation. *Annual Review of Biochemistry*, *85*(Volume 85, 2016), 743-763. https://doi.org/https://doi.org/10.1146/annurev-biochem-060815-014830

Newton, K., Strasser, A., Kayagaki, N., & Dixit, V. M. (2024). Cell death. *Cell*, *187*(2), 235-256. https://doi.org/10.1016/j.cell.2023.11.044

Newton, K., Wickliffe, K. E., Dugger, D. L., Maltzman, A., Roose-Girma, M., Dohse, M., Kőműves, L., Webster, J. D., & Dixit, V. M. (2019). Cleavage of RIPK1 by caspase-8 is crucial for limiting apoptosis and necroptosis. *Nature*, *574*(7778), 428-431. https://doi.org/10.1038/s41586-019-1548-x

Nicholson, D. W. (1999). Caspase structure, proteolytic substrates, and function during apoptotic cell death. *Cell Death & Differentiation*, *6*(11), 1028-1042. https://doi.org/10.1038/sj.cdd.4400598

Niemann, S., & Müller, U. (2000). Mutations in SDHC cause autosomal dominant paraganglioma, type 3. *Nat Genet*, *26*(3), 268-270. https://doi.org/10.1038/81551

Nigro, J. M., Baker, S. J., Preisinger, A. C., Jessup, J. M., Hostetter, R., Cleary, K., Bigner, S. H., Davidson, N., Baylin, S., Devilee, P., & et al. (1989). Mutations in the p53 gene occur in diverse human tumour types. *Nature*, *342*(6250), 705-708. https://doi.org/10.1038/342705a0

NIH. (2021). *What is Cancer?* Retrieved January 19, 2024 from https://www.cancer.gov/about-cancer/understanding/what-is-cancer

NIH. (2024a). *Anatomy of the Prostate*. NIH. Retrieved April 28, 2024 from https://training.seer.cancer.gov/prostate/anatomy/

NIH. (2024b). *Annual Report to the Nation on the Status of Cancer*. Retrieved January 19, 2024 from https://seer.cancer.gov/report_to_nation/

NIH. (2024c). *Cancer: A Historic Perspective*. Retrieved January 19, 2024 from https://training.seer.cancer.gov/disease/history/

NIH. (2024d). *PT-112 in Subjects with Thymoma and Thymic Carcinoma*. Retrieved April 29, 2024 from https://www.cancer.gov/research/participate/clinical-trials-search/v?id=NCI-2021-13371&r=1

Ning, X., Wang, Y., Jing, M., Sha, M., Lv, M., Gao, P., Zhang, R., Huang, X., Feng, J. M., & Jiang, Z. (2019). Apoptotic Caspases Suppress Type I Interferon Production via the Cleavage of cGAS, MAVS, and IRF3. *Mol Cell*, *74*(1), 19-31.e17. https://doi.org/10.1016/j.molcel.2019.02.013

O'Donnell, J. S., Teng, M. W. L., & Smyth, M. J. (2019). Cancer immunoediting and resistance to T cell-based immunotherapy. *Nature Reviews Clinical Oncology*, *16*(3), 151-167. https://doi.org/10.1038/s41571-018-0142-8

Oberst, A., Dillon, C. P., Weinlich, R., McCormick, L. L., Fitzgerald, P., Pop, C., Hakem, R., Salvesen, G. S., & Green, D. R. (2011). Catalytic activity of the caspase-8–FLIPL complex inhibits RIPK3-dependent necrosis. *Nature*, *471*(7338), 363-367. https://doi.org/10.1038/nature09852

Observatory, G. C. (2024). *Cancer today* Retrieved January 19, 2024 from https://gco.iarc.fr/

Ong, S. B., Subrayan, S., Lim, S. Y., Yellon, D. M., Davidson, S. M., & Hausenloy, D. J. (2010). Inhibiting mitochondrial fission protects the heart against ischemia/reperfusion injury. *Circulation*, *121*(18), 2012-2022. https://doi.org/10.1161/circulationaha.109.906610

Orrantia-Borunda, E., Anchondo-Nuñez, P., Acuña-Aguilar, L. E., Gómez-Valles, F. O., & Ramírez-Valdespino, C. A. (2022). Subtypes of Breast Cancer. In H. N. Mayrovitz (Ed.), *Breast Cancer*. Exon Publications

Orsini, F., Pavelic, Z., & Mihich, E. (1977). Increased primary cell-mediated immunity in culture subsequent to adriamycin or daunorubicin treatment of spleen donor mice. *Cancer Res*, *37*(6), 1719-1726.

Pagès, F., Berger, A., Camus, M., Sanchez-Cabo, F., Costes, A., Molidor, R., Mlecnik, B., Kirilovsky, A., Nilsson, M., Damotte, D., Meatchi, T., Bruneval, P., Cugnenc, P. H., Trajanoski, Z., Fridman, W. H., & Galon, J. (2005). Effector memory T cells, early metastasis, and survival in colorectal cancer. *N Engl J Med*, *353*(25), 2654-2666. https://doi.org/10.1056/NEJMoa051424

Palikaras, K., Lionaki, E., & Tavernarakis, N. (2018). Mechanisms of mitophagy in cellular homeostasis, physiology and pathology. *Nature Cell Biology*, *20*(9), 1013-1022. https://doi.org/10.1038/s41556-018-0176-2

Pan, H., Liu, P., Zhao, L., Pan, Y., Mao, M., Kroemer, G., & Kepp, O. (2024). Immunogenic cell stress and death in the treatment of cancer. *Semin Cell Dev Biol*, *156*, 11-21. https://doi.org/10.1016/j.semcdb.2023.10.007

Pantelouris, E. M. (1968). Absence of thymus in a mouse mutant. *Nature*, *217*(5126), 370-371. https://doi.org/10.1038/217370a0

Pardo, J., Aguilo, J. I., Anel, A., Martin, P., Joeckel, L., Borner, C., Wallich, R., Müllbacher, A., Froelich, C. J., & Simon, M. M. (2009). The biology of cytotoxic cell granule exocytosis pathway: granzymes have evolved to induce cell death and inflammation. *Microbes and Infection*, *11*(4), 452-459. https://doi.org/https://doi.org/10.1016/j.micinf.2009.02.004

Pardo, J., Wallich, R., Martin, P., Urban, C., Rongvaux, A., Flavell, R. A., Müllbacher, A., Borner, C., & Simon, M. M. (2008). Granzyme B-induced cell death exerted by ex vivo CTL: discriminating requirements for cell death and some of its signs. *Cell Death Differ*, *15*(3), 567-579. https://doi.org/10.1038/sj.cdd.4402289

Pardo , J. n., Bosque , A., Brehm , R., Wallich , R., Naval , J., Müllbacher , A., Anel , A., & Simon , M. M. (2004). Apoptotic pathways are selectively activated by granzyme A and/or granzyme B in CTL-mediated target cell lysis. *Journal of Cell Biology*, *167*(3), 457-468. https://doi.org/10.1083/jcb.200406115

Park, J. S., Gamboni-Robertson, F., He, Q., Svetkauskaite, D., Kim, J.-Y., Strassheim, D., Sohn, J.-W., Yamada, S., Maruyama, I., Banerjee, A., Ishizaka, A., & Abraham, E. (2006). High mobility group box 1 protein interacts with multiple Toll-like receptors. *American Journal of Physiology-Cell Physiology*, *290*(3), C917-C924. https://doi.org/10.1152/ajpcell.00401.2005

Park, J. S., Gamboni-Robertson, F., He, Q., Svetkauskaite, D., Kim, J. Y., Strassheim, D., Sohn, J. W., Yamada, S., Maruyama, I., Banerjee, A., Ishizaka, A., & Abraham, E. (2006). High mobility group

box 1 protein interacts with multiple Toll-like receptors. *Am J Physiol Cell Physiol*, *290*(3), C917-924. https://doi.org/10.1152/ajpcell.00401.2005

Park, S. Y., Chang, I., Kim, J. Y., Kang, S. W., Park, S. H., Singh, K., & Lee, M. S. (2004). Resistance of mitochondrial DNA-depleted cells against cell death: role of mitochondrial superoxide dismutase. *J Biol Chem*, *279*(9), 7512-7520. https://doi.org/10.1074/jbc.M307677200

Parker, B. S., Rautela, J., & Hertzog, P. J. (2016). Antitumour actions of interferons: implications for cancer therapy. *Nat Rev Cancer*, *16*(3), 131-144. https://doi.org/10.1038/nrc.2016.14

Parkin, J., & Cohen, B. (2001). An overview of the immune system. *Lancet*, *357*(9270), 1777-1789. https://doi.org/10.1016/s0140-6736(00)04904-7

Peng, R. Q., Chen, Y. B., Ding, Y., Zhang, R., Zhang, X., Yu, X. J., Zhou, Z. W., Zeng, Y. X., & Zhang, X. S. (2010). Expression of calreticulin is associated with infiltration of T-cells in stage IIIB colon cancer. *World J Gastroenterol*, *16*(19), 2428-2434. https://doi.org/10.3748/wjg.v16.i19.2428

Perego, P., & Robert, J. (2016). Oxaliplatin in the era of personalized medicine: from mechanistic studies to clinical efficacy. *Cancer Chemotherapy and Pharmacology*, *77*(1), 5-18. https://doi.org/10.1007/s00280-015-2901-x

Perretti, M., & D'Acquisto, F. (2009). Annexin A1 and glucocorticoids as effectors of the resolution of inflammation. *Nat Rev Immunol*, *9*(1), 62-70. https://doi.org/10.1038/nri2470

Peters, P. J., Borst, J., Oorschot, V., Fukuda, M., Krähenbühl, O., Tschopp, J., Slot, J. W., & Geuze, H. J. (1991). Cytotoxic T lymphocyte granules are secretory lysosomes, containing both perforin and granzymes. *J Exp Med*, *173*(5), 1099-1109. https://doi.org/10.1084/jem.173.5.1099

Petersen, O. W., Høyer, P. E., & van Deurs, B. (1987). Frequency and distribution of estrogen receptor-positive cells in normal, nonlactating human breast tissue. *Cancer Res*, *47*(21), 5748-5751.

Petros, J. A., Baumann, A. K., Ruiz-Pesini, E., Amin, M. B., Sun, C. Q., Hall, J., Lim, S., Issa, M. M., Flanders, W. D., Hosseini, S. H., Marshall, F. F., & Wallace, D. C. (2005). mtDNA mutations increase tumorigenicity in prostate cancer. *Proc Natl Acad Sci U S A*, *102*(3), 719-724. https://doi.org/10.1073/pnas.0408894102

Pfister, A. S. (2019). Emerging Role of the Nucleolar Stress Response in Autophagy. *Front Cell Neurosci*, *13*, 156. https://doi.org/10.3389/fncel.2019.00156

Piskounova, E., Agathocleous, M., Murphy, M. M., Hu, Z., Huddlestun, S. E., Zhao, Z., Leitch, A. M., Johnson, T. M., DeBerardinis, R. J., & Morrison, S. J. (2015). Oxidative stress inhibits distant metastasis by human melanoma cells. *Nature*, *527*(7577), 186-191. https://doi.org/10.1038/nature15726

Pittis, A. A., & Gabaldón, T. (2016). Late acquisition of mitochondria by a host with chimaeric prokaryotic ancestry. *Nature*, *531*(7592), 101-104. https://doi.org/10.1038/nature16941

Polgár, C., Kahán, Z., Ivanov, O., Chorváth, M., Ligačová, A., Csejtei, A., Gábor, G., Landherr, L., Mangel, L., Mayer, Á., & Fodor, J. (2022). Radiotherapy of Breast Cancer-Professional Guideline 1st Central-Eastern European Professional Consensus Statement on Breast Cancer. *Pathol Oncol Res*, *28*, 1610378. https://doi.org/10.3389/pore.2022.1610378

Pollak, M. N. (2012). Investigating Metformin for Cancer Prevention and Treatment: The End of the Beginning. *Cancer Discovery*, *2*(9), 778-790. https://doi.org/10.1158/2159-8290.Cd-12-0263

Polyak, K., Li, Y., Zhu, H., Lengauer, C., Willson, J. K., Markowitz, S. D., Trush, M. A., Kinzler, K. W., & Vogelstein, B. (1998). Somatic mutations of the mitochondrial genome in human colorectal tumours. *Nat Genet*, *20*(3), 291-293. https://doi.org/10.1038/3108

Porporato, P. E., Filigheddu, N., Pedro, J. M. B., Kroemer, G., & Galluzzi, L. (2018). Mitochondrial metabolism and cancer. *Cell Res*, *28*(3), 265-280. https://doi.org/10.1038/cr.2017.155

Prehn, R. T., & Main, J. M. (1957). Immunity to Methylcholanthrene-Induced Sarcomas. *JNCI: Journal of the National Cancer Institute*, *18*(6), 769-778. https://doi.org/10.1093/jnci/18.6.769

Promontory Therapeutics. (2024). *Key Milestones*. Retrieved April 28, 2024 from https://promontorytx.com/key-milestones

Prostate Cancer Foundation. (2024). *How Prostate Cancer Grows*. Retrieved April 28, 2024 from https://www.pcf.org/about-prostate-cancer/what-is-prostate-cancer/how-it-grows/

Qiu, L., Yang, H., Lv, G., Li, K., Liu, G., Wang, W., Wang, S., Zhao, X., Xie, M., & Lin, J. (2017). Insights into the mevalonate pathway in the anticancer effect of a platinum complex on human gastric cancer cells. *European Journal of Pharmacology*, *810*, 120-127. https://doi.org/https://doi.org/10.1016/j.ejphar.2017.06.035

Quail, D. F., & Joyce, J. A. (2013). Microenvironmental regulation of tumor progression and metastasis. *Nature Medicine*, *19*(11), 1423-1437. https://doi.org/10.1038/nm.3394

Quintana-Cabrera, R., & Scorrano, L. (2023). Determinants and outcomes of mitochondrial dynamics. *Molecular Cell*, *83*(6), 857-876. https://doi.org/https://doi.org/10.1016/j.molcel.2023.02.012

Quintana-Cabrera, R., & Scorrano, L. (2023). Determinants and outcomes of mitochondrial dynamics. *Mol Cell*, *83*(6), 857-876. https://doi.org/10.1016/j.molcel.2023.02.012

Raimondi, V., Ciccarese, F., & Ciminale, V. (2020). Oncogenic pathways and the electron transport chain: a dangeROS liaison. *British Journal of Cancer*, *122*(2), 168-181. https://doi.org/10.1038/s41416-019-0651-y

Ramakrishnan, R., Huang, C., Cho, H.-I., Lloyd, M., Johnson, J., Ren, X., Altiok, S., Sullivan, D., Weber, J., Celis, E., & Gabrilovich, D. I. (2012). Autophagy Induced by Conventional Chemotherapy Mediates Tumor Cell Sensitivity to Immunotherapy. *Cancer Research*, *72*(21), 5483-5493. https://doi.org/10.1158/0008-5472.Can-12-2236

Rasmussen, S. B., Horan, K. A., Holm, C. K., Stranks, A. J., Mettenleiter, T. C., Simon, A. K., Jensen, S. B., Rixon, F. J., He, B., & Paludan, S. R. (2011). Activation of autophagy by α-herpesviruses in myeloid cells is mediated by cytoplasmic viral DNA through a mechanism dependent on stimulator of IFN genes. *J Immunol*, *187*(10), 5268-5276. https://doi.org/10.4049/jimmunol.1100949

Reznik, E., Miller, M. L., Şenbabaoğlu, Y., Riaz, N., Sarungbam, J., Tickoo, S. K., Al-Ahmadie, H. A., Lee, W., Seshan, V. E., Hakimi, A. A., & Sander, C. (2016). Mitochondrial DNA copy number variation across human cancers. *eLife*, *5*. https://doi.org/10.7554/eLife.10769

Riera Romo, M., Pérez-Martínez, D., & Castillo Ferrer, C. (2016). Innate immunity in vertebrates: an overview. *Immunology*, *148*(2), 125-139. https://doi.org/10.1111/imm.12597

Riley, J. S., Quarato, G., Cloix, C., Lopez, J., O'Prey, J., Pearson, M., Chapman, J., Sesaki, H., Carlin, L. M., Passos, J. F., Wheeler, A. P., Oberst, A., Ryan, K. M., & Tait, S. W. (2018). Mitochondrial inner membrane permeabilisation enables mtDNA release during apoptosis. *Embo j*, *37*(17). https://doi.org/10.15252/embj.201899238

Riley, J. S., & Tait, S. W. (2020). Mitochondrial DNA in inflammation and immunity. *EMBO Rep*, *21*(4), e49799. https://doi.org/10.15252/embr.201949799

Rodríguez-Nuevo, A., & Zorzano, A. (2019). The sensing of mitochondrial DAMPs by non-immune cells. *Cell Stress*, *3*(6), 195-207. https://doi.org/10.15698/cst2019.06.190

Rodriguez-Ruiz, M. E., Buqué, A., Hensler, M., Chen, J., Bloy, N., Petroni, G., Sato, A., Yamazaki, T., Fucikova, J., & Galluzzi, L. (2019). Apoptotic caspases inhibit abscopal responses to radiation and identify a new prognostic biomarker for breast cancer patients. *OncoImmunology*, *8*(11), e1655964. https://doi.org/10.1080/2162402x.2019.1655964

Rodríguez, T., Rengifo, E., Gavilondo, J., Tormo, B., & Fernández, A. (1984). Morphologic and cytochemical study of L929 cell variants with different metastasizing ability in C3HA/Hab mice. *Neoplasma*, *31*(3), 271-279.

Rohle, D., Popovici-Muller, J., Palaskas, N., Turcan, S., Grommes, C., Campos, C., Tsoi, J., Clark, O., Oldrini, B., Komisopoulou, E., Kunii, K., Pedraza, A., Schalm, S., Silverman, L., Miller, A., Wang, F., Yang, H., Chen, Y., Kernytsky, A., . . . Mellinghoff, I. K. (2013). An inhibitor of mutant IDH1 delays growth

and promotes differentiation of glioma cells. *Science*, *340*(6132), 626-630. https://doi.org/10.1126/science.1236062

Rongvaux, A., Jackson, R., Harman, C. C., Li, T., West, A. P., de Zoete, M. R., Wu, Y., Yordy, B., Lakhani, S. A., Kuan, C. Y., Taniguchi, T., Shadel, G. S., Chen, Z. J., Iwasaki, A., & Flavell, R. A. (2014). Apoptotic caspases prevent the induction of type I interferons by mitochondrial DNA. *Cell*, *159*(7), 1563-1577. https://doi.org/10.1016/j.cell.2014.11.037

Rongvaux, A., Jackson, R., Harman, Christian C. D., Li, T., West, A. P., de Zoete, Marcel R., Wu, Y., Yordy, B., Lakhani, Saquib A., Kuan, C.-Y., Taniguchi, T., Shadel, Gerald S., Chen, Zhijian J., Iwasaki, A., & Flavell, Richard A. (2014). Apoptotic Caspases Prevent the Induction of Type I Interferons by Mitochondrial DNA. *Cell*, *159*(7), 1563-1577. https://doi.org/https://doi.org/10.1016/j.cell.2014.11.037

Rosenberg, B., Van Camp, L., & Krigas, T. (1965). Inhibition of Cell Division in Escherichia coli by Electrolysis Products from a Platinum Electrode. *Nature*, *205*(4972), 698-699. https://doi.org/10.1038/205698a0

Rottenberg, S., Disler, C., & Perego, P. (2021). The rediscovery of platinum-based cancer therapy. *Nat Rev Cancer*, *21*(1), 37-50. https://doi.org/10.1038/s41568-020-00308-y

Roy, N., Deveraux, Q. L., Takahashi, R., Salvesen, G. S., & Reed, J. C. (1997). The c-IAP-1 and c-IAP-2 proteins are direct inhibitors of specific caspases. *Embo j*, *16*(23), 6914-6925. https://doi.org/10.1093/emboj/16.23.6914

Russell, R. G., Watts, N. B., Ebetino, F. H., & Rogers, M. J. (2008). Mechanisms of action of bisphosphonates: similarities and differences and their potential influence on clinical efficacy. *Osteoporos Int*, *19*(6), 733-759. https://doi.org/10.1007/s00198-007-0540-8

Saad, F., Gleason, D. M., Murray, R., Tchekmedyian, S., Venner, P., Lacombe, L., Chin, J. L., Vinholes, J. J., Goas, J. A., & Zheng, M. (2004). Long-term efficacy of zoledronic acid for the prevention of skeletal complications in patients with metastatic hormone-refractory prostate cancer. *J Natl Cancer Inst*, *96*(11), 879-882. https://doi.org/10.1093/jnci/djh141

Sagan, L. (1967). On the origin of mitosing cells. *Journal of Theoretical Biology*, *14*(3), 225-IN226. https://doi.org/https://doi.org/10.1016/0022-5193(67)90079-3

Sainero-Alcolado, L., Liaño-Pons, J., Ruiz-Pérez, M. V., & Arsenian-Henriksson, M. (2022). Targeting mitochondrial metabolism for precision medicine in cancer. *Cell Death & Differentiation*, *29*(7), 1304-1317. https://doi.org/10.1038/s41418-022-01022-y

Saitoh, T., Fujita, N., Hayashi, T., Takahara, K., Satoh, T., Lee, H., Matsunaga, K., Kageyama, S., Omori, H., Noda, T., Yamamoto, N., Kawai, T., Ishii, K., Takeuchi, O., Yoshimori, T., & Akira, S. (2009). Atg9a controls dsDNA-driven dynamic translocation of STING and the innate immune response. *Proceedings of the National Academy of Sciences*, *106*(49), 20842-20846. https://doi.org/doi:10.1073/pnas.0911267106

Samson, N., & Ablasser, A. (2022). The cGAS–STING pathway and cancer. *Nature Cancer*, *3*(12), 1452-1463. https://doi.org/10.1038/s43018-022-00468-w

Sanford, K. K., Hobbs, G. L., & Earle, W. R. (1956). The tumor-producing capacity of strain L mouse cells after 10 years in vitro. *Cancer Res*, *16*(2), 162-166.

Sanz, L., Ibáñez-Pérez, R., Guerrero-Ochoa, P., Lacadena, J., & Anel, A. (2021). Antibody-Based Immunotoxins for Colorectal Cancer Therapy. *Biomedicines*, *9*(11). https://doi.org/10.3390/biomedicines9111729

Sartor, O., de Bono, J., Chi, K. N., Fizazi, K., Herrmann, K., Rahbar, K., Tagawa, S. T., Nordquist, L. T., Vaishampayan, N., El-Haddad, G., Park, C. H., Beer, T. M., Armour, A., Pérez-Contreras, W. J., DeSilvio, M., Kpamegan, E., Gericke, G., Messmann, R. A., Morris, M. J., & Krause, B. J. (2021). Lutetium-177-PSMA-617 for Metastatic Castration-Resistant Prostate Cancer. *N Engl J Med*, *385*(12), 1091-1103. https://doi.org/10.1056/NEJMoa2107322

Sato, A., Bloy, N., Galassi, C., Jiménez-Cortegana, C., Klapp, V., Aretz, A., Guilbaud, E., Yamazaki, T., Petroni, G., Galluzzi, L., & Buqué, A. (2022). Quantification of cytosolic DNA species by immunofluorescence microscopy and automated image analysis. *Methods Cell Biol*, *172*, 115-134. https://doi.org/10.1016/bs.mcb.2022.05.004

Sato, A., Buque, A., Yamazaki, T., Bloy, N., Petroni, G., & Galluzzi, L. (2021). Immunofluorescence microscopy-based assessment of cytosolic DNA accumulation in mammalian cells. *STAR protocols*, *2*(2), 100488. https://doi.org/10.1016/j.xpro.2021.100488

Scaffidi, C., Fulda, S., Srinivasan, A., Friesen, C., Li, F., Tomaselli, K. J., Debatin, K. M., Krammer, P. H., & Peter, M. E. (1998). Two CD95 (APO-1/Fas) signaling pathways. *Embo j*, *17*(6), 1675-1687. https://doi.org/10.1093/emboj/17.6.1675

Scaffidi, P., Misteli, T., & Bianchi, M. E. (2002). Release of chromatin protein HMGB1 by necrotic cells triggers inflammation. *Nature*, *418*(6894), 191-195. https://doi.org/10.1038/nature00858

Scaglia, N., Frontini-López, Y. R., & Zadra, G. (2021). Prostate Cancer Progression: as a Matter of Fats. *Front Oncol*, *11*, 719865. https://doi.org/10.3389/fonc.2021.719865

Schaeffer, E. M., Srinivas, S., Adra, N., An, Y., Barocas, D., Bitting, R., Bryce, A., Chapin, B., Cheng, H. H., D'Amico, A. V., Desai, N., Dorff, T., Eastham, J. A., Farrington, T. A., Gao, X., Gupta, S., Guzzo, T., Ippolito, J. E., Kuettel, M. R., . . . Freedman-Cass, D. A. (2022). NCCN Guidelines® Insights: Prostate Cancer, Version 1.2023. *J Natl Compr Canc Netw*, *20*(12), 1288-1298. https://doi.org/10.6004/jnccn.2022.0063

Schägger, H., & Pfeiffer, K. (2000). Supercomplexes in the respiratory chains of yeast and mammalian mitochondria. *The EMBO Journal*, *19*(8), 1777-1783. https://doi.org/https://doi.org/10.1093/emboj/19.8.1777

Schardt, J. A., Weber, D., Eyholzer, M., Mueller, B. U., & Pabst, T. (2009). Activation of the unfolded protein response is associated with favorable prognosis in acute myeloid leukemia. *Clin Cancer Res*, *15*(11), 3834-3841. https://doi.org/10.1158/1078-0432.Ccr-08-2870

Schiavoni, G., Mattei, F., Di Pucchio, T., Santini, S. M., Bracci, L., Belardelli, F., & Proietti, E. (2000). Cyclophosphamide induces type I interferon and augments the number of CD44(hi) T lymphocytes in mice: implications for strategies of chemoimmunotherapy of cancer. *Blood*, *95*(6), 2024-2030.

Schindl, M., Schoppmann, S. F., Samonigg, H., Hausmaninger, H., Kwasny, W., Gnant, M., Jakesz, R., Kubista, E., Birner, P., Oberhuber, G., & Group, t. A. B. C. C. S. (2002). Overexpression of Hypoxia-inducible Factor 1α Is Associated with an Unfavorable Prognosis in Lymph Node-positive Breast Cancer. *Clinical Cancer Research*, *8*(6), 1831-1837.

Schmidt, O., Pfanner, N., & Meisinger, C. (2010). Mitochondrial protein import: from proteomics to functional mechanisms. *Nat Rev Mol Cell Biol*, *11*(9), 655-667. https://doi.org/10.1038/nrm2959

Schoggins, J. W. (2019). Interferon-Stimulated Genes: What Do They All Do? *Annual Review of Virology*, *6*(1), 567-584. https://doi.org/10.1146/annurev-virology-092818-015756

Schreiber, R. D., Old, L. J., & Smyth, M. J. (2011). Cancer immunoediting: integrating immunity's roles in cancer suppression and promotion. *Science*, *331*(6024), 1565-1570. https://doi.org/10.1126/science.1203486

Semenza, G. L. (2003). Targeting HIF-1 for cancer therapy. *Nature Reviews Cancer*, *3*(10), 721-732. https://doi.org/10.1038/nrc1187

Sen Santara, S., Lee, D.-J., Crespo, Â., Hu, J. J., Walker, C., Ma, X., Zhang, Y., Chowdhury, S., Meza-Sosa, K. F., Lewandrowski, M., Zhang, H., Rowe, M., McClelland, A., Wu, H., Junqueira, C., & Lieberman, J. (2023). The NK cell receptor NKp46 recognizes ecto-calreticulin on ER-stressed cells. *Nature*, *616*(7956), 348-356. https://doi.org/10.1038/s41586-023-05912-0

Senovilla, L., Vitale, I., Martins, I., Tailler, M., Pailleret, C., Michaud, M., Galluzzi, L., Adjemian, S., Kepp, O., Niso-Santano, M., Shen, S., Mariño, G., Criollo, A., Boilève, A., Job, B., Ladoire, S., Ghiringhelli, F.,

Sistigu, A., Yamazaki, T., . . . Kroemer, G. (2012). An immunosurveillance mechanism controls cancer cell ploidy. *Science*, *337*(6102), 1678-1684. https://doi.org/10.1126/science.1224922

Serrano-Del Valle, A., Anel, A., Naval, J., & Marzo, I. (2019). Immunogenic Cell Death and Immunotherapy of Multiple Myeloma. *Front Cell Dev Biol*, *7*, 50. https://doi.org/10.3389/fcell.2019.00050

Serrano-Mendioroz, I., Garate-Soraluze, E., & Rodriguez-Ruiz, M. E. (2023). A simple method to assess clonogenic survival of irradiated cancer cells. *Methods Cell Biol*, *174*, 127-136. https://doi.org/10.1016/bs.mcb.2022.08.002

Serrano Del Valle, A., Beltrán-Visiedo, M., de Poo-Rodríguez, V., Jiménez-Alduán, N., Azaceta, G., Díez, R., Martínez-Lázaro, B., Izquierdo, I., Palomera, L., Naval, J., Anel, A., & Marzo, I. (2022). Ecto-calreticulin expression in multiple myeloma correlates with a failed anti-tumoral immune response and bad prognosis. *OncoImmunology*, *11*(1), 2141973. https://doi.org/10.1080/2162402X.2022.2141973

Seshadri, R., Matthews, C., Dobrovic, A., & Horsfall, D. J. (1989). The significance of oncogene amplification in primary breast cancer. *Int J Cancer*, *43*(2), 270-272. https://doi.org/10.1002/ijc.2910430218

Shahbandi, A., Nguyen, H. D., & Jackson, J. G. (2020). TP53 Mutations and Outcomes in Breast Cancer: Reading beyond the Headlines. *Trends Cancer*, *6*(2), 98-110. https://doi.org/10.1016/j.trecan.2020.01.007

Sharma, P., & Allison, J. P. (2015). The future of immune checkpoint therapy. *Science*, *348*(6230), 56-61. https://doi.org/10.1126/science.aaa8172

Siegel, R. L., Giaquinto, A. N., & Jemal, A. (2024). Cancer statistics, 2024. *CA: A Cancer Journal for Clinicians*, *74*(1), 12-49. https://doi.org/https://doi.org/10.3322/caac.21820

Singh, R., Letai, A., & Sarosiek, K. (2019). Regulation of apoptosis in health and disease: the balancing act of BCL-2 family proteins. *Nature Reviews Molecular Cell Biology*, *20*(3), 175-193. https://doi.org/10.1038/s41580-018-0089-8

Sisirak, V., Sally, B., D'Agati, V., Martinez-Ortiz, W., Özçakar, Z. B., David, J., Rashidfarrokhi, A., Yeste, A., Panea, C., Chida, A. S., Bogunovic, M., Ivanov, II, Quintana, F. J., Sanz, I., Elkon, K. B., Tekin, M., Yalçınkaya, F., Cardozo, T. J., Clancy, R. M., . . . Reizis, B. (2016). Digestion of Chromatin in Apoptotic Cell Microparticles Prevents Autoimmunity. *Cell*, *166*(1), 88-101. https://doi.org/10.1016/j.cell.2016.05.034

Slamon, D. J., Clark, G. M., Wong, S. G., Levin, W. J., Ullrich, A., & McGuire, W. L. (1987). Human Breast Cancer: Correlation of Relapse and Survival with Amplification of the HER-2/neu Oncogene. *Science*, *235*(4785), 177-182. https://doi.org/doi:10.1126/science.3798106

Solari, J. I. G., Filippi-Chiela, E., Pilar, E. S., Nunes, V., Gonzalez, E. A., Figueiró, F., Andrade, C. F., & Klamt, F. (2020). Damage-associated molecular patterns (DAMPs) related to immunogenic cell death are differentially triggered by clinically relevant chemotherapeutics in lung adenocarcinoma cells. *BMC Cancer*, *20*(1), 474. https://doi.org/10.1186/s12885-020-06964-5

Soler-Agesta, R., Ames, T. D., Price, M., Jimeno, J., Yim, C. Y., Moreno-Loshuertos, R., & Anel, A. (2022). PT-112 induces potent mitochondrial stress and immunogenic cell death in human prostate cancer cell lines [Meeting Abstract]. *Cancer Research*, *82*(12), 2. <Go to ISI>://WOS:000892509505402

Soler-Agesta, R., Marco-Brualla, J., Fernández-Silva, P., Mozas, P., Anel, A., & Loshuertos, R. M. (2023). Transmitochondrial Cybrid Generation Using Cancer Cell Lines. *JoVE*(193), e65186. https://doi.org/doi:10.3791/65186

Soler-Agesta, R., Marco-Brualla, J., Minjárez-Sáenz, M., Yim, C. Y., Martínez-Júlvez, M., Price, M. R., Moreno-Loshuertos, R., Ames, T. D., Jimeno, J., & Anel, A. (2022a). PT-112 Induces Mitochondrial Stress and Immunogenic Cell Death, Targeting Tumor Cells with Mitochondrial Deficiencies. *Cancers (Basel)*, *14*(16). https://doi.org/10.3390/cancers14163851

Soler-Agesta, R., Marco-Brualla, J., Minjárez-Sáenz, M., Yim, C. Y., Martínez-Júlvez, M., Price, M. R., Moreno-Loshuertos, R., Ames, T. D., Jimeno, J., & Anel, A. (2022b). PT-112 Induces Mitochondrial Stress and Immunogenic Cell Death, Targeting Tumor Cells with Mitochondrial Deficiencies [Article]. *Cancers*, *14*(16), 21, Article 3851. https://doi.org/10.3390/cancers14163851

Soler-Agesta, R., Ripollés-Yuba, C., Marco-Brualla, J., et al. (2024). Generation of transmitochondrial cybrids in cancer cells. *Methods Cell Biol*.

Soller, M. J., Isaksson, M., Elfving, P., Soller, W., Lundgren, R., & Panagopoulos, I. (2006). Confirmation of the high frequency of the TMPRSS2/ERG fusion gene in prostate cancer. *Genes Chromosomes Cancer*, *45*(7), 717-719. https://doi.org/10.1002/gcc.20329

Srinivasainagendra, V., Sandel, M. W., Singh, B., Sundaresan, A., Mooga, V. P., Bajpai, P., Tiwari, H. K., & Singh, K. K. (2017). Migration of mitochondrial DNA in the nuclear genome of colorectal adenocarcinoma. *Genome Med*, *9*(1), 31. https://doi.org/10.1186/s13073-017-0420-6

Stagg, J., Beavis, P. A., Divisekera, U., Liu, M. C. P., Möller, A., Darcy, P. K., & Smyth, M. J. (2012). CD73-Deficient Mice Are Resistant to Carcinogenesis. *Cancer Research*, *72*(9), 2190-2196. https://doi.org/10.1158/0008-5472.Can-12-0420

Stetson, D. B., & Medzhitov, R. (2006). Recognition of cytosolic DNA activates an IRF3-dependent innate immune response. *Immunity*, *24*(1), 93-103. https://doi.org/10.1016/j.immuni.2005.12.003

Stewart, J. B., & Chinnery, P. F. (2015). The dynamics of mitochondrial DNA heteroplasmy: implications for human health and disease. *Nature Reviews Genetics*, *16*(9), 530-542. https://doi.org/10.1038/nrg3966

Stinchcombe, J. C., Salio, M., Cerundolo, V., Pende, D., Arico, M., & Griffiths, G. M. (2011). Centriole polarisation to the immunological synapse directs secretion from cytolytic cells of both the innate and adaptive immune systems. *BMC Biology*, *9*(1), 45. https://doi.org/10.1186/1741-7007-9-45

Stine, Z. E., Schug, Z. T., Salvino, J. M., & Dang, C. V. (2022). Targeting cancer metabolism in the era of precision oncology. *Nature Reviews Drug Discovery*, *21*(2), 141-162. https://doi.org/10.1038/s41573-021-00339-6

Stutman, O. (1974). Tumor development after 3-methylcholanthrene in immunologically deficient athymic-nude mice. *Science*, *183*(4124), 534-536. https://doi.org/10.1126/science.183.4124.534

Stutman, O., Dien, P., Wisun, R. E., & Lattime, E. C. (1980). Natural cytotoxic cells against solid tumors in mice: blocking of cytotoxicity by D-mannose. *Proc Natl Acad Sci U S A*, *77*(5), 2895-2898. https://doi.org/10.1073/pnas.77.5.2895

Sui, X., Chen, R., Wang, Z., Huang, Z., Kong, N., Zhang, M., Han, W., Lou, F., Yang, J., Zhang, Q., Wang, X., He, C., & Pan, H. (2013). Autophagy and chemotherapy resistance: a promising therapeutic target for cancer treatment. *Cell Death Dis*, *4*(10), e838. https://doi.org/10.1038/cddis.2013.350

Sun, L., Wang, H., Wang, Z., He, S., Chen, S., Liao, D., Wang, L., Yan, J., Liu, W., Lei, X., & Wang, X. (2012). Mixed lineage kinase domain-like protein mediates necrosis signaling downstream of RIP3 kinase. *Cell*, *148*(1-2), 213-227. https://doi.org/10.1016/j.cell.2011.11.031

Sun, L., Wu, J., Du, F., Chen, X., & Chen, Z. J. (2013). Cyclic GMP-AMP synthase is a cytosolic DNA sensor that activates the type I interferon pathway. *Science*, *339*(6121), 786-791. https://doi.org/10.1126/science.1232458

Sung, H., Ferlay, J., Siegel, R. L., Laversanne, M., Soerjomataram, I., Jemal, A., & Bray, F. (2021). Global Cancer Statistics 2020: GLOBOCAN Estimates of Incidence and Mortality Worldwide for 36 Cancers in 185 Countries. *CA: A Cancer Journal for Clinicians*, *71*(3), 209-249. https://doi.org/https://doi.org/10.3322/caac.21660

Swanson, G. P., Trevathan, S., Hammonds, K. A. P., Speights, V. O., & Hermans, M. R. (2021). Gleason Score Evolution and the Effect on Prostate Cancer Outcomes. *Am J Clin Pathol*, *155*(5), 711-717. https://doi.org/10.1093/ajcp/aqaa130

Swinnen, J. V., Van Veldhoven, P. P., Esquenet, M., Heyns, W., & Verhoeven, G. (1996). Androgens markedly stimulate the accumulation of neutral lipids in the human prostatic adenocarcinoma cell line LNCaP. *Endocrinology*, *137*(10), 4468-4474. https://doi.org/10.1210/endo.137.10.8828509

Tait, S. W. G., & Green, D. R. (2010). Mitochondria and cell death: outer membrane permeabilization and beyond. *Nature reviews. Molecular cell biology*, *11*(9), 621-632. https://doi.org/10.1038/nrm2952

Tan, A. S., Baty, J. W., Dong, L. F., Bezawork-Geleta, A., Endaya, B., Goodwin, J., Bajzikova, M., Kovarova, J., Peterka, M., Yan, B., Pesdar, E. A., Sobol, M., Filimonenko, A., Stuart, S., Vondrusova, M., Kluckova, K., Sachaphibulkij, K., Rohlena, J., Hozak, P., . . . Berridge, M. V. (2015). Mitochondrial genome acquisition restores respiratory function and tumorigenic potential of cancer cells without mitochondrial DNA. *Cell Metab*, *21*(1), 81-94. https://doi.org/10.1016/j.cmet.2014.12.003

Tan, M. H. E., Li, J., Xu, H. E., Melcher, K., & Yong, E.-l. (2015). Androgen receptor: structure, role in prostate cancer and drug discovery. *Acta Pharmacologica Sinica*, *36*(1), 3-23. https://doi.org/10.1038/aps.2014.18

Tang, C. H., Zundell, J. A., Ranatunga, S., Lin, C., Nefedova, Y., Del Valle, J. R., & Hu, C. C. (2016). Agonist-Mediated Activation of STING Induces Apoptosis in Malignant B Cells. *Cancer Res*, *76*(8), 2137-2152. https://doi.org/10.1158/0008-5472.Can-15-1885

Tang, D. G. (2022). Understanding and targeting prostate cancer cell heterogeneity and plasticity. *Semin Cancer Biol*, *82*, 68-93. https://doi.org/10.1016/j.semcancer.2021.11.001

Tashiro, T., Kawada, Y., Sakurai, Y., & Kidani, Y. (1989). Antitumor activity of a new platinum complex, oxalato (trans-l-1,2-diaminocyclohexane)platinum (II): new experimental data. *Biomed Pharmacother*, *43*(4), 251-260. https://doi.org/10.1016/0753-3322(89)90004-8

Tataranni, T., & Piccoli, C. (2019). Dichloroacetate (DCA) and Cancer: An Overview towards Clinical Applications. *Oxid Med Cell Longev*, *2019*, 8201079. https://doi.org/10.1155/2019/8201079

Tesniere, A., Schlemmer, F., Boige, V., Kepp, O., Martins, I., Ghiringhelli, F., Aymeric, L., Michaud, M., Apetoh, L., Barault, L., Mendiboure, J., Pignon, J. P., Jooste, V., van Endert, P., Ducreux, M., Zitvogel, L., Piard, F., & Kroemer, G. (2010a). Immunogenic death of colon cancer cells treated with oxaliplatin. *Oncogene*, *29*(4), 482-491. https://doi.org/10.1038/onc.2009.356

Tesniere, A., Schlemmer, F., Boige, V., Kepp, O., Martins, I., Ghiringhelli, F., Aymeric, L., Michaud, M., Apetoh, L., Barault, L., Mendiboure, J., Pignon, J. P., Jooste, V., van Endert, P., Ducreux, M., Zitvogel, L., Piard, F., & Kroemer, G. (2010b). Immunogenic death of colon cancer cells treated with oxaliplatin. *Oncogene*, *29*(4), 482-491. https://doi.org/10.1038/onc.2009.356

Thomas, R. K., Baker, A. C., DeBiasi, R. M., Winckler, W., LaFramboise, T., Lin, W. M., Wang, M., Feng, W., Zander, T., MacConaill, L. E., Lee, J. C., Nicoletti, R., Hatton, C., Goyette, M., Girard, L., Majmudar, K., Ziaugra, L., Wong, K.-K., Gabriel, S., . . . Garraway, L. A. (2007). High-throughput oncogene mutation profiling in human cancer. *Nature Genetics*, *39*(3), 347-351. https://doi.org/10.1038/ng1975

Tilekar, K., Upadhyay, N., Iancu, C. V., Pokrovsky, V., Choe, J. Y., & Ramaa, C. S. (2020). Power of two: combination of therapeutic approaches involving glucose transporter (GLUT) inhibitors to combat cancer. *Biochim Biophys Acta Rev Cancer*, *1874*(2), 188457. https://doi.org/10.1016/j.bbcan.2020.188457

Tomlins, S. A., Rhodes, D. R., Perner, S., Dhanasekaran, S. M., Mehra, R., Sun, X. W., Varambally, S., Cao, X., Tchinda, J., Kuefer, R., Lee, C., Montie, J. E., Shah, R. B., Pienta, K. J., Rubin, M. A., & Chinnaiyan, A. M. (2005). Recurrent fusion of TMPRSS2 and ETS transcription factor genes in prostate cancer. *Science*, *310*(5748), 644-648. https://doi.org/10.1126/science.1117679

Topalian, S. L., Hodi, F. S., Brahmer, J. R., Gettinger, S. N., Smith, D. C., McDermott, D. F., Powderly, J. D., Carvajal, R. D., Sosman, J. A., Atkins, M. B., Leming, P. D., Spigel, D. R., Antonia, S. J., Horn, L.,

Drake, C. G., Pardoll, D. M., Chen, L., Sharfman, W. H., Anders, R. A., . . . Sznol, M. (2012). Safety, Activity, and Immune Correlates of Anti–PD-1 Antibody in Cancer. *New England Journal of Medicine*, *366*(26), 2443-2454. https://doi.org/doi:10.1056/NEJMoa1200690

Tortorella, E., Giantulli, S., Sciarra, A., & Silvestri, I. (2023). AR and PI3K/AKT in Prostate Cancer: A Tale of Two Interconnected Pathways. *Int J Mol Sci*, *24*(3). https://doi.org/10.3390/ijms24032046

Tsung, A., Sahai, R., Tanaka, H., Nakao, A., Fink, M. P., Lotze, M. T., Yang, H., Li, J., Tracey, K. J., Geller, D. A., & Billiar, T. R. (2005). The nuclear factor HMGB1 mediates hepatic injury after murine liver ischemia-reperfusion. *J Exp Med*, *201*(7), 1135-1143. https://doi.org/10.1084/jem.20042614

Vacchelli, E., Ma, Y., Baracco, E. E., Sistigu, A., Enot, D. P., Pietrocola, F., Yang, H., Adjemian, S., Chaba, K., Semeraro, M., Signore, M., De Ninno, A., Lucarini, V., Peschiaroli, F., Businaro, L., Gerardino, A., Manic, G., Ulas, T., Günther, P., . . . Kroemer, G. (2015). Chemotherapy-induced antitumor immunity requires formyl peptide receptor 1. *Science*, *350*(6263), 972-978. https://doi.org/10.1126/science.aad0779

Vacchelli, E., Ma, Y., Baracco, E. E., Sistigu, A., Enot, D. P., Pietrocola, F., Yang, H., Adjemian, S., Chaba, K., Semeraro, M., Signore, M., De Ninno, A., Lucarini, V., Peschiaroli, F., Businaro, L., Gerardino, A., Manic, G., Ulas, T., Günther, P., . . . Kroemer, G. (2015). Chemotherapy-induced antitumor immunity requires formyl peptide receptor 1. *Science*, *350*(6263), 972-978. https://doi.org/doi:10.1126/science.aad0779

van Parijs, L., Perez, V. L., & Abbas, A. K. (1998). Mechanisms of peripheral T cell tolerance. *Novartis Found Symp*, *215*, 5-14; discussion 14-20, 33-40. https://doi.org/10.1002/9780470515525.ch2

Vander Heiden, M. G., Cantley, L. C., & Thompson, C. B. (2009). Understanding the Warburg effect: the metabolic requirements of cell proliferation. *Science*, *324*(5930), 1029-1033. https://doi.org/10.1126/science.1160809

Vanlangenakker, N., Bertrand, M. J., Bogaert, P., Vandenabeele, P., & Vanden Berghe, T. (2011). TNF-induced necroptosis in L929 cells is tightly regulated by multiple TNFR1 complex I and II members. *Cell Death Dis*, *2*(11), e230. https://doi.org/10.1038/cddis.2011.111

Varfolomeev, E. E., Schuchmann, M., Luria, V., Chiannilkulchai, N., Beckmann, J. S., Mett, I. L., Rebrikov, D., Brodianski, V. M., Kemper, O. C., Kollet, O., Lapidot, T., Soffer, D., Sobe, T., Avraham, K. B., Goncharov, T., Holtmann, H., Lonai, P., & Wallach, D. (1998). Targeted Disruption of the Mouse Caspase 8 Gene Ablates Cell Death Induction by the TNF Receptors, Fas/Apo1, and DR3 and Is Lethal Prenatally. *Immunity*, *9*(2), 267-276. https://doi.org/https://doi.org/10.1016/S1074-7613(00)80609-3

Vargas, J. N. S., Hamasaki, M., Kawabata, T., Youle, R. J., & Yoshimori, T. (2023). The mechanisms and roles of selective autophagy in mammals. *Nature Reviews Molecular Cell Biology*, *24*(3), 167-185. https://doi.org/10.1038/s41580-022-00542-2

Vaupel, P., & Multhoff, G. (2021). Revisiting the Warburg effect: historical dogma versus current understanding. *J Physiol*, *599*(6), 1745-1757. https://doi.org/10.1113/jp278810

Vaupel, P., & Multhoff, G. (2021). Revisiting the Warburg effect: historical dogma versus current understanding. *The Journal of Physiology*, *599*(6), 1745-1757. https://doi.org/https://doi.org/10.1113/JP278810

Vazquez, A., & Oltvai, Z. N. (2011). Molecular crowding defines a common origin for the Warburg effect in proliferating cells and the lactate threshold in muscle physiology. *PLoS One*, *6*(4), e19538. https://doi.org/10.1371/journal.pone.0019538

Vercammen, D., Beyaert, R., Denecker, G., Goossens, V., Van Loo, G., Declercq, W., Grooten, J., Fiers, W., & Vandenabeele, P. (1998). Inhibition of caspases increases the sensitivity of L929 cells to necrosis mediated by tumor necrosis factor. *J Exp Med*, *187*(9), 1477-1485. https://doi.org/10.1084/jem.187.9.1477

Vercammen, D., Brouckaert, G., Denecker, G., Van de Craen, M., Declercq, W., Fiers, W., & Vandenabeele, P. (1998). Dual signaling of the Fas receptor: initiation of both apoptotic and necrotic cell death pathways. *J Exp Med*, *188*(5), 919-930. https://doi.org/10.1084/jem.188.5.919

Verze, P., Cai, T., & Lorenzetti, S. (2016). The role of the prostate in male fertility, health and disease. *Nat Rev Urol*, *13*(7), 379-386. https://doi.org/10.1038/nrurol.2016.89

Vijayan, D., Young, A., Teng, M. W. L., & Smyth, M. J. (2017). Targeting immunosuppressive adenosine in cancer. *Nature Reviews Cancer*, *17*(12), 709-724. https://doi.org/10.1038/nrc.2017.86

Villa, E., Proïcs, E., Rubio-Patiño, C., Obba, S., Zunino, B., Bossowski, J. P., Rozier, R. M., Chiche, J., Mondragón, L., Riley, J. S., Marchetti, S., Verhoeyen, E., Tait, S. W. G., & Ricci, J. E. (2017). Parkin-Independent Mitophagy Controls Chemotherapeutic Response in Cancer Cells. *Cell Rep*, *20*(12), 2846-2859. https://doi.org/10.1016/j.celrep.2017.08.087

Vitale, I., Pietrocola, F., Guilbaud, E., Aaronson, S. A., Abrams, J. M., Adam, D., Agostini, M., Agostinis, P., Alnemri, E. S., Altucci, L., Amelio, I., Andrews, D. W., Aqeilan, R. I., Arama, E., Baehrecke, E. H., Balachandran, S., Bano, D., Barlev, N. A., Bartek, J., . . . Galluzzi, L. (2023). Apoptotic cell death in disease—Current understanding of the NCCD 2023. *Cell Death & Differentiation*, *30*(5), 1097-1154. https://doi.org/10.1038/s41418-023-01153-w

Vogelstein, B., & Kinzler, K. W. (1993). The multistep nature of cancer. *Trends in Genetics*, *9*(4), 138-141. https://doi.org/https://doi.org/10.1016/0168-9525(93)90209-Z

Vringer, E., & Tait, S. W. G. (2023). Mitochondria and cell death-associated inflammation. *Cell Death & Differentiation*, *30*(2), 304-312. https://doi.org/10.1038/s41418-022-01094-w

Vyas, S., Zaganjor, E., & Haigis, M. C. (2016). Mitochondria and Cancer. *Cell*, *166*(3), 555-566. https://doi.org/10.1016/j.cell.2016.07.002

Wang, H., Bloom, O., Zhang, M., Vishnubhakat, J. M., Ombrellino, M., Che, J., Frazier, A., Yang, H., Ivanova, S., Borovikova, L., Manogue, K. R., Faist, E., Abraham, E., Andersson, J., Andersson, U., Molina, P. E., Abumrad, N. N., Sama, A., & Tracey, K. J. (1999). HMG-1 as a late mediator of endotoxin lethality in mice. *Science*, *285*(5425), 248-251. https://doi.org/10.1126/science.285.5425.248

Wang, H., Hu, S., Chen, X., Shi, H., Chen, C., Sun, L., & Chen, Z. J. (2017). cGAS is essential for the antitumor effect of immune checkpoint blockade. *Proc Natl Acad Sci U S A*, *114*(7), 1637-1642. https://doi.org/10.1073/pnas.1621363114

Wang, Y., Martins, I., Ma, Y., Kepp, O., Galluzzi, L., & Kroemer, G. (2013). Autophagy-dependent ATP release from dying cells via lysosomal exocytosis. *Autophagy*, *9*(10), 1624-1625. https://doi.org/10.4161/auto.25873

Wang, Y., & Patti, G. J. (2023). The Warburg effect: a signature of mitochondrial overload. *Trends Cell Biol*, *33*(12), 1014-1020. https://doi.org/10.1016/j.tcb.2023.03.013

Warburg, O. (1924). Über den Stoffwechsel der Carcinomzelle. *Naturwissenschaften*, *12*(50), 1131-1137. https://doi.org/10.1007/BF01504608

Warburg, O. (1956). On respiratory impairment in cancer cells. *Science*, *124*(3215), 269-270.

Warburg, O. (1956). On the Origin of Cancer Cells. *Science*, *123*(3191), 309-314. https://doi.org/doi:10.1126/science.123.3191.309

Watt, M. J., Clark, A. K., Selth, L. A., Haynes, V. R., Lister, N., Rebello, R., Porter, L. H., Niranjan, B., Whitby, S. T., Lo, J., Huang, C., Schittenhelm, R. B., Anderson, K. E., Furic, L., Wijayaratne, P. R., Matzaris, M., Montgomery, M. K., Papargiris, M., Norden, S., . . . Taylor, R. A. (2019). Suppressing fatty acid uptake has therapeutic effects in preclinical models of prostate cancer. *Science Translational Medicine*, *11*(478), eaau5758. https://doi.org/doi:10.1126/scitranslmed.aau5758

Wei, M. C., Zong, W. X., Cheng, E. H. Y., Lindsten, T., Panoutsakopoulou, V., Ross, A. J., Roth, K. A., Macgregor, G. R., Thompson, C. B., & Korsmeyer, S. J. (2001). Proapoptotic BAX and BAK: A requisite gateway to mitochondrial dysfunction and death [Article]. *Science*, *292*(5517), 727-730. https://doi.org/10.1126/science.1059108

Wei, S. C., Duffy, C. R., & Allison, J. P. (2018). Fundamental Mechanisms of Immune Checkpoint Blockade Therapy. *Cancer Discovery*, *8*(9), 1069-1086. https://doi.org/10.1158/2159-8290.Cd-18-0367

Weinberg, S. E., Sena, L. A., & Chandel, N. S. (2015). Mitochondria in the regulation of innate and adaptive immunity. *Immunity*, *42*(3), 406-417. https://doi.org/10.1016/j.immuni.2015.02.002

Weiss, A., & Littman, D. R. (1994). Signal transduction by lymphocyte antigen receptors. *Cell*, *76*(2), 263-274. https://doi.org/https://doi.org/10.1016/0092-8674(94)90334-4

West, A. P., Khoury-Hanold, W., Staron, M., Tal, M. C., Pineda, C. M., Lang, S. M., Bestwick, M., Duguay, B. A., Raimundo, N., MacDuff, D. A., Kaech, S. M., Smiley, J. R., Means, R. E., Iwasaki, A., & Shadel, G. S. (2015). Mitochondrial DNA stress primes the antiviral innate immune response. *Nature*, *520*(7548), 553-557. https://doi.org/10.1038/nature14156

White, E., Lattime, E. C., & Guo, J. Y. (2021). Autophagy Regulates Stress Responses, Metabolism, and Anticancer Immunity. *Trends Cancer*, *7*(8), 778-789. https://doi.org/10.1016/j.trecan.2021.05.003

White, M. J., McArthur, K., Metcalf, D., Lane, R. M., Cambier, J. C., Herold, M. J., van Delft, M. F., Bedoui, S., Lessene, G., Ritchie, M. E., Huang, D. C., & Kile, B. T. (2014). Apoptotic caspases suppress mtDNA-induced STING-mediated type I IFN production. *Cell*, *159*(7), 1549-1562. https://doi.org/10.1016/j.cell.2014.11.036

WHO. (2024). *Global health estimates: Leading causes of death*. Retrieved January 19, 2024 from https://www.who.int/data/gho/data/themes/mortality-and-global-health-estimates/ghe-leading-causes-of-death

Wittig, I., Karas, M., & Schägger, H. (2007). High resolution clear native electrophoresis for in-gel functional assays and fluorescence studies of membrane protein complexes. *Mol Cell Proteomics*, *6*(7), 1215-1225. https://doi.org/10.1074/mcp.M700076-MCP200

Woo, S. R., Fuertes, M. B., Corrales, L., Spranger, S., Furdyna, M. J., Leung, M. Y., Duggan, R., Wang, Y., Barber, G. N., Fitzgerald, K. A., Alegre, M. L., & Gajewski, T. F. (2014). STING-dependent cytosolic DNA sensing mediates innate immune recognition of immunogenic tumors. *Immunity*, *41*(5), 830-842. https://doi.org/10.1016/j.immuni.2014.10.017

Wooster, R., Bignell, G., Lancaster, J., Swift, S., Seal, S., Mangion, J., Collins, N., Gregory, S., Gumbs, C., Micklem, G., Barfoot, R., Hamoudi, R., Patel, S., Rices, C., Biggs, P., Hashim, Y., Smith, A., Connor, F., Arason, A., . . . Stratton, M. R. (1995). Identification of the breast cancer susceptibility gene BRCA2. *Nature*, *378*(6559), 789-792. https://doi.org/10.1038/378789a0

Xia, L., Oyang, L., Lin, J., Tan, S., Han, Y., Wu, N., Yi, P., Tang, L., Pan, Q., Rao, S., Liang, J., Tang, Y., Su, M., Luo, X., Yang, Y., Shi, Y., Wang, H., Zhou, Y., & Liao, Q. (2021). The cancer metabolic reprogramming and immune response. *Molecular Cancer*, *20*(1), 28. https://doi.org/10.1186/s12943-021-01316-8

Xia, M., Zhang, Y., Jin, K., Lu, Z., Zeng, Z., & Xiong, W. (2019). Communication between mitochondria and other organelles: a brand-new perspective on mitochondria in cancer. *Cell & Bioscience*, *9*(1), 27. https://doi.org/10.1186/s13578-019-0289-8

Yakes, F. M., & Van Houten, B. (1997). Mitochondrial DNA damage is more extensive and persists longer than nuclear DNA damage in human cells following oxidative stress. *Proc Natl Acad Sci U S A*, *94*(2), 514-519. https://doi.org/10.1073/pnas.94.2.514

Yamamoto, H., Zhang, S., & Mizushima, N. (2023). Autophagy genes in biology and disease. *Nature Reviews Genetics*, *24*(6), 382-400. https://doi.org/10.1038/s41576-022-00562-w

Yamashiro, L. H., Wilson, S. C., Morrison, H. M., Karalis, V., Chung, J.-Y. J., Chen, K. J., Bateup, H. S., Szpara, M. L., Lee, A. Y., Cox, J. S., & Vance, R. E. (2020). Interferon-independent STING signaling promotes resistance to HSV-1 in vivo. *Nature Communications*, *11*(1), 3382. https://doi.org/10.1038/s41467-020-17156-x

Yamazaki, T., Ames, T. D., & Galluzzi, L. (2019). Potent induction of immunogenic cell death by PT-112 [Meeting Abstract]. *Cancer Immunology Research*, *7*(2), 2. https://doi.org/10.1158/2326-6074.Cricimteatiaacr18-b199

Yamazaki, T., Buqué, A., Ames, T. D., & Galluzzi, L. (2020). PT-112 induces immunogenic cell death and synergizes with immune checkpoint blockers in mouse tumor models. *OncoImmunology*, *9*(1), 1721810. https://doi.org/10.1080/2162402x.2020.1721810

Yamazaki, T., & Galluzzi, L. (2020). Mitochondrial control of innate immune signaling by irradiated cancer cells. *OncoImmunology*, *9*(1), 1797292. https://doi.org/10.1080/2162402x.2020.1797292

Yamazaki, T., Galluzzi, L., Yim, C., & Ames, T. (2022). 1118 Immunologically relevant effects of PT-112 on cancer cell mitochondria. *Journal for ImmunoTherapy of Cancer*, *10*(Suppl 2), A1162-A1162. https://doi.org/10.1136/jitc-2022-SITC2022.1118

Yamazaki, T., Kirchmair, A., Sato, A., Buqué, A., Rybstein, M., Petroni, G., Bloy, N., Finotello, F., Stafford, L., Navarro Manzano, E., Ayala de la Peña, F., García-Martínez, E., Formenti, S. C., Trajanoski, Z., & Galluzzi, L. (2020). Mitochondrial DNA drives abscopal responses to radiation that are inhibited by autophagy. *Nature Immunology*, *21*(10), 1160-1171. https://doi.org/10.1038/s41590-020-0751-0

Yamazaki, T., Kirchmair, A., Sato, A., Buqué, A., Rybstein, M., Petroni, G., Bloy, N., Finotello, F., Stafford, L., Navarro Manzano, E., Ayala de la Peña, F., García-Martínez, E., Formenti, S. C., Trajanoski, Z., & Galluzzi, L. (2020). Mitochondrial DNA drives abscopal responses to radiation that are inhibited by autophagy. *Nat Immunol*, *21*(10), 1160-1171. https://doi.org/10.1038/s41590-020-0751-0

Yan, C., Luo, L., Guo, C. Y., Goto, S., Urata, Y., Shao, J. H., & Li, T. S. (2017). Doxorubicin-induced mitophagy contributes to drug resistance in cancer stem cells from HCT8 human colorectal cancer cells. *Cancer Lett*, *388*, 34-42. https://doi.org/10.1016/j.canlet.2016.11.018

Yanai, H., Ban, T., & Taniguchi, T. (2011). Essential role of high-mobility group box proteins in nucleic acid-mediated innate immune responses. *Journal of Internal Medicine*, *270*(4), 301-308. https://doi.org/https://doi.org/10.1111/j.1365-2796.2011.02433.x

Yanai, H., Ban, T., Wang, Z., Choi, M. K., Kawamura, T., Negishi, H., Nakasato, M., Lu, Y., Hangai, S., Koshiba, R., Savitsky, D., Ronfani, L., Akira, S., Bianchi, M. E., Honda, K., Tamura, T., Kodama, T., & Taniguchi, T. (2009). HMGB proteins function as universal sentinels for nucleic-acid-mediated innate immune responses. *Nature*, *462*(7269), 99-103. https://doi.org/10.1038/nature08512

Yang, H., Hreggvidsdottir, H. S., Palmblad, K., Wang, H., Ochani, M., Li, J., Lu, B., Chavan, S., Rosas-Ballina, M., Al-Abed, Y., Akira, S., Bierhaus, A., Erlandsson-Harris, H., Andersson, U., & Tracey, K. J. (2010). A critical cysteine is required for HMGB1 binding to Toll-like receptor 4 and activation of macrophage cytokine release. *Proceedings of the National Academy of Sciences*, *107*(26), 11942-11947. https://doi.org/doi:10.1073/pnas.1003893107

Yang, H., Wang, H., Ren, J., Chen, Q., & Chen, Z. J. (2017). cGAS is essential for cellular senescence. *Proceedings of the National Academy of Sciences*, *114*(23), E4612-E4620. https://doi.org/doi:10.1073/pnas.1705499114

Yang, K., Halima, A., & Chan, T. A. (2023). Antigen presentation in cancer - mechanisms and clinical implications for immunotherapy. *Nat Rev Clin Oncol*, *20*(9), 604-623. https://doi.org/10.1038/s41571-023-00789-4

Yang, Y., Karakhanova, S., Hartwig, W., D'Haese, J. G., Philippov, P. P., Werner, J., & Bazhin, A. V. (2016). Mitochondria and Mitochondrial ROS in Cancer: Novel Targets for Anticancer Therapy. *J Cell Physiol*, *231*(12), 2570-2581. https://doi.org/10.1002/jcp.25349

Yang, Y., Wang, H., Kouadir, M., Song, H., & Shi, F. (2019). Recent advances in the mechanisms of NLRP3 inflammasome activation and its inhibitors. *Cell Death & Disease*, *10*(2), 128. https://doi.org/10.1038/s41419-019-1413-8

Yang, Z., Schumaker, L. M., Egorin, M. J., Zuhowski, E. G., Guo, Z., & Cullen, K. J. (2006). Cisplatin preferentially binds mitochondrial DNA and voltage-dependent anion channel protein in the

mitochondrial membrane of head and neck squamous cell carcinoma: possible role in apoptosis. *Clin Cancer Res*, *12*(19), 5817-5825. https://doi.org/10.1158/1078-0432.Ccr-06-1037

Yao, N., Wang, C., Hu, N., Li, Y., Liu, M., Lei, Y., Chen, M., Chen, L., Chen, C., Lan, P., Chen, W., Chen, Z., Fu, D., Ye, W., & Zhang, D. (2019). Inhibition of PINK1/Parkin-dependent mitophagy sensitizes multidrug-resistant cancer cells to B5G1, a new betulinic acid analog. *Cell Death & Disease*, *10*(3), 232. https://doi.org/10.1038/s41419-019-1470-z

Yim, C. Y., Congenie, M. T., Johnson, H. L., Mancini, M. G., Stossi, F., Mancini, M. A., Azofeifa, J., Price, M. R., Baeck, J., & Ames, T. D. (2023). Abstract C128: PT-112, a novel immunogenic cell death inducer, causes ribosomal biogenesis inhibition and organelle stress in cancer cells. *Molecular Cancer Therapeutics*, *22*(12_Supplement), C128-C128. https://doi.org/10.1158/1535-7163.Targ-23-c128

Yim, C. Y., Congenie, M. T., Johnson, H. L., Mancini, M. G., Stossi, F., Mancini, M. A., Azofeifa, J., Price, M. R., Baeck, J., & Ames, T. D. (2023). PT-112, a novel immunogenic cell death inducer, causes ribosomal biogenesis inhibition and organelle stress in cancer cells [Meeting Abstract]. *Molecular Cancer Therapeutics*, *22*(12), 2. https://doi.org/10.1158/1535-7163.Targ-23-c128

Youn, J. H., & Shin, J.-S. (2006). Nucleocytoplasmic Shuttling of HMGB1 Is Regulated by Phosphorylation That Redirects It toward Secretion1. *The Journal of Immunology*, *177*(11), 7889-7897. https://doi.org/10.4049/jimmunol.177.11.7889

Yu, L., Chen, X., Wang, L., & Chen, S. (2016). The sweet trap in tumors: aerobic glycolysis and potential targets for therapy. *Oncotarget*, *7*(25), 38908-38926. https://doi.org/10.18632/oncotarget.7676

Yuan, Y., Ju, Y. S., Kim, Y., Li, J., Wang, Y., Yoon, C. J., Yang, Y., Martincorena, I., Creighton, C. J., Weinstein, J. N., Xu, Y., Han, L., Kim, H. L., Nakagawa, H., Park, K., Campbell, P. J., & Liang, H. (2023). Publisher Correction: Comprehensive molecular characterization of mitochondrial genomes in human cancers. *Nat Genet*, *55*(5), 893. https://doi.org/10.1038/s41588-020-0587-4

Yuda, J., Will, C., Phillips, D. C., Abraham, L., Alvey, C., Avigdor, A., Buck, W., Besenhofer, L., Boghaert, E., Cheng, D., Cojocari, D., Doyle, K., Hansen, T. M., Huang, K., Johnson, E. F., Judd, A. S., Judge, R. A., Kalvass, J. C., Kunzer, A., . . . Souers, A. J. (2023). Selective MCL-1 inhibitor ABBV-467 is efficacious in tumor models but is associated with cardiac troponin increases in patients. *Commun Med (Lond)*, *3*(1), 154. https://doi.org/10.1038/s43856-023-00380-z

Zhang, Z., Zhang, Y., Xia, S., Kong, Q., Li, S., Liu, X., Junqueira, C., Meza-Sosa, K. F., Mok, T. M. Y., Ansara, J., Sengupta, S., Yao, Y., Wu, H., & Lieberman, J. (2020). Gasdermin E suppresses tumour growth by activating anti-tumour immunity. *Nature*, *579*(7799), 415-420. https://doi.org/10.1038/s41586-020-2071-9

Zhao, X., Hu, S., Zeng, L., Liu, X., Song, Y., Zhang, Y., Chen, Q., Bai, Y., Zhang, J., Zhang, H., Pan, Y., & Shao, C. (2022). Irradiation combined with PD-L1(-/-) and autophagy inhibition enhances the antitumor effect of lung cancer via cGAS-STING-mediated T cell activation. *iScience*, *25*(8), 104690. https://doi.org/10.1016/j.isci.2022.104690

Zhou, Z., He, H., Wang, K., Shi, X., Wang, Y., Su, Y., Wang, Y., Li, D., Liu, W., Zhang, Y., Shen, L., Han, W., Shen, L., Ding, J., & Shao, F. (2020). Granzyme A from cytotoxic lymphocytes cleaves GSDMB to trigger pyroptosis in target cells. *Science*, *368*(6494). https://doi.org/10.1126/science.aaz7548

Zitvogel, L., Apetoh, L., Ghiringhelli, F., & Kroemer, G. (2008). Immunological aspects of cancer chemotherapy. *Nature Reviews Immunology*, *8*(1), 59-73. https://doi.org/10.1038/nri2216

Zitvogel, L., Tesniere, A., & Kroemer, G. (2006). Cancer despite immunosurveillance: immunoselection and immunosubversion. *Nature Reviews Immunology*, *6*(10), 715-727. https://doi.org/10.1038/nri1936

Zong, W. X., Rabinowitz, J. D., & White, E. (2016). Mitochondria and Cancer. *Mol Cell*, *61*(5), 667-676. https://doi.org/10.1016/j.molcel.2016.02.011